

**THE CORRELATION BETWEEN CRANIAL AND POST-
CRANIAL SKELETAL ELEMENTS FOR RESOLVING AND
RECONSTRUCTION OF COMINGLED SKELETAL REMAINS IN
VICTIM IDENTIFICATION**

by
Johan Christian Marais

*Thesis presented in partial fulfilment of the requirements for the degree of Masters of Science (in
Anatomy) in the Faculty of Medicine and Health Sciences at Stellenbosch University*



Supervisor: Mrs A Alblas

Co-Supervisor: Mrs LM Greyling

DIVISION OF CLINICAL ANATOMY

April 2019

DECLARATION

By submitting this dissertation electronically, I declare that the entirety of the work contained therein is my own, original work, that I am the sole author thereof (save to the extent explicitly otherwise stated), that reproduction and publication thereof by Stellenbosch University will not infringe any third party rights and that I have not previously in its entirety or in part submitted it for obtaining any qualification.

JC Marais

April 2019

Date

ABSTRACT

Upon discovery of comingled disarticulated skeletons, actual matching of different skeletal elements to a particular individual can be extremely difficult. Available literature regarding the matching of skeletal elements, show few studies correlating skull measurements with post-cranial elements, with the majority of cases determining correlations with stature. The aim of this study is to assess the degree of correlation between cranial and post-cranial skeletal elements, of the three dominant South African population groups, by means of direct correlations of measurements.

Skeletons of individuals (N=296) of both males (n=148) and females (n=148) of South African black (n=100), South African white (n=97) and South African coloured (n=99) population groups, were assessed in three distinct manners. Firstly, three correlation sets were recorded: 21 cephalometric elements were correlated with eight long-bone measurements, and six occipital condyle measurements with morphologically mirrored measurements on the superior articular facet of the first cervical vertebra were correlated. The last of the correlation sets consisted of the lengths and breadths of the neural foramina from foramen magnum up to C2. Secondly, Principal Component Analyses were conducted on the 21 cephalometric elements, the eight long-bones measurements, the 12 articular facet measurements, and the six neural canal measurements. Lastly, t-tests were conducted to determine if any of the measurements were sexually different.

From these assessments, a connection between some of the cephalometric elements and the long bones were observed. Most notably, the novel construct known as representative facial height (NLH.MRH), which is the summation of the nasal height and the maximum ramus height of the mandible for all three population groups. The South African white males, however, showed a much weaker connection with NLH.MRH, though, the basion-bregma height correlated well with the long bones. It was determined that the length measurements outperformed the breadth measurements in terms of correlative strength for the three population groups, in the atlanto-occipital joint. A direct relationship was established within the neural canal from foramen magnum up until C2 for all three population groups.

A clear platform is created for future research into constructing regression formulae for matching skulls with long bones. The articular facet and neural canal results can be used in a combined assessment for matching a skull with a body that has an intact cervical spine, by developing a regression model from a grouping of both measurement sets. These regression models may then be implemented in the sorting of comingled remains in situations such as mass graves and mass disasters.

ABSTRAK/OPSOMMING

Met die ontdekking van gemengde gedisartikuleerde skelette, kan die werklike ooreenstemming van verskillende skeletelemente met 'n spesifieke individu uiters moeilik wees. Die beskikbare literatuur, aangaande die ooreenstemming van skeletelemente, toon dat weinige studies, met betrekking tot korrelasies van post-kraniale elemente en skedelmates, beskikbaar is, waar die meeste gevalle wat korrelasies met staturus bepaal is. Die doel van hierdie studie was om die mate van korrelasie tussen kraniale en post-kraniale skeletelemente van die drie dominante Suid-Afrikaanse bevolkingsgroepe te bepaal, deur middel van direkte korrelasies van metings.

Skelette van individue (N=296) van beide mans (n=148) en vrouens (n=148) van Suid-Afrikaanse swart (n=100), Suid-Afrikaanse blank (n=97) en Suid-Afrikaanse kleurling (n=99) bevolkingsgroepe, is op drie verskillende maniere beoordeel. Eerstens is drie korrelasiestelle aangeteken: 21 kefalometriese elemente is gekorreleer met agt langbeenmetings, en ses oksipitale kondiele metings met morfologies gewoenspeëlde metings, van die superieure artikulêre faset van die eerste servikale werwel, is gekorreleer. Die laaste van die korrelasiestelle het bestaan uit die lengtes en breedtes van die neurale foramina van foramen magnum tot die tweede servikale werwels (C2). Tweedens is hoofkomponentanalises uitgevoer op die 21 kefalometriese elemente, die agt langbene metings, die 12 artikulêre fasetmetings en die ses neurale kanaalmetings. Laastens is t-toetse uitgevoer om vas te stel of enige van die metings verskil tussen die geslagte.

Uit hierdie assesserings is 'n verband tussen sommige van die kefalometriese elemente en die langbene waargeneem. Opmerklik, die nuut geskepte metode bekend as die gesigshoogte verteenwoordiger (NLH.MRH), wat die som van die neushoogte en die maksimum ramushoogte van die mandibel is. Die Suid-Afrikaanse blanke mans het egter 'n baie swakker assosiasie met NLH.MRH getoon, alhoewel die basion-bregma-hoogte goed met die langbene gekorreleer het. Met betrekking tot die atlanto-oksipitale gewrig is waargeneem dat die lengtemetings beter as die breedtemetings was in terme van korrelatiewe sterkte vir al drie populasies. 'n Direkte verhouding is binne die neurale kanaal van foramen magnum tot C2 vir al drie populasies bevind.

'n Duidelike platform is geskep vir toekomstige navorsing, sowel as die opstel van regressieformules vir die passing van skedels met langbene. Die artikulêre faset- en neurale kanaal resultate kan gebruik word in 'n gekombineerde assessering vir die passing van 'n skedel met 'n liggaam wat 'n ongeskonde servikale ruggraat het, deur 'n regressiemodel te ontwikkel wat van beide stelle resultate gebruik maak. Hierdie regressie modelle kan dan geïmplementeer word in die sorteer van gemengde skelette in situasies soos massagrafte en massa-rampe.

ACKNOWLEDGEMENTS

First of all, I would like to thank each and every person who has helped me along the way in writing this thesis. It has been quite the learning experience and I treasure everything I have learned.

I would like to thank Prof. Daan Nel, former director of the Centre for Statistical Consultation at Stellenbosch University, personally for his assistance with the statistical component of this thesis.

I would further like to thank my interobservers Christy L. Hagelthorn and Alisa Naude

I would like to thank each of the universities that opened their doors and allowed me to measure their skeletal specimens.

The biggest thank you to my two supervisors Amanda Alblas and Linda M. Greyling, without you, this thesis would never have happened.

Laaste wil ek net bitterlik dankie sê vir al die vriende en familie wat my ondersteun het gedurende die skryf van die tesis, sonder julle sou ek lankal my kop verloor het. 'n Groot dankie aan een spesifieke persoon wie altyd my moed in gepraat het wanneer ek voel ek kon nie meer nie, maar nooit 'n oorlas gemaak het om honderd keer 'n dag te gevra het hoe dit gaan met die tesis nie.

CONTENTS

ACKNOWLEDGEMENTS	v
Chapter 1: INTRODUCTION	1
1.1 Problem statement	2
1.2 Aims	2
1.3 Objectives	2
Chapter 2: LITERATURE REVIEW	3
2.1 Population distribution and study cohort.....	3
2.2 Standardisation of measurements and the importance of population based research .	4
2.3 Cephalometric size and stability with age	5
2.4 Vertebral osteology	5
2.5 Foramen magnum osteology	8
2.6 Development and growth of the long bones.....	8
2.7 Previous research on correlations of cranial and post-cranial elements.....	9
Chapter 3: MATERIALS AND METHODS.....	11
3.1 Materials.....	11
3.2 Methods.....	12
3.2.1 Cephalometric measurements	12
3.2.2 Articular facets measurements of C0-C1	16
3.2.3 Neural foramina measurements	17
3.2.4 Post-cranial measurements.....	18
3.3 Statistics.....	19
3.4 Limitations.....	21
3.5 Assumptions	22
3.6 Ethical consideration	22
Chapter 4: RESULTS	23
4.1 Descriptive statistics.....	23
4.1.1 Cephalometric measurements	23
4.1.2 Articular facets measurements of C0-C1	24
4.1.3 Neural foramina measurements	30
4.1.4 Post-cranial measurements.....	30
4.2 Factor analyses	36

4.2.1	Cephalometric measurements	37
4.2.2	Articular facet measurements of C0-C1.....	41
4.2.3	Neural foramina measurements	46
4.2.4	Post-cranial measurements.....	49
4.2.5	All variables combined	53
4.3	Correlative statistics	60
4.3.1	Cephalometric measurements with post-cranial measurements	60
4.3.2	Articular facets measurements of C0-C1	66
4.3.3	Neural foramina measurements	70
Chapter 5:	DISCUSSION	77
5.1	Cephalometric-long bones.....	77
5.2	Articular facets measurements of C0-C1	80
5.3	Neural foramina measurements.....	81
Chapter 6:	CONCLUSION.....	83
Chapter 7:	REFERENCE LIST	84
APPENDIX A	88
APPENDIX B	93
7.1	South African Black Males	93
7.2	South African Black Females.....	102
7.3	South African White Males	111
7.4	South African White Females	121
7.5	South African Coloured Males.....	130
7.6	South African Coloured Females	140

TABLES

Table 3.1: Distribution of samples in the Bone Collections.	11
Table 3.2: Sample numbers used in the current study after exclusions were finalised during data processing all three population groups.....	11
Table 3.3: Discriptions of cephalometric points as seen in Fig. 3.1 and Fig. 3.2 (Buikstra & Ubelaker, 1994; Langley <i>et al.</i> , 2016)	13
Table 3.4: Standard cephalometric measurements used in this study as described by Buikstra & Ubelaker (1994) and Langley <i>et al.</i> (2016).....	14
Table 3.5: Condylar measurements used from Naderi <i>et al.</i> (2005) and superior articular facet measurements as reflections of condylar measurements.	17
Table 3.6: Measurements of the first and second cervical vertebrae designed to reflect the standard measurements for the foramen magnum (Buikstra & Ubelaker, 1994).....	18
Table 3.7: Long bone measurements for post-cranial assessment in accordance with the standards set by Buikstra & Ubelaker, (1994) and Langley <i>et al.</i> (2016).....	18
Table 3.8: Inter-observer reliability for all measurements.	20
Table 4.1: Results of the t-test for the cephalometric measurements of the three population groups and the combined study population.	24
Table 4.2: Results of the t-test for the articular facet measurements of C0-C1 of the three population groups and the combined study population.	25
Table 4.3: Results of the t-test for the neural foramina measurements of C1 and C2 the three population groups and the combined study population.	25
Table 4.4: Results of the t-test for the long bone measurements of the three population groups and the combined study population.	26
Table 4.5: Descriptive statistics for cephalometric variables of SAB sample.	27
Table 4.6: Descriptive statistics for cephalometric variables of SAW sample.	28
Table 4.7: Descriptive statistics for cephalometric variables of SAC sample.	29
Table 4.8: Descriptive statistics for articular facets of C0-C1 of SAB sample.....	31
Table 4.9: Descriptive statistics for articular facets of C0-C1 of SAW sample.	31
Table 4.10: Descriptive statistics for articular facets of C0-C1 of SAC sample.....	32
Table 4.11: Descriptive statistics for neural foramina measurements of C1 and C2 for the SAB sample.	33
Table 4.12: Descriptive statistics for neural foramina measurements of C1 and C2 for the SAW sample.	33
Table 4.13: Descriptive statistics for neural foramina measurements of C1 and C2 for the SAC sample.	34

Table 4.14: Descriptive statistics for long bone measurements of SAB sample.	34
Table 4.15: Descriptive statistics for long bone measurements of SAW sample.	35
Table 4.16: Descriptive statistics for long bone measurements of SAC sample.	35
Table 4.17: Eigenvalues of the cephalometric measurements listed for the SAB sample with percentage of variance explained by each factor.	37
Table 4.18: Factor loadings from a principal component extraction for the cephalometric measurements of the SAB sample after a varimax rotation was implemented.....	37
Table 4.19: Eigenvalues of the cephalometric measurements listed for the SAW sample with percentage of variance explained by each factor.	38
Table 4.20: Factor loadings from a principal component extraction for the cephalometric measurements of the SAW sample after a varimax rotation was implemented.....	38
Table 4.21: Eigenvalues of the cephalometric measurements listed for the SAC sample with percentage of variance explained by each factor.	39
Table 4.22: Factor loadings from a principal component extraction for the cephalometric measurements of the SAC sample after a varimax rotation was implemented.....	39
Table 4.23: Eigenvalues of the cephalometric measurements listed for the combined sample with percentage of variance explained by each factor.	40
Table 4.24: Factor loadings from a principal component extraction for the cephalometric measurements of the combined sample after a varimax rotation was implemented.....	41
Table 4.25: Eigenvalues of all C0-C1 articular facet measurements for the SAB sample with percentage of variance explained by each factor.	42
Table 4.26: Factor loadings from a principal component extraction for the C0-C1 articular facet measurements of the SAB sample after a varimax rotation was implemented.....	42
Table 4.27: Eigenvalues of all C0-C1 articular facet measurements for the SAW sample with percentage of variance explained by each factor.	43
Table 4.28: Factor loadings from a principal component extraction for the C0-C1 articular facet measurements of the SAW sample after a varimax normalised rotation was implemented.....	43
Table 4.29: Eigenvalues of all C0-C1 articular facet measurements for the SAC sample with percentage of variance explained by each factor.	44
Table 4.30: Factor loadings from a principal component extraction for the C0-C1 articular facet measurements of the SAC sample after a varimax normalised rotation was implemented.....	44
Table 4.31: Eigenvalues of all C0-C1 articular facet measurements for the combined sample with percentage of variance explained by each factor.	45
Table 4.32: Factor loadings from a principal component extraction for the C0-C1 articular facet measurements of the combined sample after a varimax normalised rotation was implemented.....	45

Table 4.33: Eigenvalues of the neural foramina measurements for the SAB sample with percentage of variance explained by each factor.....	46
Table 4.34: Factor loadings from a principal component extraction for the neural foramina measurements of the SAB sample after a varimax normalised rotation was implemented.....	46
Table 4.35: Eigenvalues of the neural foramina measurements for the SAW sample with percentage of variance explained by each factor.....	47
Table 4.36: Factor loadings from a principal component extraction for the neural foramina measurements of the SAW sample after a varimax normalised rotation was implemented.....	47
Table 4.37: Eigenvalues of the neural foramina measurements for the SAC sample with percentage of variance explained by each factor.....	47
Table 4.38: Factor loadings from a principal component extraction for the neural foramina measurements of the SAC sample after a varimax normalised rotation was implemented.....	48
Table 4.39: Eigenvalues of the neural foramina measurements for the combined sample with percentage of variance explained by each factor.	48
Table 4.40: Factor loadings from a principal component extraction for the neural foramina measurements of the combined sample after a varimax normalised rotation was implemented.....	49
Table 4.41: Eigenvalues of the post-cranial measurements for the SAB sample with percentage of variance explained by each factor.....	49
Table 4.42: Factor loadings from a principal component extraction for the post-cranial measurements of the SAB sample after a varimax normalised rotation was implemented.....	50
Table 4.43: Eigenvalues of the post-cranial measurements for the SAW sample with percentage of variance explained by each factor.....	50
Table 4.44: Factor loadings from a principal component extraction for the post-cranial measurements of the SAW sample after a varimax normalised rotation was implemented.....	50
Table 4.45: Eigenvalues of the post-cranial measurements for the SAC sample with percentage of variance explained by each factor.....	51
Table 4.46: Factor loadings from a principal component extraction for the post-cranial measurements of the SAC sample after a varimax normalised rotation was implemented.....	51
Table 4.47: Eigenvalues of the post-cranial measurements for the combined sample with percentage of variance explained by each factor.	52
Table 4.48: Factor loadings from a principal component extraction for the post-cranial measurements of the combined sample after a varimax normalised rotation was implemented.....	52
Table 4.49: Eigenvalues of all measurements for the SAB sample with percentage of variance explained by each factor.	53

Table 4.50: Factor loadings from a principal component extraction for all measurements of the SAB sample after a varimax normalised rotation was implemented.	53
Table 4.51: Eigenvalues of all measurements for the SAW sample with percentage of variance explained by each factor.	54
Table 4.52: Factor loadings from a principal component extraction for all measurements of the SAW sample after a varimax normalised rotation was implemented.	55
Table 4.53: Eigenvalues of all measurements for the SAC sample with percentage of variance explained by each factor.	56
Table 4.54: Factor loadings from a principal component extraction for all measurements of the SAC sample after a varimax normalised rotation was implemented.	56
Table 4.55: Eigenvalues of all measurements for the combined sample with percentage of variance explained by each factor.	58
Table 4.56: Factor loadings from a principal component extraction for all measurements of the SAC sample after a varimax normalised rotation was implemented.	58
Table 4.57: Cephalometric-Long bone correlations of SAB males.	60
Table 4.58: Cephalometric-Long bone correlations of SAB females.	61
Table 4.59: Cephalometric-Long bone correlations of SAW males.	62
Table 4.60: Cephalometric-Long bone correlations of SAW females.	63
Table 4.61: Cephalometric-Long bone correlations of SAC males.	64
Table 4.62: Cephalometric-Long bone correlations of SAC females.	65
Table 4.63: Atlanto-occipital articular facet correlations of SAB males.	66
Table 4.64: Atlanto-occipital articular facet correlations of SAB females.	67
Table 4.65: Atlanto-occipital articular facet correlations of SAW males.	68
Table 4.66: Atlanto-occipital articular facet correlations of SAW females.	68
Table 4.67: Atlanto-occipital articular facet correlations of SAC males.	69
Table 4.68: Atlanto-occipital articular facet correlations of SAC females.	70
Table 4.69: Foramina correlations for SAB males.	71
Table 4.70: Foramina correlations for SAB females.	71
Table 4.71: Foramina correlations for SAW males.	72
Table 4.72: Foramina correlations for SAW females.	73
Table 4.73: Foramina correlations for SAC males.	74
Table 4.74: Foramina correlations for SAC females.	75

FIGURES

Figure 2.1: Illustrations of the differences seen in the cervical vertebrae. (Netter, 2010).....	6
Figure 2.2: Posterior view of the internal ligaments of the upper part of the cervical spine (the spinous processes have been removed) (Netter, 2010).....	7
Figure 2.3: The articulation of the dens process of the second vertebra with the anterior arch of the first cervical vertebra. (Netter, F.H., 2010).....	7
Figure 2.4: The growth centres of the lower limb long-bones and when the epiphyses fuse. (Scheuer & Black, 2000).....	8
Figure 2.5: The growth centres of the upper limb long-bones and when the epiphyses fuse. (Scheuer & Black, 2000).....	9
Figure 3.1: Diagrams showing standard cephalometric landmarks and measurements used in the study. Figures adapted from Moore-Jansen <i>et al.</i> 1994 in Buikstra & Ubelaker (1994).	12
Figure 3.2: Indications of cephalometric measurements (Table 3.4). Figure adapted from Moore-Jansen <i>et al.</i> 1994 in Buikstra & Ubelaker (1994).....	13
Figure 3.3: A- A lateral view of a skull illustrating the warped calvarium and the gap created by it. B- A lateral view of the cranium illustrating the anterior tilt method. C – The shim position as the anterior tilt is employed. D- A lateral view of the cranium illustrating the posterior tilt method.	15
Figure 3.4: An illustration of the measurements taken of the superior articular surface of the first cervical vertebra.	16
Figure 3.5: Illustrations of the measurements listed in Table 3.6 of the neural foramen of the first and second vertebra.....	17

ABBREVIATIONS

Abbr	-	Abbreviation
AICD	-	Anterior inter-condylar distances
AIFD	-	Anterior inter-facet distance
Ant.	-	Anterior
AUB	-	Biauricular breadth
b	-	Bregma
ba	-	Basion
BBH	-	Basion-bregma height
BNL	-	Cranial base length
C0	-	Occipital condyles
C1	-	First cervical vertebra
C2	-	Second cervical vertebra
CCV	-	Combined Cords Variable
cdl	-	Condylion
CdILL	-	Condylar lengths (left)
CdILR	-	Condylar lengths (right)
CdIWL	-	Condylar widths (left)
CdIWR	-	Condylar widths (right)
CLAXLN	-	Clavicle maximum length
d	-	Dacryon
ec	-	Ectoconchion
EKB	-	Biorbital breadth
eu	-	Euryon
FEMXLN	-	Femur maximum length
FEMBLN	-	Femur bicondylar length
FIBXLN	-	Fibula maximum length
FM	-	Foramen magnum
fnt	-	Frontomolare temporal
FOB	-	Foramen magnum breadth
FOL	-	Foramen magnum length
FRC	-	Frontal cord
ft	-	Frontotemporale
g	-	Glabella
go	-	Gonion
GOL	-	Maximum cranial length
Hox	-	Homeobox
HSC	-	University of Cape Town Human Skeletal Collection
HUMXLN	-	Humerus maximum length
id	-	Infradentale
inf.	-	Inferior
KSC	-	Kirsten Skeletal Collection
L	-	Left
l	-	Lambda
MRH	-	Mandibular Ramus Height

ms	- Mastoidale
n	- Nasion
ns	- Nasospinale
NLH	- Nasal height
o	- Opisthion
OBB	- Orbital breadth
OBH	- Orbital height
OCC	- Occipital cord
op	- Opisthocranium
PAC	- Parietal cord
PCA	- Principal component analysis
PCAs	- Principal component analyses
PCC	- Pearson's correlation coefficient
PICD	- Posterior inter-condylar distances
PIFD	- Posterior inter-facet distance
post.	- Posterior
R	- Right
ra	- Radiculare
RAD	- University of the Witwatersrand Raymond A. Dart Collection
RADXLN	- Radius maximum length
SD	- Standard deviation
SAB	- South African Black
SAC	- South African Coloured
SAFLL	- Superior articular facet length (left)
SAFLR	- Superior articular facet length (right)
SAFWL	- Superior articular facet width (left)
SAFWR	- Superior articular facet width (right)
SAI	- South Africa Indian
SAW	- South African White
sup.	- Superior
SAF	- Superior articular facet
SAFs	- Superior articular facets
TIBXLN	- Tibia maximum length
ULNXLN	- Ulna maximum length
WFB	- Minimum frontal breadth
XCB	- Maximal cranial breadth

SYMBOLS

♀	- Female
♂	- Male

CHAPTER 1: INTRODUCTION

During anthropogenic or natural disasters it is often the case that dismemberment of either the limbs or head is found. During recovery of individuals from mass graves, it is often untrained individuals who do some of the recovery before specialists step in. In these cases, it is easy to have comingled bodies and it falls upon the physical anthropologists to be able to reconstruct these individuals and to help ascertain the identity of each individual.

It is essential that individuals are as complete as possible, and have as few as possible parts missing from their bodies, in order to make a positive identification from the skeletal remains (Lundy, 1983; Lundy & Feldesman, 1987; Sauer, 1992), as not all morphometric and anthropological data can be attained from the same areas. In creating a network of traits in the body it becomes possible to translate information through these traits and arrive at the same conclusion, even in the absence of missing body parts that can usually provide the information.

In events where large numbers of DNA analysis is needed to ensure that all parts of dismembered bodies are returned to the family, having an anthropologist identify possible matches will decrease the workload on the genetic analysts. One such event that shook the United States of America in the year 2001 was the four coordinated attacks of al-Qaeda in which 2977 individuals were killed (Plumer, 2013; CNN, 2018). In the aftermath DNA testing was used in the identification of victims and their body parts. These cases can account for the identification of individuals in a mass grave or for individuals dismembered in explosions from purpose or accidental origin.

This study has, therefore, been conducted to determine correlations between cranial and post-cranial measurements. Having a clear link between cranial and post-cranial measurements will complement the identification process of individual in mixed remains cases. As previous research in the subject of whole body proportions in the field of physical anthropology is limited to determining stature from cephalometric measurements (Pelin *et al.*, 2010; Giurazza *et al.*, 2012; Agarwal *et al.*, 2014), the correlations between cranial and post-cranial elements will allow for further research in the field of anthropology by providing a renewed basis to work from.

Since no standards exist for fitting disarticulated skulls with bodies for South African population groups, the findings of this thesis can be used in identification of comingled cases from mass disasters. Distinct genetic differences between population groups in South Africa allow for comparison of morphological traits.

1.1 PROBLEM STATEMENT

In cases where skulls are disarticulated and not paired with their corresponding bodies it is difficult to fully assess the individual, since the skull and body hold different information from one another. Each part of the body can hold information, although not necessarily the same information. The face, for instance, is used predominantly to determine ancestral decent (Sauer, 1992), while the long bones are used to determine stature. When considering the natural proportions of *Homo sapiens* (Carroll, 1995) and how overall size differs among the large and small of stature, it is likely that correlative size variables are apparent with regards to the entire body, and by extension the cranial and post-cranial proportions. This observation is based on individuals with unaffected proportions and excludes individuals with dwarfism and gigantism.

1.2 AIMS

To assess the degree of correlation between cranium and some post-cranial aspects of the three dominant South African population groups, namely the South African Black (SAB), South African Coloured (SAC) and South African White (SAW) population groups.

The following three correlations are proposed:

1. Determine whether a correlation exists between cranial lengths that are determined by skull size and body size (through long-bone lengths)
2. Ascertain how accurately the size of the occipital condyles correlate with the size of the superior articular facets of the first cervical vertebra (C1).
3. Determine whether a direct metric relationship exists between the foramen magnum and vertebral foramina of the first or second (C2) cervical vertebrae.

1.3 OBJECTIVES

1. To determine through statistical evaluation whether a significant correlation between cranial and post-cranial measurements exist by:
 - a. Measuring lengths determined by cephalometric points on the skull.
 - b. Measuring post-cranial elements pertaining to the specificities of body size, specifically the lengths of the long bones found in the upper and lower limbs.
2. To measure and statistically compare the mirrored morphological aspects of the occipital condyles and superior articular facet of the C1 vertebra.
3. To statistically compare the foramen magnum with vertebral foramina measurements of the first and second cervical vertebrae.

CHAPTER 2: LITERATURE REVIEW

2.1 POPULATION DISTRIBUTION AND STUDY COHORT

The Western Cape has a unique population distribution within South Africa, as can be seen in the census data of 2011 (Statistics South Africa, 2012). This data shows within the Western Cape the highest density of SAC individuals at 48.8%, as well as the highest density for SAW individuals, at 15.7%. It has, however, the lowest distribution of SAB individuals at 32.9%, compared to the other provinces of South Africa. The remainder of the population in this Province is made up of Indian (SAI) or Asian individuals at 1.0%, and a class designated as “other” which makes up the remaining 1.6% (Statistics South Africa, 2012). The SAC individuals are, furthermore, found with a high distribution in the Northern Cape, forming 40.3% of the region’s population, while 15.6% of SAW individuals are also found in the Gauteng Province, although slightly lower than the percentage found in the Western Cape. The SAB individuals are found abundantly throughout South Africa and make up 79.2% of the population, with the exclusion of the Western Cape, as stated above, and Northern Cape, where they form 50.4% of the regional population.

The Kirsten Skeletal Collection (KSC) is housed within the FISAN building on Tygerberg campus, and managed by the Division of Clinical Anatomy. The collection is derived from cadavers used in the education and training of medical students (Labuschagne & Mathey, 2000; Alblas *et al.*, 2018). The collection currently consists of 1161 skeletonised individuals with known cadaver records (Alblas *et al.*, 2018) and include a few archaeological and some forensic cases (3.6%). The collection is predominantly made up of skeletonised male individuals at approximately 60% (Pfeiffer *et al.*, 2016; Alblas *et al.*, 2018). The SAC individuals make up approximately 60% of the KSC, with the SAB and SAW individuals making up approximately 16.5% and 12.2% of the population, respectively. The mean age of all individuals at death is 51 years-of-age (range 10–103 years-of-age), as noted by Pfeiffer *et al.* (2016) and Alblas *et al.* (2018). The majority of individuals (41.8%) died between the ages of 40 and 60 years-of-age (Alblas *et al.*, 2018).

The Raymond A. Dart Collection of Human Skeletons, held in the School of Anatomical Sciences at the University of Witwatersrand, comprises 2605 skeletonised individuals primarily derived from cadaver origin (Dayal *et al.*, 2009). The collection houses remains from individuals of 24 population groups indigenous to South Africa, with approximately 71% of individuals being male, 72% classified as SAB, and 18% as SAW, with considerably smaller proportions of other population groups, less than 1% in total (Dayal *et al.*, 2009). The age distribution of the collection, in general, is normally distributed, but becomes skewed when examining smaller population groups, such as the SAI or SAC groups, and population groups biased with regards to age, such as SAW individuals due to the limitations of receiving enough individuals or individuals from all age ranges

(Dayal *et al.*, 2009). Individuals are documented in a categorical age distribution with the youngest category at 0-10 years and the oldest 90+ years.

The UCT Human Skeletal Collection is based in the Department of Human Biology under the Division of Clinical Anatomy and Biological Anthropology, at the University of Cape Town, with the skeletal material originating from bodies donated to the university (UCT, 2018). The portion of the collection used for research purposes consists of 352 skeletons of cadaver origin (Dayal *et al.*, 2009; UCT, 2018). The majority of individuals within the collection are over the age of 50 years, with a mean of 64 years-of-age (Dayal *et al.*, 2009).

2.2 STANDARDISATION OF MEASUREMENTS AND THE IMPORTANCE OF POPULATION BASED RESEARCH

Each human is unique in bone structure, due to normal variation, and it is thus easy to establish unique physical characteristics, which allows each person to be identified individually. Only identical twins would cause great difficulty in being identified as separate individuals. Four major factors relating to bone variation include ontogeny, sexual dimorphism, geographic/population based, and idiosyncratic variation (White *et al.*, 2011).

The standardised methods for collecting skeletal measurements have been thoroughly described by Buikstra & Ubelaker (1994) and later by Langley *et al.* (2016) for both cephalometric and post-cranial measurements. Moore-Jansen *et al.* (1994) used the exact same landmarks and measurements to describe data collection in forensics, but was later updated by Langley *et al.* (2016). By keeping standardised measurements, all skeletal samples can be compared across the world. This can be most easily seen in the famous Howell's data set, which contains data from 1348 males and 1156 females, that originate from 28 specific populations and was compiled over a period of 15 years by W.W. Howells. The dataset was made available by him upon completion (Howells, 1996).

Although standardised landmarks and measurements help with the comparison between individuals, not all populations have the same degree of variability, and the conclusions made within one population group may not be applicable in another (İşcan & Steyn, 1986). İşcan & Steyn (1999) compiled specific osteometric standards for SAB and SAW population groups and concluded that previously used standards, based on North American population groups, were not representative of the South African populations. The population specificity in anthropology is most appropriately seen when comparing population standards or applying regression formulae, based on one population, across other populations not incorporated into the original analysis.

A large variety of unique body shapes are found in animals. The body shapes are largely thought to be influenced by the homeobox (Hox) cluster of genes in each animal, which are encoded for specific transcription factors (Carroll, 1995; Pearson *et al.*, 2005). Changes in the number of these Hox genes can cause changes in an animal body pattern (Carroll, 1955), which makes the Hox set of genes very specific for every animal species, including *Homo sapiens*. The Hox gene cluster suggest that an underlying pattern of growth and development within a species could possibly be observed.

2.3 CEPHALOMETRIC SIZE AND STABILITY WITH AGE

It is well documented (Moore *et al.*, 2009; White *et al.*, 2011) that the skull is made up of several bones defined as facial or cranial in nature. These bones are observed to grow along the edges to facilitate the growth of the skull. The skull is reported to cease its growth at the time of sexual maturity of an individual (Morris-Kay & Wilkie, 2005). The study of Bastir *et al.* (2006), which looked at 66 landmarks and semi-landmarks of the 28 individuals in the longitudinal Denver Growth Study, used two methods to determine when the head reached adult size by observing the growing features of the skull. They found that final adult size and morphology of the head ended with the face reaching maturity, which occurred at 15.7 years-of-age in both methods of estimation for males and females.

The work of Albert *et al.* (2007) reviewed and analysed the changes related to the skull caused by aging, after adulthood was reached. In their paper they concluded that there are changes seen in the skeletal and soft tissue, with regards to shape, size, and configuration with relation to age over the adult lifespan. These changes, include slight craniofacial bone growth, a slight increase in facial height, and mandibular length from the second to third decade of life. The third to fourth decades showed further mandibular length increases. During the fourth to fifth decades of life, craniofacial skeletal remodelling progresses, while the size of the dental arches for both mandible and maxilla decreases. Further remodelling continues in the fifth to sixth decades of life. From the sixth decade onward, a decrease in craniofacial size is noted, along with greater craniofacial convexity and temporomandibular joint flattening. It should be noted that not all reviewed studies of Albert *et al.* (2007) were longitudinal in nature and changes that were noted may be due to secular changes. The reviewed studies were, furthermore, not conducted on the same population groups, which might have affected the conclusions that were made (Pearson, 1899). The degrees of growth were noted to be a few millimetres, which diminish their importance on the current study.

2.4 VERTEBRAL OSTEOLOGY

The vertebral foramen is a large opening in each vertebra, bordered by the posterior aspect of the vertebral body anterior to it and the vertebral arch posterior, and together with other vertebral

foramina forms the vertebral canal, which houses the spinal cord, spinal roots, meninges, fat, and the associated blood vessels (Moore *et al.*, 2009). In the cervical vertebrae, the vertebral foramen is triangular in shape and quite large and wide in size in relation to the smaller vertebral body (White *et al.*, 2011), and houses the cervical enlargement of the spinal cord (Williams *et al.*, 1995). Both the atlas (C1) and axis (C2) vertebrae deviate from the typical shape of cervical vertebrae.

The atlas is located between the skull and the axis, and deviates from the typical cervical vertebrae in that it has no spinous process and no vertebral centrum or body (White *et al.*, 2011; Moore *et al.*, 2009). The atlas centrum has instead partially fused to the centrum of the axis, contributing to form the dens (odontoid process) of the axis (Williams *et al.*, 1995). An oval articular facet that receives the dens is located on the posterior aspect of the anterior arch of the atlas (Williams *et al.*, 1995; White *et al.*, 2011).

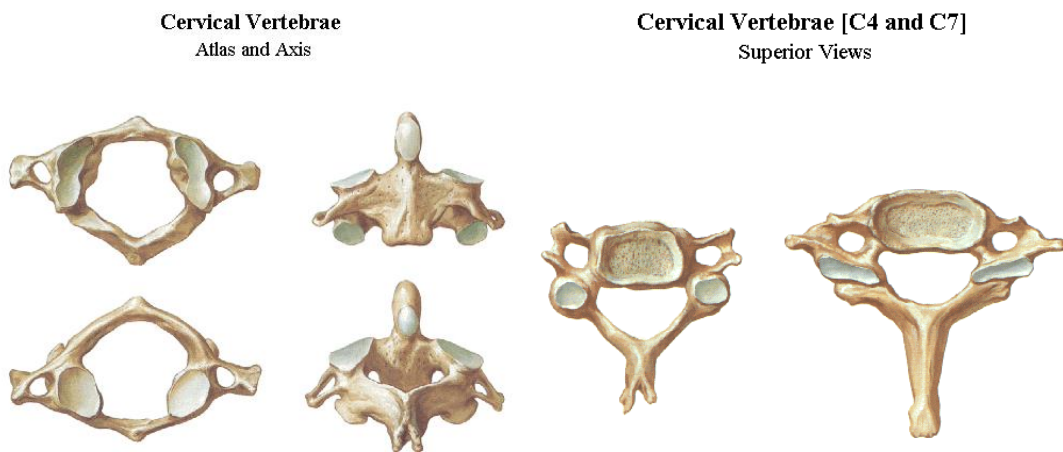


Figure 2.1: Illustrations of the differences seen in the cervical vertebrae. (Netter, 2010)

On the ovoid lateral masses of the atlas, the reniform superior articular facets (SAFs) are found, which articulate with the respective ipsilateral occipital condyles (Williams *et al.*, 1995; Moore *et al.*, 2009; White *et al.*, 2011). The transverse ligament divides the C1 vertebral foramen into two regions: a larger posterior section that houses the spinal cord and meninges, and an anterior section that houses the dens (Williams *et al.*, 1995, Moore *et al.*, 2009). The spinal cord, meninges and posterior longitudinal ligament continue through the vertebral foramen of C2 (Figure 2.2) (Williams *et al.*, 1995; Moore *et al.*, 2009).

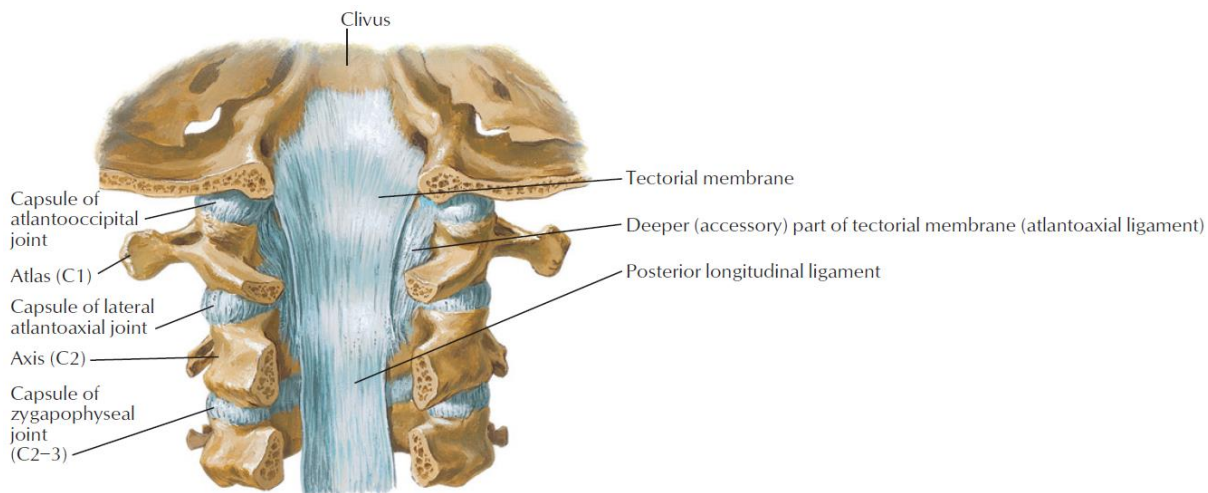


Figure 2.2: Posterior view of the internal ligaments of the upper part of the cervical spine (the spinous processes have been removed) (Netter, 2010).

The attachments for the transverse ligament are two tubercles on the medial aspects of the lateral masses, with the transverse ligament being slightly longer than the distance between the tubercles (Williams *et al.*, 1995). It has been noted that the C1 anterior arch, along with the transverse ligament, which helps to keep the dens in articulation with the anterior arch, represents a modified intervertebral disk into which the dens is received (Figure 2.3) (Jenkins, 1969; O’Rahilly *et al.*, 1983).

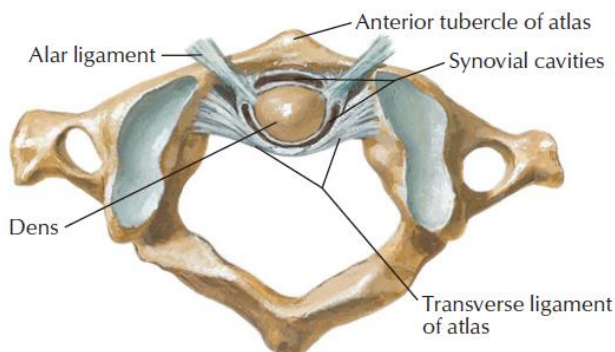


Figure 2.3: The articulation of the dens process of the second vertebra with the anterior arch of the first cervical vertebra. (Netter, F.H., 2010)

The atlanto-occipital joint connects the skull to the vertebral column and is made up of reciprocally curved articular surfaces (Williams *et al.*, 1995) found on the occipital condyles and the superior surface of the lateral masses of the atlas (Williams *et al.*, 1995, Moore *et al.*, 2009). The atlanto-occipital joint primarily facilitates the nodding or “yes” motion, while the atlanto-axial joint contributes to the side-to-side or “no” motion, where the atlas rotates around the dens (Moore *et al.*, 2009; White *et al.*, 2011).

2.5 FORAMEN MAGNUM OSTEOLOGY

The foramen magnum is the large foramen situated at the base of the skull in the occipital bone just posterior to the basilar part and between the occipital condyles (Williams *et al.*, 1995). Several structures traverse the foramen, including the spinal cord/medulla oblongata junction, the meninges, vertebral arteries, anterior and posterior spinal arteries, dural veins, and the spinal accessory nerve (Williams *et al.*, 1995; Moore *et al.*, 2009;). The apical ligament and the tectorial membrane also pass through the foramen (Williams *et al.*, 1995).

2.6 DEVELOPMENT AND GROWTH OF THE LONG BONES

The human skeleton has a distinct pattern of growth, with growth sites usually completing growth at different rates. This phenomenon has been extensively studied and reviewed in detail by the heavily cited Scheuer & Black (2000). As the aim of this study is not to review this phenomenon, the major points of complete fusion will be highlighted in the following paragraphs, as it pertains to this study.

The femur has five ossification centres, which complete fusion at different rates. The final fusion, indicated by the fusion of the distal epiphysis, occurs at 14-18 years-of-age for females and 16-20 years-of-age for males. The tibia has three ossification centres, of which the proximal epiphysis is the last to fuse; with females completing fusion at 13-17 years-of-age and males at 15-19 years-of-age. The fibula also has three ossification centres, with various fusion times of which the proximal epiphysis fuses last at 12-17 years-of-age for females, and 15-20 years-of-age for males (Scheuer & Black, 2000).

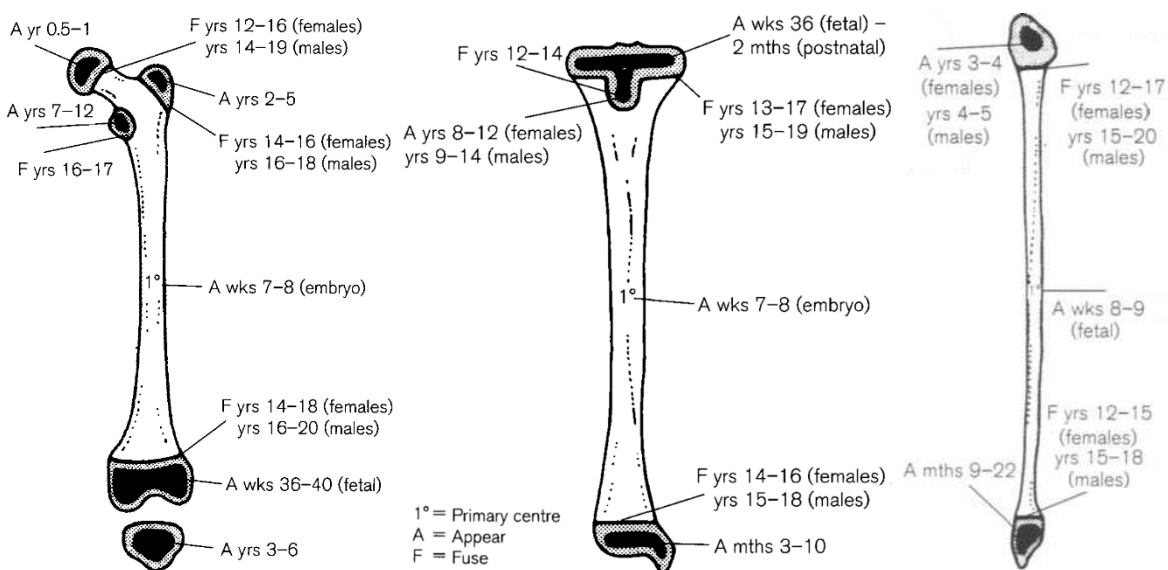


Figure 2.4: The growth centres of the lower limb long-bones and when the epiphyses fuse. (Scheuer & Black, 2000)

With regards to the upper limb, growth in the humerus is documented to originate from eight centres, with proximal centres fusing first, and the distal centres thereafter. Final bone length is achieved when the proximal epiphysis fuses at 13-17 years-of-age in females and 16-20 years-of-age in males. The radius originates from three centres forming two epiphyseal lines, with the distal epiphyseal line fusing last at 14-17 years-of-age in females, and 16-20 years-of-age in males. The ulna, similar to the radius, has of three fusion centres, with the final fusion occurring in the distal epiphysis at 15-17 years-of-age in females, and 17-20 years-of-age in males. The clavicle is unique in that it has two primary ossification centres, which fuse at seven weeks in utero, after which the bone then forms a medial and possible lateral epiphysis, of which the medial fusion occurs from 16-20 years-of-age, but may persist until 29 years-of-age.

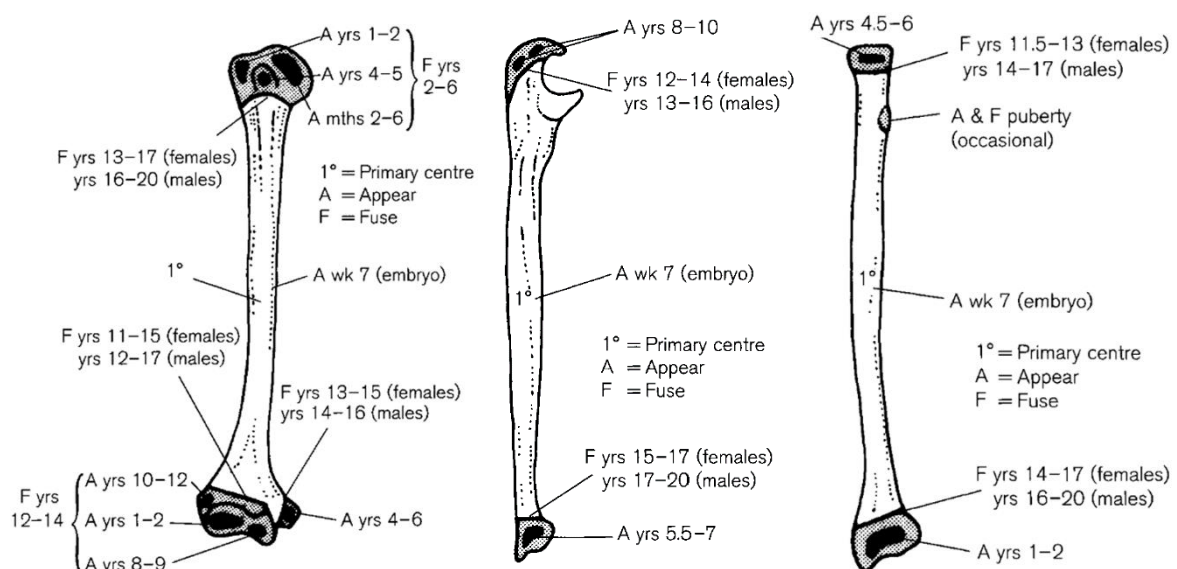


Figure 2.5: The growth centres of the upper limb long-bones and when the epiphyses fuse. (Scheuer & Black, 2000)

2.7 PREVIOUS RESEARCH ON CORRELATIONS OF CRANIAL AND POST-CRANIAL ELEMENTS

It is a well-known fact that the length of long bones hold a high correlation with stature (Telkkä, 1950; Trotter & Gleser 1958; Lundy, 1983; Lundy & Feldesman, 1987; Özaslan *et al.*, 2003). The lower limb contributes directly to stature and is the obvious choice when it comes to reconstruction of living stature from skeletal remains. The bones of the lower limb have also proved to have some of the highest correlations with stature (Özaslan *et al.*, 2003). It is, however, not always possible to use the bones of the lower limb, as they may be lost or damaged. Using other bones with equal, or close to equal, levels of correlation with stature, or contributes directly to stature, is the next logical choice. Such bones include the remaining long bones, the skull and some small bones, including the vertebrae and calcanei.

The conclusions that living stature can be estimated from long bones, indicate a definitive relation to the body in its totality. There is a possibility that long bone relations are not strictly restricted to stature alone, but to each other as well, since they can all accurately determine skeletal height (Radoinova *et al.*, 2002; Özaslan *et al.*, 2003; Dayal *et al.*, 2008). It has been noted by Özaslan *et al.* (2003) as well, that the lower limbs are more related to stature than the upper limbs, and explains the unsatisfactory results that Mall *et al.* (2001) found in their study on the upper limb. From the review work by Scheuer and Black (2000) it is apparent that a distinct pattern exists in skeletal fusion, although some overlap does exist, which might hint at why the long bones correlate well with stature. Multiple studies have been conducted on stature and long bones across various population groups, allowing for the formulation of regression formulas (Telkkä, 1950; Trotter & Gleaser 1958; Lundy, 1983; Lundy & Feldesman, 1987; Dayal *et al.*, 2008).

Apart from correlations within the group of long bones, correlations outside of the group may exist. The skull, along its vertical axis, contributes directly to the stature and may have correlations with the long bones in some of its aspects. Very limited literature exists on studies aiming to correlate craniofacial measurements with post-cranial measurements. One study by Pelin *et al.* (2010) correlated craniofacial measurements with stature in a living population, but with limited success. They found no significant correlations between the craniofacial measurements and stature. It should, however, be noted that their study design did not account for the high variability in the facial region previously reported by other authors (Relethford, 1994; İşcan & Steyn, 1999; Relethford, 2002).

CHAPTER 3: MATERIALS AND METHODS

3.1 MATERIALS

Complete skeletal specimens (N=300) were selected according to whether the bones to be measured were present and if the cephalometric components to be measured for the study, were intact. Skeletal samples were taken from the cadaver derived Stellenbosch University Kirsten Skeletal Collection (KSC), the University of the Witwatersrand Raymond A. Dart Collection (RAD), and University of Cape Town Human Skeletal Collection (HSC). The study was conducted on both sexes of the SAB, SAW and SAC population groups. The total sample aimed to include 100 individuals in each population group, with 50 males and 50 females each. The population sizes and the collections they were assessed at, are shown in Table 3.1. The measured skeletal components include the skull and mandible (Table 3.3); C1 and C2 vertebrae (Table 3.4 – 3.5); femur, tibia, fibula, humerus, radius, ulna and clavicle (Table 3.5).

Table 3.1: Distribution of samples in the Bone Collections.

		KSC	RAD	HSC	Total
SAB	♂	50	-	-	50
	♀	17	33	-	50
SAW	♂	32	-	18	50
	♀	8	36	6	50
SAC	♂	50	-	-	50
	♀	50	-	-	50

KSC = Stellenbosch University Kirsten Skeletal Collection, RAD = University of the Witwatersrand Raymond A. Dart Collection; HSC = University of Cape Town Human Skeletal Collection. ♂ = Male; ♀ = Female; SAB = South African Black; SAW = South African White; SAC = South African Coloured.

Individuals who did not show complete fusion of the medial ends of the clavulae, which is generally accepted as the last epiphysis of long bones to fuse at <30 years-of-age (White *et al.*, 2012), were excluded. Individuals over 70 years-of-age were excluded to limit the long-term effects of bone resorption with age. Individuals with damage in the areas of interest or pathology that altered measurement sizes were excluded as well. The left side was preferred over the right, where a single side was measured, as dictated by convention (Langley *et al.*, 2016), unless pathology or trauma was evident on the left side, in which case the right was assessed and measured.

Table 3.2: Sample numbers used in the current study after exclusions were finalised during data processing all three population groups.

	SAB	SAW	SAC	Total
Male	50	48	50	148
Female	50	49	49	148
Total	100	97	99	296

SAB=South African Black; SAW=South African White; SAC=South African Coloured.

The availability of skeletal specimens that fit the inclusion criteria did not allow for perfect numbers of individuals after outliers were excluded. Individuals included (Table 3.2) in the study were selected in sets, where the first set of individuals adhered to all stipulations of the inclusion criteria. The second set included individuals missing only one long bone with minimal overlapping of missing bones among individuals, which included the long bones and the mandible. Where samples did not have a full count of 100 individuals per population group, a third round of inclusions were made to include individuals with up to four bones missing. One round of outlier eliminations, by using box and whisker plots was conducted where two SAW males, one SAW female and one SAC female were removed from the sample, which brought the total of the study samples to 296 individuals with, as mentioned, a few bones missing for some individuals.

3.2 METHODS

Dedicated digital sliding and spreading callipers (Paleo-Tech Inc., USA), and a standard osteometric board were used to take measurements as described in the standards set by Buikstra & Ubelaker (1994), and corroborated by Langley *et al.* (2016).

3.2.1 Cephalometric measurements

Cephalometric measurements pertaining to skull size or size of the foramen magnum (FM) were selected for this correlation study. Definitions of the standard cephalometric landmarks (Table 3.2) and cephalometric measurements (Table 3.3) constructed from these points (Fig. 3.1; Fig. 3.2), are explained in the tables and images.

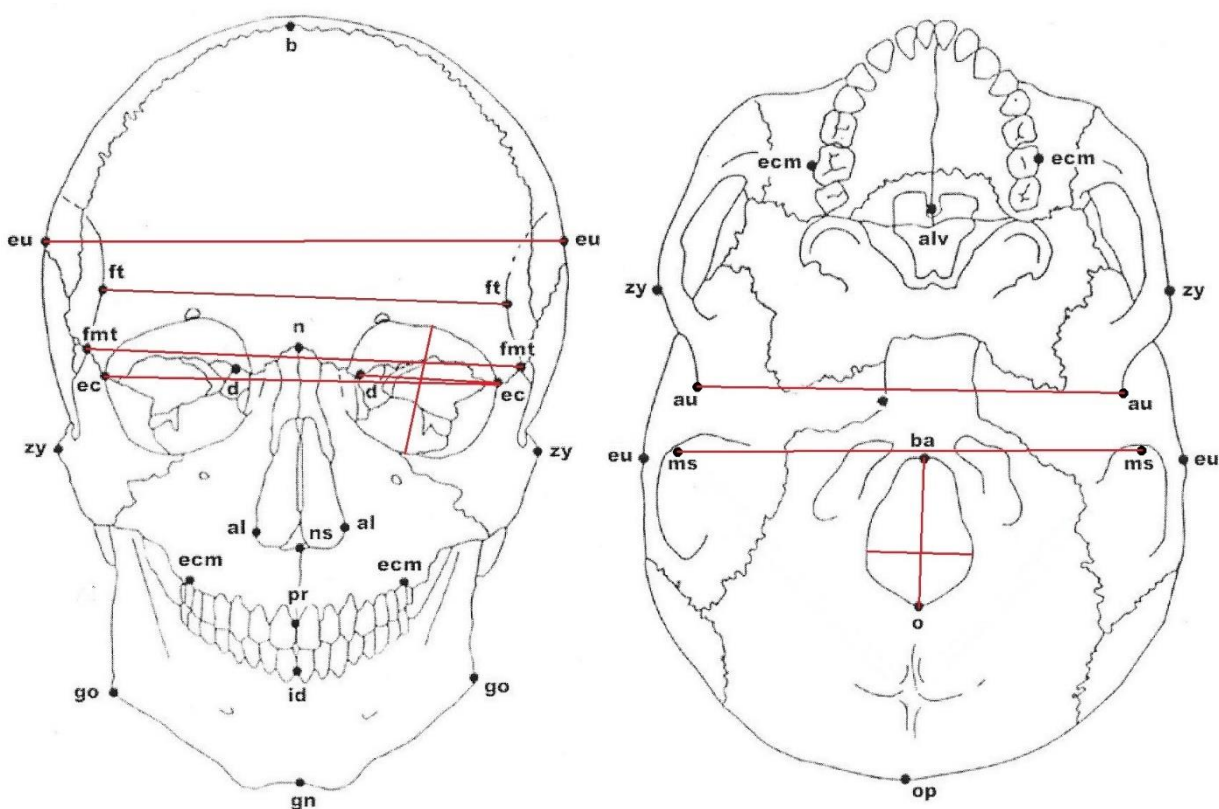


Figure 3.1: Diagrams showing standard cephalometric landmarks and measurements used in the study. Figures adapted from Moore-Jansen *et al.* 1994 in Buikstra & Ubelaker (1994).

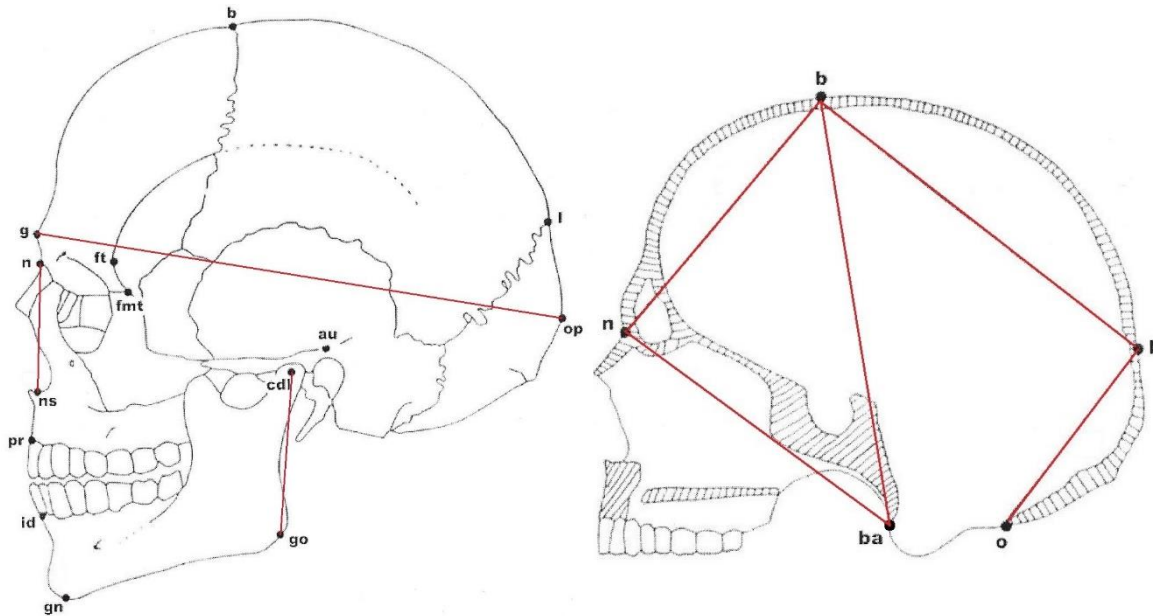


Figure 3.2: Indications of cephalometric measurements (Table 3.4). Figure adapted from Moore-Jansen *et al.* 1994 in Buikstra & Ubelaker (1994)

Table 3.3: Descriptions of cephalometric points as seen in Fig. 3.1 and Fig. 3.2 (Buikstra & Ubelaker, 1994; Langley *et al.*, 2016)

Name	Abbr.	Description
Bregma	b	The posterior border of the frontal bone in the mid-sagittal plane
Basion	ba	The point at which the anterior border of the foramen magnum is intersected by the mid-sagittal plane opposite nasion
Condylion	cdl	The most lateral points of the mandibular condyles
Dacryon	d	Dacryon is located on the frontal bone. When the lacrimomaxillary suture is easily found, the dacryon is the point on the frontal bone where the frontal, lacrimal and maxillary sutures meet
Ectoconchion	ec	The intersection of the most anterior edge of the lateral orbital border and a line parallel to the superior orbital border that bisects the orbit into two equal halves
Euryon	eu	The most laterally positioned point on the side of the braincase
Frontomolare temporale	fnt	The most laterally positioned point on the fronto-malar suture
Frontotemporale	ft	A point located generally forward and inward on the superior temporal line directly above the zygomatic process of the frontal bone
Glabella	g	The most anteriorly projecting point in the mid-sagittal plane at the lower margin of the frontal bone, which lies above the nasal root and between the superciliary arches
Gonion	go	The point on the mandible where the inferior margin of the mandibular corpus and the posterior margin of the ramus meet, i.e. the point on the mandibular angle which is directed most inferiorly, posteriorly, and laterally
Lambda	l	The apex of the occipital bone at its junction with the parietal bones, in the midline
Mastoidale	ms	The most inferior point on the tip of the mastoid process
Nasion	n	The point of intersection of the naso-frontal suture and the mid-sagittal plane

Nasospinale	ns	The point where a line drawn between the inferiormost points of the nasal (piriform) aperture crosses the midsagittal plane.
Opisthion	o	The point on the inner border of the posterior margin of the foramen magnum in the mid-sagittal plane.
Opisthocranion	op	The most distant point posteriorly from the glabella on the occipital bone, located in the mid-sagittal plane.
Radiculare	ra(au)	The point on the lateral aspect of the root of the zygomatic process at the deepest incurvature

Abbr. = Abbreviation

Table 3.4: Standard cephalometric measurements used in this study as described by Buikstra & Ubelaker (1994) and Langley *et al.* (2016).

Measurement	Abbr.	Instrument	Measurement Description
g-op	GOL	Spreading calliper	Maximum Cranial Length
g-op-g***	GOG*	Tape measure	Skull Circumference
eu-eu	XCB	Spreading calliper	Maximal Cranial Breadth
fmt-fmt	UFB*	Spreading calliper	Upper Facial Breadth
ft-ft	WFB	Spreading calliper	Minimum Frontal Breadth
ec-ec	EKB	Sliding calliper	Biorbital Breadth
d-ec	OBB	Sliding calliper	Orbital Breadth
Perpendicular to d-ec	OBH	Sliding calliper	Orbital Height
n-ns	NLH	Sliding calliper	Nasal Height
n-b	FRC	Sliding calliper	Frontal Cord
b-l	PAC	Sliding calliper	Parietal Cord
l-o	OCC	Sliding calliper	Occipital Cord
ba-b	BBH	Spreading calliper	Basion-Bregma Height
ba-n	BNL	Spreading calliper	Cranial Base Length
ra-ra	AUB	Sliding calliper	Biauricular Breadth
ms-ms	MM*	Sliding calliper	Inter-mastoid breadth
ba-o	FOL	Sliding calliper	FM Length
FM greatest lateral curvature	FOB	Sliding calliper	FM Breadth
Highest point of cdl-go**	MRH*	Sliding calliper	Maximum Ramus Height
Combined cords variable	CCV	-	Mean of FRC, PAC & OCC
Representative facial height	NLH.MRH	-	Summation of NLH & MRH

*Not standard abbreviations; **Cephalometric point 'go' adapted to the point of most posterior, inferior and eversion/inversion and cdl adapted to most superior point of the condyle; ***Measurement is taken around skull along the g-op line. FM= foramen magnum; Abbr. = abbreviation.

The non-standard combined cords variable (CCV) (Table 3.4) is the arithmetic mean of the three cranial cords listed as the frontal cord (FRC), parietal cord (PAC) and occipital cord (OCC), and was added as a variable after large variability within the three separate cranial cords was observed. The CCV is a novel approach used to even out the variability of the three cranial cords within themselves, but still using the total length of the three cords. The CCV measurement can, therefore, be used as a representative of the three cords while still allowing for the variation between individuals. The non-standard combined measurement NHL.MRH (Table 3.5) is the summation of

the nasal height (NLH) and mandibular ramus height (MRH) measurements and is used to represent total facial height, since the measured areas are stable and shows no significant changes with age or after tooth loss (Şakar *et al.*, 2008; Chole *et al.*, 2013; Ozturk *et al.*, 2013). It should be noted that differences exist between the sexes, with females presenting with more obtuse gonial angles in comparison with males (Şakar *et al.*, 2008; Chole *et al.*, 2013) and that the right side, compared to the left, is found to be significantly more obtuse in both sexes (Ozturk *et al.*, 2013). The measurements and cephalometric points set out in this study are not used in the measurement of the gonial angle. The sex differences seen in gonial angle should therefore only be used to show that the mandible displays traits with sexual dimorphism.

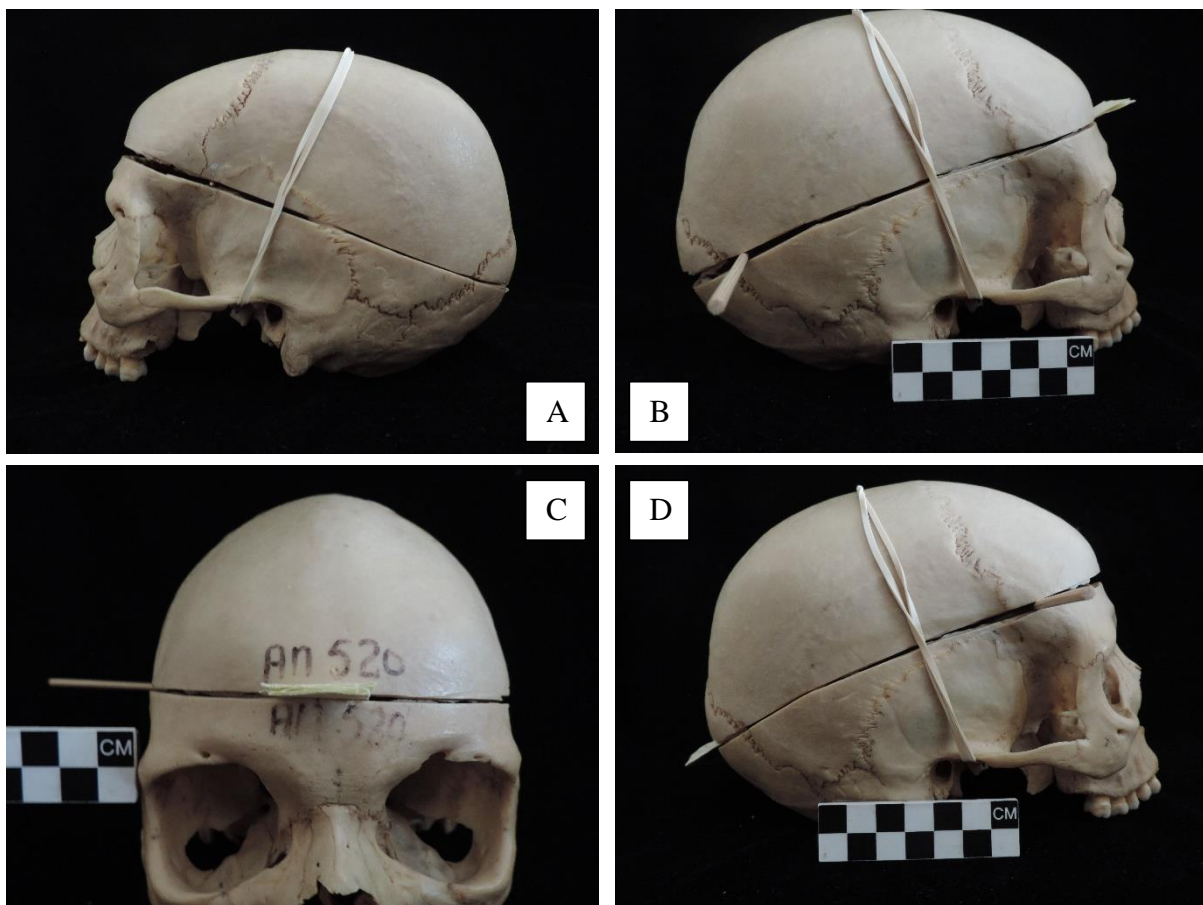


Figure 3.3: A- A lateral view of a skull illustrating the warped calvarium and the gap created by it. B- A lateral view of the cranium illustrating the anterior tilt method. C – The shim position as the anterior tilt is employed. D- A lateral view of the cranium illustrating the posterior tilt method.

A limitation to overcome during vault measurements derived from cadaver-dissection methods. The majority of skulls in all three collections have been sectioned horizontally through the cranium for removal of the brain during dissection, which is used to train medical students in neuroanatomy. The procedure involves removal of the scalp, followed by a circumferential cut around the cranial vault using an oscillating bone saw with a blade thickness of 1mm. This procedure removes bone at the thickness of the blade, which is 1mm, and to offset this loss of bone, shims with the appropriate

thickness were added into the gap created from the circular cut (Figure 3.3C). To ensure that the gap between the calvarium and remainder of the skull was the thickness of the removed bone, the skull and calvarium, with inserted shims of 1mm thickness, were fixed into position with rubber bands. The bands were placed across the radiculare (ra) and the vertex.

In some instances, the release of internal stress had distorted the skull or calvarium to cause a large gap between the calvarium and free border of the remainder of the skull in the plane of some measurements (Figure 3.3A). In most cases the calvarium or skull remainder warped so that the anterior and posterior borders did not make contact simultaneously, but instead a rocking motion was possible around a mid-point. In these cases the calvarium was tilted to close the gap until a shim was firmly pressed between the two borders over which the measurement occurred (Figure 3.3B). In these cases the shims would be periodically moved to fall directly across the measured plane. An anterior tilt was implemented when the frontal cord was measured (Figure 3.3B) and a posterior tilt when the occipital cord was measured (Figure 3.3D). The tilts were always performed over the central rocking point and had shims inserted at these points. These tilting methods have not been previously described in the literature; however, the method is standardised within the study and allows for a more accurate measurement compared to the tape-fixing technique, which leaves large gaps between the calvarium and skull in some cases. The tilted state, furthermore causes the calvarium to be in the same position relatively to the skull for every researcher.

3.2.2 Articular facets measurements of C0-C1

Measurements were taken of the occipital condyles (C0) and the superior articular facet (SAF) of C1 vertebra as seen in Table 3.4. Occipital condyle measurements were taken in accordance with the methods used by Naderi *et al.* (2005), while SAF measurements were taken as reflected measurements of the measurements taken of the occipital condyles and are displayed in Figure 3.4. The measurement descriptions and abbreviations are displayed in Table 3.5 and were determined with a digital sliding calliper.



Figure 3.4: An illustration of the measurements taken of the superior articular surface of the first cervical vertebra.

Table 3.5: Condylar measurements used from Naderi *et al.* (2005) and superior articular facet measurements as reflections of condylar measurements.

Measurement	Abbr.	Measurement Description
Condylar lengths (Left)	CdILL	Direct length between most anterior and post. tips
Condylar lengths (Right)	CdILR	Direct length between most anterior and post. tips
Condylar widths (Left)	CdiWL	Widest area perpendicular to length line
Condylar widths (Right)	CdiWR	Widest area perpendicular to length line
Ant. Inter-condylar distances	AICD	Distance between most superior tips
Post. Inter-condylar distances	PICD	Distance between most posterior tips
SAF length (Left)	SAFLL	Direct length between most anterior and posterior tips
SAF length (Right)	SAFLR	Direct length between most anterior and posterior tips
SAF Width (Left)	SAFWL	Widest area perpendicular to length line
SAF Width (Right)	SAFWR	Widest area perpendicular to length line
Ant. Inter-facet distance	AIFD	Distance between most superior tips
Post. Inter-facet distance	PIFD	Distance between most posterior tips

Abbr. = abbreviation, SAF=superior articular facet; ant=anterior; post=posterior

3.2.3 Neural foramina measurements

Additional measurements on the C1 and C2 vertebrae were taken (Table 3.6) which are reflected in Figure 3.5A & 3.5B, respectively. The vertebral foramina measurements were designed to reflect the standard measurements of the foramen magnum, as no standards are explicitly stated for the C1 and C2 vertebral foramen (Langley *et al.*, 2016) with the purpose of correlating the foramen magnum and cervical vertebrae. These measurements were determined with a digital sliding calliper.

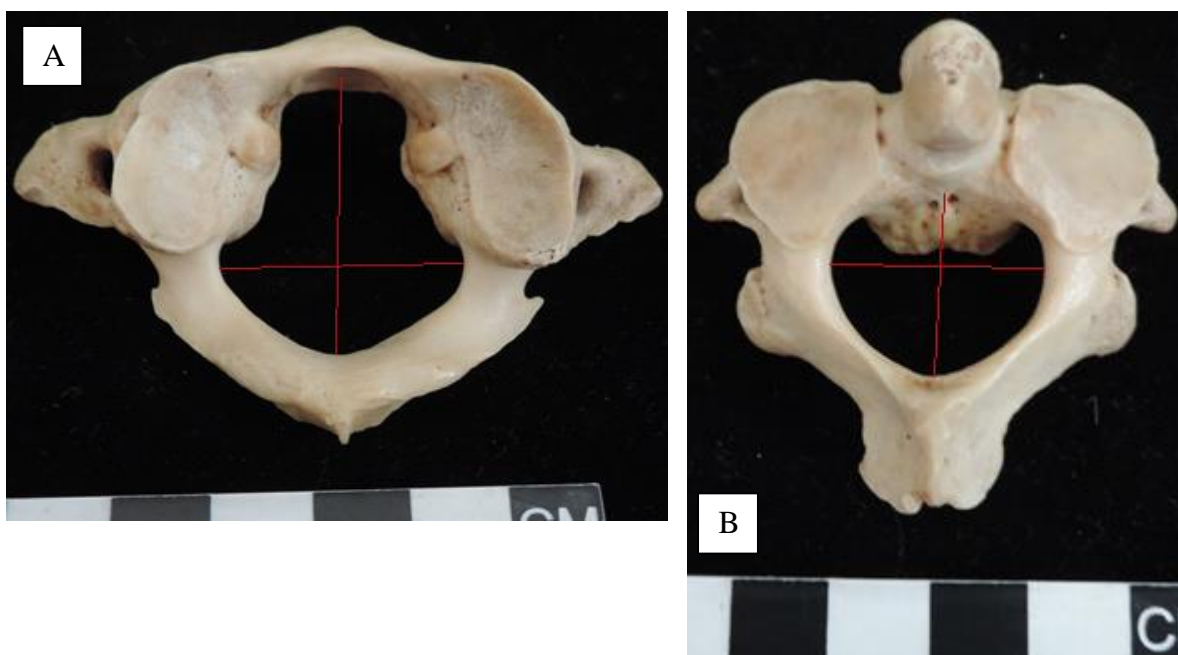


Figure 3.5: Illustrations of measurements listed in Table 3.6 of the neural foramen of the first and second vertebra

Table 3.6: Measurements of the first and second cervical vertebrae designed to reflect the standard measurements for the foramen magnum (Buikstra & Ubelaker, 1994).

Bone	Measurement	Abbr.	Measurement Description
C1	Vertebral foramen maximum length	C1VFML	Direct distance from the most anterior aspect of the vertebral foramen to the most posterior aspect (in the most superior plane).
	Vertebral foramen maximum breadth	C1VFMB	Direct distance between the most lateral ends within the vertebral canal.
C2	Vertebral foramen maximum length	C2VFML	Direct distance from the most anterior aspect of the vertebral foramen to the most posterior aspect (in the most superior plane).
	Vertebral foramen maximum breadth	C2VFMB	Direct distance between the most lateral ends within the vertebral canal.

Abbr. = Abbreviation; C1 = First cervical vertebra; C2 = Second cervical vertebra

3.2.4 Post-cranial measurements

Post-cranial measurements of long bones (Table 3.7) were all determined with a standard osteometric board. Within the study the long bones act as the “body” portion to assess whether a skull can be statistically matched to a body after disarticulation. These measurements were chosen based on the principal of normal proportion seen in organisms of the same species (Carroll, 1995; Pearson et al., 2005), with a human analogue as shown by Da Vinci’s Vitruvian man (c. 1490) being one of the first documented examples to be applied to humans.

Table 3.7: Long bone measurements for post-cranial assessment in accordance with the standards set by Buikstra & Ubelaker, (1994) and Langley *et al.* (2016).

Measurement	Abbr.	Measurement Description
Femur bicondylar length	FEMBLN	The distance from the femoral head to the condyles, with both condyles being in the same plane.
Femur maximum length	FEMXLN	The distance from the most superior tip of the femoral head to the most inf. tip of the condyles.
Tibia maximum length	TIBXLN	The distance from the lateral tibial plateau (associated with the lateral femoral condyle) to the tip of the medial malleolus.
Fibula maximum length	FIBXLN	The maximum distance from the most superior tip of the fibular head to the most inf. tip of the lateral malleolus.
Humerus maximum length	HUMXLN	Direct distance from most superior tip of humeral head to the most inf. end of the trochlea.
Radius maximum length	RADXLN	The distance from the most proximal part of the head to the most distal tip of the styloid process (disregarding the long axis)
Ulna maximum length	ULNXLN	The distance from the most proximal part of the olecranon to the most distal part of the styloid process.
Clavicle maximum length	CLAXLN	The distance between the sternal and acromial ends.

Abbr. = Abbreviation

Many organisms have characteristics showing distinct ratios and correlations within themselves as seen with the well-known Fibonacci spiral and Phi ratio (Fett, 2006). In addition to the longitudinal nature of the bones that are measured, the clavicle was chosen as a representation of shoulder breadth and was specifically, but not exclusively, included to be correlated with ms-ms and ra-ra, as they are measured on the same horizontal plane.

3.3 STATISTICS

As this is novel research, sample size was determined by the estimation of availability of skeletal samples in collections and that a sample size of ≥ 25 per tested population (David, 1938) allows for accurate Pearson's correlations to still exist as long as the data is normally distributed (Bonett & Wright, 2000). Only one round of outlier removal was conducted to preserve the sample as much as possible and limit bias.

All data entries were captured in Microsoft® Excel 2013 v15.0.5041.1000. For both the descriptive statistics and the correlative analysis, the statistical program IBM SPSS v23.0.0.0 was used to determine all statistics, which included the Pearson's Correlation Coefficient (PCC) for linear correlations, with a bootstrapped analysis of 1000 resamplings of the data sets. Principal component analyses (PCA) and t-tests was determined through the statistical program STATISTICA v13.2.92.1.

The 19 cephalometric measurements, and the two novel measurements, were correlatively tested against the eight long bone lengths, providing an output of 168 correlations. The six mirrored measurements of the articular facets of the atlanto-occipital joint had 36 correlative tests, by which the condylar measurements were correlated with those of C1. The focus of the articular correlations was placed on the matched mirrored traits, even if all combinations of correlations were conducted. The foramen magnum and C1-C2 foramen correlations yielded 30 correlations, where all measurements were correlated with each other. Only the strongest correlations that held strong significance ($p \leq 0.01$) found in each correlation set of population and sex were further assessed.

For simplicity, a PCA can be seen as a linear correlation of the variables with the factors, which allows for underlying trends to be found within data, where all factors are orthogonal to one another. Factor analyses were conducted on each set of males and females within each population group on the cephalometric measurements, articular facet measurements, neural foramina measurements, and post-cranial measurements. In addition, the population groups were combined into a single data set, which had undergone PCAs exactly as conducted on the individual populations groups. For the cephalometric component three factors were examined. The articular facet portion had three factors examined as well, but because two different bones, C1 and C2, were measured, each was assessed individually, after which the two bones were assessed together. The six neural foramina measurements for each bone were too few to be assessed in isolation and all 12 measurements had to be assessed together, of which two factors were examined. The post-cranial portion consisted of the long bones and allowed only two factors to be assessed. Finally, all measurements were assessed in a combined group, which contained all measurements to corroborate the correlations seen between and among the cephalometric measurements, articular

facet measurements, neural foramina measurements, and post-cranial measurements. During the assessment a varimax normalised rotation of the factors was conducted. This technique is used to create maximum variance in the loading by dividing the factors with the square root of the variable's communalities. Communalities are a representative of the variance seen for each variable as expressed by the factors. It is defined as the sum of the squared factor loadings. By implementing the rotation, it allows for good contrast to form between the factors and highlights which factor the variable is best associated with. The variables were sorted according to the factors they correlated best with and the cut off was determined by the lowest correlation that ensured the variable was not shared by two factors.

Inter-observer agreement was assessed by having a postgraduate student in anthropology measure 10 samples. By using the reliability function in IBM SPSS v23.0.0.0 the inter-observer agreement was established for every measurement. The results can be seen in Table 3.8 were the numbers in bold are reliable measurements. It should be noted that when inspecting the data, especially for the cephalometric measurements, a large number of measurements differ extremely from the mean and are likely errors in inputting the data, which influences the data to produce type one errors.

Table 3.8: Inter-observer reliability for all measurements.

Measurements	Intraclass Correlation	95% CI	
		Lower	Upper
GOL	0.338	-2.370	0.844
GOG	0.971	0.794	0.994
XCB	-0.030	-0.580	0.572
UFB	0.847	-0.080	0.968
WFB	0.093	-0.430	0.633
EKB	0.440	-0.600	0.846
OBB	0.033	-2.670	0.756
OBH	0.997	0.988	0.999
NLH	0.978	0.913	0.995
FRC	-0.460	-5.220	0.642
PAC	0.012	-4.790	0.772
OCC	0.492	-1.460	0.879
BBH	0.074	-0.470	0.627
BNL	0.105	-0.100	0.497
AUB	0.898	0.585	0.975
MM	0.958	-0.020	0.993
FOL	0.953	0.785	0.989
FOB	0.947	0.578	0.989
MRH	0.853	0.391	0.964
CdILL	0.977	0.908	0.994
CdILR	0.896	0.601	0.974
CdIWL	0.445	-0.326	0.836
CdIWR	0.688	-0.259	0.928

AICD	0.535	-0.360	0.873
PICD	0.724	-0.060	0.931
SAFLL	0.782	0.107	0.946
SAFLR	0.769	0.014	0.943
SAFWL	0.108	-0.736	0.698
SAFWR	0.124	-2.480	0.782
AIFD	0.975	0.899	0.994
PIFD	0.950	0.805	0.988
C1VFML	0.986	0.946	0.996
C1VFMB	0.952	0.791	0.988
C2VFML	0.879	0.190	0.974
C2VFMB	0.986	0.937	0.997
FEMBLN	0.997	0.477	1.000
FEMXLN	0.997	0.705	1.000
TIBXLN	0.966	0.868	0.992
FIBXLN	0.996	0.982	0.999
HUMXLN	0.984	0.933	0.996
RADXLN	0.999	0.945	1.000
ULNXLN	0.998	0.992	0.999
CLAXLN	0.976	0.885	0.994

CI = Confidence Interval; GOL = Maximum Cranial Length; GOG = Skull Circumference; XCB = Maximal Cranial Breadth; UFB = Upper Facial Breadth; WFB = Minimum Frontal Breadth; EKB = Biorbital Breadth; OBB = Orbital Breadth; OBH = Orbital Height; NLH = Nasal Height; FRC = Frontal Cord; PAC = Parietal Cord; OCC = Occipital Cord; BBH = Basion-Bregma Height; BNL = Cranial Base Length; AUB = Biauricular Breadth; MM = Inter-mastoid breadth; FOL = FM Length; FOB = FM Breadth; MRH = Maximum Ramus Height; CCV = Mean of FRC, PAC & OCC; NLH.MRH = Summation of NLH & MRH; CdlLL = Condylar lengths (Left); CdlLR = Condylar lengths (Right); CdlWL = Condylar widths (Left); CdlWR = Condylar widths (Right); AICD = Ant. Inter-condylar distances; PICD = Post. Inter-condylar distances; SAFLL = SAF length (Left); SAFLR = SAF length (Right); SAFWL = SAF Width (Left); SAFWR = SAF Width (Right); AIFD = Ant. Inter-facet distance; PIFD = Post. Inter-facet distance; C1VFML = Vertebral foramen maximum length of first cervical vertebra; C1VFMB = Vertebral foramen maximum breadth of first cervical vertebra; C2VFML = Vertebral foramen maximum length of second cervical vertebra; C2VFMB = Vertebral foramen maximum breadth of second cervical vertebra; FEMBLN = Femur bicondylar length; FEMXLN = Femur maximum length; TIBXLN = Tibia maximum length; FIBXLN = Fibula maximum length; HUMXLN = Humerus maximum length; RADXLN = Radius maximum length; ULNXLN = Ulna maximum length; CLAXLN = Clavicle maximum length. **Bold:** values in bold indicate measurements which are reliably measured.

3.4 LIMITATIONS

1. The research conducted in the field of physical anthropology is always demographic specific. Conclusions determined in one population group should be applied with caution to other unrelated populations due to this specificity of demographics (Pearson, 1899).
2. Measurements were conducted on dry bone samples. This makes it incomparable with anthropometric measurements on living individuals with intact soft tissue; an exception occurs for research based on precise scanning methods such as Magnetic resonance imaging and Computed tomography scans.
3. Individuals who have died more recently were preferred, for the study, to keep the data as applicable as possible to the current living population.

4. With sectioning of the skulls, for brain removal, some deformation occurs in the form of bone loss along the cut as well as releases of internal stress, within the skull, causing the calvarium or remaining skull to warp.
5. Wormian bones forming within the lambda cephalometric point may cause an inaccurate reading.
6. Inter-observer reliability test was conducted solely on the skeletal samples from the KSC and no samples were testes for reliability for the other university collections.

3.5 ASSUMPTIONS

1. The records kept for date of birth are accurate.
2. Date of death is accurate.
3. Ancestral descent is accurate.
4. Measured bones of an individual belong together, as indicated by records of collections, with no comingling of remains having occurred prior to their measurement in this study.

3.6 ETHICAL CONSIDERATION

The Human Tissues Act (No 65 of 1983) and the National Health Act (No 61 of 2003) governs and oversees research on human skeletal remains in collections. Within the limits of these two laws the Inspector of Anatomy can invoke consent by proxy for paupers donated by the state. Individuals who donate their bodies for scientific research before death have given their own consent. The individuals used within this study adhere to the stipulations of the Helsinki declaration concerning informed consent in both cases as stated within the laws of South Africa.

Ethical clearance was granted by the Human Research Ethical Committee of Stellenbosch, with the Ethics # S13/05/100. Permission to take measurements from the Raymond A. Dart and UCT Bone Collection were obtained by petitioning the collection managers and submitting a synopsis of the study outlining procedures and samples and subsequent signing of collections documents on site.

CHAPTER 4: RESULTS

4.1 DESCRIPTIVE STATISTICS

In Tables 4.1-4.4 the results for the t-tests can be seen, while in Table 4.5-4.16, various descriptive statistics for each measurement of each population group is listed. These descriptive statistics include the minimum (Min), maximum (Max), Range, Mean, standard deviation (SD), skewness, coefficient of variation (CV) and standard error of the mean (SEM). For all data sets a normal distribution (skewness $< |2|$) was determined for all measurements taken (Table 4.1 - 4.12), allowing for parametric testing to be conducted. In addition to the descriptive statistics the t-test results of each section for differences between males and females of each population group and a holistic group is described. A t-test is used to determine whether two data sets are statistically different from one another by assessing the means and variance.

The CV works best with data that is on the ratio scale and is an expression of variability, constructed as a ratio between the standard deviation and mean, allowing for accurate comparisons of variability with reference to variables that have large differences in means. By using the CV of each measurement, a variability from the SD relative to the mean of each measurement is ascertained; generating a dimensionless number always in reference to the mean of the measurement. The CV is useful in this study to compare the variations within the males and females of each population group, as well as indicate which variables have the highest and lowest levels of variability, which helps to explain correlation strengths.

4.1.1 Cephalometric measurements

The t-test showed that the orbital height (OBH) between males and females for the SAB sample ($p=0.13$) and SAW sample ($p=0.86$) did not have a statistical difference between males and females (Table 4.1). However, the SAC sample showed no statistical difference for two traits, namely the OBH ($p=0.61$) and occipital cord (OCC) ($p=0.39$) measurement (Table 4.1). When all the data is pooled as one set, the t-test reveal no significant difference between males and females for only one trait, namely the OBH ($p=0.51$) measurement (Table 4.1).

The descriptive measurements for the 19 standard cephalometric and two novel (CCV and NLH.MRH) measurements for the three population groups, which will later be statistically compared with the long bone measurements, can be seen in Tables 4.5-4.7. The CV column indicates which measurements have the most variability within the sample groups and assist in determining the viability of the two novel measurements in comparison with the established measurements. As seen in the skewness column, for each of the tables, the measurements falls well within the prescribed range of $|2|$ to allow for parametric testing.

Table 4.1: Results of the t-test for the cephalometric measurements of the three population groups and the combined study population.

Variable	SAB			SAW			SAC			Combined		
	t-value	df	p	t-value	df	p	t-value	df	p	t-value	df	p
GOL	7.59	98	0.00	8.38	95	0.00	7.49	97	0.00	13.30	294	0.00
GOG	8.01	98	0.00	8.83	95	0.00	8.37	97	0.00	14.19	294	0.00
XCB	4.79	98	0.00	4.34	95	0.00	3.87	97	0.00	6.69	294	0.00
UFB	5.31	98	0.00	7.32	95	0.00	6.16	97	0.00	9.81	294	0.00
WFB	3.26	98	0.00	3.24	95	0.00	3.74	97	0.00	5.80	294	0.00
EKB	4.99	98	0.00	7.40	95	0.00	7.56	97	0.00	10.34	294	0.00
OBB	6.14	98	0.00	5.34	95	0.00	3.99	97	0.00	8.35	294	0.00
OBH	1.54	98	0.13	0.18	95	0.86	-0.51	97	0.61	0.65	294	0.51
NLH	6.65	98	0.00	7.88	95	0.00	5.75	97	0.00	10.18	294	0.00
FRC	3.24	98	0.00	5.83	94	0.00	6.92	97	0.00	9.10	293	0.00
PAC	4.34	98	0.00	2.92	95	0.00	5.32	97	0.00	7.22	294	0.00
OCC	2.05	98	0.04	2.91	95	0.00	0.86	96	0.39	3.10	293	0.00
BBH	5.19	98	0.00	8.38	94	0.00	5.38	97	0.00	9.98	293	0.00
BNL	6.70	98	0.00	11.05	95	0.00	6.51	97	0.00	13.22	294	0.00
AUB	7.16	98	0.00	7.28	95	0.00	6.92	97	0.00	11.07	294	0.00
MM	5.50	98	0.00	8.24	95	0.00	5.22	97	0.00	10.51	294	0.00
FOL	3.71	98	0.00	2.63	95	0.01	4.56	97	0.00	6.27	294	0.00
FOB	4.54	98	0.00	2.68	94	0.01	4.32	96	0.00	5.94	292	0.00
MRH	8.96	97	0.00	9.10	92	0.00	9.45	97	0.00	14.88	290	0.00
Cords	5.06	98	0.00	6.07	95	0.00	6.06	97	0.00	9.62	294	0.00
NLH.MRH	10.15	97	0.00	11.18	92	0.00	9.39	97	0.00	15.47	290	0.00

SAB = South African black; SAW = South African white; SAC = South African coloured; df = degrees of freedom; p = probability value; GOL = Maximum Cranial Length; GOG = Skull Circumference; XCB = Maximal Cranial Breadth; UFB = Upper Facial Breadth; WFB = Minimum Frontal Breadth; EKB = Biorbital Breadth; OBB = Orbital Breadth; OBH = Orbital Height; NLH = Nasal Height; FRC = Frontal Cord; PAC = Parietal Cord; OCC = Occipital Cord; BBH = Basion-Bregma Height; BNL = Cranial Base Length; AUB = Biauricular Breadth; MM = Inter-mastoid breadth; FOL = FM Length; FOB = FM Breadth; MRH = Maximum Ramus Height; CCV = Mean of FRC, PAC & OCC; NLH.MRH = Summation of NLH & MRH. **Bold** font indicates insignificant p-values.

4.1.2 Articular facets measurements of C0-C1

When considering the measurements of the articular facets of C0 and C1, where sexes were compared within population groups, the t-test for the SAB sample showed that 8/12 measurements showed no difference between males and females. The other 4/12 measurements (CdLLR, SAFLL, SAFLR and PIFD) showed a difference between the sexes (Table 4.2). On the other hand, when comparing sex to the SAW sample group, all the measurements showed a significant difference between the sexes, except for AICD (p=0.121) (Fig. 4.2). The SAC sample showed some similarities with the SAB sample group in regards to the measurements that showed no sex difference, these measurements included SAFWL, SAFWR, and AIFD measurements (Fig. 4.2). The pooled data, which comprise all three population groups, showed that all measurements differed significantly between males and females.

The 12 mirrored morphological measurements of the occipital condyles and superior articular facet (SAF) of C1 were attained and assessed through descriptive statistics showed in Table 4.8-4.10. The six measurements of the occipital bone and the C1 vertebra had a counterpart on the other bone, making them mirrored. These 12 mirrored measurements will later be cross examined by assessing their correlations with one another. The CV column was once again included and indicated large values in the column, showing the distinct variability of each individual within the sample. These large variables can possibly indicate that the articular facet measurements are unique enough in individuals from the population to allow them to be used as individualising characteristics. The variables proved to stay within the prescribed values for skewness at a value of |2|.

Table 4.2: Results of the t-test for the articular facet measurements of C0-C1 of the three population groups and the combined study population.

Variable	SAB			SAW			SAC			Combined		
	t-value	df	p	t-value	df	p	t-value	df	p	t-value	df	p
CdILL	1.95	98	0.05	5.59	95	0.00	4.12	97	0.00	6.15	294	0.00
CdILR	2.55	98	0.01	4.87	95	0.00	2.77	97	0.01	5.50	294	0.00
CdIWL	0.91	98	0.37	4.19	95	0.00	2.50	97	0.01	4.10	294	0.00
CdIWR	0.71	98	0.48	4.14	95	0.00	4.17	97	0.00	4.87	294	0.00
AICD	0.27	98	0.78	1.56	95	0.12	2.25	97	0.03	2.27	294	0.02
PICD	1.92	98	0.06	2.03	95	0.05	5.29	97	0.00	4.96	294	0.00
SAFLL	2.18	98	0.03	5.01	95	0.00	4.71	97	0.00	6.39	294	0.00
SAFLR	2.69	98	0.01	5.44	95	0.00	4.65	97	0.00	6.91	294	0.00
SAFWL	-0.71	98	0.48	4.24	95	0.00	1.61	96	0.11	2.39	293	0.02
SAFWR	-0.17	98	0.86	3.89	94	0.00	0.94	96	0.35	2.29	292	0.02
AIFD	1.79	98	0.08	2.67	95	0.01	0.78	97	0.44	2.93	294	0.00
PIFD	3.84	98	0.00	4.66	95	0.00	5.08	95	0.00	7.17	292	0.00

SAB = South African black; SAW = South African white; SAC = South African coloured; df = degrees of freedom; p = probability value; CdILL = Condylar lengths (Left); CdILR = Condylar lengths (Right); CdIWL = Condylar widths (Left); CdIWR = Condylar widths (Right); AICD = Ant. Inter-condylar distances; PICD = Post. Inter-condylar distances; SAFLL = SAF length (Left); SAFLR = SAF length (Right); SAFWL = SAF Width (Left); SAFWR = SAF Width (Right); AIFD = Ant. Inter-facet distance; PIFD = Post. Inter-facet distance. **Bold** font indicates insignificant p-values.

Table 4.3: Results of the t-test for the neural foramina measurements of C1 and C2 the three population groups and the combined study population.

Variable	SAB			SAW			SAC			Combined		
	t-value	df	p	t-value	df	p	t-value	df	p	t-value	df	p
C1VFML	6.29	98	0.00	4.00	95	0.00	5.61	97	0.00	8.33	294	0.00
C1VFMB	3.38	98	0.00	2.09	91	0.04	3.69	97	0.00	4.89	290	0.00
C2VFML	2.48	97	0.02	2.35	95	0.02	3.10	97	0.00	4.20	293	0.00
C2VFMB	4.07	98	0.00	2.64	94	0.01	4.77	97	0.00	5.81	293	0.00

SAB = South African black; SAW = South African white; SAC = South African coloured; df = degrees of freedom; p = probability value; C1VFML = Vertebral foramen maximum length of first cervical vertebra; C1VFMB = Vertebral foramen maximum breadth of first cervical vertebra; C2VFML = Vertebral foramen maximum length of second cervical vertebra; C2VFMB = Vertebral foramen maximum breadth of second cervical vertebra.

Table 4.4: Results of the t-test for the long bone measurements of the three population groups and the combined study population.

Variable	SAB			SAW			SAC			Combined		
	t-value	df	p	t-value	df	p	t-value	df	p	t-value	df	p
FEMBLN	7.82	98	0.00	8.55	91	0.00	8.12	97	0.00	13.45	290	0.00
FEMXLN	8.01	98	0.00	8.29	91	0.00	7.80	97	0.00	13.22	290	0.00
TIBXLN	6.70	97	0.00	9.25	91	0.00	7.89	97	0.00	13.39	289	0.00
FIBXLN	7.26	97	0.00	9.55	91	0.00	8.08	97	0.00	13.94	289	0.00
HUMXLN	7.46	98	0.00	9.94	94	0.00	9.90	97	0.00	14.66	293	0.00
RADXLN	8.09	98	0.00	12.50	93	0.00	10.00	97	0.00	16.69	292	0.00
ULNXLN	7.66	98	0.00	11.66	94	0.00	10.16	97	0.00	16.21	293	0.00
CLAXLN	7.36	96	0.00	10.54	88	0.00	9.26	96	0.00	15.32	284	0.00

SAB = South African black; SAW = South African white; SAC = South African coloured; df = degrees of freedom; p = probability value; FEMBLN = Femur bicondylar length; FEMXLN = Femur maximum length; TIBXLN = Tibia maximum length; FIBXLN = Fibula maximum length; HUMXLN = Humerus maximum length; RADXLN = Radius maximum length; ULNXLN = Ulna maximum length; CLAXLN = Clavicle maximum length.

Table 4.5: Descriptive statistics for cephalometric variables of SAB sample.

	N		Min		Max		Range		Mean		SD		CV		SEM		Skewness	
	♂	♀	♂	♀	♂	♀	♂	♀	♂	♀	♂	♀	♂	♀	♂	♀	♂	♀
GOL	50	50	174.00	170.00	204.00	191.00	30.00	21.00	188.50	179.64	6.29	5.35	3.34	<u>2.98</u>	0.89	0.76	<u>0.00</u>	0.20
GOG	50	50	492.00	481.00	560.00	530.00	68.00	49.00	526.34	504.50	14.64	12.55	2.78	2.49	2.07	1.77	-0.16	0.21
XCB	50	50	124.00	120.00	145.00	143.00	21.00	23.00	135.76	131.00	4.99	4.95	3.67	3.78	0.71	0.70	-0.47	0.09
UFB	50	50	102.00	96.00	118.00	114.00	16.00	18.00	108.86	104.60	4.05	3.96	3.72	3.79	0.57	0.56	0.31	0.05
WFB	50	50	87.00	83.00	111.00	109.00	24.00	26.00	98.22	94.74	5.08	5.60	5.17	5.91	0.72	0.79	0.16	0.28
EKB	50	50	90.94	88.29	110.72	102.70	19.78	14.41	99.36	95.80	3.83	3.28	3.86	3.43	0.54	0.46	0.40	-0.12
OBB	50	50	36.04	34.48	43.94	41.82	7.90	7.34	40.30	38.23	1.64	1.73	4.06	4.52	0.23	0.24	-0.02	-0.17
OBH	50	50	28.55	29.09	43.58	38.52	15.03	9.43	34.33	33.61	2.60	2.06	7.57	6.14	0.37	0.29	0.50	<u>0.04</u>
NLH	50	50	44.48	41.85	57.84	55.24	13.36	13.39	50.82	46.99	3.22	2.50	6.33	5.33	0.46	0.35	-0.05	0.45
FRC	50	50	103.48	101.15	126.19	124.99	22.71	23.84	113.51	110.12	5.54	4.94	4.88	4.49	0.78	0.70	0.34	0.53
PAC	50	50	98.30	95.84	126.23	126.26	27.93	30.42	117.07	111.99	5.67	6.02	4.84	5.38	0.80	0.85	-0.81	-0.26
OCC	50	50	86.57	83.79	110.68	115.29	24.11	31.50	97.90	95.63	5.04	6.02	5.15	6.29	0.71	0.85	-0.11	0.99
BBH	50	50	119.00	115.00	145.00	141.00	26.00	26.00	133.92	127.98	5.67	5.77	4.23	4.51	0.80	0.82	-0.29	-0.06
BNL	50	50	91.00	84.00	112.00	106.00	21.00	22.00	102.62	96.22	4.87	4.68	4.75	4.86	0.69	0.66	-0.20	-0.38
AUB	50	50	109.00	104.86	130.18	121.18	21.18	16.32	119.19	113.19	4.66	3.66	3.91	3.23	0.66	0.52	-0.08	-0.05
MM	50	50	92.43	89.08	111.47	106.26	19.04	17.18	102.92	98.09	4.60	4.18	4.47	4.26	0.65	0.59	-0.38	0.08
FOL	50	50	32.46	30.17	42.99	39.76	10.53	9.59	37.19	35.56	2.42	1.96	6.52	5.52	0.34	0.28	0.07	-0.47
FOB	50	50	24.92	24.01	34.72	32.03	9.80	8.02	29.89	28.13	1.96	1.92	6.54	6.82	0.28	0.27	-0.02	-0.14
MRH	50	49	52.97	43.05	75.11	62.15	22.14	19.10	60.96	53.05	4.28	4.50	7.02	8.49	0.61	0.64	0.41	0.11
CCV	50	50	102.18	98.72	117.04	114.43	14.86	15.71	109.49	105.91	3.62	3.45	<u>3.31</u>	3.26	0.51	0.49	-0.34	-0.09
NLH.MRH	50	49	101.78	88.26	130.66	116.11	28.88	27.85	111.79	100.00	5.95	5.60	5.32	5.60	0.84	0.80	0.52	0.56

SAB = South African black; N = sample; Min = minimum; Max = maximum; SD = standard deviation; CV = coefficient of variation; SEM = standard error of mean; GOL = Maximum Cranial Length; GOG = Skull Circumference; XCB = Maximal Cranial Breadth; UFB = Upper Facial Breadth; WFB = Minimum Frontal Breadth; EKB = Biorbital Breadth; OBB = Orbital Breadth; OBH = Orbital Height; NLH = Nasal Height; FRC = Frontal Cord; PAC = Parietal Cord; OCC = Occipital Cord; BBH = Basion-Bregma Height; BNL = Cranial Base Length; AUB = Biauricular Breadth; MM = Inter-mastoid breadth; FOL = FM Length; FOB = FM Breadth; MRH = Maximum Ramus Height; CCV = Mean of FRC, PAC & OCC; NLH.MRH = Summation of NLH & MRH. **Bold** font indicates the highest value and underlined the lowest value for the column.

Table 4.6: Descriptive statistics for cephalometric variables of SAW sample.

	N		Min		Max		Range		Mean		SD		CV		SEM		Skewness	
	♂	♀	♂	♀	♂	♀	♂	♀	♂	♀	♂	♀	♂	♀	♂	♀	♂	♀
GOL	48	49	171.00	167.00	204.00	189.00	33.00	22.00	187.88	177.67	6.68	5.24	3.56	2.95	0.96	0.75	0.20	0.13
GOG	48	49	503.00	487.00	563.00	530.00	60.00	43.00	528.98	505.96	14.21	11.33	<u>2.69</u>	<u>2.24</u>	2.05	1.62	0.22	0.25
XCB	48	49	131.00	128.00	151.00	149.00	20.00	21.00	140.90	136.84	4.66	4.56	3.31	3.33	0.67	0.65	-0.14	0.22
UFB	48	49	98.00	90.00	114.00	110.00	16.00	20.00	105.10	99.82	3.33	3.76	3.17	3.77	0.48	0.54	0.30	0.28
WFB	48	49	87.00	82.00	103.00	104.00	16.00	22.00	96.35	93.63	3.40	4.76	3.53	5.08	0.49	0.68	-0.07	-0.50
EKB	48	49	90.78	87.44	104.34	97.42	13.56	9.98	96.16	91.76	3.14	2.71	3.26	2.95	0.45	0.39	0.41	0.48
OBB	48	49	36.62	36.36	44.53	42.36	7.91	6.00	40.93	39.15	1.79	1.49	4.38	3.82	0.26	0.21	-0.04	0.25
OBH	48	49	29.53	30.27	37.14	37.42	7.61	7.15	34.03	33.97	1.85	1.71	5.44	5.04	0.27	0.24	-0.36	<u>0.00</u>
NLH	48	49	46.84	44.66	59.69	56.81	12.85	12.15	53.54	49.45	2.55	2.56	4.76	5.19	0.37	0.37	-0.55	0.40
FRC	48	48	105.67	100.05	125.61	121.33	19.94	21.28	115.20	109.26	4.65	5.30	4.03	4.85	0.67	0.76	0.24	0.46
PAC	48	49	100.54	101.63	126.75	120.53	26.21	18.90	114.48	111.24	6.11	4.73	5.34	4.25	0.88	0.68	-0.11	0.15
OCC	48	49	90.18	88.79	118.31	106.75	28.13	17.96	100.48	97.27	5.98	4.84	5.95	4.97	0.86	0.69	0.64	0.05
BBH	48	48	127.00	120.00	151.00	139.00	24.00	19.00	138.77	130.77	5.32	3.93	3.83	3.00	0.77	0.57	0.48	-0.41
BNL	48	49	96.00	88.00	110.00	103.00	14.00	15.00	104.10	96.10	3.38	3.74	3.25	3.89	0.49	0.53	-0.33	-0.14
AUB	48	49	113.79	108.91	130.19	125.31	16.40	16.40	122.47	116.88	4.11	3.43	3.35	2.94	0.59	0.49	-0.11	-0.08
MM	48	49	97.19	88.79	112.36	108.15	15.17	19.36	105.36	98.90	3.94	3.79	3.74	3.83	0.57	0.54	<u>0.03</u>	0.40
FOL	48	49	31.25	30.96	45.29	41.10	14.04	10.14	37.26	35.95	2.48	2.40	6.66	6.69	0.36	0.34	0.52	0.05
FOB	47	49	26.09	26.10	36.56	34.72	10.47	8.62	31.63	30.53	2.22	1.79	7.03	5.86	0.32	0.26	-0.10	-0.18
MRH	45	49	56.28	47.73	75.68	67.43	19.40	19.70	64.66	56.56	4.37	4.26	6.76	7.54	0.65	0.61	0.09	0.38
CCV	48	49	102.12	97.23	119.29	111.68	17.17	14.45	110.05	105.83	3.73	3.10	3.39	2.93	0.54	0.44	0.15	-0.03
NLH.MRH	45	49	109.66	96.15	133.11	119.96	23.45	23.81	118.24	106.00	5.23	5.36	4.43	5.05	0.78	0.77	0.49	0.60

SAW = South African white; N = sample; Min = minimum; Max = maximum; SD = standard deviation; CV = coefficient of variation; SEM = standard error of mean; GOL = Maximum Cranial Length; GOG = Skull Circumference; XCB = Maximal Cranial Breadth; UFB = Upper Facial Breadth; WFB = Minimum Frontal Breadth; EKB = Biorbital Breadth; OBB = Orbital Breadth; OBH = Orbital Height; NLH = Nasal Height; FRC = Frontal Cord; PAC = Parietal Cord; OCC = Occipital Cord; BBH = Basion-Bregma Height; BNL = Cranial Base Length; AUB = Biauricular Breadth; MM = Inter-mastoid breadth; FOL = FM Length; FOB = FM Breadth; MRH = Maximum Ramus Height; CCV = Mean of FRC, PAC & OCC; NLH.MRH = Summation of NLH & MRH. Bold font indicates the highest value and underlined the lowest value for the column.

Table 4.7: Descriptive statistics for cephalometric variables of SAC sample.

	N		Min		Max		Range		Mean		SD		CV		SEM		Skewness	
	♂	♀	♂	♀	♂	♀	♂	♀	♂	♀	♂	♀	♂	♀	♂	♀	♂	♀
GOL	50	49	170.00	158.00	200.00	193.00	30.00	35.00	186.46	176.04	6.61	7.22	3.54	4.10	0.93	1.03	-0.25	0.05
GOG	50	49	488.00	453.00	560.00	537.00	72.00	84.00	525.32	496.86	16.74	17.09	3.19	<u>3.44</u>	2.37	2.44	-0.18	-0.07
XCB	50	49	123.00	122.00	152.00	141.00	29.00	19.00	136.06	131.94	5.93	4.54	4.36	<u>3.44</u>	0.84	0.65	0.21	-0.24
UFB	50	49	98.00	90.00	116.00	111.00	18.00	21.00	106.22	101.22	3.80	4.27	3.58	4.22	0.54	0.61	0.23	-0.16
WFB	50	49	87.00	81.00	108.00	101.00	21.00	20.00	96.14	92.41	4.96	4.97	5.16	5.38	0.70	0.71	0.60	-0.24
EKB	50	49	90.65	82.19	103.10	102.39	12.45	20.20	97.63	92.46	2.74	3.97	<u>2.81</u>	4.29	0.39	0.57	<u>-0.03</u>	0.09
OBB	50	49	36.03	33.98	43.04	42.07	7.01	8.09	39.24	37.85	1.48	1.96	3.77	5.19	0.21	0.28	0.26	<u>-0.02</u>
OBH	50	49	26.72	26.31	37.27	36.82	10.55	10.51	32.41	32.65	2.52	2.19	7.78	6.71	0.36	0.31	-0.11	-0.41
NLH	50	49	44.26	37.68	57.11	53.15	12.85	15.47	49.71	46.02	3.16	3.22	6.36	7.00	0.45	0.46	0.29	<u>0.02</u>
FRC	50	49	97.84	100.39	125.50	116.75	27.66	16.36	114.91	107.90	5.96	3.88	5.19	3.60	0.84	0.55	-0.34	0.18
PAC	50	49	102.64	93.94	124.73	124.14	22.09	30.20	115.48	109.35	5.29	6.15	4.58	5.62	0.75	0.88	-0.10	0.15
OCC	50	48	82.45	82.90	107.13	107.75	24.68	24.85	94.47	93.55	5.52	4.92	5.85	5.26	0.78	0.71	-0.10	0.30
BBH	50	49	121.00	112.00	144.00	138.00	23.00	26.00	133.08	127.20	5.77	5.07	4.33	3.99	0.82	0.72	0.09	-0.15
BNL	50	49	94.00	85.00	109.00	107.00	15.00	22.00	101.06	95.27	3.73	5.04	3.69	5.30	0.53	0.72	-0.12	0.27
AUB	50	49	110.76	96.45	132.42	123.22	21.66	26.77	118.16	111.68	4.72	4.59	4.00	4.11	0.67	0.66	0.75	-0.41
MM	50	49	92.32	85.62	110.27	106.71	17.95	21.09	102.35	97.64	4.63	4.34	4.53	4.44	0.66	0.62	-0.22	-0.17
FOL	50	49	32.00	29.72	42.12	39.91	10.12	10.19	37.08	34.63	2.57	2.77	6.94	8.00	0.36	0.40	<u>0.03</u>	-0.20
FOB	49	49	26.18	24.43	34.97	32.74	8.79	8.31	29.95	28.21	2.00	1.98	6.69	7.01	0.29	0.28	0.49	0.21
MRH	50	49	52.15	43.51	70.72	61.83	18.57	18.32	61.70	53.31	4.63	4.18	7.51	7.84	0.66	0.60	-0.13	<u>-0.02</u>
CCV	50	49	99.50	93.22	115.02	111.81	15.52	18.60	108.29	103.48	3.95	3.93	3.65	3.80	0.56	0.56	-0.18	0.05
NLH.MRH	50	49	97.11	84.42	126.98	109.56	29.87	25.14	111.41	99.33	6.90	5.85	6.19	5.89	0.98	0.84	-0.12	-0.26

SAC = South African coloured; N = sample; Min = minimum; Max = maximum; SD = standard deviation; CV = coefficient of variation; SEM = standard error of mean; GOL = Maximum Cranial Length; GOG = Skull Circumference; XCB = Maximal Cranial Breadth; UFB = Upper Facial Breadth; WFB = Minimum Frontal Breadth; EKB = Biorbital Breadth; OBB = Orbital Breadth; OBH = Orbital Height; NLH = Nasal Height; FRC = Frontal Cord; PAC = Parietal Cord; OCC = Occipital Cord; BBH = Basion-Bregma Height; BNL = Cranial Base Length; AUB = Biauricular Breadth; MM = Inter-mastoid breadth; FOL = FM Length; FOB = FM Breadth; MRH = Maximum Ramus Height; CCV = Mean of FRC, PAC & OCC; NLH.MRH = Summation of NLH & MRH. Bold font indicates the highest value and underlined the lowest value for the column.

4.1.3 Neural foramina measurements

The t-tests (Table 4.3) revealed that all three population groups showed significant differences between the sexes. Additionally, when all the data is pooled, all measurements showed significant differences between males and females.

The vertebral foramina of C1 and C2 were assessed with two measurements each, totalling four measurements shown with descriptive statistics in Table 4.11-4.13. These four measurements, along with the cephalometric measurements listed as foramen magnum length (FOL) and foramen magnum breadth (FOB) will later be assessed correlatively, where every measurement is correlated with all neural foramina measurements, which include the FM and C1/C2 neural foramina. The CV was once again included to assess the variability of the measurements among themselves. The skewness values fell within $|2|$ indicating normal distribution of the data set.

4.1.4 Post-cranial measurements

When comparing the sexes of each population group with t-test analyses (Table 4.4), all three population groups showed significant differences between males and females. When pooling the data as a single set, all measurements showed a significant difference between the sexes.

The eight measurements displayed in Tables 4.14-4.16 show the descriptive statistics for the long bone measurements. These measurements were correlated with the cephalometric measurements present in Tables 4.5-4.7. The CV was included again and indicated little difference in the variability among the long bones, but shows marked variability within each of the long bone measurements. The skewness was, as with the other groups of measurements, in accordance with the prescribed value of $|2|$.

Table 4.8: Descriptive statistics for articular facets of C0-C1 of SAB sample.

	N		Min		Max		Mean		SD		CV		SEM		Skewness	
	♂	♀	♂	♀	♂	♀	♂	♀	♂	♀	♂	♀	♂	♀	♂	♀
CdILL	50	50	15.29	14.83	29.91	28.18	21.96	20.90	2.88	2.53	13.12	12.12	0.41	0.36	<u>0.10</u>	0.34
CdILR	50	50	17.07	13.91	29.51	26.30	21.94	20.74	2.52	2.17	11.48	10.47	0.36	0.31	0.50	-0.49
CdIWL	50	50	9.64	9.71	15.16	14.81	12.37	12.16	1.13	1.12	9.11	9.24	0.16	0.16	0.18	0.15
CdIWR	50	50	9.57	8.91	15.18	14.96	12.03	11.86	1.06	1.32	8.80	11.14	0.15	0.19	0.28	-0.08
AICD	50	50	20.39	17.59	34.77	33.97	25.29	25.11	3.21	3.50	12.70	13.96	0.45	0.50	0.97	0.06
PICD	50	50	31.20	30.17	47.76	46.67	40.23	38.86	3.62	3.52	9.00	9.05	0.51	0.50	-0.11	-0.13
SAFLL	50	50	16.41	15.29	29.10	26.03	21.33	20.32	2.57	2.06	12.03	10.15	0.36	0.29	0.38	0.54
SAFLR	50	50	16.94	15.94	28.81	25.57	21.38	20.16	2.54	1.96	11.90	9.72	0.36	0.28	0.84	0.48
SAFWL	50	50	8.41	8.86	14.14	14.02	10.95	11.13	1.20	1.33	11.01	11.97	0.17	0.19	0.48	0.44
SAFWR	50	50	8.31	8.54	13.78	13.29	10.95	10.99	1.30	1.24	11.84	11.33	0.18	0.18	0.22	<u>-0.05</u>
AIFD	50	50	16.64	13.26	31.05	30.86	22.85	21.49	3.70	3.87	16.19	18.03	0.52	0.55	0.65	<u>0.05</u>
PIFD	50	50	29.89	28.24	46.84	44.14	39.89	37.52	3.08	3.08	<u>7.72</u>	<u>8.20</u>	0.44	0.44	-0.14	-0.35

SAB = South African black N = sample; Min = minimum; Max = maximum; SD = standard deviation; CV = coefficient of variation; SEM = standard error of mean; CdILL = Condylar lengths (Left); CdILR = Condylar lengths (Right); CdIWL = Condylar widths (Left); CdIWR = Condylar widths (Right); AICD = Ant. Inter-condylar distances; PICD = Post. Inter-condylar distances; SAFLL = SAF length (Left); SAFLR = SAF length (Right); SAFWL = SAF Width (Left); SAFWR = SAF Width (Right); AIFD = Ant. Inter-facet distance; PIFD = Post. Inter-facet distance. **Bold** font indicates the highest value and underlined the lowest value for the column.

Table 4.9: Descriptive statistics for articular facets of C0-C1 of SAW sample.

	N		Min		Max		Mean		SD		CV		SEM		Skewness	
	♂	♀	♂	♀	♂	♀	♂	♀	♂	♀	♂	♀	♂	♀	♂	♀
CdILL	48	49	18.77	16.07	29.58	25.78	24.69	22.00	2.32	2.41	9.38	10.96	0.33	0.34	-0.21	-0.66
CdILR	48	49	18.40	15.76	30.10	26.98	24.73	22.29	2.42	2.50	9.79	11.20	0.35	0.36	-0.27	-0.45
CdIWL	48	49	9.37	7.77	14.12	13.28	11.65	10.69	1.15	1.11	9.84	10.42	0.17	0.16	0.21	0.20
CdIWR	48	49	9.79	7.30	14.45	12.61	11.62	10.67	1.20	1.05	10.35	9.86	0.17	0.15	0.41	-0.48
AICD	48	49	19.14	19.36	32.15	30.46	25.24	24.35	2.95	2.65	11.70	10.89	0.43	0.38	-0.13	0.28
PICD	48	49	35.06	34.64	47.52	47.17	42.19	40.94	3.13	2.97	7.42	7.25	0.45	0.42	-0.33	0.11
SAFLL	48	49	19.61	14.94	27.97	24.67	23.68	21.36	2.27	2.30	9.58	10.75	0.33	0.33	<u>0.02</u>	-0.85

SAFLR	48	49	18.15	16.06	29.39	26.06	23.73	21.25	2.39	2.11	10.07	9.91	0.34	0.30	0.25	<u>-0.09</u>
SAFWL	48	49	8.79	8.21	13.11	11.91	10.94	10.16	1.01	0.82	9.21	8.07	0.15	0.12	0.32	-0.29
SAFWR	47	49	9.37	8.23	13.18	12.86	10.86	10.10	0.88	1.04	8.08	10.26	0.13	0.15	0.56	0.57
AIFD	48	49	18.41	16.80	30.25	30.54	23.98	22.36	2.78	3.18	11.61	14.21	0.40	0.45	0.10	0.56
PIFD	48	49	37.92	34.52	50.96	46.56	42.48	39.88	2.87	2.63	<u>6.76</u>	<u>6.60</u>	0.41	0.38	0.50	0.35

SAW = South African white; N = sample; Min = minimum; Max = maximum; SD = standard deviation; CV = coefficient of variation; SEM = standard error of mean; CdLL = Condylar lengths (Left); CdLR = Condylar lengths (Right); CdWL = Condylar widths (Left); CdWR = Condylar widths (Right); AICD = Ant. Inter-condylar distances; PICD = Post. Inter-condylar distances; SAFLL = SAF length (Left); SAFLR = SAF length (Right); SAFWL = SAF Width (Left); SAFWR = SAF Width (Right); AIFD = Ant. Inter-facet distance; PIFD = Post. Inter-facet distance. Bold font indicates the highest value and underlined the lowest value for the column.

Table 4.10: Descriptive statistics for articular facets of C0-C1 of SAC sample.

C	N		Min		Max		Mean		SD		CV		SEM		Skewness	
	♂	♀	♂	♀	♂	♀	♂	♀	♂	♀	♂	♀	♂	♀	♂	♀
CdLL	50	49	17.54	15.83	28.51	26.08	22.83	20.95	2.27	2.26	9.96	10.77	0.32	0.32	-0.23	-0.16
CdLR	50	49	16.09	17.47	27.94	26.61	22.70	21.38	2.53	2.18	11.16	10.18	0.36	0.31	-0.08	0.40
CdWL	50	49	9.25	9.91	15.97	14.37	12.14	11.50	1.57	0.89	12.92	7.76	0.22	0.13	0.39	0.62
CdWR	50	49	9.89	9.12	15.78	12.95	12.11	11.21	1.22	0.89	10.07	7.94	0.17	0.13	0.46	-0.11
AICD	50	49	18.43	16.12	33.15	34.44	24.56	23.06	3.15	3.48	12.83	15.09	0.45	0.50	0.45	0.60
PICD	50	49	32.35	31.73	49.66	45.24	40.93	37.58	3.28	3.02	8.02	8.04	0.46	0.43	<u>-0.06</u>	0.30
SAFLL	50	49	18.08	14.71	26.53	23.87	21.94	19.94	2.08	2.15	9.48	10.76	0.29	0.31	0.14	-0.38
SAFLR	50	49	17.85	16.48	26.34	24.32	22.10	20.18	2.24	1.85	10.13	9.16	0.32	0.26	0.21	0.09
SAFWL	49	49	8.53	8.42	13.56	12.26	10.76	10.41	1.15	0.98	10.70	9.46	0.16	0.14	0.56	<u>-0.10</u>
SAFWR	49	49	8.89	7.97	13.64	13.24	10.63	10.42	1.03	1.21	9.73	11.59	0.15	0.17	0.79	0.24
AIFD	50	49	15.97	15.93	30.13	30.91	22.70	22.17	3.35	3.41	14.74	15.38	0.47	0.49	0.57	0.52
PIFD	48	49	35.04	30.79	46.98	43.99	39.90	37.08	2.67	2.78	<u>6.69</u>	<u>7.50</u>	0.39	0.40	0.94	0.40

SAC = South African coloured; N = sample; Min = minimum; Max = maximum; SD = standard deviation; CV = coefficient of variation; SEM = standard error of mean; CdLL = Condylar lengths (Left); CdLR = Condylar lengths (Right); CdWL = Condylar widths (Left); CdWR = Condylar widths (Right); AICD = Ant. Inter-condylar distances; PICD = Post. Inter-condylar distances; SAFLL = SAF length (Left); SAFLR = SAF length (Right); SAFWL = SAF Width (Left); SAFWR = SAF Width (Right); AIFD = Ant. Inter-facet distance; PIFD = Post. Inter-facet distance. Bold font indicates the highest value and underlined the lowest value for the column.

Table 4.11: Descriptive statistics for neural foramina measurements of C1 and C2 for the SAB sample.

	N		Min		Max		Mean		SD		CV		SEM		Skewness	
	♂	♀	♂	♀	♂	♀	♂	♀	♂	♀	♂	♀	♂	♀	♂	♀
C1VFML	50	50	28.66	24.41	33.77	32.59	31.08	28.86	1.49	2.00	<u>4.80</u>	6.92	0.21	0.28	0.14	-0.14
C1VFMB	50	50	24.34	23.49	32.98	32.75	28.15	26.85	2.00	1.87	7.11	6.95	0.28	0.26	0.40	0.81
C2VFML	50	49	16.57	13.89	22.68	22.61	19.21	18.46	1.38	1.64	7.16	8.88	0.19	0.23	0.54	<u>-0.01</u>
C2VFMB	50	50	20.15	18.82	26.52	25.36	23.34	22.19	1.45	1.36	6.23	<u>6.12</u>	0.21	0.19	<u>-0.13</u>	-0.05

SAB = South African black; N = sample; Min = minimum; Max = maximum; SD = standard deviation; CV = coefficient of variation; SEM = standard error of mean; C1VFML = Vertebral foramen maximum length of first cervical vertebra; C1VFMB = Vertebral foramen maximum breadth of first cervical vertebra; C2VFML = Vertebral foramen maximum length of second cervical vertebra; C2VFMB = Vertebral foramen maximum breadth of second cervical vertebra. **Bold** font indicates the highest value and underlined the lowest value for the column.

Table 4.12: Descriptive statistics for neural foramina measurements of C1 and C2 for the SAW sample.

	N		Min		Max		Mean		SD		CV		SEM		Skewness	
	♂	♀	♂	♀	♂	♀	♂	♀	♂	♀	♂	♀	♂	♀	♂	♀
C1VFML	48	49	28.67	26.87	38.28	36.49	32.65	30.92	2.23	2.02	6.84	6.54	0.32	0.29	0.62	0.42
C1VFMB	46	47	25.91	25.90	33.18	34.16	29.70	28.91	1.89	1.78	6.35	<u>6.17</u>	0.28	0.26	0.06	0.86
C2VFML	48	49	16.62	16.68	25.42	24.88	20.68	19.84	1.91	1.63	9.22	8.23	0.28	0.23	0.43	<u>0.36</u>
C2VFMB	47	49	21.85	21.06	27.90	29.39	24.73	23.92	1.47	1.53	<u>5.96</u>	6.38	0.22	0.22	<u>-0.05</u>	0.59

SAW = South African white; N = sample; Min = minimum; Max = maximum; SD = standard deviation; CV = coefficient of variation; SEM = standard error of mean; C1VFML = Vertebral foramen maximum length of first cervical vertebra; C1VFMB = Vertebral foramen maximum breadth of first cervical vertebra; C2VFML = Vertebral foramen maximum length of second cervical vertebra; C2VFMB = Vertebral foramen maximum breadth of second cervical vertebra. **Bold** font indicates the highest value and underlined the lowest value for the column.

Table 4.13: Descriptive statistics for neural foramina measurements of C1 and C2 for the SAC sample.

	N		Min		Max		Mean		SD		CV		SEM		Skewness	
	♂	♀	♂	♀	♂	♀	♂	♀	♂	♀	♂	♀	♂	♀	♂	♀
C1VFML	50	49	27.02	23.84	37.42	33.04	31.23	28.74	2.22	2.20	7.12	7.66	0.31	0.31	0.35	-0.25
C1VFMB	50	49	24.00	23.57	36.69	31.78	28.38	26.87	2.24	1.80	7.88	<u>6.71</u>	0.32	0.26	1.10	0.54
C2VFML	50	49	15.77	14.60	23.08	23.27	19.34	18.25	1.72	1.77	8.87	9.68	0.24	0.25	<u>0.11</u>	<u>0.04</u>
C2VFMB	50	49	19.98	18.90	26.28	25.74	23.33	21.80	1.57	1.62	<u>6.74</u>	7.41	0.22	0.23	-0.21	0.29

SAC = South African coloured; N = sample; Min = minimum; Max = maximum; SD = standard deviation; CV = coefficient of variation; SEM = standard error of mean; C1VFML = Vertebral foramen maximum length of first cervical vertebra; C1VFMB = Vertebral foramen maximum breadth of first cervical vertebra; C2VFML = Vertebral foramen maximum length of second cervical vertebra; C2VFMB = Vertebral foramen maximum breadth of second cervical vertebra. **Bold** font indicates the highest value and underlined the lowest value for the column.

Table 4.14: Descriptive statistics for long bone measurements of SAB sample.

	N		Min		Max		Mean		SD		CV		SEM		Skewness	
	♂	♀	♂	♀	♂	♀	♂	♀	♂	♀	♂	♀	♂	♀	♂	♀
FEMBLN	50	50	412	368	500	480	453.48	420.20	19.45	22.94	<u>4.29</u>	5.46	2.75	3.24	0.17	0.09
FEMXLN	50	50	412	373	505	481	458.08	424.10	19.88	22.45	4.34	<u>5.29</u>	2.81	3.18	<u>0.09</u>	0.06
TIBXLN	50	49	338	313	428	400	385.48	356.49	21.61	21.44	5.61	6.01	3.06	3.06	-0.37	0.14
FIBXLN	50	49	334	308	417	393	379.82	349.47	21.26	20.32	5.60	5.82	3.01	2.90	-0.38	0.12
HUMXLN	50	50	287	248	358	339	322.16	296.36	16.39	18.14	5.09	6.12	2.32	2.57	-0.12	<u>-0.05</u>
RADXLN	50	50	208	198	329	255	254.52	227.88	18.91	15.03	7.43	6.60	2.67	2.13	0.81	0.12
ULNXLN	50	50	228	213	303	278	270.22	245.38	15.90	16.51	5.89	6.73	2.25	2.34	-0.53	0.08
CLAXLN	50	48	124	121	170	162	153.36	140.48	8.92	8.37	5.82	5.96	1.26	1.21	-0.53	0.58

SAB = South African black; N = sample; Min = minimum; Max = maximum; SD = standard deviation; CV = coefficient of variation; SEM = standard error of mean; FEMBLN = Femur bicondylar length; FEMXLN = Femur maximum length; TIBXLN = Tibia maximum length; FIBXLN = Fibula maximum length; HUMXLN = Humerus maximum length; RADXLN = Radius maximum length; ULNXLN = Ulna maximum length; CLAXLN = Clavicle maximum length. **Bold** font indicates the highest value and underlined the lowest value for the column.

Table 4.15: Descriptive statistics for long bone measurements of SAW sample.

	N		Min		Max		Mean		SD		CV		SEM		Skewness	
	♂	♀	♂	♀	♂	♀	♂	♀	♂	♀	♂	♀	♂	♀	♂	♀
FEMBLN	44	49	413	372	515	461	466.61	426.88	25.83	18.73	5.53	<u>4.39</u>	3.89	2.68	-0.02	-0.42
FEMXLN	44	49	417	375	524	467	470.75	431.43	26.08	19.51	5.54	4.52	3.93	2.79	<u>0.01</u>	-0.35
TIBXLN	44	49	338	303	427	386	386.32	350.51	20.54	16.76	5.32	4.78	3.10	2.39	0.04	-0.47
FIBXLN	45	48	336	302	416	381	380.98	345.85	19.89	15.43	5.22	4.46	2.97	2.23	-0.06	-0.36
HUMXLN	47	49	311	257	386	350	338.57	304.10	17.15	16.83	5.06	5.53	2.50	2.40	0.75	<u>0.05</u>
RADXLN	46	49	221	193	274	246	250.00	221.14	11.45	11.04	<u>4.58</u>	4.99	1.69	1.58	0.04	-0.14
ULNXLN	47	49	232	210	288	266	267.19	238.22	12.49	11.86	4.67	4.98	1.82	1.69	-0.42	0.08
CLAXLN	44	46	131	126	185	154	159.11	140.20	10.28	6.36	6.46	4.54	1.55	0.94	0.09	-0.27

SAW = South African white; N = sample; Min = minimum; Max = maximum; SD = standard deviation; CV = coefficient of variation; SEM = standard error of mean; FEMBLN = Femur bicondylar length; FEMXLN = Femur maximum length; TIBXLN = Tibia maximum length; FIBXLN = Fibula maximum length; HUMXLN = Humerus maximum length; RADXLN = Radius maximum length; ULNXLN = Ulna maximum length; CLAXLN = Clavicle maximum length. **Bold** font indicates the highest value and underlined the lowest value for the column.

Table 4.16: Descriptive statistics for long bone measurements of SAC sample.

	N		Min		Max		Mean		SD		CV		SEM		Skewness	
	♂	♀	♂	♀	♂	♀	♂	♀	♂	♀	♂	♀	♂	♀	♂	♀
FEMBLN	50	49	406	363	502	448	448.76	411.24	23.06	22.90	5.14	5.57	3.26	3.27	0.13	-0.11
FEMXLN	50	49	410	366	506	454	452.32	415.67	23.76	22.95	<u>5.25</u>	<u>5.52</u>	3.36	3.28	0.10	-0.14
TIBXLN	50	49	344	296	438	389	379.10	344.45	21.56	22.17	5.69	6.44	3.05	3.17	0.50	-0.02
FIBXLN	50	49	338	290	425	380	372.82	338.18	20.95	21.71	5.62	6.42	2.96	3.10	0.43	-0.11
HUMXLN	50	49	294	253	358	326	323.42	289.71	17.12	16.76	5.29	5.79	2.42	2.39	0.07	-0.13
RADXLN	50	49	220	186	284	250	247.12	218.08	14.60	14.29	5.91	6.55	2.07	2.04	0.08	<u>0.00</u>
ULNXLN	50	49	238	203	305	266	265.00	235.10	14.88	14.39	5.61	6.12	2.10	2.06	0.22	0.01
CLAXLN	49	49	135	121	175	157	154.80	137.47	9.12	9.39	5.89	6.83	1.30	1.34	<u>-0.03</u>	0.22

SAC = South African coloured; N = sample; Min = minimum; Max = maximum; SD = standard deviation; CV = coefficient of variation; SEM = standard error of mean; FEMBLN = Femur bicondylar length; FEMXLN = Femur maximum length; TIBXLN = Tibia maximum length; FIBXLN = Fibula maximum length; HUMXLN = Humerus maximum length; RADXLN = Radius maximum length; ULNXLN = Ulna maximum length; CLAXLN = Clavicle maximum length. **Bold** font indicates the highest value and underlined the lowest value for the column.

4.2 FACTOR ANALYSES

A principal component analysis (PCA), sometimes referred to as a factor analysis, is a statistical test in which observed data is condensed into interpretable underlying factors. Factors can be viewed as a reason why variables react in a similar manner, where the factor is the driving force for the similar response. By using a PCA, structure can be found in data sets showing which variables are closely related with each other, through the factor, within the factor loadings. By looking at the factor loadings, variables that correlate strongly with the same factor likely correlate well with each another. Factor loadings can be understood as the correlation of a variable with the factor.

Factors originate from eigenvectors, where an eigenvector is a line within a data set that describes the variance of the data set; eigenvectors exist along with eigenvalues. An eigenvalue is described as the sum of the squared loadings for a factor. These eigenvalues describe the amount of variance seen along the eigenvector; the higher the variance is, the higher the eigenvalue will be. When an eigenvalue is zero it shows no variance along the eigenvector and is considered useless. The eigenvector/eigenvalue pair is equal to the number of variables entered into the analyses, whereas every eigenvector is orthogonal to the other eigenvectors. The eigenvector with the highest eigenvalue is the principal component (first factor) as it has the most variance, which allows it to describe the data variability the best. Within PCA, the second factor is extracted on the remaining variability after the first factor is extracted, which is why the first factor will always have the highest eigenvalue. The third factor is extracted in the same manner as the second, but is conducted on the remaining variability. This process of sequential extraction continues for further extracted factors.

By using algorithms, the factors can be transformed/rotated to facilitate easier interpretation without changing the correlations between the variables. The varimax normalised rotation aims to maximize variance among the squared values of loadings of each factor. After the varimax rotation is implemented, the factors are no longer orthogonal, but still exist within the same amount of dimensions as they did before the rotation. With the rotation, the eigenvalues and the amount of variance each factor explains changes. This change does not alter the cumulative values for either the eigenvalues or the explained variance.

A threshold, identical across the sampled population groups, was chosen for each set of tested variables and all variables above the selected threshold is highlighted in red. The threshold was chosen so that a variable will only be highlighted under one factor.

4.2.1 Cephalometric measurements

For the cephalometric proportion of the analyses several factors were extracted, of which three were further assessed by means of the varimax normalised rotation to create a sharp contrast in the factor loading for clarity of the variable-factor associations. For all population groups, a factor for both skull-breadth associated measurements and measurements found along the sagittal plane were found. Some of the factors had some variables included that did not fit within these broad terms, but were generally seen to be weaker in correlation with the factor they were associated with than other variables within the factor.

Table 4.17: Eigenvalues of the cephalometric measurements listed for the SAB sample with percentage of variance explained by each factor.

Value	Eigenvalue*	% Total	Cumulative	Cumulative
1	9.892188	47.10566	9.89219	47.10566
2	2.012622	9.58391	11.90481	56.68957
3	1.677056	7.98598	13.58187	64.67555
4	1.295479	6.16895	14.87734	70.84449

% Total = percentage of total variance explained; *Extraction: Principal components.

From Table 4.17 it can be seen that 64.68% of the SAB sample's variance is explained by the first three factors. When looking at the Scree plot for the cephalometric component of the SAB in Appendix A a linearity within the scree plot starts after the third factor, which is why three factors were chosen, even though all four factors have eigenvalues above one (eigenvalues >1).

Table 4.18: Factor loadings from a principal component extraction for the cephalometric measurements of the SAB sample after a varimax rotation was implemented.

Variable	Factor 1	Factor 2	Factor 3
GOL	0.444872	0.421772	0.692881
GOG	0.542155	0.439337	0.642800
XCB	0.462100	0.330136	0.442408
UFB	0.919003	0.150093	0.146186
WFB	0.862071	-0.003642	0.168276
EKB	0.865856	0.234706	0.169503
OBB	0.641501	0.429329	0.192384
OBH	0.078981	0.484184	0.127250
NLH	0.245919	0.758640	0.204145
FRC	0.242522	0.180023	0.729906
PAC	0.480944	0.027157	0.484759
OCC	-0.126348	0.134951	0.633736
BBH	0.215929	0.233060	0.810699
BNL	0.434599	0.428355	0.513722
AUB	0.504866	0.629354	0.242237
MM	0.244495	0.632783	0.370861
FOL	0.107746	0.573283	-0.004832
FOB	-0.137193	0.626629	0.084890
MRH	0.190538	0.657711	0.291478
CCV	0.311311	0.162659	0.901812

NLH.MRH	0.239891	0.790096	0.294571
Expl.Var	4.598512	4.442092	4.541261
Prp.Totl	0.218977	0.211528	0.216251

Bold values are above the prescribed lower limit of 0.63. This value is chosen based on the lowest level of which a variable will only be highlighted by one factor. This value is identical for all sample groups and serves as an indicator of strong correlations. Expl.Var = Explained variance in the form of an eigenvalue following rotation; Prp.Totl = Proportion of the total variance that is explained by the new eigenvalue following rotation.

The SAB varimax rotation seen in Table 4.18 indicates that the first factor correlates well with variables associated with the region related to the breadth of the forehead and eyes. All four strongly correlated factors increase with the increase of the factor. The second factor is associated with the representative facial height value NLH.MRH and its components, all of which increase with the increase of the factor and additionally associated well with the inter-mastoid breadth (MM) variable, which increased as well. The third and final factor is associated with measurements taken along the sagittal plane related to cranial size, all of which increase with the increase of the factor.

Table 4.19: Eigenvalues of the cephalometric measurements listed for the SAW sample with percentage of variance explained by each factor.

Value	Eigenvalue*	% Total	Cumulative	Cumulative
1	9.854399	46.92571	9.85440	46.92571
2	1.867445	8.89260	11.72184	55.81831
3	1.600299	7.62047	13.32214	63.43878
4	1.181563	5.62649	14.50371	69.06527

% Total = percentage of total variance explained; *Extraction: Principal components.

Concerning the eigenvalues of cephalometric measurements with regards to the SAW sample in Table 4.19, the first three factors were selected, as with the SAB group, due to the general linearity seen in the scree plot after three factors were extracted (Appendix A). These three factors represent 63.44% of the variance seen in the sample.

Table 4.20: Factor loadings from a principal component extraction for the cephalometric measurements of the SAW sample after a varimax rotation was implemented.

Variable	Factor 1	Factor 2	Factor 3
GOL	0.301873	0.278380	0.821197
GOG	0.499061	0.173503	0.770425
XCB	0.610969	-0.199102	0.280651
UFB	0.808897	0.096616	0.271526
WFB	0.691654	-0.030777	0.143097
EKB	0.793044	0.206210	0.250972
OBB	0.525998	0.515781	0.240812
OBH	0.002323	0.700011	-0.011185
NLH	0.475964	0.400772	0.452878
FRC	0.352268	0.200953	0.635552
PAC	-0.086973	0.002938	0.821138
OCC	0.432596	0.031780	0.333401
BBH	0.429046	0.137760	0.667248

BNL	0.498676	0.208504	0.546080
AUB	0.805458	0.108918	0.129861
MM	0.750339	0.228244	0.193863
FOL	0.013108	0.787595	0.168023
FOB	0.130940	0.680751	0.222884
MRH	0.523349	0.124474	0.525513
CCV	0.336842	0.115846	0.864549
NLH.MRH	0.577428	0.254982	0.569566
Expl.Var	5.679735	2.462178	5.180230
Prp.Totl	0.270464	0.117247	0.246678

Bold values are above the prescribed lower limit of 0.63. This value is chosen based on the lowest level of which a variable will only be highlighted by one factor. This value is identical for all sample groups and serves as an indicator of strong correlations. Expl.Var = Explained variance in the form of an eigenvalue following rotation; Prp.Totl = Proportion of the total variance that is explained by the new eigenvalue following rotation.

The varimax rotation augmented factor analyses for the SAW sample (Table 4.20) indicates that the first factor correlates best with the region associated with forehead breadth, outer eye distance and general skull base breadth. All strongly associated variables increase with the increase of the factor. The second factor correlates well with the foramen magnum measurements and interestingly with the orbital height; all strongly correlated measurements increase with the increase of the factor. The third factor showed its best correlations with measurements taken along the sagittal plane, all of which increased with an increase in the factor as well.

Table 4.21: Eigenvalues of the cephalometric measurements listed for the SAC sample with percentage of variance explained by each factor.

Value	Eigenvalue*	% Total	Cumulative	Cumulative
1	11.41562	54.36011	11.41562	54.36011
2	1.57285	7.48978	12.98848	61.84990
3	1.38145	6.57835	14.36993	68.42824
4	1.24960	5.95046	15.61953	74.37871

% Total = percentage of total variance explained; *Extraction: Principal components.

In Table 4.21 the eigenvalues from a factor analysis for cephalometric measurements of the SAC sample is seen; and as with the SAB and SAW sample, the first three factors were selected for further analyses bases on the linearity seen in the scree plot (Appendix A). These three factors account for 68.43% of the sample variance.

Table 4.22: Factor loadings from a principal component extraction for the cephalometric measurements of the SAC sample after a varimax rotation was implemented.

Variable	Factor 1	Factor 2	Factor 3
GOL	0.512860	0.376106	0.687147
GOG	0.626573	0.329918	0.662959
XCB	0.543154	0.076318	0.580973
UFB	0.850783	0.070542	0.303934
WFB	0.748208	-0.112108	0.375308
EKB	0.818169	0.139807	0.346477

OBB	0.464297	0.321856	0.415985
OBH	-0.013678	0.336064	0.241671
NLH	0.571590	0.589260	0.177197
FRC	0.391896	0.430945	0.617377
PAC	0.382963	0.318614	0.578717
OCC	0.056572	0.012826	0.715568
BBH	0.343264	0.351812	0.700468
BNL	0.599554	0.256112	0.483557
AUB	0.764126	0.309534	0.270413
MM	0.469284	0.442521	0.323577
FOL	0.128080	0.687891	0.235019
FOB	0.075072	0.781624	0.155523
MRH	0.644439	0.549921	-0.049013
CCV	0.379293	0.349544	0.824812
NLH.MRH	0.685311	0.627963	0.041718
Expl.Var	6.081866	3.528430	4.759634
Prp.Totl	0.289613	0.168020	0.226649

Bold values are above the prescribed lower limit of 0.63. This value is chosen based on the lowest level of which a variable will only be highlighted by one factor. This value is identical for all sample groups and serves as an indicator of strong correlations. Expl.Var = Explained variance in the form of an eigenvalue following rotation; Prp.Totl = Proportion of the total variance that is explained by the new eigenvalue following rotation.

Displayed in Table 4.22 a varimax rotation augmented factor analyses for the cephalometric measurements of the SAC sample is displayed. The first factor shows that it has a strong correlation with the breadth of the forehead, the distance of the outsides of the eyes from one another, the base of the cranium, the height of the mandibular ramus, and by extension the representative of the facial height (NLH.MRH). All of the strong correlations with the first factor are seen to increase with an increase in the factor. The second factor is seen to strongly correlate with only the foramen magnum measurements, which increase with an increase in the factor. The third factor associates strongly with the measurements found along the sagittal plane, with the addition of the skull circumference; and it is seen that all strongly associated variables increase with an increase in the factor.

Table 4.23: Eigenvalues of the cephalometric measurements listed for the combined sample with percentage of variance explained by each factor.

Value	Eigenvalue*	% Total	Cumulative	Cumulative
1	10.25955	48.85502	10.25955	48.85502
2	1.98879	9.47044	12.24835	58.32546
3	1.33347	6.34984	13.58181	64.67530
4	1.19304	5.68114	14.77485	70.35644

% Total = percentage of total variance explained; *Extraction: Principal components.

The sampled populations can be grouped together as a single sample to look at any underlying traits apparent with all three population samples. Looking at Table 4.23 the eigenvalues of a factor analyses for the cephalometric variables of the combined sample can be seen. Three factors were

further looked at for the same reason of linearity seen in the scree plot as with the three sample populations. The three factors make up 64.67% of the variance seen for the combined sample.

Table 4.24: Factor loadings from a principal component extraction for the cephalometric measurements of the combined sample after a varimax rotation was implemented.

Variable	Factor 1	Factor 2	Factor 3
GOL	0.336953	0.398367	0.759929
GOG	0.435730	0.447170	0.721231
XCB	0.497822	0.209026	0.419235
UFB	0.140347	0.899743	0.236838
WFB	0.130872	0.792621	0.250088
EKB	0.201293	0.872337	0.245892
OBB	0.576997	0.444565	0.248469
OBH	0.471233	0.105577	0.017902
NLH	0.796896	0.184710	0.259275
FRC	0.273032	0.209748	0.735261
PAC	0.022133	0.306581	0.704732
OCC	0.315928	-0.003472	0.476243
BBH	0.418590	0.092667	0.745761
BNL	0.431564	0.396211	0.533255
AUB	0.691296	0.371673	0.276508
MM	0.644945	0.249129	0.318060
FOL	0.473884	0.056578	0.204032
FOB	0.665464	-0.221054	0.222813
MRH	0.677662	0.173140	0.284116
CCV	0.280349	0.244445	0.899504
NLH.MRH	0.811519	0.199211	0.308041
Expl.Var	5.112546	3.529266	4.940002
Prp.Totl	0.243455	0.168060	0.235238

Bold values are above the prescribed lower limit of 0.63. This value is chosen based on the lowest level of which a variable will only be highlighted by one factor. This value is identical for all sample groups and serves as an indicator of strong correlations. Expl.Var = Explained variance in the form of an eigenvalue following rotation; Prp.Totl = Proportion of the total variance that is explained by the new eigenvalue following rotation.

Table 4.24 shows the results from a varimax rotation transformed factor analyses for the combined sample. The first factor shows strong correlations with the components of the facial height representative NLH.MRH, with the breadth of the skull and skull base, and the foramen magnum breadth. All strongly correlated variables increase with an increase in the first factor. The second factor correlates very strongly with the forehead breadth area and the distance between the most lateral points of the eyes; all variables increase with an increase in the factor. The third factor correlates best with the variables found along the sagittal plane and best with the CCV.

4.2.2 Articular facet measurements of C0-C1

In regards to the analyses of the articular facets of the first cervical vertebrae and the occipital condyles a factor analysis was conducted on the measurements of each bone and on the measurements as a whole. Of the several factors that were extracted four factors for all

measurements together were further assessed, by means of the varimax normalised rotation for the same reason as with the cephalometric portion, to create a strong contrast between weak and strong correlations. All eigenvalues cut off points for factor determination was determined by looking at the scree plot (Appendix A) for each analyses and finding the point where the curve becomes mostly linear.

Table 4.25: Eigenvalues of all C0-C1 articular facet measurements for the SAB sample with percentage of variance explained by each factor.

Value	Eigenvalue*	% Total	Cumulative	Cumulative
1	4.083425	34.02854	4.083425	34.02854
2	2.687231	22.39360	6.770657	56.42214
3	1.546719	12.88933	8.317376	69.31146
4	0.782472	6.52060	9.099848	75.83206

% Total = percentage of total variance explained; *Extraction: Principal components.

In Table 4.25, the eigenvalues for a principal component analysis conducted on the articular facets of the occipital condyles and the superior articular facets of the SAB sample is found. Four factors were used due to the shape of the scree plot (Appendix A), as discussed above. These four factors explain 75.83% of the sample variance.

Table 4.26: Factor loadings from a principal component extraction for the C0-C1 articular facet measurements of the SAB sample after a varimax rotation was implemented.

Variable	Factor 1	Factor 2	Factor 3	Factor 4
CdILL	0.842911	-0.002293	0.174370	0.257396
CdILR	0.808966	-0.026390	0.295183	0.132316
CdIWL	-0.004164	0.771123	-0.190998	-0.121832
CdIWR	0.000334	0.801988	0.045746	0.023911
AICD	-0.136157	0.076099	0.002033	-0.918088
PICD	0.243144	0.094442	0.880558	0.006767
SAFLL	0.881574	-0.098207	0.122568	0.197680
SAFLR	0.877409	0.115748	0.185760	0.014058
SAFWL	-0.085181	0.796899	0.252758	0.062830
SAFWR	0.074596	0.784807	0.124695	-0.082568
AIFD	-0.444835	0.012766	0.161381	-0.675731
PIFD	0.334471	0.094001	0.833466	-0.146592
Expl.Var	3.312188	2.536239	1.781173	1.470248
Prp.Totl	0.276016	0.211353	0.148431	0.122521

Bold values are above the prescribed lower limit of 0.60. This value is chosen based on the lowest level of which a variable will only be highlighted by one factor. This value is identical for all sample groups and serves as an indicator of strong correlations. Expl.Var = Explained variance in the form of an eigenvalue following rotation; Prp.Totl = Proportion of the total variance that is explained by the new eigenvalue following rotation.

The results of the varimax normalised rotation of the factor analyses of the articular facets for the SAB sample can be seen in Table 4.26. The first factor is strongly correlated with the length measurements of both the condyles and SAFs and show a positive increase in the variables with an increase of the factor. The second factor is seen to correlate best with the width measurements of

both the condyles and SAFs, which increase with an increase in the factor. The third factor shows the best correlation with the posterior inter-facet distances on the condyles and SAFs and shows a positive increase of the variables with an increase in the factor. The fourth factor correlates strongly with the anterior inter-facet distances, contrary to the third factor. The variables correlated with the fourth factor decrease with an increase in the factor and are, as such negatively correlated.

Table 4.27: Eigenvalues of all C0-C1 articular facet measurements for the SAW sample with percentage of variance explained by each factor.

Value	Eigenvalue*	% Total	Cumulative	Cumulative
1	4.511753	37.59794	4.511753	37.59794
2	2.666834	22.22361	7.178587	59.82156
3	1.426230	11.88525	8.604817	71.70680
4	0.797371	6.64476	9.402188	78.35156

% Total = percentage of total variance explained; *Extraction: Principal components.

The eigenvalues for the factor analysis on the C0-C1 articular facets of the SAW sample are seen in Table 4.27. The amount of factors were chosen based on the shape of the scree plot (Appendix A). These four factors explain 78.35% of the variance seen in the SAW sample.

Table 4.28: Factor loadings from a principal component extraction for the C0-C1 articular facet measurements of the SAW sample after a varimax normalised rotation was implemented.

Variable	Factor 1	Factor 2	Factor 3	Factor 4
CdILL	0.926100	0.087309	-0.004177	0.045145
CdILR	0.840178	0.096061	-0.104516	0.261692
CdIWL	0.162163	0.881725	0.150660	-0.004112
CdIWR	0.046458	0.852420	0.056334	0.185398
AICD	-0.175776	0.031490	0.853024	0.127079
PICD	0.248208	0.097222	0.351952	0.782044
SAFLL	0.879900	0.124837	-0.176586	0.044624
SAFLR	0.812931	0.092798	-0.169502	0.304453
SAFWL	0.233291	0.618310	0.065525	0.449870
SAFWR	-0.028868	0.535055	-0.184036	0.621875
AIFD	-0.160362	0.140260	0.898278	0.139885
PIFD	0.376851	0.176508	0.250890	0.701680
Expl.Var	3.342592	2.274968	1.856258	1.928369
Prp.Totl	0.278549	0.189581	0.154688	0.160697

Bold values are above the prescribed lower limit of 0.60. This value is chosen based on the lowest level of which a variable will only be highlighted by one factor. This value is identical for all sample groups and serves as an indicator of strong correlations. Expl.Var = Explained variance in the form of an eigenvalue following rotation; Prp.Totl = Proportion of the total variance that is explained by the new eigenvalue following rotation.

Table 4.28 shows the results of the varimax normalised rotation of the C0-C1 articular facets for the SAW sample. The first factor indicates it is strongly correlated with the length measurements of the condyles and the SAFs and that the variables increase with an increase of the factor. The second factor shows its best correlations with both condyle width measurements, but has a strong correlation with only the left width measurement of the SAFs; these three variables increase with an

increase in the factor. The third factor has a strong correlation with the anterior inter-facet distances, which increase with an increase of the third factor. The fourth factor correlates well best with the posterior inter-facet distances and, interestingly, with the right SAF width. All three strongly correlated variables with the fourth factor are seen to increase with an increase in the fourth factor.

Table 4.29: Eigenvalues of all C0-C1 articular facet measurements for the SAC sample with percentage of variance explained by each factor.

Value	Eigenvalue*	% Total	Cumulative	Cumulative
1	3.971548	33.09623	3.971548	33.09623
2	3.022573	25.18811	6.994121	58.28434
3	1.505299	12.54416	8.499420	70.82850
4	0.794474	6.62061	9.293893	77.44911

% Total = percentage of total variance explained; *Extraction: Principal components.

Regarding Table 4.29, the eigenvalues for the factor analyses of the C0-C1 articular facet of the SAC sample is displayed. The four factors were further assessed based on were the curve of the scree plot became linear (Appendix A). The four factors explain a cumulative variance of 77.45%.

Table 4.30: Factor loadings from a principal component extraction for the C0-C1 articular facet measurements of the SAC sample after a varimax normalised rotation was implemented.

Variable	Factor 1	Factor 2	Factor 3	Factor 4
CdILL	0.879045	-0.020140	0.096007	0.013701
CdILR	0.847437	-0.065404	-0.100508	-0.000409
CdIWL	0.003526	0.799929	0.139598	0.306169
CdIWR	0.157243	0.866838	0.128770	0.200299
AICD	-0.176055	0.266121	0.741399	0.040836
PICD	0.574882	0.082849	0.666907	0.059377
SAFLL	0.836257	0.135356	-0.154993	0.030166
SAFLR	0.873047	0.160872	-0.165833	-0.064618
SAFWL	0.013645	0.226192	0.200835	0.840899
SAFWR	0.009947	0.236587	0.029288	0.849490
AIFD	-0.324983	0.010845	0.841073	0.160831
PIFD	0.613205	0.063921	0.586506	0.226432
Expl.Var	3.820547	1.629202	2.193935	1.650209
Prp.Totl	0.318379	0.135767	0.182828	0.137517

Bold values are above the prescribed lower limit of 0.60. This value is chosen based on the lowest level of which a variable will only be highlighted by one factor. This value is identical for all sample groups and serves as an indicator of strong correlations. Expl.Var = Explained variance in the form of an eigenvalue following rotation; Prp.Totl = Proportion of the total variance that is explained by the new eigenvalue following rotation.

Within Table 4.30 the results of the varimax normalised rotation augmentation of the factor analyses for the C0-C1 articular facets of the SAC sample can be seen. The first factor shows a strong correlation with the length variable of the condyles and the SAFs and, additionally the posterior inter-facet distance of the SAFs. All variables that correlate strongly with the first factor increase as the first factor increases. The second factor correlates best with only the condylar length measurements, which both increase with an increase in the factor. The third factor correlates well

with three variables; the anterior inter-facet distance for the condyles and the SAFs and with the posterior inter-facet distance for the condyle. All three variables increase as the third factor increases. The fourth factor has the best correlation with the width of the articular surfaces of the SAFs, which increase with an increase in the fourth factor.

Table 4.31: Eigenvalues of all C0-C1 articular facet measurements for the combined sample with percentage of variance explained by each factor.

Value	Eigenvalue*	% Total	Cumulative	Cumulative
1	4.032028	33.60023	4.032028	33.60023
2	2.835596	23.62997	6.867624	57.23020
3	1.712080	14.26733	8.579704	71.49754
4	0.677718	5.64765	9.257422	77.14518

% Total = percentage of total variance explained; *Extraction: Principal components.

By taking the combined sample and analysing it, underlying traits may be discovered that all three populations might have in common, or highlight differences between the samples Table 4.31 displays the eigenvalues for a factor analysis of the C0-C1 articular facets for the combined sample. The factor number was determined by the curve of the scree plot, as with the sampled population groups. The four factors that are further assessed make up 77.15% of the variance seen in the combined sample, which falls within the explained variance of the individual sampled populations, as is expected.

Table 4.32: Factor loadings from a principal component extraction for the C0-C1 articular facet measurements of the combined sample after a varimax normalised rotation was implemented.

Variable	Factor 1	Factor 2	Factor 3	Factor 4
CdILL	0.891107	0.026284	-0.103827	-0.050929
CdILR	0.872782	-0.046882	-0.105248	0.013054
CdIWL	-0.045592	0.865319	0.076918	0.248496
CdIWR	0.045087	0.813429	0.073196	0.323478
AICD	-0.142010	0.172040	0.806962	-0.001028
PICD	0.605418	-0.103470	0.504972	0.309041
SAFLL	0.868958	0.045301	-0.194785	-0.053934
SAFLR	0.873035	0.037299	-0.140599	0.063278
SAFWL	0.045450	0.358259	0.092509	0.786230
SAFWR	0.013623	0.288472	0.002101	0.828583
AIFD	-0.204525	0.022458	0.846830	0.031607
PIFD	0.665141	-0.110392	0.464037	0.332211
Expl.Var	3.950403	1.681337	1.938038	1.687643
Prp.Totl	0.329200	0.140111	0.161503	0.140637

Bold values are above the prescribed lower limit of 0.60. This value is chosen based on the lowest level of which a variable will only be highlighted by one factor. This value is identical for all sample groups and serves as an indicator of strong correlations. Expl.Var = Explained variance in the form of an eigenvalue following rotation; Prp.Totl = Proportion of the total variance that is explained by the new eigenvalue following rotation.

Within Table 4.32 the results of the factor analysis, with a varimax normalised rotation, on the C0-C1 articular facets of the combined sample can be seen. The first factor indicates a strong

correlation with the articular facet lengths and posterior inter-facet distances for the condyles and SAFs. These variables increase as the factor increase. The second factor has a strong correlation with the condylar widths and indicates that these variables increase with an increase in the factor. The third factor has the best correlation with the anterior inter-facet distances of the condyles and SAFs, of which the positive correlation indicates the variables increase with an increase in the factor. The fourth and final factor shows a strong correlation with the widths of the SAFs, which increase as the factor increase.

4.2.3 Neural foramina measurements

The foramina portion of the factor analyses was conducted by extracting several factors, of which two factors were analysed per population group and with all samples as one group. The extended analyses was done by means of a varimax normalised rotation, which allows for the best contrast between high and low correlation values.

Table 4.33: Eigenvalues of the neural foramina measurements for the SAB sample with percentage of variance explained by each factor.

Value	Eigenvalue*	% Total	Cumulative	Cumulative
1	3.451240	57.52067	3.451240	57.52067
2	1.050669	17.51115	4.501909	75.03182

% Total = percentage of total variance explained; *Extraction: Principal components.

Table 4.33 shows the eigenvalues of the factors generated for the neural foramina of the SAB sample. The factor amounts were determined with the help of a scree plot (Appendix A) where linearity became apparent in the curve was designated as the cut-off point for the amount of factors. In this case with the SAB sample the two factors account for 75.03% of the sample variance.

Table 4.34: Factor loadings from a principal component extraction for the neural foramina measurements of the SAB sample after a varimax normalised rotation was implemented.

Variable	Factor 1	Factor 2
FOL	0.857462	0.184602
FOB	0.310563	0.785707
C1VFML	0.837831	0.341494
C1VFMB	0.179664	0.863233
C2VFML	0.840648	0.218876
C2VFMB	0.216726	0.788170
Expl.Var	2.319588	2.182321
Prp.Totl	0.386598	0.363720

Bold values are above the prescribed lower limit of 0.69. This value is chosen based on the lowest level of which a variable will only be highlighted by one factor. This value is identical for all sample groups and serves as an indicator of strong correlations. Expl.Var = Explained variance in the form of an eigenvalue following rotation; Prp.Totl = Proportion of the total variance that is explained by the new eigenvalue following rotation.

The results in Table 4.34 are of the factor analysis, following a varimax normalised rotation, on the neural foramina measurements for the SAB sample. A good segregation between lengths and breadths was seen, with the first factor associating with the length variables and the second associating with the breadth variables. All variables increased as the relevant factor increased.

Table 4.35: Eigenvalues of the neural foramina measurements for the SAW sample with percentage of variance explained by each factor.

Value	Eigenvalue*	% Total	Cumulative	Cumulative
1	3.822899	63.71498	3.822899	63.71498
2	0.749016	12.48359	4.571915	76.19858

% Total = percentage of total variance explained; *Extraction: Principal components.

Displayed in Table 4.35 are the eigenvalues for the factor analyses of the neural foramina measurements for the SAW sample. Two factors were determine as the cut-off point for further analysis by using the curvature of the scree plot (Appendix A) as a guide. The two factors for the SAW sample explain 76.20% of the sample variance.

Table 4.36: Factor loadings from a principal component extraction for the neural foramina measurements of the SAW sample after a varimax normalised rotation was implemented.

Variable	Factor 1	Factor 2
FOL	0.467955	0.693275
FOB	0.834406	0.313873
C1VFML	0.317659	0.871778
C1VFMB	0.838180	0.266973
C2VFML	0.244617	0.851929
C2VFMB	0.743046	0.324175
Expl.Var	2.330623	2.241291
Prp.Totl	0.388437	0.373549

Bold values are above the prescribed lower limit of 0.69. This value is chosen based on the lowest level of which a variable will only be highlighted by one factor. This value is identical for all population groups and serves as an indicator of strong correlations. Expl.Var = Explained variance in the form of an eigenvalue following rotation; Prp.Totl = Proportion of the total variance that is explained by the new eigenvalue following rotation.

The factor analysis augmented with a varimax normalised rotation for the neural foramina measurements of the SAW sample can be seen in Table 4.36. The measurements are divided into breadths and lengths by the two factors. The first factor showing the best correlation with the breadth values of the neural foramina measurements and the second factor the best correlation with the length variables. All variables are seen to increase as the relevant factor increases, as all correlations are positive.

Table 4.37: Eigenvalues of the neural foramina measurements for the SAC sample with percentage of variance explained by each factor.

Value	Eigenvalue*	% Total	Cumulative	Cumulative
1	4.131914	68.86524	4.131914	68.86524
2	0.764509	12.74181	4.896423	81.60705

% Total = percentage of total variance explained; *Extraction: Principal components.

The eigenvalues for the factor analyse of the neural foramina for the SAC sample are displayed, along with the variances they explain, in Table 4.37. Two factors were determined for further assessment when looking at the curve of the scree plot (Appendix A). The two factors account for 81.61% of the total variance seen in the SAC sample.

Table 4.38: Factor loadings from a principal component extraction for the neural foramina measurements of the SAC sample after a varimax normalised rotation was implemented.

Variable	Factor 1	Factor 2
FOL	0.802477	0.349118
FOB	0.340719	0.816110
C1VFML	0.858193	0.409070
C1VFMB	0.234581	0.913971
C2VFML	0.871240	0.228274
C2VFMB	0.515752	0.690705
Expl.Var	2.576642	2.319782
Prp.Totl	0.429440	0.386630

Bold values are above the prescribed lower limit of 0.69. This value is chosen based on the lowest level of which a variable will only be highlighted by one factor. This value is identical for all sample groups and serves as an indicator of strong correlations. Expl.Var = Explained variance in the form of an eigenvalue following rotation; Prp.Totl = Proportion of the total variance that is explained by the new eigenvalue following rotation.

Looking at Table 4.38 it is apparent that there is a clear segregation between the neural foramina lengths and breadths, as with the SAB and SAW samples. The first factor is strongly associated with the lengths, while the second factor correlates best with the breadths. All variables increase as the relevant factor increases.

Table 4.39: Eigenvalues of the neural foramina measurements for the combined sample with percentage of variance explained by each factor.

Value	Eigenvalue*	% Total	Cumulative	Cumulative
1	3.993703	66.56171	3.993703	66.56171
2	0.780515	13.00859	4.774218	79.57030

% Total = percentage of total variance explained; *Extraction: Principal components.

By looking at the samples as a single group, it can be possible to ascertain underlying similarities and differences among and between the selected sample population groups and, as such, the eigenvalues for the grouped sample can be seen in Table 4.39. Two factors were apparent according to the scree plot curve, as is seen with the individual sample groups, furthermore, the two factors make up 79.57% of the sample, which is higher than the explained variance of the SAB and SAW, but lower than the SAC group, as expected based on the individual sample results

Table 4.40: Factor loadings from a principal component extraction for the neural foramina measurements of the combined sample after a varimax normalised rotation was implemented.

Variable	Factor 1	Factor 2
FOL	0.218045	0.851546
FOB	0.811722	0.354712
C1VFML	0.418951	0.830951
C1VFMB	0.892557	0.238802
C2VFML	0.354786	0.791385
C2VFMB	0.778001	0.373762
Expl.Var	2.409773	2.364445
Prp.Totl	0.401629	0.394074

Bold values are above the prescribed lower limit of 0.69. This value is chosen based on the lowest level of which a variable will only be highlighted by one factor. This value is identical for all sample groups and serves as an indicator of strong correlations. Expl.Var = Explained variance in the form of an eigenvalue following rotation; Prp.Totl = Proportion of the total variance that is explained by the new eigenvalue following rotation.

The Table 4.40 shows the results for the varimax normalised rotation of the factor analyses done for the neural foramina measurements for the combined sample group. There is a clear segregation between the neural foramina length and breadth variables generated by the two factor, as seen with the constituent sample populations. The first factor associates best with the breadth variables and the second factor with the length variables. All variables are seen to increase with an increase of the relevant factor associated with the variable.

4.2.4 Post-cranial measurements

The post-cranial measurements, pertaining to the long bones, of the factor analyses had several factors extracted, but only had two factors assessed per population group and as a united group based on the shape of the shape of the scree plots in Appendix A. The analyses was conducted with a varimax normalized rotation to gain most apparent view of the correlations within the factor and with the factor itself, due to the high contrast the rotation displays between high and low correlation values.

Table 4.41: Eigenvalues of the post-cranial measurements for the SAB sample with percentage of variance explained by each factor.

Value	Eigenvalue*	% Total	Cumulative	Cumulative
1	7.020869	87.76086	7.020869	87.76086
2	0.393712	4.92140	7.414581	92.68227
3	0.268639	3.35798	7.683220	96.04025

% Total = percentage of total variance explained; *Extraction: Principal components.

In Table 4.41 the eigenvalues for the SAB sample can be seen, with regards to the post-cranial measurements. Two factors were chosen based on the shape of the scree plot, which explained 92.68% of the sample variance. Of these two factors, the first contribute a significant 92.68% of the explained variance.

Table 4.42: Factor loadings from a principal component extraction for the post-cranial measurements of the SAB sample after a varimax normalised rotation was implemented.

Variable	Factor 1	Factor 2
FEMBLN	0.887503	0.363155
FEMXLN	0.885579	0.370489
TIBXLN	0.859649	0.440062
FIBXLN	0.865323	0.442708
HUMXLN	0.851764	0.386540
RADXLN	0.812063	0.514604
ULNXLN	0.783563	0.552395
CLAXLN	0.395928	0.906119
Expl.Var	5.215370	2.199211
Prp.Totl	0.651921	0.274901

Bold values are above the prescribed lower limit of 0.68. This value is chosen based on the lowest level of which a variable will only be highlighted by one factor. This value is identical for all sample groups and serves as an indicator of strong correlations. Expl.Var = Explained variance in the form of an eigenvalue following rotation; Prp.Totl = Proportion of the total variance that is explained by the new eigenvalue following rotation.

Within Table 4.42 the results for the factor analyses altered with a varimax normalised rotation can be seen. The first factor included all true long bones, while the second factor included only the clavicle, which is considered a pseudo long bone. All variables increases as the relevant factor increases.

Table 4.43: Eigenvalues of the post-cranial measurements for the SAW sample with percentage of variance explained by each factor.

Value	Eigenvalue*	% Total	Cumulative	Cumulative
1	7.164004	89.55005	7.164004	89.55005
2	0.290627	3.63284	7.454631	93.18289
3	0.256491	3.20614	7.711122	96.38903

% Total = percentage of total variance explained; *Extraction: Principal components.

The eigenvalues for the SAW sample following a factor analysis can be seen in Table 4.43. Two factors were chosen for further analyses based on the shape of the scree plot having linearity after this point. The factors accounted for 93.39% of the variance seen in the sample, with the first factor explaining the majority of the variance.

Table 4.44: Factor loadings from a principal component extraction for the post-cranial measurements of the SAW sample after a varimax normalised rotation was implemented.

Variable	Factor 1	Factor 2
FEMBLN	0.855676	0.501916
FEMXLN	0.858329	0.497968
TIBXLN	0.781776	0.581766
FIBXLN	0.694076	0.678480
HUMXLN	0.653512	0.676659
RADXLN	0.530128	0.813782
ULNXLN	0.517075	0.819471

CLAXLN	0.452023	0.789101
Expl.Var	3.741629	3.713002
Prp.Totl	0.467704	0.464125

Bold values are above the prescribed lower limit of 0.68. This value is chosen based on the lowest level of which a variable will only be highlighted by one factor. This value is identical for all sample groups and serves as an indicator of strong correlations. Expl.Var = Explained variance in the form of an eigenvalue following rotation; Prp.Totl = Proportion of the total variance that is explained by the new eigenvalue following rotation.

In Table 4.44 the results of the factor analyses following a varimax normalised rotation can be seen for the SAW sample. The SAW sample showed segregation between the upper and lower limb by means of the two factors. The first factor is seen to correlate best with the lower limb, while the second factor correlates best with the upper limb. The humerus and fibula lengths have very similar results for both factors, only very slightly preferring the limb-associated factor. All variables can be seen to increase as the relevant factor value is increased.

Table 4.45: Eigenvalues of the post-cranial measurements for the SAC sample with percentage of variance explained by each factor.

Value	Eigenvalue*	% Total	Cumulative	Cumulative
1	7.190157	89.87697	7.190157	89.87697
2	0.362630	4.53288	7.552787	94.40984
3	0.204566	2.55707	7.757353	96.96691

% Total = percentage of total variance explained; *Extraction: Principal components.

Table 4.45 displays the eigenvalues after a factor analyses on the post-cranial measurements of the SAC sample. There were two factors chosen for further analysis, which explained 94.41% of the variance within the sample. The majority of the variance is explained by the first factor.

Table 4.46: Factor loadings from a principal component extraction for the post-cranial measurements of the SAC sample after a varimax normalised rotation was implemented.

Variable	Factor 1	Factor 2
FEMBLN	0.891895	0.406991
FEMXLN	0.892653	0.400718
TIBXLN	0.865596	0.444830
FIBXLN	0.859006	0.474835
HUMXLN	0.746578	0.582897
RADXLN	0.763732	0.597911
ULNXLN	0.744074	0.608984
CLAXLN	0.394970	0.897405
Expl.Var	4.929765	2.623022
Prp.Totl	0.616221	0.327878

Bold values are above the prescribed lower limit of 0.68. This value is chosen based on the lowest level of which a variable will only be highlighted by one factor. This value is identical for all sample groups and serves as an indicator of strong correlations. Expl.Var = Explained variance in the form of an eigenvalue following rotation; Prp.Totl = Proportion of the total variance that is explained by the new eigenvalue following rotation.

Regarding Table 4.46, the results of a varimax normalised rotation augmenting a factor analyses of the post-cranial measurements can be seen for the SAC sample. The first factor clearly associates strongly with the true long bones, while the second factor is strongly associated with only the clavicle. All variables are positively correlated with the relevant factors.

Table 4.47: Eigenvalues of the post-cranial measurements for the combined sample with percentage of variance explained by each factor.

Value	Eigenvalue*	% Total	Cumulative	Cumulative
1	7.049275	88.11593	7.049275	88.11593
2	0.343478	4.29348	7.392753	92.40941
3	0.297691	3.72114	7.690444	96.13055

% Total = percentage of total variance explained; *Extraction: Principal components.

As with the other sets of variables, a combined set was used for the post-cranial measurements as well. This set encompassed all three sample populations for the purpose of determining underlying trends among the population, which might differ or be similar to the individual sample populations. Within Table 4.47 the eigenvalues of the combined sample can be seen, following a factor analysis. As with the individual sample populations, two factors were determined for further analyses. These two factors explain 92.41% of the sample variance, with the first factor explaining the majority of the variance, similar to the individual sample populations.

Table 4.48: Factor loadings from a principal component extraction for the post-cranial measurements of the combined sample after a varimax normalised rotation was implemented.

Variable	Factor 1	Factor 2
FEMBLN	0.888991	0.399595
FEMXLN	0.889156	0.398181
TIBXLN	0.821988	0.505436
FIBXLN	0.813680	0.532081
HUMXLN	0.783415	0.498905
RADXLN	0.723135	0.625005
ULNXLN	0.700756	0.643685
CLAXLN	0.392973	0.883907
Expl.Var	4.700792	2.691961
Prp.Totl	0.587599	0.336495

Bold values are above the prescribed lower limit of 0.68. This value is chosen based on the lowest level of which a variable will only be highlighted by one factor. This value is identical for all sample groups and serves as an indicator of strong correlations. Expl.Var = Explained variance in the form of an eigenvalue following rotation; Prp.Totl = Proportion of the total variance that is explained by the new eigenvalue following rotation.

Within Table 4.48 are the results of the factor analyse with a varimax normalised rotation implemented. This indicates that the first factor is strongly correlated with the true long bones and the second factor is associated with the clavicle. It is interesting to note the strength of the lower limb measurements seen in factor two, which highlights the results of the SAW sample within the combined sample.

4.2.5 All variables combined

A holistic approach can be taken with the variables, identifying any underlying connections between variables and help to provide some explanation to correlations between them. By keeping this in mind several factors were extracted for all variables, examined as a group for each sample population groups and a combined population group, encompassing all samples. Of these factors, five were used in further analyses by means of a varimax normalized rotation for the purpose of easing the identification of trends within the correlations of the variables and the trends of the variables with the factors. Five factors were chosen based on the shape of the scree plots (Appendix A) and where they became linear.

Table 4.49: Eigenvalues of all measurements for the SAB sample with percentage of variance explained by each factor.

Value	Eigenvalue*	% Total	Cumulative	Cumulative
1	15.35459	34.12131	15.35459	34.12131
2	4.43744	9.86098	19.79203	43.98229
3	3.95068	8.77929	23.74271	52.76158
4	2.83329	6.29619	26.57600	59.05777
5	2.59720	5.77155	29.17319	64.82932

% Total = percentage of total variance explained; *Extraction: Principal components.

The Table 4.49 displays the eigenvalues of a factor analyses on all measurements taken for the SAB sample group. Of the factors that were determined, five were used in further analyses. Even though the sample shows that six factors can be used before linearity sets in for the scree plot, it was kept at five to standardise the results. These five factors are seen to account for 64.82% of the sample.

Table 4.50: Factor loadings from a principal component extraction for all measurements of the SAB sample after a varimax normalised rotation was implemented.

Variable	Factor 1	Factor 2	Factor 3	Factor 4	Factor 5
GOL	0.395298	0.781445	0.086316	0.147624	0.098516
GOG	0.357902	0.852823	0.040811	0.113836	0.141721
XCB	0.159723	0.719208	-0.005274	0.057755	0.097845
UFB	0.165546	0.776997	-0.067406	-0.005809	-0.041983
WFB	0.001783	0.732463	0.014844	-0.069597	-0.072396
EKB	0.192523	0.751724	0.019267	-0.040095	0.063283
OBB	0.336649	0.657225	0.079361	-0.107858	0.194384
OBH	0.330905	0.202083	0.088305	-0.187263	0.181250
NLH	0.639327	0.394228	-0.126476	0.015916	0.123302
FRC	0.052773	0.674377	0.127634	0.072032	0.106603
PAC	0.072592	0.653317	-0.014785	0.035442	0.061894
OCC	0.311343	0.246618	0.155052	0.223153	-0.132972
BBH	0.219708	0.655123	0.262177	0.202022	0.114434
BNL	0.456813	0.620395	0.079433	0.264672	0.062949
AUB	0.491676	0.610261	0.004954	-0.064087	0.184818
MM	0.378582	0.540366	0.072494	-0.048236	0.263768
FOL	0.204645	0.184328	0.116559	-0.082136	0.662446
FOB	0.239977	0.015478	-0.022628	0.057815	0.790522
MRH	0.676913	0.368366	0.036772	-0.027158	0.039514

CCV	0.206866	0.782875	0.123720	0.155555	0.022623
NLH.MRH	0.750201	0.427677	-0.026871	-0.012663	0.079860
CdILL	0.216108	0.145657	0.874282	-0.002895	0.111014
CdILR	0.136458	0.193847	0.807650	0.007045	0.190712
CdIWL	0.023996	0.186968	-0.142911	0.667449	-0.085399
CdIWR	0.006605	0.195826	-0.024054	0.767494	0.031281
AICD	0.150598	-0.009734	-0.487303	0.197365	0.201439
PICD	0.087128	-0.030333	0.314716	0.292589	0.647124
SAFL	0.148997	0.071350	0.865298	-0.100099	0.160584
SAFLR	0.101947	0.099143	0.793859	0.165466	0.183254
SAFWL	0.061803	-0.003331	-0.014515	0.803398	0.019279
SAFWR	0.051897	-0.080472	0.039103	0.776239	0.124612
AIFD	0.344912	0.106721	-0.660151	0.067759	0.151628
PIFD	0.197837	0.007480	0.307518	0.250045	0.665807
C1VFML	0.352180	0.133960	0.059854	-0.112083	0.667985
C1VFMB	0.125618	0.027112	0.060563	0.139318	0.754772
C2VFML	0.058661	0.087536	-0.118855	-0.179219	0.703529
C2VFMB	0.201435	0.236688	-0.081640	-0.057738	0.596771
FEMBLN	0.914753	0.156474	-0.016471	0.027663	0.133494
FEMXLN	0.926523	0.140008	-0.019824	0.046157	0.128475
TIBXLN	0.901602	0.159095	0.039810	0.058836	0.222116
FIBXLN	0.901842	0.174393	0.036777	0.050752	0.257380
HUMXLN	0.857891	0.189799	0.041253	-0.002407	0.240692
RADXLN	0.899605	0.183521	0.079600	0.073784	0.210417
ULNXLN	0.887025	0.166895	0.083502	0.097056	0.231620
CLAXLN	0.700109	0.279332	0.150064	0.149799	0.259977
Expl.Var	9.537101	8.099088	3.951141	2.925580	4.660285
Prp.Totl	0.211936	0.179980	0.087803	0.065013	0.103562

Bold values are above the prescribed lower limit of 0.60. This value is chosen based on the lowest level of which a variable will only be highlighted by one factor. This value is identical for all sample groups and serves as an indicator of strong correlations. Expl.Var = Explained variance in the form of an eigenvalue following rotation; Prp.Totl = Proportion of the total variance that is explained by the new eigenvalue following rotation.

The results for the varimax normalised rotation of the factor analysis of the SAB sample can be seen in Table of 4.50. Among the results seen in this table only the first factor shows the inclusion of sub sets of measurements, namely cephalometric and post-cranial measurements, indicating these measurements are linked in some way within the sample.

Table 4.51: Eigenvalues of all measurements for the SAW sample with percentage of variance explained by each factor.

Value	Eigenvalue*	% Total	Cumulative	Cumulative
1	18.95052	42.11227	18.95052	42.11227
2	3.50952	7.79893	22.46004	49.91120
3	2.99634	6.65854	25.45638	56.56974
4	2.59135	5.75855	28.04773	62.32829
5	2.38138	5.29195	30.42911	67.62025

% Total = percentage of total variance explained; *Extraction: Principal components.

Within Table 4.51 the eigenvalues for the SAW sample regarding a factor analyses on all the measurements used in the study is seen. The scree plot for the SAW sample indicates a linearity after the fifth factor, making it the deciding point for the amount of factors that are further assessed. These factors account for 67.62% of the sample variance.

Table 4.52: Factor loadings from a principal component extraction for all measurements of the SAW sample after a varimax normalised rotation was implemented.

Variable	Factor 1	Factor 2	Factor 3	Factor 4	Factor 5
GOL	0.650381	0.228917	0.127275	0.140312	0.39701
GOG	0.791193	0.167575	0.071401	0.162317	0.39612
XCB	0.585447	-0.167042	-0.086127	0.058514	0.23268
UFB	0.655002	0.157682	0.066628	0.093462	0.45415
WFB	0.643200	0.062233	-0.129860	-0.051059	0.12294
EKB	0.562842	0.201514	0.104441	0.044438	0.46017
OBB	0.371533	0.446872	0.078291	-0.211552	0.47951
OBH	-0.083429	0.374332	0.067076	-0.437947	0.32294
NLH	0.423479	0.207974	0.029233	0.125788	0.63396
FRC	0.658842	0.181878	-0.065412	0.080339	0.36318
PAC	0.573905	0.062616	0.293922	0.135475	-0.06018
OCC	0.449358	0.309635	0.023888	0.227189	-0.02486
BBH	0.557501	0.183347	0.200735	0.308578	0.35598
BNL	0.409763	0.033207	0.169334	0.247726	0.62319
AUB	0.440527	0.064663	-0.058943	0.192434	0.49959
MM	0.404916	0.219866	0.020607	0.319487	0.53387
FOL	0.110274	0.736956	0.103872	-0.131958	0.27330
FOB	0.226920	0.773244	-0.003115	0.298950	0.11513
MRH	0.556757	-0.020556	0.131435	0.299391	0.46074
CCV	0.815259	0.259690	0.118601	0.206297	0.14870
NLH.MRH	0.580958	0.069890	0.108253	0.270767	0.59657
CdILL	0.204244	0.197121	0.732262	0.149805	0.35872
CdILR	0.121696	0.221224	0.745277	0.223385	0.36722
CdIWL	0.085037	0.030176	-0.029038	0.563382	0.36237
CdIWR	0.201452	-0.086718	-0.083660	0.621826	0.28700
AICD	0.134691	0.199974	-0.624593	0.224873	0.21822
PICD	0.079341	0.557556	-0.028553	0.654515	0.04683
SAFLL	0.204417	0.183126	0.789395	0.113088	0.22866
SAFLR	0.122361	0.169017	0.725641	0.193381	0.37645
SAFWL	0.188759	0.114507	0.133707	0.682834	0.30964
SAFWR	0.124622	-0.088889	0.091719	0.699689	0.20027
AIFD	0.196219	0.105888	-0.693159	0.298289	0.29541
PIFD	0.285182	0.436688	0.178836	0.574757	0.15676
C1VFML	0.192427	0.685862	0.140197	-0.132194	0.45677
C1VFMB	0.077228	0.790712	-0.001088	0.300476	0.10283
C2VFML	0.066952	0.710007	0.154410	-0.117357	0.22275
C2VFMB	0.186783	0.639595	-0.005754	-0.016627	0.40894
FEMBLN	0.201530	0.281190	0.043078	0.161765	0.86549
FEMXLN	0.199503	0.280384	0.039089	0.154557	0.86682
TIBXLN	0.211208	0.249348	0.082089	0.134953	0.87259
FIBXLN	0.213386	0.246623	0.087890	0.154916	0.88447
HUMXLN	0.158294	0.280035	0.074207	0.242630	0.83872

RADXLN	0.300440	0.157278	0.161469	0.203304	0.85450
ULNXLN	0.303267	0.148019	0.116743	0.150915	0.86595
CLAXLN	0.242476	0.201008	0.189266	0.196415	0.78503
Expl.Var	6.929006	5.181762	3.611642	4.055889	10.65081
Prp.Totl	0.153978	0.115150	0.080259	0.090131	0.23668

Bold values are above the prescribed lower limit of 0.60. This value is chosen based on the lowest level of which a variable will only be highlighted by one factor. This value is identical for all sample groups and serves as an indicator of strong correlations. Expl.Var = Explained variance in the form of an eigenvalue following rotation; Prp.Totl = Proportion of the total variance that is explained by the new eigenvalue following rotation.

The results of the factor analysis with the augmentation of the varimax normalised on all measurements taken for the SAW sample population is visible in Table 4.48. Only one factor showed correlations with more than one sub-set of measurement, more specifically, a few cephalometric measurements with the post-cranial measurements group that includes the long-bones. The factor in question can be seen as factor 5 in Table 4.52.

Table 4.53: Eigenvalues of all measurements for the SAC sample with percentage of variance explained by each factor.

Value	Eigenvalue*	% Total	Cumulative	Cumulative
1	19.48395	43.29766	19.48395	43.29766
2	3.47406	7.72013	22.95800	51.01779
3	3.11477	6.92171	26.07277	57.93949
4	2.83184	6.29297	28.90461	64.23246
5	1.86346	4.14102	30.76806	68.37348

% Total = percentage of total variance explained; *Extraction: Principal components.

The eigenvalues of the SAC sample for all of the measurements following a factor analysis, can be observed in Table 4.53. Of the large amounts of factors that were extracted only five were further assessed. The number of factors are based on the shape of the scree plot, which is seen to become linear after this point (Appendix A). These five factors for the SAC sample are seen to account for 68.37% of the sample variance.

Table 4.54: Factor loadings from a principal component extraction for all measurements of the SAC sample after a varimax normalised rotation was implemented.

Variable	Factor 1	Factor 2	Factor 3	Factor 4	Factor 5
GOL	0.378251	0.098512	0.292861	0.784084	0.106426
GOG	0.409762	0.115589	0.276188	0.818968	0.116115
XCB	0.235429	0.067869	0.111480	0.740639	0.134227
UFB	0.317364	0.162343	0.084302	0.716655	0.145235
WFB	0.094507	0.113693	0.014932	0.759659	0.183839
EKB	0.371531	0.145557	0.108264	0.698225	0.231555
OBB	0.392179	-0.102756	0.209901	0.552037	0.206618
OBH	0.027814	-0.136679	0.264531	0.229075	0.092076
NLH	0.466102	-0.029268	0.332841	0.507948	0.068992
FRC	0.400682	0.129522	0.345639	0.632637	-0.028004
PAC	0.396211	0.110990	0.249694	0.548618	0.184606
OCC	-0.009474	0.050243	0.036051	0.589542	-0.028719
BBH	0.430185	0.238155	0.279609	0.585803	0.070449

BNL	0.458502	0.170324	0.114209	0.608371	0.250595
AUB	0.494695	0.213155	0.121554	0.556546	0.315932
MM	0.335272	0.287194	0.278341	0.425337	0.266250
FOL	0.190861	0.027175	0.739976	0.243980	0.061614
FOB	0.332011	0.159596	0.742961	0.007964	0.180594
MRH	0.531970	0.152368	0.248757	0.330322	0.108635
CCV	0.365316	0.129743	0.287682	0.765274	0.064678
NLH.MRH	0.562398	0.090168	0.313038	0.444422	0.103437
CdILL	0.286866	0.733468	0.276368	0.129333	0.036551
CdILR	0.282990	0.727629	0.238295	0.166654	-0.084972
CdIWL	0.011710	-0.091902	-0.001665	0.189297	0.711415
CdIWR	0.047193	0.037279	0.109474	0.390655	0.627150
AICD	0.114960	-0.457719	0.364449	0.103987	0.331101
PICD	0.314629	0.246718	0.518975	0.108284	0.335071
SAFLL	0.189857	0.780242	0.146800	0.225654	0.062083
SAFLR	0.235573	0.798576	0.206098	0.225449	-0.029267
SAFWL	0.095041	-0.147894	0.224595	0.076319	0.677594
SAFWR	0.023997	-0.018545	-0.043551	0.105698	0.731974
AIFD	0.190209	-0.664886	0.376232	-0.071608	0.302837
PIFD	0.375214	0.294852	0.602571	-0.025313	0.383472
C1VFML	0.182826	0.122676	0.795460	0.326378	-0.036854
C1VFMB	0.236746	0.143102	0.726472	0.096086	0.216472
C2VFML	-0.060169	0.061846	0.773996	0.185013	-0.128992
C2VFMB	0.228760	0.022551	0.702406	0.301974	-0.062663
FEMBLN	0.905644	0.081720	0.132055	0.237782	0.015884
FEMXLN	0.912307	0.077101	0.127651	0.214409	0.018756
TIBXLN	0.901558	0.104071	0.146065	0.227247	0.027528
FIBXLN	0.906946	0.118396	0.136019	0.273329	0.041094
HUMXLN	0.868286	0.140280	0.181356	0.294514	0.030192
RADXLN	0.895631	0.111940	0.178899	0.284020	0.053178
ULNXLN	0.886804	0.098970	0.169302	0.295963	0.063726
CLAXLN	0.734198	0.202636	0.261400	0.277038	0.170565
Expl.Var	9.805235	3.743645	5.783858	8.413814	3.021513
Prp.Totl	0.217894	0.083192	0.128530	0.186974	0.067145

Bold values are above the prescribed lower limit of 0.60. This value is chosen based on the lowest level of which a variable will only be highlighted by one factor. This value is identical for all sample groups and serves as an indicator of strong correlations. Expl.Var = Explained variance in the form of an eigenvalue following rotation; Prp.Totl = Proportion of the total variance that is explained by the new eigenvalue following rotation.

Table 4.54 shows the results for the further assessment of the factor analyses by means of a varimax normalised rotation for the SAC sample. Among the five factors, none showed strong correlations with more than one sub-set of measurements. The first factor showed the strongest correlations for possible underlying factors existing between sub-sets of measurements. The facial height representative measurement (NLH.MRH) shows the best correlation for measurements not associated with the post-cranial measurements, which are correlated best with the first factor. It should be noted that the value for the facial height representative measurement is still strong enough

to imply some connection between the cephalometric measurement and the post-cranial measurements of the long bones.

Table 4.55: Eigenvalues of all measurements for the combined sample with percentage of variance explained by each factor.

Value	Eigenvalue*	% Total	Cumulative	Cumulative
1	17.66984	39.26632	17.66984	39.26632
2	4.17934	9.28742	21.84918	48.55374
3	2.97753	6.61672	24.82671	55.17046
4	2.62932	5.84294	27.45603	61.01340
5	2.36136	5.24748	29.81740	66.26088

% Total = percentage of total variance explained; *Extraction: Principal components.

The eigenvalues for the factor analysis on all measurements for the combined sample group is seen in Table 4.55. As with the constituent samples, the combined group has five factors that are further assessed. These five factors were determined by the shape of the scree plot and where the linearity of it starts. A total of 61.01% of the sample variance is explained by these five factors.

Table 4.56: Factor loadings from a principal component extraction for all measurements of the SAC sample after a varimax normalised rotation was implemented.

Variable	Factor 1	Factor 2	Factor 3	Factor 4	Factor 5
GOL	0.778308	0.172727	0.058151	0.350039	0.183090
GOG	0.844996	0.223380	0.060222	0.341017	0.115188
XCB	0.636841	0.264299	0.058787	0.137488	-0.125333
UFB	0.711758	-0.148988	-0.014935	0.265636	0.260224
WFB	0.748085	-0.064205	-0.003483	0.044461	0.092314
EKB	0.696198	-0.083182	0.010583	0.285121	0.258199
OBB	0.564472	0.317538	0.016122	0.353536	-0.073964
OBH	0.210209	0.271765	-0.061394	0.200512	-0.136998
NLH	0.460661	0.381654	-0.040807	0.517365	-0.077630
FRC	0.679699	0.211722	0.074671	0.222425	0.058442
PAC	0.622351	0.050750	0.065269	0.159377	0.182768
OCC	0.424570	0.274862	0.063831	0.069229	-0.011541
BBH	0.603810	0.337009	0.243166	0.278826	0.073170
BNL	0.592866	0.135920	0.123812	0.464777	0.225676
AUB	0.578226	0.298618	0.067761	0.427655	-0.009780
MM	0.497582	0.345422	0.109116	0.369190	0.065344
FOL	0.216144	0.570956	0.043210	0.223129	0.081748
FOB	0.078663	0.829481	0.049223	0.214723	0.021909
MRH	0.404646	0.250846	0.106386	0.533972	-0.049211
CCV	0.806395	0.242641	0.094533	0.211745	0.112185
NLH.MRH	0.477185	0.337175	0.055755	0.590726	-0.067334
CdILL	0.158576	0.291236	0.778345	0.254544	-0.035985
CdILR	0.151359	0.313010	0.765755	0.234870	-0.031040
CdIWL	0.182438	-0.099387	-0.131275	0.094795	0.736965
CdIWR	0.260999	-0.035223	-0.048939	0.072046	0.758320
AICD	0.101640	0.346539	-0.557662	0.139403	0.178868
PICD	0.083898	0.680086	0.176859	0.142364	0.263598
SAFLL	0.177254	0.266447	0.790804	0.179349	-0.039707

SAFLR	0.155776	0.285182	0.780783	0.208841	0.057641
SAFWL	0.088068	0.131313	-0.044683	0.117235	0.772879
SAFWR	0.036553	0.066151	0.020238	0.073251	0.768146
AIFD	0.056719	0.311155	-0.677754	0.264095	0.063785
PIFD	0.084474	0.713931	0.253034	0.222311	0.219842
C1VFML	0.237226	0.688148	0.111446	0.297498	-0.076230
C1VFMB	0.080904	0.816819	0.077566	0.131724	0.069067
C2VFML	0.115541	0.691549	0.041257	0.080291	-0.133850
C2VFMB	0.249052	0.705615	0.002019	0.235624	-0.162687
FEMBLN	0.239543	0.240398	0.050101	0.882710	0.036817
FEMXLN	0.226164	0.241055	0.044976	0.887388	0.039593
TIBXLN	0.246623	0.162622	0.054348	0.889003	0.130558
FIBXLN	0.269695	0.182810	0.062518	0.892157	0.126539
HUMXLN	0.252702	0.310025	0.108885	0.836615	0.020415
RADXLN	0.301065	0.127122	0.079558	0.874261	0.181364
ULNXLN	0.295666	0.120489	0.066919	0.872177	0.187645
CLAXLN	0.310198	0.256381	0.179354	0.718267	0.166046
Expl.Var	8.233888	6.258315	3.550269	8.761322	3.013601
Prp.Totl	0.182975	0.139074	0.078895	0.194696	0.066969

Bold values are above the prescribed lower limit of 0.60. This value is chosen based on the lowest level of which a variable will only be highlighted by one factor. This value is identical for all sample groups and serves as an indicator of strong correlations. Expl.Var = Explained variance in the form of an eigenvalue following rotation; Prp.Totl = Proportion of the total variance that is explained by the new eigenvalue following rotation.

In Table 4.56 results of the extended analysis with a varimax normalised rotation of the factor analysis on all the measurements for the combined sample can be seen. As with the SAC sample, no factor displays a strong correlation with more than one sub-set of measurements at a time, but as with the SAC sample, the representative facial height and its constituents are shown to correlate best with the factor that correlates well strongly with the post-cranial sub-set. Of these measurements, the NLH.MRH is the strongest correlation with a factor loading of 0.59, which still indicates an underlying connection between the representative facial height and the post-cranial measurements.

4.3 CORRELATIVE STATISTICS

A large number of correlations (N=234) were calculated for each population group in regards to the three correlation subsets: cephalometric-long bone correlations, articular surface correlations for the atlanto-occipital joint, and correlations for the neural canal's foramina up to the second cervical vertebra; with many correlations showing significance ($p \leq 0.05$). As such, the main focus will be placed on values with a strong degree of significance ($p \leq 0.01$). The complete set of scatterplots for the correlations can be seen in Appendix B

4.3.1 Cephalometric measurements with post-cranial measurements

The cephalometric-long bone correlations consisted of 168 sets. The SAB males showed significance ($p \leq 0.05$) in 52 correlations, while the SAB females only showed significance ($p \leq 0.05$) in 40 sets. Of these sets, the SAB males showed a high significance ($p \leq 0.01$) within 21, and the SAB females within 20 of the sets. The correlations for the high significance ($p \leq 0.01$) are displayed in Table 4.53 and 4.54 for SAB males and SAB females respectively, with the strongest correlations in bold.

Table 4.57: Cephalometric-Long bone correlations of SAB males.

Measurements		PCC	95% CI	
1	2		Lower	Upper
OBH	TIBXLN	0.404	0.121	0.635
	FIBXLN	0.405	0.162	0.621
	RADXLN	0.492	0.245	0.696
	ULNXLN	0.463	0.227	0.678
NLH	FIBXLN	0.400	0.161	0.602
	RADXLN	0.400	0.138	0.592
	ULNXLN	0.386	0.118	0.601
OCC	CLAXLN	0.434	0.155	0.678
AUB	CLAXLN	0.384	0.097	0.588
FOL	RADXLN	0.377	0.120	0.589
	ULNXLN	0.381	0.126	0.584
FOB	TIBXLN	0.365	0.088	0.612
	FIBXLN	0.403	0.126	0.629
MRH	FEMXLN	0.382	0.093	0.597
NLH.MRH	FEMBLN	0.420	0.148	0.616
	FEMXLN	0.466	0.205	0.649
	TIBXLN	0.435	0.163	0.645
	FIBXLN	0.458	0.205	0.653
	HUMXLN	0.388	0.115	0.616
	RADXLN	0.467	0.159	0.662
	ULNXLN	0.440	0.145	0.642

PCC = Pearson's correlation coefficient, CI = Confidence Interval.

As seen in Table 4.53, the SAB males had strong significant correlation that include the OBH, NLH, OCC, AUB, FOL, FOB and BM cephalometric measurements; all of which were weak ($r > |0.3|$, $r < |0.5|$) positive. The OBH measurements showed the strongest correlation with the RADXLN ($r = 0.492$). The NLH measurement showed equal strength with the FIBXLN and RADXLN ($r = 0.400$). Interestingly, the OCC ($r = 0.434$) and AUB ($r = 0.384$) both showed the highest significant correlations with the CLAXLN. The FOL and FOB measurements surprisingly showed their strongest most significant correlations with analogous structures in the upper and lower body respectively, with the FOL-ULNXLN ($r = 0.381$) and FOB-FIBXLN ($r = 0.403$) sets being the strongest. The MRH measurement had only one strong significant correlation, which was with the FEMXLN ($r = 0.382$). The combined measurement NLH.MRH had highly significant correlations which included all long bones, except the CLAXLN, but showed the strongest correlation with the RADXLN ($r = 0.467$).

Table 4.58: Cephalometric-Long bone correlations of SAB females.

Measurements		PCC	95% CI	
1	2		Lower	Upper
NLH	FEMBLN	0.524	0.307	0.716
	FEMXLN	0.518	0.294	0.715
	TIBXLN	0.587	0.388	0.735
	FIBXLN	0.581	0.359	0.744
	HUMXLN	0.444	0.180	0.638
	RADXLN	0.501	0.290	0.682
	ULNXLN	0.467	0.202	0.675
	CLAXLN	0.437	0.200	0.623
BNL	TIBXLN	0.389	0.145	0.581
	FIBXLN	0.385	0.138	0.594
	CLAXLN	0.466	0.157	0.700
AUB	TIBXLN	0.384	0.122	0.594
	HUMXLN	0.395	0.081	0.624
NLH.MRH	FEMBLN	0.536	0.363	0.671
	FEMXLN	0.520	0.338	0.666
	TIBXLN	0.547	0.274	0.720
	FIBXLN	0.534	0.279	0.709
	HUMXLN	0.448	0.253	0.597
	RADXLN	0.433	0.177	0.638
	ULNXLN	0.409	0.122	0.638

PCC = Pearson's correlation coefficient, CI = Confidence Interval.

The SAB females showed high statistical significance, as displayed in Table 4.54, with only four of the 21 cephalometric variables: the NLH, BNL, AUB, NLH.MRH measurements, with NLH and NLH.MRH having moderate ($r > |0.5|$, $r < |0.7|$) positive and the rest weak ($r > |0.3|$, $r < |0.5|$) positive correlations. The NLH measurement showed a high significance with all the measured long bones

and showed the strongest correlation with the TIBXLN ($r=0.587$), with the FIBXLN coming in to a close second ($r=0.581$). The BNL-CLAXLN correlation was the strongest ($r=0.466$) of the three sets that were highly significant pertaining to the BNL variable. Unlike the SAB males, the AUB of the SAB females correlated best with the HUMXLN ($r=0.395$). The combined measurement NLH.MRH of the SAB females had similar results compared to the males in that they both show high significance with all long bone correlations; the females differed in that their strongest correlation is with the TIBXLN ($r=0.547$).

When observing the SAW males; it can be seen that of the 168 cephalometric-long bone correlations 52 showed significance ($p\leq 0.05$), with SAW females showing significance with 35 sets of correlations. A high significance ($p\leq 0.01$) was seen in 15 sets of correlations for SAW males (Table 4.55) and nine sets for SAW females (Table 4.56), and displays the strongest correlations in bold.

Table 4.59: Cephalometric-Long bone correlations of SAW males.

Measurements		PCC	95% CI	
1	2		Lower	Upper
GOL	RADXLN	0.420	0.195	0.613
GOG	RADXLN	0.533	0.335	0.706
	ULNXLN	0.452	0.222	0.682
OBB	ULNXLN	0.420	-0.004	0.705
OBH	ULNXLN	0.434	0.029	0.696
NLH	FEMXLN	0.435	0.107	0.699
	TIBXLN	0.490	0.163	0.742
	FIBXLN	0.495	0.057	0.681
	RADXLN	0.498	0.204	0.716
	ULNXLN	0.475	0.168	0.709
	CLAXLN	0.426	0.024	0.795
FRC	RADXLN	0.440	0.170	0.639
	ULNXLN	0.452	0.180	0.671
BNL	ULNXLN	0.444	0.168	0.658
FOB	HUMXLN	0.432	0.199	0.635

PCC = Pearson's correlation coefficient, CI = Confidence Interval.

In the correlation sets of the SAW males the GOL, GOG, OBB, OBH, NLH, FRC, BNL, and FOB cephalometric measurements showed high ($p\leq 0.01$) significance. The skull circumference (GOG) is the only measurement that had a moderate positive correlation, while the rest had weak positive correlations. GOL had high significance with only the RADXLN ($r=0.420$). GOG showed high significance with both RADXLN and ULNXLN, but had a stronger correlation with RADXLN ($r=0.533$). OBB ($r=0.420$) and OBH ($r=0.434$) both showed high significance with only the ULNXLN. The NLH measurement showed a high significance with six long bone variables, with the RADXLN as the strongest ($r=0.498$). FRC showed a high significance and strongest correlation

with the ULNXLN ($r=0.452$) similar to BNL with the ULNXLN ($r=0.444$). FOB is unique in that it is the only cephalometric measurement in the SAW male sample group that showed a high significance with the HUMXLN ($r=0.432$).

The high ($p \leq 0.01$) statistically significant correlations of the SAW female group were much fewer than the values seen for the SAW males. Only the OBH, NLH, BNL and NLH.MRH variables were seen to have high significance, with all correlations being weak positive correlations. The OBH measurement showed the strongest correlation with the FIBXLN ($r=0.437$); similar to the NLH that also showed the strongest correlation with the FIBXLN ($r=0.396$). BNL was the only measurement that had a highly significant correlation with the upper limb for SAW females and had the strongest correlation with the RADXLN ($r=0.422$). NLH.MRH showed equal strength in its correlation with FEMBLN and FEMXLN ($r=0.404$), which were its only sets of correlations with high statistical significance.

Table 4.60: Cephalometric-Long bone correlations of SAW females.

Measurements		PCC	95% CI	
1	2		Lower	Upper
OBH	FEMBLN	0.415	0.109	0.638
	FEMXLN	0.418	0.107	0.639
	FIBXLN	0.437	0.203	0.624
NLH	FIBXLN	0.396	0.149	0.586
BNL	HUMXLN	0.417	0.162	0.646
	RADXLN	0.422	0.150	0.636
	ULNXLN	0.416	0.148	0.627
NLH.MRH	FEMBLN	0.404	0.099	0.628
	FEMXLN	0.404	0.096	0.632

PCC = Pearson's correlation coefficient, CI = Confidence Interval.

The SAC sample showed good significance ($p \leq 0.05$), out of the possible 168 correlation, with 51 correlations for SAC males and 145 correlations with the SAC females. Of these sets, correlations with high significance ($p \leq 0.01$) accounted for 16 correlations within the SAC males and 107 correlations with the SAC females and are displayed in Table 4.57 and 4.58 respectively, with the strongest correlations in bold.

The SAC male correlations (Table 4.57), which showed a high significance, were limited to the OBB, FRC, BBH, BNL, CCV, and NLH.MRH cephalometric variables; all of which were weak positive correlations. The OBB measurement had only one highly significant correlation which was with the CLAXLN ($r=0.437$). FRC had its strongest correlation with the FIBXLN ($r=0.423$). BBH also revealed its strongest correlation to be with the FIBXLN ($r=0.467$). BNL only had one highly significant correlation which was with the CLAXLN ($r=0.385$). The CCV showed highly significant correlations with the same long bones as BBH had had and has the strongest correlation with the

FIBXLN ($r=0.449$), similar to BBH. NLH.MRH only showed one highly significant correlation, which was with the CLAXLN ($r=0.373$).

Table 4.61: Cephalometric-Long bone correlations of SAC males.

Measurements		PCC	95% CI	
1	2		Lower	Upper
OBB	CLAXLN	0.437	0.201	0.613
FRC	TIBXLN	0.394	0.162	0.605
	FIBXLN	0.423	0.202	0.607
	RADXLN	0.378	0.115	0.615
BBH	TIBXLN	0.454	0.222	0.648
	FIBXLN	0.467	0.216	0.663
	HUMXLN	0.388	0.070	0.670
	RADXLN	0.411	0.118	0.652
	ULNXLN	0.439	0.152	0.685
BNL	CLAXLN	0.385	0.090	0.625
CCV	TIBXLN	0.432	0.189	0.634
	FIBXLN	0.449	0.212	0.632
	HUMXLN	0.416	0.109	0.682
	RADXLN	0.403	0.161	0.605
	ULNXLN	0.393	0.149	0.591
NLH.MRH	CLAXLN	0.373	0.119	0.581

PCC = Pearson's correlation coefficient, CI = Confidence Interval.

The SAC females, contrary to expectation, showed significance for almost all correlation sets and involved 18 of the 21 cephalometric components in its highly significant correlations (Table 4.58): GOL, GOG, XCB, UFB, WFB, EKB, OBB, OBH, NLH, FRC, PAC, BBH, BNL, AUB, MM, FOB, CCV, and NLH.MRH. Regardless of the large number of highly significant correlations, eight were moderate positive correlations: GOG, UFB, NLH, BBH, BNL, AUB, FOB, NLH.MRH and the rest weak positive correlations. The GOL measurement had its strongest correlation with the RADXLN ($r=0.466$), while GOG ($r=0.531$), XCB ($r=0.460$) and UFB ($r=0.535$) had theirs with HUMXLN. The strongest correlation of WFB was with the ULNXLN ($r=0.439$) and for EKB it was, once again, the HUMXLN ($r=0.453$). OBB and OBH correlated strongest with the RADXLN ($r=0.482$) and ULNXLN ($r=0.467$) respectively. NLH exhibited its strongest correlation with the HUMXLN ($r=0.557$). The FRC and PAC were the only cord measurements that showed a high significance; and contrary to many of the cephalometric measurements for SAC females, FRC showed a high significance with only one long bone, the CLAXLN ($r=0.406$), while PAC, which had strong significance with all but one, showed its strongest correlation with the FEMXLN ($r=0.467$). The BBH ($r=0.568$) and BNL ($r=0.631$) both had their strongest correlation with the RADXLN. The AUB continued the trend of having the highest correlation with the HUMXLN ($r=0.639$). The MM only had on highly significant correlation, which was with the CLAXLN ($r=0.380$). The FOB had

more high significant correlation than MM, but similarly had its strongest correlation with the CLAXLN ($r=0.524$). The CCV showed similar results compared to PAC with the strongest correlation being with the FEMXLN ($r=0.445$). The NLH.MRH also correlated with high significance with all but one, and showed its highest correlation with the HUMXLN; bringing the cephalometric measurements that had their strongest correlation with the HUMXLN up to seven of the 18.

Table 4.62: Cephalometric-Long bone correlations of SAC females.

Measurements		PCC	95% CI		Measurements		PCC	95% CI	
1	2		Lower	Upper	1	2		Lower	Upper
GOL	FEMBLN	0.444	0.217	0.627	FRC	CLAXLN	0.406	0.162	0.63
	FEMXLN	0.457	0.226	0.644	PAC	FEMBLN	0.447	0.175	0.663
	FIBXLN	0.437	0.17	0.649		FEMXLN	0.467	0.196	0.681
	HUMXLN	0.456	0.192	0.67		TIBXLN	0.393	0.111	0.621
	RADXLN	0.466	0.211	0.679		FIBXLN	0.443	0.138	0.694
	ULNXLN	0.448	0.178	0.674		HUMXLN	0.435	0.122	0.667
GOG	FEMBLN	0.508	0.273	0.681		RADXLN	0.428	0.166	0.654
	FEMXLN	0.512	0.272	0.694		ULNXLN	0.419	0.17	0.637
	TIBXLN	0.428	0.179	0.629	BBH	FEMBLN	0.414	0.119	0.627
	FIBXLN	0.503	0.26	0.691		FEMXLN	0.438	0.139	0.657
	HUMXLN	0.531	0.261	0.719		TIBXLN	0.396	0.118	0.596
	RADXLN	0.52	0.282	0.717		FIBXLN	0.508	0.209	0.696
	ULNXLN	0.517	0.272	0.723		HUMXLN	0.528	0.228	0.716
	CLAXLN	0.456	0.191	0.659		RADXLN	0.568	0.348	0.717
XCB	FEMBLN	0.409	0.138	0.625		ULNXLN	0.524	0.298	0.685
	FEMXLN	0.418	0.134	0.628		CLAXLN	0.37	0.091	0.582
	FIBXLN	0.418	0.151	0.616	BNL	FEMBLN	0.403	0.118	0.638
	HUMXLN	0.46	0.134	0.683		FEMXLN	0.411	0.125	0.644
	RADXLN	0.392	0.119	0.62		TIBXLN	0.454	0.165	0.677
	ULNXLN	0.418	0.157	0.624		FIBXLN	0.507	0.226	0.713
UFB	FEMBLN	0.408	0.129	0.618		HUMXLN	0.45	0.166	0.656
	FEMXLN	0.402	0.108	0.62		RADXLN	0.631	0.396	0.794
	TIBXLN	0.424	0.167	0.638		ULNXLN	0.621	0.389	0.793
	FIBXLN	0.435	0.166	0.655		CLAXLN	0.452	0.19	0.665
	HUMXLN	0.535	0.25	0.738	AUB	FEMBLN	0.579	0.365	0.721
	RADXLN	0.48	0.19	0.692		FEMXLN	0.592	0.369	0.733
	ULNXLN	0.483	0.204	0.696		TIBXLN	0.544	0.325	0.693
	CLAXLN	0.426	0.118	0.635		FIBXLN	0.581	0.357	0.722
WFB	TIBXLN	0.376	0.108	0.599		HUMXLN	0.639	0.418	0.771
	FIBXLN	0.371	0.089	0.602		RADXLN	0.488	0.209	0.679
	HUMXLN	0.402	0.097	0.617		ULNXLN	0.505	0.243	0.687
	RADXLN	0.404	0.108	0.629		CLAXLN	0.54	0.259	0.727
	ULNXLN	0.439	0.158	0.659	MM	CLAXLN	0.38	0.124	0.567
EKB	FIBXLN	0.374	0.075	0.624	FOB	FEMXLN	0.372	0.078	0.618
	HUMXLN	0.453	0.111	0.707		TIBXLN	0.376	0.106	0.591
	RADXLN	0.425	0.139	0.657		HUMXLN	0.401	0.199	0.576

	ULNXLN	0.406	0.106	0.646		CLAXLN	0.524	0.331	0.701
	CLAXLN	0.392	0.137	0.583	CCV	FEMBLN	0.427	0.196	0.611
OBB	FEMBLN	0.443	0.136	0.68		FEMXLN	0.445	0.207	0.633
	FEMXLN	0.436	0.129	0.678		FIBXLN	0.43	0.128	0.657
	FIBXLN	0.403	0.114	0.625		HUMXLN	0.437	0.153	0.642
	HUMXLN	0.454	0.152	0.667		RADXLN	0.423	0.162	0.647
	RADXLN	0.482	0.243	0.679		ULNXLN	0.393	0.118	0.626
	ULNXLN	0.463	0.228	0.663	NLH.MRH	FEMBLN	0.47	0.22	0.669
	CLAXLN	0.443	0.165	0.635		FEMXLN	0.464	0.206	0.665
OBH	FEMBLN	0.389	0.158	0.604		FIBXLN	0.383	0.146	0.587
	FEMXLN	0.376	0.144	0.597		HUMXLN	0.544	0.324	0.705
	HUMXLN	0.39	0.151	0.622		RADXLN	0.451	0.206	0.667
	RADXLN	0.401	0.166	0.603		ULNXLN	0.475	0.243	0.674
	ULNXLN	0.467	0.268	0.636		CLAXLN	0.422	0.099	0.644
NLH	FEMBLN	0.468	0.163	0.711					
	FEMXLN	0.472	0.158	0.717					
	FIBXLN	0.45	0.194	0.67					
	HUMXLN	0.557	0.293	0.739					
	RADXLN	0.484	0.23	0.68					
	ULNXLN	0.524	0.285	0.7					
	CLAXLN	0.417	0.101	0.643					

PCC = Pearson's correlation coefficient, CI = Confidence Interval.

4.3.2 Articular facets measurements of C0-C1

The articular facet correlations consisted of 36 sets. Of these 36 sets the SAB males showed significance ($p \leq 0.05$) with 16 of the correlations, while the SAB females showed significant correlations with 14 sets. Highly significant ($p \leq 0.01$) correlation for SAB males were seen in 14 sets and in 12 sets for the SAB females, as seen in Table 4.59 and 4.60 with the strongest correlations displayed in bold.

Of the six condylar measurements that were used in the articular facet correlations, all of them showed high significance ($p \leq 0.01$) for the SAB males with the CdILL, CdILR, AICD, and PICD having strong ($r > |0.7|$, $r < |1.0|$) positive correlations, the CdiWL a weak positive and the CdiWR a moderate positive correlation. The condylar measurement, CdILL, CdiWL, AICD, and PICD had their strongest correlations with their mirrored measurements, the SAFLL ($r=0.824$), SAFWL ($r=0.434$), AIFD ($r=0.602$), and PIFD ($r=0.773$) respectively, while CdILR and CdiWR correlated best with their contralateral components SAFLL ($r=0.803$) and SAFWL ($r=0.598$) respectively.

Table 4.63: Atlanto-occipital articular facet correlations of SAB males.

Measurements		PCC	95% CI	
1	2		Lower	Upper
CdILL	SAFLL	0.824	0.678	0.914
	SAFLR	0.685	0.490	0.820
	AIFD	-0.376	-0.610	-0.112

CdILR	PIFD	0.369	0.075	0.589
	SAFLL	0.803	0.660	0.890
	SAFLR	0.771	0.580	0.888
CdIWL	AIFD	-0.423	-0.602	-0.192
	PIFD	0.379	0.090	0.597
	SAFWL	0.434	0.191	0.643
CdIWR	SAFWL	0.598	0.349	0.769
	SAFWR	0.444	0.188	0.645
AICD	AIFD	0.602	0.353	0.788
PICD	SAFLL	0.393	0.179	0.577
	PIFD	0.773	0.620	0.880

PCC = Pearson's correlation coefficient, CI = Confidence Interval.

Table 4.64: Atlanto-occipital articular facet correlations of SAB females.

Measurements		PCC	95% CI	
1	2		Lower	Upper
CdILL	SAFLL	0.822	0.690	0.908
	SAFLR	0.565	0.305	0.768
	AIFD	-0.494	-0.703	-0.252
CdILR	SAFLL	0.443	0.232	0.636
	SAFLR	0.626	0.432	0.814
CdIWL	SAFWL	0.536	0.266	0.731
	SAFWR	0.553	0.336	0.703
CdIWR	SAFWL	0.421	0.205	0.589
	SAFWR	0.579	0.343	0.755
AICD	SAFLL	-0.558	-0.722	-0.370
	AIFD	0.439	0.161	0.682
PICD	PIFD	0.678	0.489	0.850

PCC = Pearson's correlation coefficient, CI = Confidence Interval.

Similar to the SAB males, the SAB females had highly significant ($p \leq 0.01$) correlations for all the condylar measurements. The condylar measurements CdILL, CdILR, CdIWL, CdIWR, AICD, and PICD were correlated strongest with their matched mirrored traits SAFLL ($r=0.822$), SAFLR ($r=0.626$), SAFWL ($r=0.536$), SAFWR ($r=0.579$), AIFD ($r=0.439$), and PIFD ($r=0.679$) respectively. Some condylar measurements had stronger correlations with other measurements, where CdIWL showed a moderate positive correlation with SAFWR ($r=0.553$) and AICD a moderate negative correlation with SAFLL ($r=-0.558$).

Within the sets of correlations that were generated by the articular surfaces the SAW males showed good significance ($p \leq 0.05$) for 20 of them, whereas the SAW females showed good significance for 14 sets. In the cases of high significance ($p \leq 0.01$) the SAW males and SAW females had 14 and 11 pairs respectively as seen in Table 4.61 and Table 4.62, where the strongest correlations are displayed in bold.

The SAW males showed highly significant correlations for all six condylar measurements and had their strongest correlations with their mirrored features on the C1 vertebrae. The CdILL, CdILR, AICD, and PICD showing strong positive correlations; CdlWR a moderate positive correlation and CdlWL a weak positive correlation. The CdILL, CdILR, CdlWL, CdlWR, AICD, and PICD found their strongest correlations with their associated mirrored measurements SAFLL ($r=0.803$), SAFLR ($r=0.819$), SAFWL ($r=0.483$), SAFWR ($r=0.577$) AIFD ($r=0.733$) and PIFD ($r=0.732$) respectively.

Table 4.65: Atlanto-occipital articular facet correlations of SAW males.

Measurements		PCC	95% CI	
1	2		Lower	Upper
CdILL	SAFLL	0.803	0.694	0.878
	SAFLR	0.555	0.378	0.715
CdILR	SAFLL	0.583	0.397	0.738
	SAFLR	0.819	0.690	0.913
CdlWL	SAFWL	0.398	0.133	0.622
	SAFWL	0.483	0.250	0.668
CdlWR	PIFD	0.453	0.161	0.666
	SAFWL	0.382	0.089	0.598
CdlWR	SAFWR	0.577	0.347	0.753
	PIFD	0.474	0.181	0.690
AICD	AIFD	0.733	0.596	0.830
PICD	SAFLL	0.374	0.117	0.588
	SAFWL	0.485	0.256	0.653
	PIFD	0.732	0.603	0.840

PCC = Pearson's correlation coefficient, CI = Confidence Interval.

The SAW female group, similar to the SAW male group, had highly significant correlations for all condylar measurements, with CdILL, CdILR, AICD and PICD also showing strong positive correlations; but CdlWL a moderate positive correlation and CdlWR a weak positive correlation. On all accounts for the strongest correlations, the SAW female group had weaker correlations compared to the SAW male group, with the exception of CdlWL and CdlWR, which had stronger correlations than the SAW males. The condylar measurements CdILL, CdILR, CdlWL, CdlWR, AICD, and PICD found their strongest correlations with their associated mirrored measurements SAFLL ($r=0.775$), SAFLR ($r=0.732$), SAFWL ($r=0.546$), SAFWR ($r=0.387$) AIFD ($r=0.723$) and PIFD ($r=0.716$) respectively.

Table 4.66: Atlanto-occipital articular facet correlations of SAW females.

Measurements		PCC	95% CI	
1	2		Lower	Upper
CdILL	SAFLL	0.775	0.597	0.914
	SAFLR	0.591	0.333	0.795
CdILR	SAFLL	0.553	0.362	0.716
	SAFLR	0.732	0.575	0.866
CdlWL	AIFD	-0.452	-0.657	-0.204
	SAFWL	0.546	0.320	0.728

CdIWR	SAFWR	0.387	0.173	0.595
AICD	SAFLL	-0.367	-0.637	-0.046
	AIFD	0.723	0.585	0.823
PICD	SAFWL	0.370	0.058	0.603
	PIFD	0.716	0.554	0.831

PCC = Pearson's correlation coefficient, CI = Confidence Interval.

Within the scope of the articular facet correlations the SAC males and females each showed significance ($p \leq 0.05$) for 15 sets of correlations, but for correlations with higher significance ($p \leq 0.01$) the SAC males had 10 sets (Table 4.63), while the females had 12 sets (Table 4.64) of correlations.

The SAC males had revealed highly significant correlations for all of condylar measurements, with only CdILR, having a strong positive correlation, CdILL, CdiWL, AICD, and PICD moderate positive correlations; and CdiWR a weak positive correlation. The strongest correlations for each condylar measurement corresponded with their mirrored trait on the C1 vertebra. As such, CdILL, CdILR, CdiWL, CdiWR, AICD, and PICD correlated best with SAFLL ($r=0.570$), SAFLR ($r=0.719$), SAFWL ($r=0.576$), SAFWR ($r=0.394$) AIFD ($r=0.528$) and PIFD ($r=0.658$) respectively. The strongest correlations are displayed in bold for both SAC male and female groups within Table 4.63 and Table 4.64.

Table 4.67: Atlanto-occipital articular facet correlations of SAC males.

Measurements		PCC	95% CI	
1	2		Lower	Upper
CdILL	SAFLL	0.570	0.295	0.752
	SAFLR	0.554	0.338	0.726
CdILR	SAFLL	0.419	0.125	0.637
	SAFLR	0.719	0.537	0.842
CdiWL	SAFWL	0.576	0.277	0.754
	SAFWR	0.476	0.150	0.705
CdiWR	SAFWR	0.394	0.065	0.614
AICD	SAFWR	0.379	0.047	0.640
	AIFD	0.528	0.234	0.735
PICD	PIFD	0.658	0.390	0.832

PCC = Pearson's correlation coefficient, CI = Confidence Interval.

Such as seen with their male counterparts, the SAC females showed correlation regarding all the condylar measurements, CdILR had a strong positive correlation, while CdILL, AICD, and PICD had medium positive correlations and CdiWL and CdiWR had weak positive correlations. The level of strength of the correlations, when compared with the SAC males differs only between the CdiWL measurements, where the level of strength is moderate for males but weak for females. Similar to the SAC males, the strongest correlations of the condylar measurements for the SAC females, were

with their morphologically mirrored aspects. More specifically the CdILL, CdILR, CdIWL, CdIWR, AICD, and PICD correlated best with SAFLL ($r=0.683$), SAFLR ($r=0.785$), SAFWL ($r=0.372$), SAFWR ($r=0.451$) AIFD ($r=0.682$) and PIFD ($r=0.667$) respectively.

Table 4.68: Atlanto-occipital articular facet correlations of SAC females.

Measurements		PCC	95% CI	
1	2		Lower	Upper
CdILL	SAFLL	0.683	0.491	0.834
	SAFLR	0.582	0.360	0.750
	PIFD	0.374	0.002	0.667
CdILR	SAFLL	0.591	0.410	0.731
	SAFLR	0.785	0.672	0.874
	AIFD	-0.386	-0.578	-0.160
	PIFD	0.388	0.133	0.621
CdIWL	SAFWL	0.372	0.106	0.584
CdIWR	SAFWL	0.402	0.169	0.603
	SAFWR	0.451	0.236	0.648
AICD	AIFD	0.682	0.454	0.818
PICD	PIFD	0.667	0.456	0.815

PCC = Pearson's correlation coefficient, CI = Confidence Interval.

4.3.3 Neural foramina measurements

Correlations for the foramina consisted of 30 sets where the foramen magnum and the C1 and C2 vertebral foramen measurements were all correlated with each other. Of these 30 sets the SAB males had 19 significant ($p \leq 0.05$) correlations, while the SAB females had 22 significant correlations. Correlations with higher significance ($p \leq 0.01$) consisted of 15 sets in the SAB males and 18 in the SAB females and can be seen in Table 4.65 and Table 4.66, respectively. The strongest correlations for each foramen measurement is displayed in bold in Table 4.65-4.66.

The SAB male group showed that the six measurements which correlated with each other all showed higher significance ($p \leq 0.01$) and all measurements showed moderate positive correlations when observing their strongest correlations. The C1VML measurement had its strongest correlation with FOL ($r=0.660$) while C1FVMB on the other hand showed its strongest correlation with FOB ($r=0.670$). When looking at the second cervical vertebra measurements C2VFML had its strongest correlations with C1VFML ($r=0.605$) and C2VFMB with C1VFMB ($r=0.654$). The cephalometric measurements indicated that FOL correlated best with C1VFML ($r=0.660$) and FOB correlated best with C1VFMB ($r=0.670$)

Table 4.69: Foramina correlations for SAB males.

Measurements		PCC	95% CI	
1	2		Lower	Upper
C1VFML	C2VFML	0.605	0.394	0.756
	FOL	0.660	0.475	0.809
C1VFMB	C1VFML	0.605	0.394	0.756
	C2VFMB	0.654	0.478	0.788
	FOB	0.670	0.517	0.785
C2VFML	C1VFML	0.605	0.394	0.756
	C2VFMB	0.417	0.166	0.620
	FOL	0.515	0.237	0.716
C2VFMB	C1VFMB	0.654	0.478	0.788
	C2VFML	0.417	0.166	0.620
	FOB	0.539	0.363	0.685
FOL	C1VFML	0.660	0.475	0.809
	C2VFML	0.515	0.237	0.716
FOB	C1VFMB	0.670	0.517	0.785
	C2VFMB	0.539	0.363	0.685

PCC = Pearson's correlation coefficient, CI = Confidence Interval.

As with the SAB males the SAB females also showed highly significant correlations with the six assessed measurements. The strength of the correlations, however, varied much more for the SAB females, when compared with the SAB males. The six foramina measurements assessed had their strongest correlations as follows: C1VFML with C2VFML ($r=0.751$), C1VFMB with FOB ($r=0.517$), C2VFML with C1VFML ($r=0.751$), C2VFMB with C1VFML ($r=0.394$), FOL with C1VFML ($r=0.675$), and FOB with C1VFMB ($r=0.517$). In order of strength for the correlations: C1VFML is strongly positive, C1VFMB moderately positive, C2VFML strongly positive, C2VFMB weakly positive, FOL moderately positive, and FOB moderately positive.

Table 4.70: Foramina correlations for SAB females.

Measurements		PCC	95% CI	
1	2		Lower	Upper
C1VFML	C1VFMB	0.415	0.159	0.610
	C2VFML	0.751	0.618	0.842
	C2VFMB	0.394	0.162	0.584
	FOL	0.675	0.466	0.819
	FOB	0.458	0.177	0.657
C1VFMB	C1VFML	0.415	0.159	0.610
	FOB	0.517	0.270	0.689
C2VFML	C1VFML	0.751	0.618	0.842
	FOL	0.644	0.383	0.802
	FOB	0.479	0.251	0.640
C2VFMB	C1VFML	0.394	0.162	0.584
FOL	C1VFML	0.675	0.466	0.819
	C2VFML	0.644	0.383	0.802

FOB	FOB	0.452	0.171	0.653
	C1VFML	0.458	0.177	0.657
	C1VFMB	0.517	0.270	0.689
	C2VFML	0.479	0.251	0.640
	FOL	0.452	0.171	0.653

PCC = Pearson's correlation coefficient, CI = Confidence Interval.

The SAW male and female groups had rather high numbers of significant correlations for the 30 sets assessed (Table 4.67-4.68). The SAW males had significance ($p \leq 0.05$) for all 30 sets and the females had significance for 28 sets. Higher significance ($p \leq 0.01$) was seen in 28 of the 30 significant sets for SAW males, and in the case of the SAW females, all 28 significant sets were of higher significance.

When further examining the SAW males for the strongest correlations, it can be seen that C1VFML correlated strongest with C2VFML ($r=0.679$), C1VFMB with FOB ($r=0.742$), C2VFML reciprocally with C1VFML ($r=0.679$), C2VFMB with FOB ($r=0.618$) as well, and FOB with C1VFMB ($r=0.742$) reciprocally as well. When assessing the correlations with the scaled levels of strength, for the strongest correlations, C1VFML and C2VFML had a moderate positive correlation with each other, C1VFMB and FOB a strong positive with each other, and C2VFMB a moderate positive correlation.

Table 4.71: Foramina correlations for SAW males.

Measurements		PCC	95% CI	
1	2		Lower	Upper
C1VFML	C2VFML	0.679	0.475	0.811
	C2VFMB	0.585	0.384	0.744
	FOL	0.626	0.387	0.789
	FOB	0.435	0.144	0.635
C1VFMB	C2VFML	0.544	0.319	0.716
	C2VFMB	0.570	0.325	0.737
	FOL	0.412	0.186	0.588
	FOB	0.742	0.619	0.831
C2VFML	C1VFML	0.679	0.475	0.811
	C1VFMB	0.544	0.319	0.716
	C2VFMB	0.553	0.373	0.707
	FOL	0.516	0.297	0.698
	FOB	0.510	0.294	0.686
C2VFMB	C1VFML	0.585	0.384	0.744
	C1VFMB	0.570	0.325	0.737
	C2VFML	0.553	0.373	0.707
	FOL	0.504	0.278	0.685
	FOB	0.618	0.427	0.765
FOL	C1VFML	0.626	0.387	0.789
	C1VFMB	0.412	0.186	0.588

	C2VFML	0.516	0.297	0.698
	C2VFMB	0.504	0.278	0.685
	FOB	0.613	0.429	0.750
FOB	C1VFML	0.435	0.144	0.635
	C1VFMB	0.742	0.619	0.831
	C2VFML	0.510	0.294	0.686
	C2VFMB	0.618	0.427	0.765
	FOL	0.613	0.429	0.750

PCC = Pearson's correlation coefficient, CI = Confidence Interval.

On closer examination of the 28 highly significant correlations for the SAW females it is seen that C1VFML had the strongest correlation with C2VFML ($r=0.735$), which is classified as a strong positive correlation. The C1VFMB measurement had a moderate positive correlation with FOB ($r=0.618$) as its strongest correlation. C2VFML revealed its strongest correlation to be reciprocal with C1VFML ($r=0.735$). The measurement C2VFMB exhibited its strongest correlation, a moderate positive correlation, with C1VFMB ($r=0.501$). The FOL indicated that the strongest correlation it could generate was a strong positive correlation with C1VFML ($r=0.729$). The FOB measurement displayed its strongest correlation with C1VFMB ($r=0.618$) as a reciprocal correlation as well.

Table 4.72: Foramina correlations for SAW females.

Measurements		PCC	95% CI	
1	2		Lower	Upper
C1VFML	C1VFMB	0.573	0.289	0.761
	C2VFML	0.735	0.610	0.851
	C2VFMB	0.457	0.191	0.640
	FOL	0.729	0.607	0.829
	FOB	0.481	0.237	0.678
C1VFMB	C1VFML	0.573	0.289	0.761
	C2VFML	0.404	0.191	0.598
	C2VFMB	0.501	0.296	0.709
	FOL	0.574	0.337	0.756
	FOB	0.618	0.425	0.778
C2VFML	C1VFML	0.735	0.610	0.851
	C1VFMB	0.404	0.191	0.598
	FOL	0.545	0.382	0.715
	FOB	0.427	0.191	0.617
C2VFMB	C1VFML	0.457	0.191	0.640
	C1VFMB	0.501	0.296	0.709
	FOL	0.485	0.290	0.662
	FOB	0.485	0.235	0.692
FOL	C1VFML	0.729	0.607	0.829
	C1VFMB	0.574	0.337	0.756
	C2VFML	0.545	0.382	0.715
	C2VFMB	0.485	0.290	0.662

FOB	FOB	0.539	0.297	0.744
	C1VFML	0.481	0.237	0.678
	C1VFMB	0.618	0.425	0.778
	C2VFML	0.427	0.191	0.617
	C2VFMB	0.485	0.235	0.692
	FOL	0.539	0.297	0.744

PCC = Pearson's correlation coefficient, CI = Confidence Interval.

The SAC males and females also showed remarkably high numbers of significant ($p \leq 0.05$) correlations with the males showing significance in 28/30 of correlations and the females in 29/30. When assessing the SAC groups for significance, the males displayed higher significance for all 28 significant findings ($p \leq 0.01$), while the females displayed higher significance in 28/29 correlation sets.

With regards to the highly significant correlations of the SAC males, it is apparent that the strongest correlations for C1VFML is a strong positive correlation with C2VFML ($r=0.754$), while C1VFMB holds a strong positive correlation with FOB ($r=0.749$). The C2VFML measurement correlated strongest with C1VFML in a reciprocal manner. The C2VFMB variable unexpectedly had its strongest correlation as a moderate positive correlation with C1VFML ($r=0.637$). The FOL measurement displayed its strongest correlation with C1VFML ($r=0.703$), as a strong positive correlation as well. The FOB measurement also had a strong positive correlation as its strongest correlation, but with C1VFMB ($r=0.749$).

Table 4.73: Foramina correlations for SAC males.

Measurements		PCC	95% CI	
1	2		Lower	Upper
C1VFML	C1VFMB	0.521	0.320	0.720
	C2VFML	0.754	0.650	0.859
	C2VFMB	0.637	0.459	0.774
	FOL	0.703	0.509	0.837
	FOB	0.597	0.375	0.770
C1VFMB	C1VFML	0.521	0.320	0.720
	C2VFML	0.438	0.240	0.661
	C2VFMB	0.605	0.019	0.563
	FOB	0.749	0.571	0.867
C2VFML	C1VFML	0.754	0.650	0.859
	C1VFMB	0.438	0.240	0.661
	C2VFMB	0.500	0.252	0.701
	FOL	0.516	0.263	0.728
	FOB	0.481	0.245	0.720
C2VFMB	C1VFML	0.637	0.459	0.774
	C1VFMB	0.605	0.408	0.769

	C2VFML	0.500	0.252	0.701
	FOL	0.369	0.060	0.620
	FOB	0.484	0.272	0.670
FOL	C1VFML	0.703	0.509	0.837
	C2VFML	0.516	0.263	0.728
	C2VFMB	0.369	0.060	0.620
	FOB	0.575	0.350	0.761
FOB	C1VFML	0.597	0.375	0.770
	C1VFMB	0.749	0.571	0.867
	C2VFML	0.481	0.245	0.720
	C2VFMB	0.484	0.272	0.670
	FOL	0.575	0.350	0.761

PCC = Pearson's correlation coefficient, CI = Confidence Interval.

The SAC female group showed on average fairly strong correlations for the cephalometric and cervical foramina. The C1VFML and C1VFMB both had strong positive correlations with their strongest correlations C2VFML ($r=0.792$) and C2VFMB ($r=0.742$) respectively. The C2VFML and C2VFMB had reciprocal correlations with C1VFML and C1VFMB. FOL and FOB both correlated best with the first cervical vertebra measurements, with FOL having a strong positive correlation with C1VFML ($r=0.781$) and FOB having a moderate positive correlation with C1VFMB ($r=0.621$).

Table 4.74: Foramina correlations for SAC females.

Measurements		PCC	95% CI	
1	2		Lower	Upper
C1VFML	C1VFMB	0.482	0.223	0.660
	C2VFML	0.792	0.645	0.893
	C2VFMB	0.694	0.528	0.818
	FOL	0.781	0.641	0.876
	FOB	0.410	0.092	0.662
C1VFMB	C1VFML	0.482	0.223	0.660
	C2VFML	0.381	0.089	0.634
	C2VFMB	0.742	0.577	0.857
	FOL	0.479	0.212	0.676
	FOB	0.621	0.364	0.793
C2VFML	C1VFML	0.792	0.645	0.893
	C1VFMB	0.381	0.089	0.634
	C2VFMB	0.558	0.328	0.750
	FOL	0.653	0.451	0.787
C2VFMB	C1VFML	0.694	0.528	0.818
	C1VFMB	0.742	0.577	0.857
	C2VFML	0.558	0.328	0.750
	FOL	0.592	0.406	0.737
	FOB	0.542	0.251	0.760
FOL	C1VFML	0.781	0.641	0.876
	C1VFMB	0.479	0.212	0.676
	C2VFML	0.653	0.451	0.787

	C2VFMB	0.592	0.406	0.737
	FOB	0.514	0.270	0.704
FOB	C1VFML	0.410	0.092	0.662
	C1VFMB	0.621	0.364	0.793
	C2VFMB	0.542	0.251	0.760
	FOL	0.514	0.270	0.704

PCC = Pearson's correlation coefficient, CI = Confidence Interval.

CHAPTER 5: DISCUSSION

5.1 CEPHALOMETRIC-LONG BONES

Within the factor analysis for the cephalometric measurements, some measurements occur within all of the three population groups, as well as in the combined group, and fall within the same factor. The factors among the groups do not all follow the same hierarchy when it comes to explaining the variance of the population groups, and as such, the factor group numbers differ between the population groups. These similarities might hint at an underlying trend that runs universally, as it runs within the three distinct population groups, as well as the combined sample group. This should be viewed with caution, however, as it can be seen that each sample population is very distinct in its proportions.

The factor analysis for the post-cranial measurements were similar for the SAB and SAC samples, while the SAW sample was completely different. This supports the notion that population specificity is necessary in research. It should be noted that the SAW sample, specifically the males, showed the highest rate of exclusions, with five males excluded from the sample concerning the mandibular ramus height, which might have influenced the presentation of the results. The exclusions in the study were done on a case bases where the individual was included, but the missing/damaged area of interest was left blank during testing.

When looking at the correlations between the cephalometric variables and the post-cranial subset, as well as the factor analysis conducted on all of the variables pooled, it shows that in the SAB sample, the representative facial height (NLH.MRH) and its constituents are the best traits for matching a disarticulated skull with a body. Even though the clavicle is included in the factor analysis of the combined variables, it is not seen in the list of significant correlations of the NLH.MRH or its constituents, for SAB males. The clavicle only correlates weakly with the nasal height measurement of the SAB females and is, as such, unreliable to use for matching skulls with bodies. The correlations with NLH.MRH for this population group, are however weak, and needs further assessment in a multivariate approach, before a working model can be placed into practice. The representative facial height and its constituents fall under the second factor of the factor analyses on the cephalometric measurements for the SAB sample. This second factor for the cephalometric factor analyses of the SAB sample is, however, not limited to the representative facial height and its constituents, since it holds a fairly strong correlation with the inter-mastoid breadth, and only marginally misses the cut-off point for the biauricular breadth and foramen magnum breadth variables. The factor analyses were, however, conducted on the SAB sample population as a whole, which might obscure the differences seen between males and females, as shown by the t-test, where the majority of cephalometric measurements show sexual dimorphism.

The factor analyses of the cephalometric measurements for the SAW sample has multiple occurrences where two or more factors show similar correlative strengths with a variable. Viewing the correlative statistics, the correlations between the cephalometric measurements and the post-cranial subset showed that males and females have minimal overlap concerning what each sex correlates best with. This disparity is likely the reason why the factor analyses has such a dual presentation of the variables, where variables such as the nasal height (NLH) and the cranial base length (BNL), are seen to have near identical factor loadings for two factors. By looking at the correlations for these two measurements with the post-cranial subset, it shows that both males and females have these two measurements as highly significant correlations, with the BNL-ulna correlation present in both sexes. The NLH, however, has a very weak correlation with the fibula in females as the only highly significant correlation, indicating that the NLH measurement is likely not suitable to link the skull with the body in SAW females. In spite of weak, but highly significant, correlations between BNL and the ulna, both sexes show that the factor loading still indicates a disparity, which points to sexual dimorphism in the SAW sample population. The SAW males did not show high significance for the representative facial height correlations with the long bones, but the females did. This can again, be attributed to sexual dimorphism seen between SAW males and females. From these results, the NLH.MRH measurement, which has a decent correlation with the femur measurements, is possibly a good measurement to link a disarticulated SAW female skull to its post-cranial elements. The correlation is weak and will need further assessment by means of multivariate or transformative tests in order to be more reliable in its predictions. The SAW males, despite showing a weak correlation for the representative facial height, showed a strong correlation between the nasal height measurement and total femur length. This is due to the mandibular height measurement showing no highly significant correlation, which excludes the representative facial height measurement as a feature for connecting a disarticulated skull with a body in SAW males. However, the skull circumference have an intermediate strength correlation with the radius, but is not seen in the factor analyses to fall within the same factor. This could be the influence of conducting a factor analysis on the entire sample population, which shows sexual dimorphism according to the t-test, which ultimately results in obscuring the factor analyses. The nasal height measurement is, in itself, the best feature for SAW males to determine whether a disarticulated skull belong to post-cranial elements, since it correlates significantly and consistently with 6/8 of the long bones, regardless of the fact that it is not the strongest correlation for the SAW males.

The correlations for the SAC population is unexpected in the sense that the SAC females held highly significant correlations for 18/21 cephalometric measurements, while the males had highly significant correlations for only 6/21 cephalometric measurements. Of the 18 cephalometric

measurements for the SAC females, five showed significant correlation with all of the long bones, and four more had highly significant correlations with 7/8 long bone measurements. With the proportional difference in the sexes, as seen in the correlations and t-test differences, it is possible for the factor analyses to give an indication of correlations that can be applied to both sexes. Such correlations are the bregma height (BBH) and combined cords variable (CCV) correlations with the long bones. Within the factor analyses, it is shown that these two cephalometric measurements have a high factor loading for only one factor, which happens to be the same factor. This factor deals with the underlying structure of the skull shape along the sagittal plane. With regards to BBH for the SAC males, it correlates most significantly with 5/8 of the long bone measurements, with the strongest correlation with the fibula, while the SAC females reveal that the best correlation for BBH is with the radius. These differences affect the factor analyses of the combined variables group for the SAC sample by causing the factor loading for BBH to split between the factor that contains the long bones, and the factor that contains the measurements along the sagittal plane. The combined cords variable associate best with the factor dealing with the sagittal plane measurements, and holds limited correlations with the factor associated with the long bones. Therefore, the combined cords variable is excluded as a possible basis for a method to match a skull with a body. By further assessing the factor analyses conducted on the combined variables it shows that the variable with the highest factor loading within the factor associated with the long bones is the representative facial height (NLH.MRH). This is unexpected, since neither of the sexes displayed a highly significant correlation for the maximum ramus height (MRH) with any of the long bone measurements. The second highest factor loading, with exclusion of the representative facial height and its constituents, within the long bone associated factor is the basion-bregma height variable. The representative facial height and basion-bregma height both hold the potential to link a disarticulated skull with a body, although both need to be refined before a reliable method can be constructed for doing so for either of the sexes.

For the combined sample group the factors did not reveal anything unexpected. It showed within the first factor the selection of variables associated with the skull breadth and the representative facial height. Similarly, the other two factors associated with the upper facial region and the sagittal plane measurements, as seen with the individual population groups. Considering these findings, it is possible that these factors, and how the variables within them associate with each another, are not limited to individual population groups but is instead applicable to the *Homo sapiens* species as a whole. Further assessment of different population groups is necessary to confirm or deny this hypothesis.

5.2 ARTICULAR FACETS MEASUREMENTS OF C0-C1

From the results of the factor analysis and the correlations of the articular facets for the SAB males, it is easy to see that distinct groups exist for the sample regarding certain measurements' associations with each other. Within the factor analyses, there is a clear segregation between the facet lengths and width. The anterior and posterior facet widths are seen to have their own factors associated with them. Furthermore, within the correlations of the articular facets, the same results can be seen, with each condylar measurement correlating with a measurement that falls within the factor group it is shown to associate with. Both males and females of the SAB group, present similarly concerning variables found within factors, and correlations showing the strongest correlations between the mirrored aspects. In both sexes, the condylar lengths hold the strongest correlations of all the correlation sets. Strangely, the SAC females show a large difference between the strength of the correlation between the left and right condylar lengths. These differences can possibly be attributed to postural changes within the C0-C1 joint, as the borders of the facets can be changed with prolonged wear due to the reciprocal plastic nature of bone. These results indicate a possibility that the facet measurements can be used in determining whether the C1 vertebra belongs to a skull. Further analyses of the vertebral joint facets are recommended in order to determine if an entire vertebral column can be correlatively matched to a skull.

The factors of the SAW sample segregated well for the facet lengths, but not for the widths. The superior articular facets of C1 seem to have an association with the posterior inter-facet distance for the SAW males, which likely disturbed the results of the factor analysis and caused a split in the weights of the factor loadings. The facet lengths for both SAW sexes have their strongest significant correlations with their mirrored counterparts. Furthermore, the inter-facet distances hold strong significant correlations with their mirrored counter parts for both sexes as well. With these results, it can be stated that the C0-C1 joints correlate well with each other for both males and females of the SAW sample group, and they can possibly be used in matching a skull with a first cervical vertebra in SAW populations. More research into the articular facets for all the vertebrae are advised so that it can be ascertained how well a skull correlates with the vertebral column.

In the SAC population group, the factor analysis showed the first factor correlating well with all facet length variables, but had the facet width measurements in two different factors. This split in the width measurements between C0 and C1, along with the results of the correlations, show that the facet widths for both SAC sexes is not reliable. The correlations were significant, but are too weak for proper application, aside from the left condylar width correlation with the left superior articular facet of C1, for the SAC males. The right articular facet length correlations are seen to be the strongest in both the SAC males and females, with the inter facet distances close behind in terms

of correlation strength. The factor analyses show a shared group for the posterior inter-facet distances, in which the posterior inter-facet distance appears in the factor associated with the articular facet lengths, while the posterior inter-condylar distance is seen in the factor associated with the anterior inter-facet distances. When looking at the correlations for the SAC males and females, it is clear that no significant correlation exists with the posterior inter-facet distances, aside from the posterior inter-condylar distance with the superior articular facet inter-facet distance, as expected. From these results, it can be stated that the facet widths are not reliable in association between the C0-C1 joint, but the facet lengths for the C0-C1 joint are reliable. As recommended with the other two population groups, further analyses of the vertebral column and the association of all joint surfaces with one another need to be determined to identify if a vertebral column in its entirety can be associated with confidence with a skull.

5.3 NEURAL FORAMINA MEASUREMENTS

The factor analysis for all population groups and the combined population showed a perfect segregation between length and breadth measurements, thereby indicating that the two dimensions in which these measurements are taken, can be isolated. It also shows great possibility to be used in conjunction with other methods to improve the outcome of predictive matching of skulls with bodies. The agreement of the factor analysis between the populations and the combined population might indicate that variation due to population affinity has little effect on the sizes of the neural foramina, but further investigation is needed to discern if this hypothesis is statistically significant.

For the SAB males' sample, the strongest correlation for the lengths was the foramen magnum with the neural foramen of C1, followed by the neural foramen length of C1 with C2. For the SAB females, the strongest correlation among the neural canal lengths was seen for the C1-C2 correlation, followed by the foramen magnum-C1 correlation. These results for the neural canal shows the possibility that the correlation trend is likely to continue down the vertebral column. As with the lengths, the breadth measurements for the neural canal in SAB males show that the foramen magnum breadth correlates best with the breadth of the C1 neural foramen, with the C2 neural foramen breadth correlating best with the C1 neural foramen breadth measurement. For SAB females, no significant correlation was seen for the C2 neural foramen breadth for either the foramen magnum or C1 neural foramen breadths, even though the factor analyses does not support this finding. A possible reason for this is the sudden change of diameter seen between the C1 neural foramen and the C2 neural foramen, where, in some cases, the C2 foramen is much smaller than the C1 vertebral foramen.

The SAW males and females shared a similar distribution of the correlations with the foramen magnum correlating best with the neural foramen length of C1, and the C1 neural foramen length

correlating best with the C2 neural foramen length. The breadth correlations of the sexes were not as similar, since both sexes shared the foramen magnum-C1 breadth as the strongest correlation, but the strongest correlation with the C2 differed between the sexes. The males have the strongest correlation between the C2 breadth and the foramen magnum breadth, while the females have the strongest correlation between the C2 neural foramen breadth and the C1 neural foramen breadth. From these results, a clear enough pattern can be seen, which shows that the neural foramina are correlated with each other, and while this was only observed in the foramen magnum and the first two cervical vertebra, the correlations may extend to the other vertebrae, which warrants further investigation.

The neural canal correlations for the SAC sample population are similar to those seen in the SAW sample population group. The neural foramina correlation related to the lengths of the foramina is the same for both sexes, regarding the strongest correlations. The foramen magnum length correlated best with the C1 foramen length, while the C1 foramen length correlated best with the C2. The widths were, however, not as similar in distribution as the lengths for the sexes. The foramen magnum breadth for both sexes is seen to correlate best with the C1 neural foramen breadth. The C2 foramen breadth is seen to correlate best with the C1 foramen breadth when studying only the breadth measurements. The correlations of the neural foramina among the SAC population display a pattern similar to the pattern in the SAW population group, and to some extent the SAB population group, which partially corroborates the hypothesis that population differences in these measured areas may be small enough not to interfere in a significant manner. Further assessment of these measurements, their correlations with one another and the influence of population affinity on these measurements is advised.

CHAPTER 6: CONCLUSION

The three dominant South African population groups have been assessed in terms of correlations between cephalometric and post-cranial skeletal elements. This was achieved by means of direct correlations between cephalometric measurements and long bones, the articular surfaces of the atlanto-occipital joint, and the neural canal foramina up to the second cervical vertebra. Principal component analyses revealed any underlying factors among and between the variables, while t-tests revealed differences between the sexes.

There are distinct correlations for each of the population groups regarding the cephalometric-long bone aspect of the study, but a general trend is seen with the representative facial height correlating moderately with some or most of the long bones for each population group. Distinct population specificity and sexual dimorphism is seen within the three sampled study populations. The articular facets of each of the three population groups are seen to correlate moderately, with a very limited number of strong correlations, with their mirrored traits. A direct relationship exists between the foramen magnum and the neural foramina of the first and second cervical vertebrae for the three population groups, with the foramen magnum generally correlating well with the first cervical vertebra, and the second cervical vertebrae better with the first vertebra than the foramen magnum.

Among the results, some aspects warrant further investigation; the cephalometric-long bone aspect should be expanded into multivariate analyses where the representative facial height is correlated with the long bones, excluding the clavicle, to determine a predictive model. The articular facet and foramina aspects can be combined and, similarly, have a predictive model constructed from their multivariate assessment. These models can be employed in the matching of disarticulated skeletal elements in conditions where comingled remains are found, such as mass graves or mass disasters. Through this study, a renewed basis in the field of whole body analyses of individuals has been created. It has brought forth a better understanding of the measured bones and their relation with one another.

CHAPTER 7: REFERENCE LIST

- Albert, A.M., Ricanek, K., Patterson, E. (2007). A review of the literature on the aging adult skull and face: Implications for forensic science research and applications. *Forensic Science International*, 172(1), 1–9. doi:10.1016/j.forsciint.2007.03.015.
- Alblas, A., Greyling, L.M., Geldenhuys, E. (2018). Composition of the Kirsten Skeletal Collection at Stellenbosch University, *South African Journal of Science*, 114(1-2), pp. 1-6. doi: 10.17159/sajs.
- Agarwal S., Agarwal, S.K., Jain, S.K. (2014). Correlation between the stature and cranial measurements in population of North India, *Acta Medica International*, 1(2) pp. 99-102
- Bastir, M., Rosas, A., O'Higgins, P. (2006). Craniofacial levels and the morphological maturation of the human skull. *Journal of Anatomy*, 209(5) pp 637–654. doi:10.1111/j.1469-7580.2006.00644.x.
- Bonett, D.G. & Wright, T.A. (2000). Sample size requirements for estimating Pearson, Kendall and Spearman correlations. *Psychometrika*, 65(1), pp 23–28. doi: 10.1007/bf02294183.
- Buikstra J.E. & Ubelaker D.H. (1994), *Standards for data collection from human skeletal remains*, Arkansas Archaeological Survey Research Series No. 44.
- Carroll, S.B. (1995). Homeotic genes and the evolution of arthropods and chordates. *Nature*, 376(6540), pp 479–485. doi: 10.1038/376479a0.
- Chole, R.H., Patil, R.N., Chole, S.B, Gondivkar, S., Gadbail, A.R., Yuwanati, M.B. (2013). Association of mandible anatomy with age, gender, and dental status: A Radiographic study. *International Scholarly Research Notices: Radiology*, pp 1–4. doi:10.5402/2013/453763.
- Da Vinci, L. (c1490). Vitruvian Man. [Pen and ink with wash over metalpoint on paper] Venice, Italy: Gallerie dell'Accademia.
- David, F.N. (1938). Tables of the Ordinates and Probability Integral of the Distribution of the Correlation Coefficient in Small Samples. *Journal of the American Statistical Association*, 33(204), 751. doi: 10.2307/2279076.
- Dayal, M.R., Kegley, A.D.T., Štrkalj, G., Bidmos, M.A., Kuykendall, K.L. (2009). The history and composition of the Raymond A. Dart Collection of Human Skeletons at the University of the Witwatersrand, Johannesburg, South Africa. *American Journal of Physical Anthropology*, 140(2), pp 324–335. doi:10.1002/ajpa.21072.

- Dayal, M.R., Steyn, M., Kuykendal, K.L. (2008). Stature estimation from bones of South African whites, *South African Journal of Science*, 104(3-4), pp. 124-128.
- Fett, B., (2006). An In-depth Investigation of the Divine Ratio. *The Mathematics Enthusiast*, [Online]. 3(2), pp 157-175. Available at: <https://scholarworks.umt.edu/tme/vol3/iss2/4>. [Accessed 20 November 2018].
- Giurazza, F., Vescovo, R.D., Schena, E., Battisti, S., Cazzato, R. L., Grasso, F. R., Silvestri, S., Denaro, V., Zobel, B.B. (2012). Determination of stature from skeletal and skull measurements by CT scan evaluation. *Forensic Science International*, 222(1-3), pp 398.e1–398.e9. doi:10.1016/j.forsciint.2012.06.008
- Howells, W.W. (1996). Howells' craniometric data on the internet. *American Journal of Physical Anthropology*, 101(3), pp 441–442. doi:10.1002/ajpa.1331010302
- İşcan, M.Y. & Steyn, M. (1986). *The human skeleton in forensic medicine*, 2nd ed., Springfield, IL: Charles C Thomas.
- İşcan, M.Y. & Steyn, M. (1999). Craniometric determination of population affinity in South Africans. *International Journal of Legal Medicine*, 112(2), pp 91–97. doi: 10.1007/s004140050208.
- Jenkins, F.A. (1969). The evolution and development of the dens of the mammalian axis. *The Anatomical Record*, 164(2), 173–184. doi:10.1002/ar.1091640205.
- Labuschagne, B.C.J., & Mathey, B. (2000). Cadaver profile at University of Stellenbosch Medical School, South Africa, 1956-1996. *Clinical Anatomy*, 13(2), pp 88–93. doi:10.1002/(sici)1098-2353(2000)13:2<88::aid-ca3>3.0.co;2-q.
- Langley R.L., Jantz L.M., Ousley S.D., Jantz R.L., Milner G. (2016). *Data collection procedures for forensic skeletal material 2.0*, Department of Anthropology. The University of Tennessee, Knoxville.
- Lundy, J.K. (1983). Living stature from long limb bones in the South African Negro, *South African Journal of Science*, 79, pp. 337–338.
- Lundy, J.K. & Feldesman, M.R. (1987). Revised equations for estimating living stature from the long bones of the South African Negro, *South African Journal of Science*, 83, pp. 54-55.
- Mall, G., Hubig, M., Büttner, A., Kuznik, J., Penning, R., Graw, M. (2001). Sex determination and estimation of stature from the long bones of the arm. *Forensic Science International*, 117(1-2), pp 23–30. doi: 10.1016/s0379-0738(00)00445-x.

Morriss-Kay, G.M., & Wilkie, A.O.M. (2005). Growth of the normal skull vault and its alteration in craniosynostosis: insights from human genetics and experimental studies. *Journal of Anatomy*, 207(5), pp 637–653. doi:10.1111/j.1469-7580.2005.00475.x.

Moore, K.L., Daly, A.F., Agur A.M.R. (2009) *Clinically Oriented Anatomy*, 6th ed., Baltimore: Lippincott Williams and Wilkins.

Moore-Jansen P.M., Ousley S.D., Jantz R.L. (1994). Data Collection Procedures for Forensic Skeletal Material, Report of Investigations No. 48, Department of Anthropology, University of Tennessee, Knoxville.

Naderi, S., Korman, E., Çıtak, G., Güvençer, M., Arman, C., Şenoğlu, M., Süleyman, T., Arda, M.N. (2005). Morphometric analysis of human occipital condyle. *Clinical Neurology and Neurosurgery*, 107(3), pp 191–199. doi:10.1016/j.clineuro.2004.07.014.

Netter, F.H. (2010) *Atlas of Human Anatomy*, 5th ed., Philadelphia, PA: Elsevier.

O'Rahilly, R., Müller, F., Meyer, D.B. (1983). The human vertebral column at the end of the embryonic period proper. 2. The occipitocervical region. *Journal of Anatomy*, 136(1), pp. 181–195. PMID: 6833119.

Özaslan, A., İşcan, M.Y., Özaslan, İ., Tuğcu, H., Koç, S. (2003). Estimation of stature from body parts. *Forensic Science International*, 132(1), pp 40–45. doi: 10.1016/s0379-0738(02)00425-5.

Ozturk, C.N., Ozturk, C., Bozkurt, M., Uygur, H.S., Papay, F.A., Zins, J.E. (2013). Dentition, bone loss, and the aging of the mandible. *Aesthetic Surgery Journal*, 33(7), pp 967–974. doi: 10.1177/1090820x13503473.

Paleo-tech Inc. (2018) Paleo-tech Inc. "We measure our success by helping you with yours", Available at: <https://paleo-tech.com/> [Accessed: 11 March 2016].

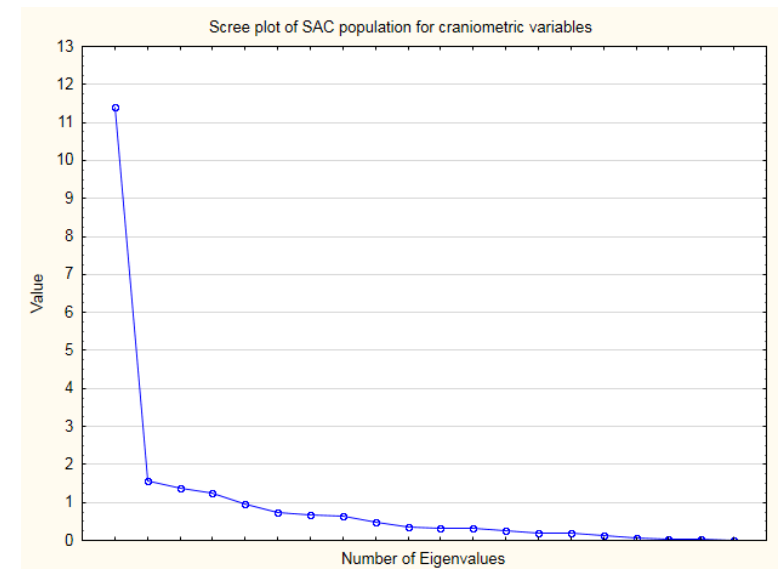
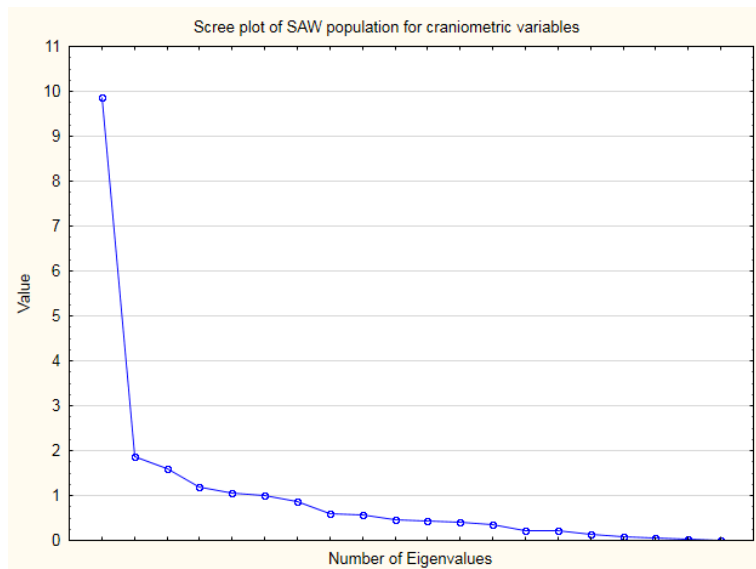
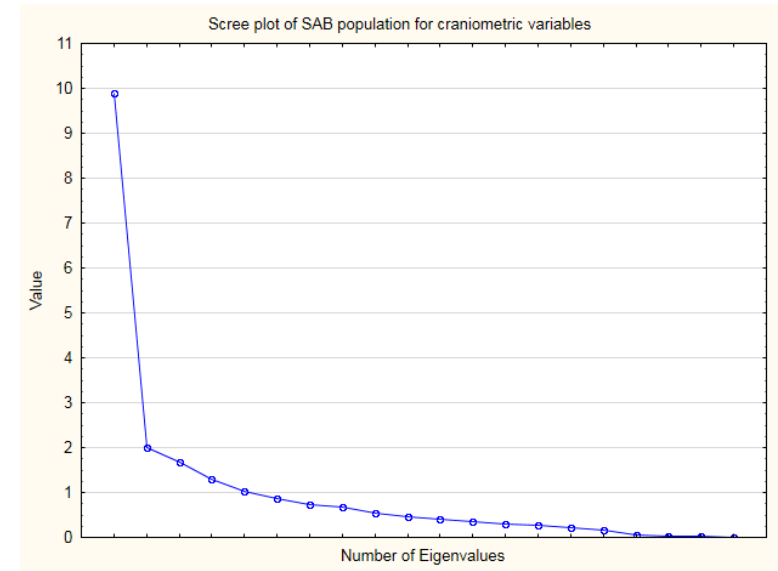
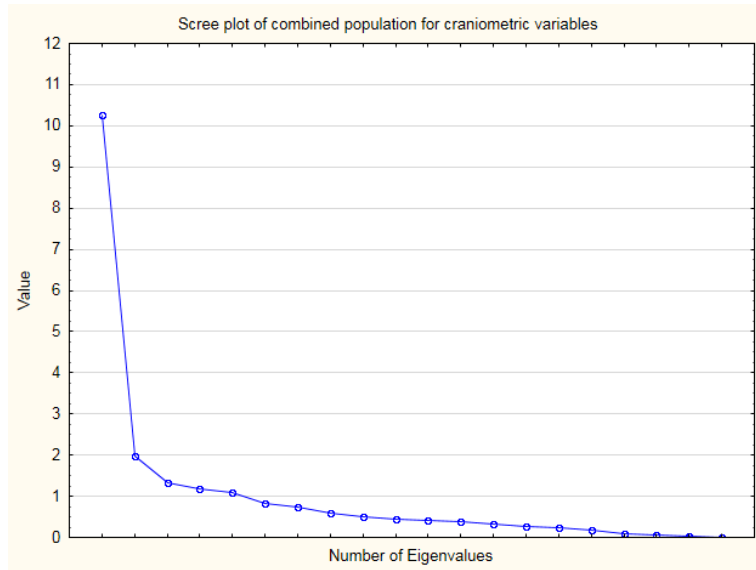
Pearson, K., (1899). Mathematical contributions to the theory of evolution. On the reconstruction of the stature of prehistoric races. *Philosophical Transactions of the Royal Society A*, [Online]. 192, pp 169-244. [Accessed 20 November 2018]. Available at:

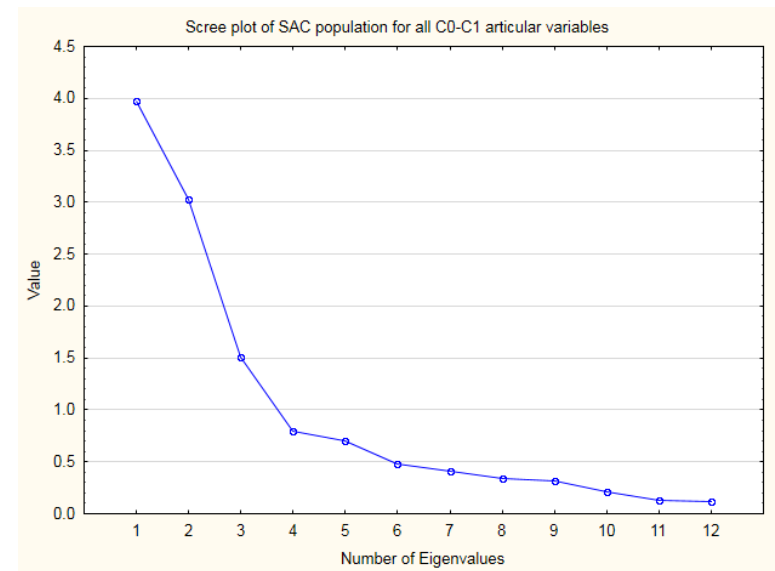
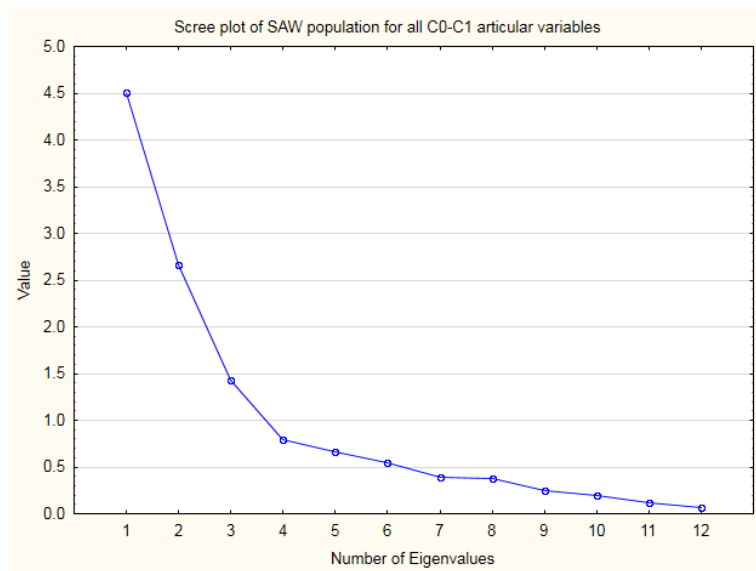
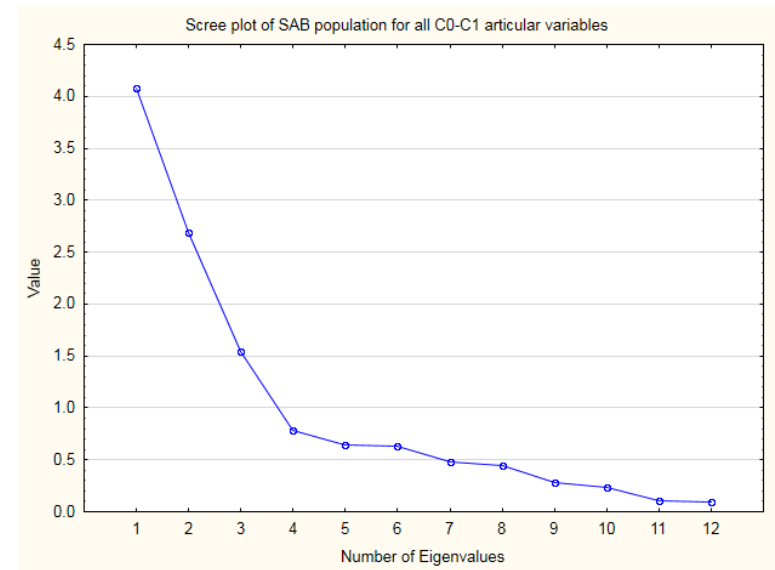
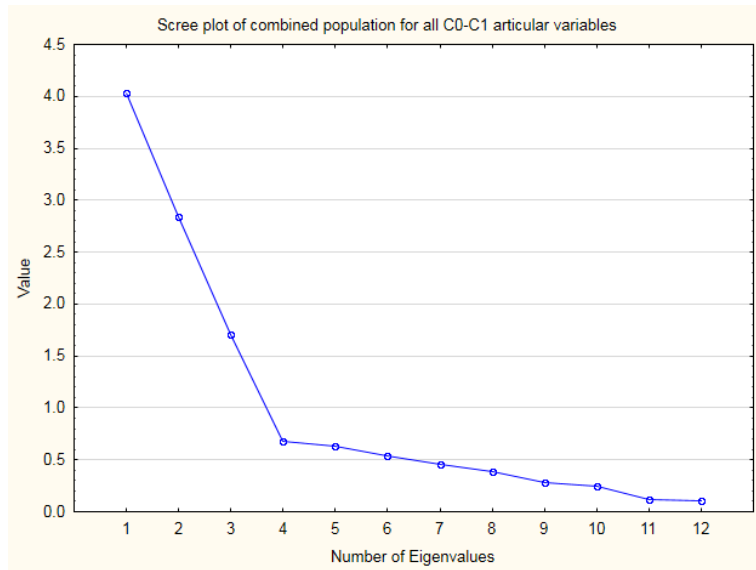
https://www.jstor.org/stable/90780?origin=JSTOR-pdf&seq=1#page_scan_tab_contents.

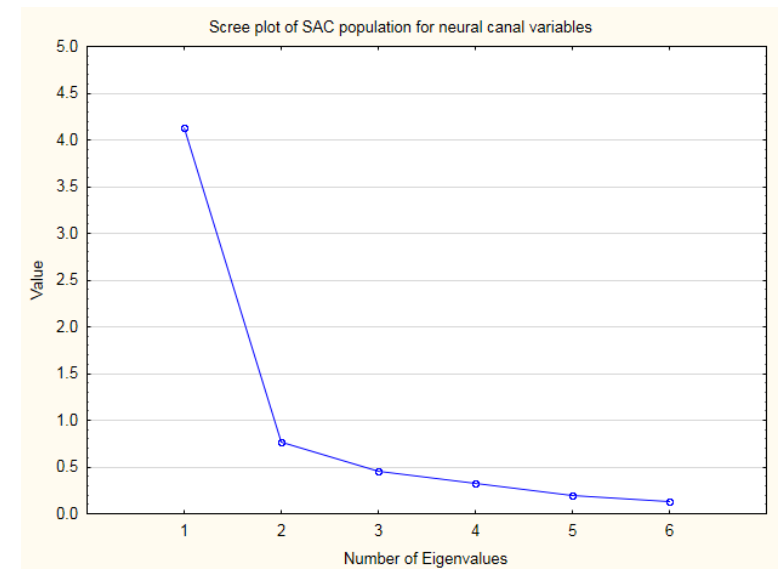
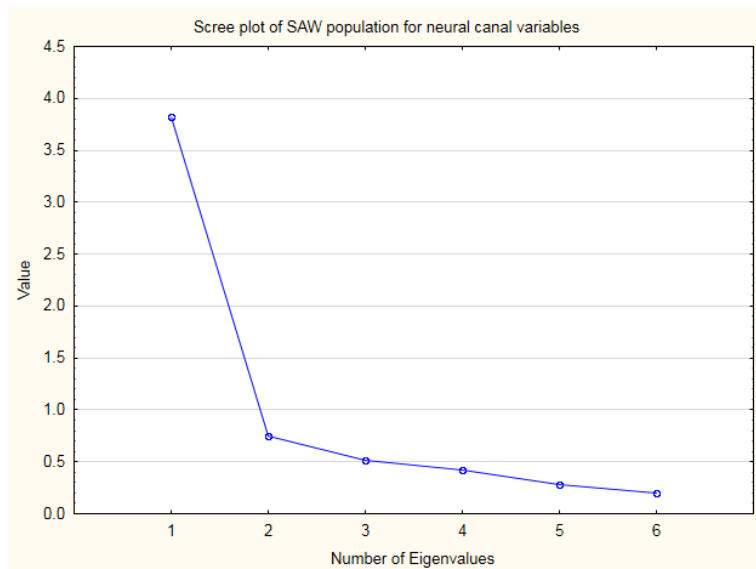
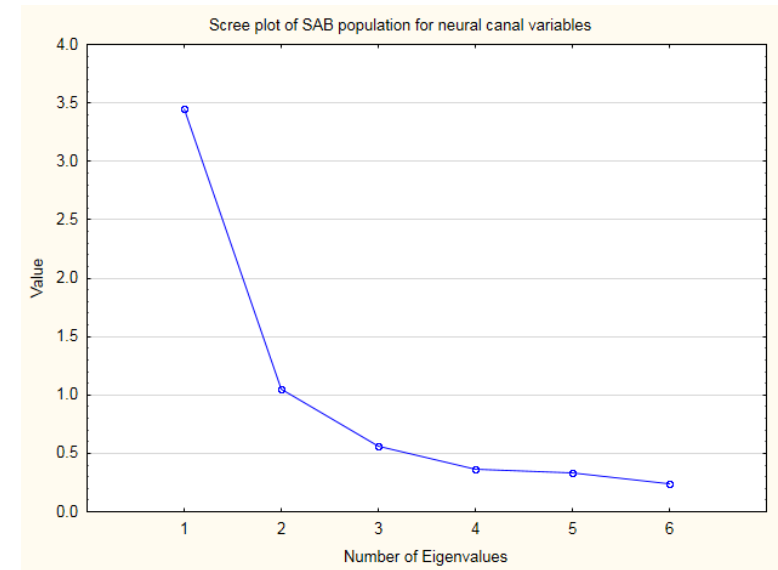
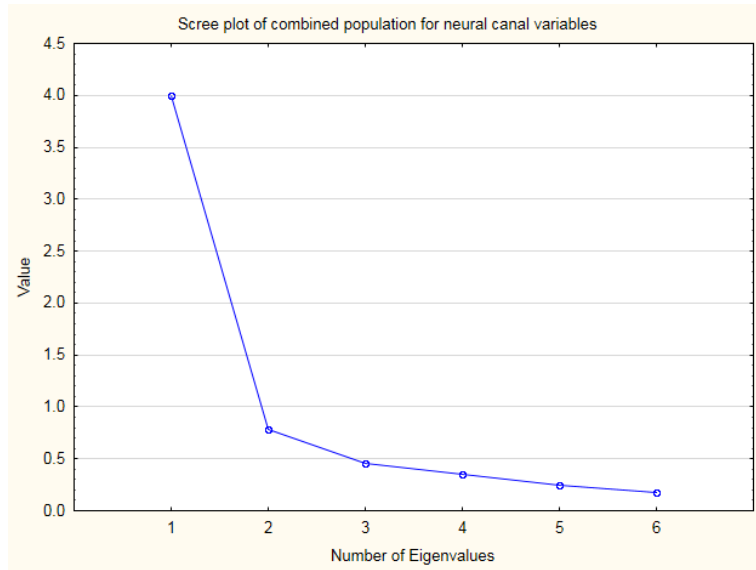
Pearson, J.C., Lemons, D., McGinnis, W. (2005). Modulating Hox gene functions during animal body patterning. *Nature Reviews Genetics*, 6(12), pp 893–904. doi: 10.1038/nrg1726.

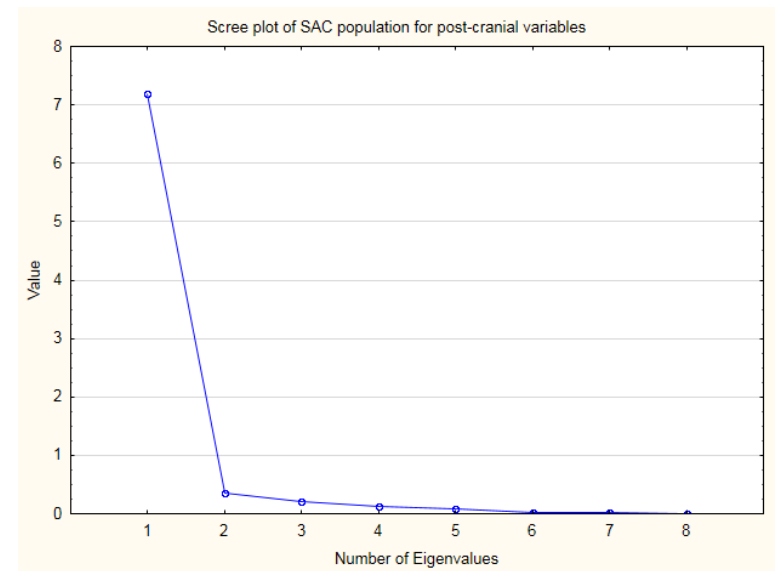
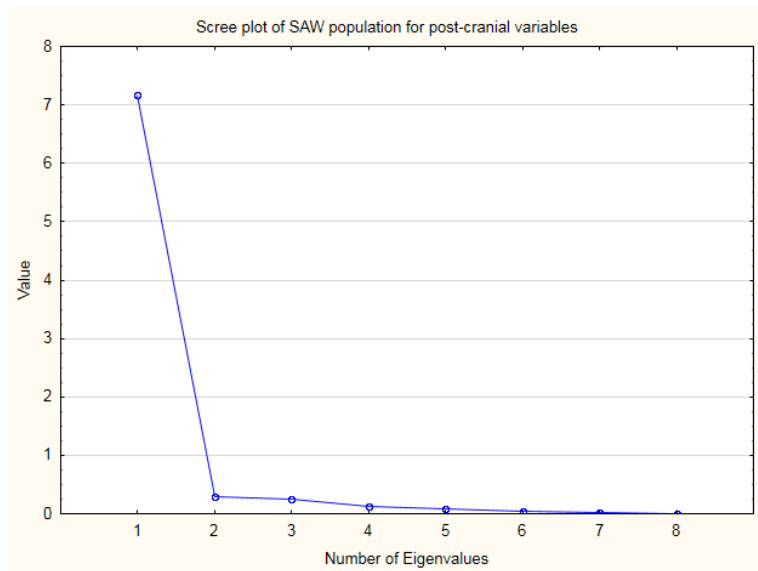
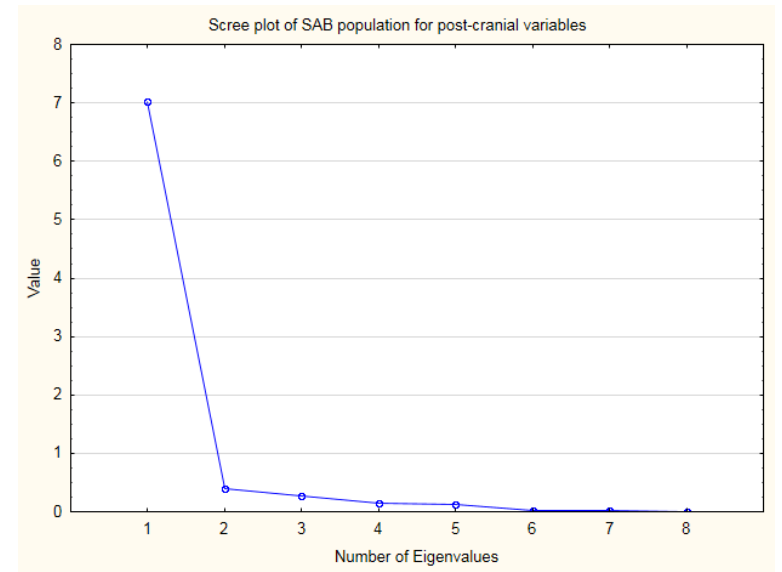
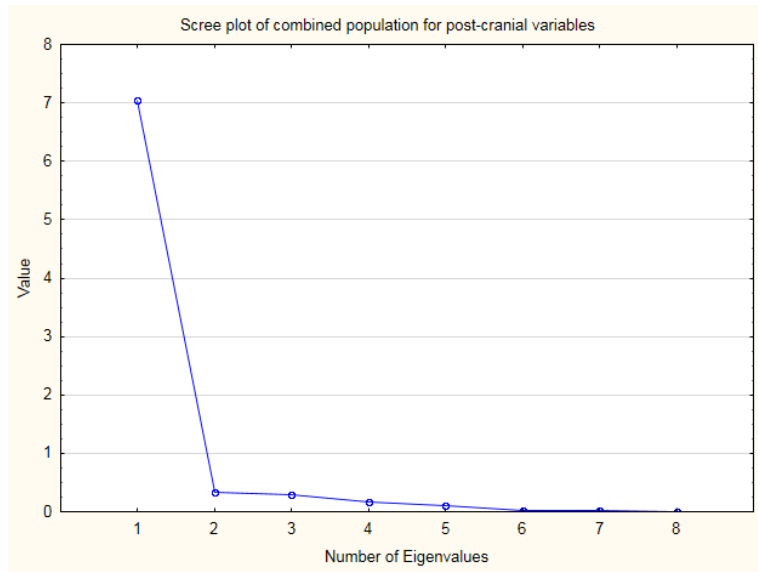
- Pelin, C., Zağyapan, R., Yazıcı, C., Kürkçüoğlu, A. (2010). Body height estimation from head and face dimensions: A Different Method. *Journal of Forensic Sciences*, 55(5), pp 1326–1330. doi:10.1111/j.1556-4029.2010.01429.x.
- Pfeiffer, S., Heinrich, J., Beresheim, A., Alblas, M. (2016). Cortical bone histomorphology of known-age skeletons from the Kirsten collection, Stellenbosch University, South Africa. *American Journal of Physical Anthropology*, 160(1), pp 137–147. doi:10.1002/ajpa.22951.
- Radoinova, D., Tenekedjiev, K., & Yordanov, Y. (2002). Stature estimation from long bone lengths in Bulgarians. *HOMO - Journal of Comparative Human Biology*, 52(3), pp 221–232. doi: 10.1078/0018-442x-00030.
- Relethford, J.H. (1994). Craniometric variation among modern human populations. *American Journal of Physical Anthropology*, 95(1), pp 53–62. doi:10.1002/ajpa.1330950105.
- Sauer, N.J. (1992). Forensic anthropology and the concept of race: if races don't exist, why are forensic anthropologists so good at identifying them? *Social Science & Medicine*, 34(2), pp. 107-111.
- Scheuer, L. & Black, S. (2000). *Developmental Juvenile Osteology*, 1st ed., California: Academic Press.
- Şakar, O., Sülün, T., İspirgi, E. (2008). Correlation of the gonial Angle size with residual ridge resorption in edentulous subjects, *Balkan Journal of Stomatology*, 12(1), pp. 38-41.
- Statistics South Africa. (2012). Census 2011: Statistical release. Pretoria: Statistics South Africa.
- Telkkä, A. (1950). On the prediction of human stature from the long bones, *Acta Anatomica*, 9, pp. 103-117. <https://doi.org/10.1159/000140434>.
- Trotter, M. & Gleser, G.C. (1958). A re-evaluation of estimation of stature based on measurements of stature taken during life and of long bones after death, *American Journal of Physical Anthropology*, 16, pp. 79-123. <https://doi.org/10.1002/ajpa.1330160106>.
- University of Cape Town (UCT) Division of Clinical Anatomy and Biological Anthropology 2018, UCT Human Skeletal Collection, accessed 6 June 2018, <<http://www.anatomybioanth.uct.ac.za/uct-human-skeletal-collection>>
- White, T.D., Black, M.T., Folkens, P.A. (2011). *Human Osteology*, 3rd ed., Academic Press.
- Williams, P.L., Bannister, L.H., Berry, M.M., Collins, P., Dyson, M., Dussek, J.E., Ferguson, M.W. (1995). *Gray's Anatomy*, 38th ed., Edinburgh: Churchill Livingstone.

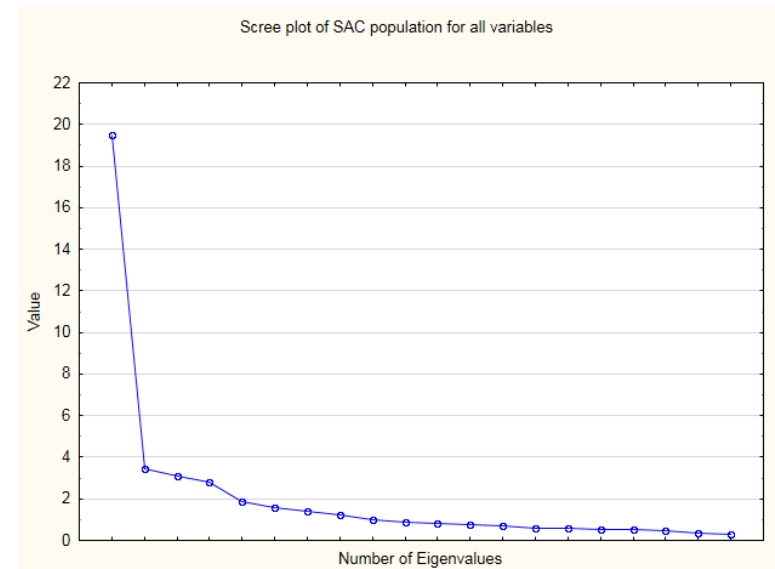
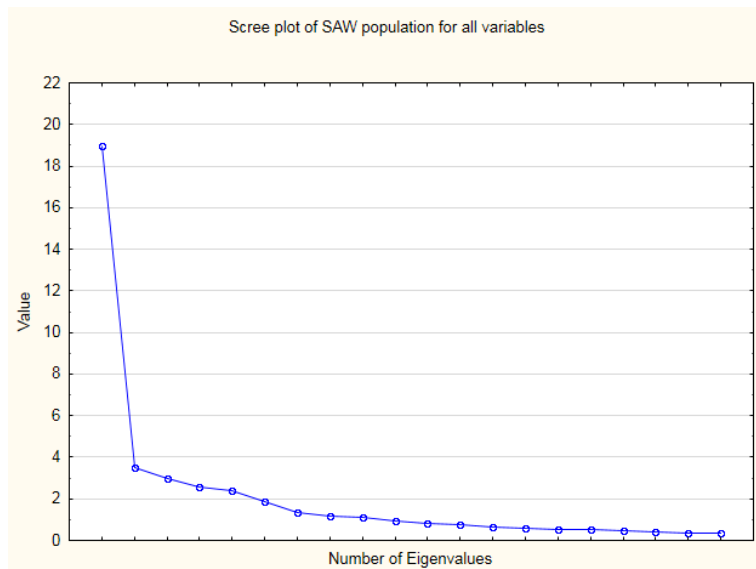
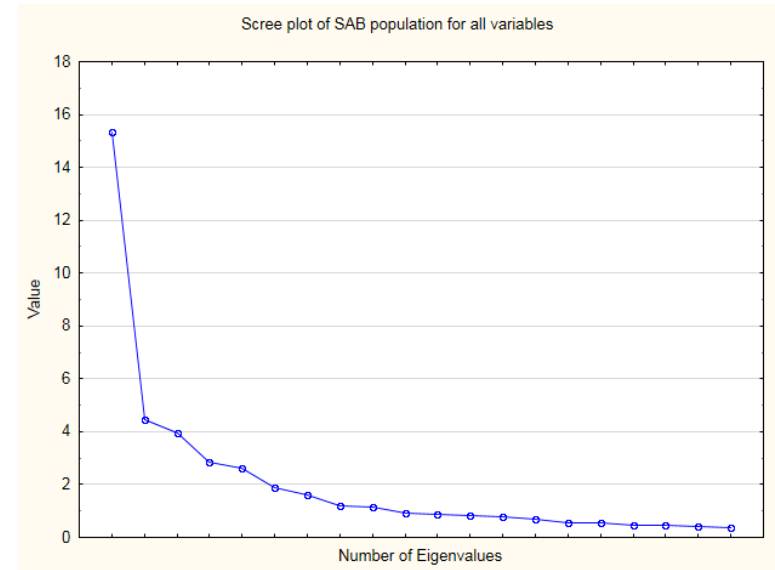
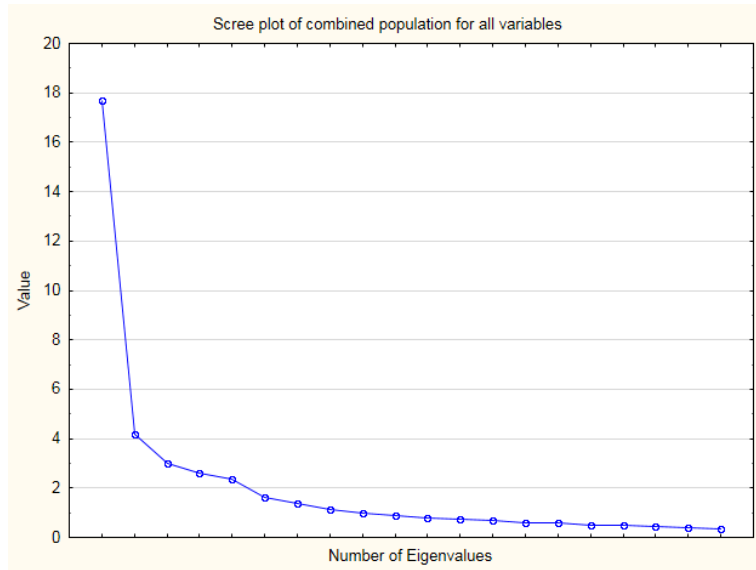
APPENDIX A







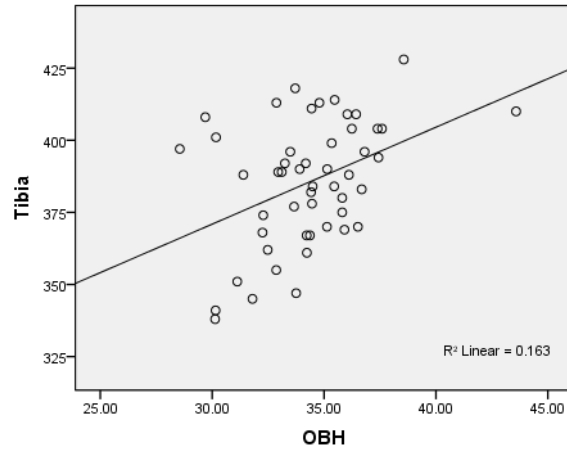




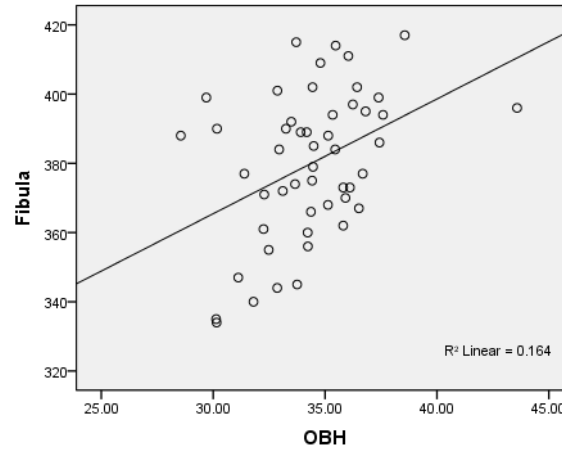
APPENDIX B

7.1 SOUTH AFRICAN BLACK MALES

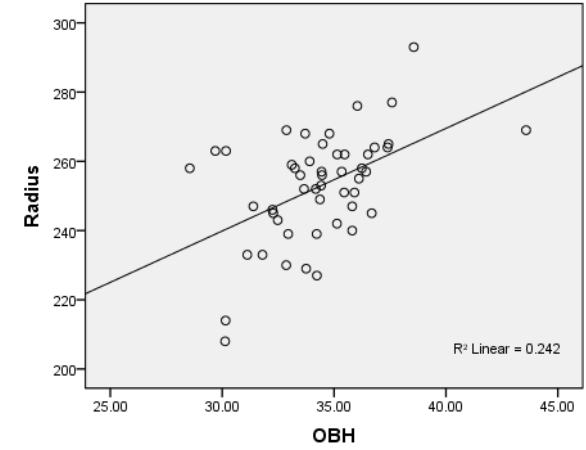
OBH-TIBXLN correlation of SAB males



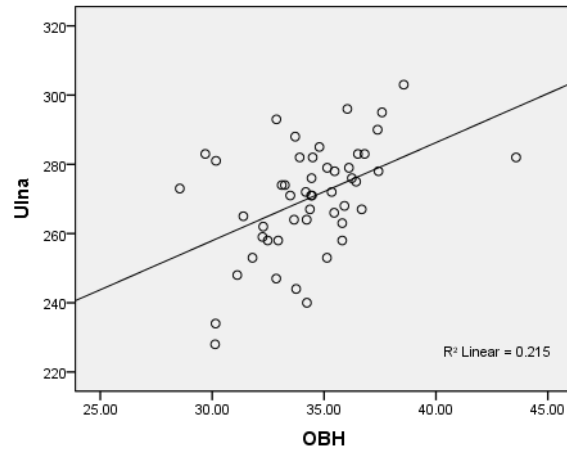
OBH-FIBXLN correlation of SAB males



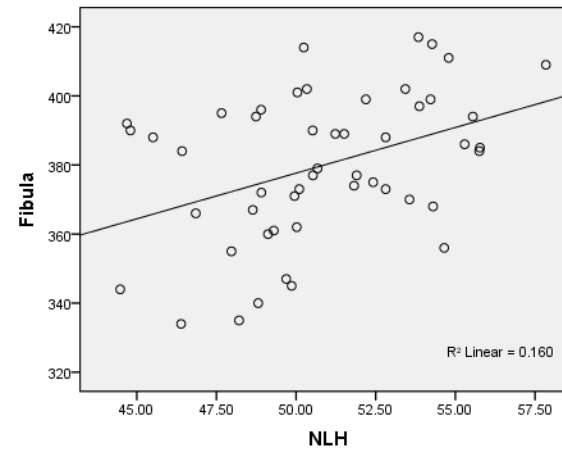
OBH-RADXLN correlation of SAB males



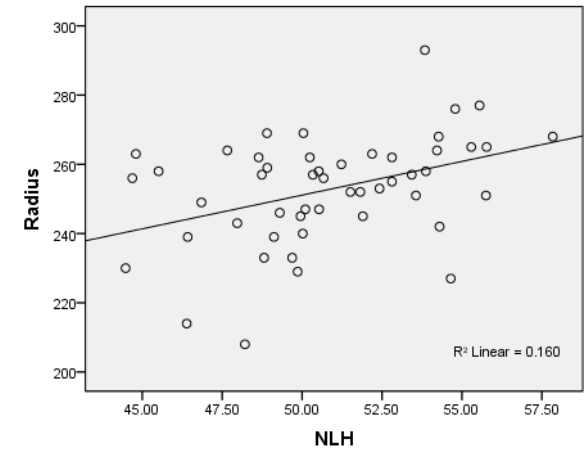
OBH-ULNXLN correlation of SAB males



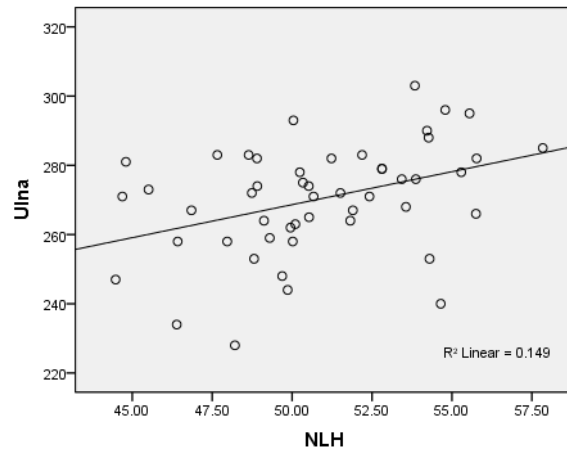
NLH-FIBXLN correlation of SAB males



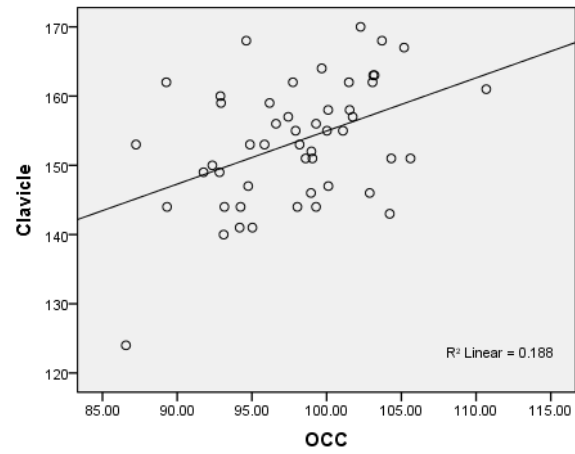
NLH-RADXLN correlation of SAB males



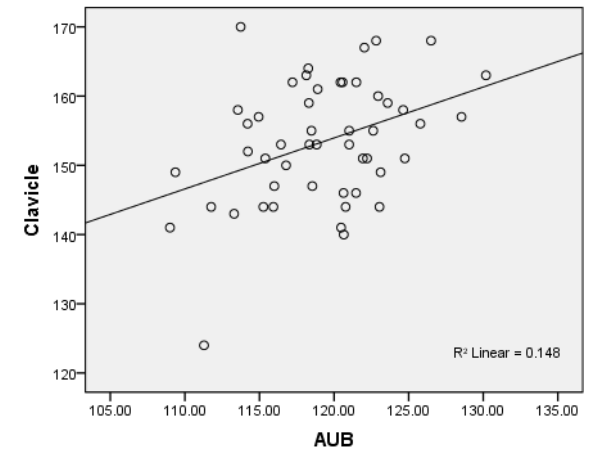
NLH-ULNXLN correlation of SAB males



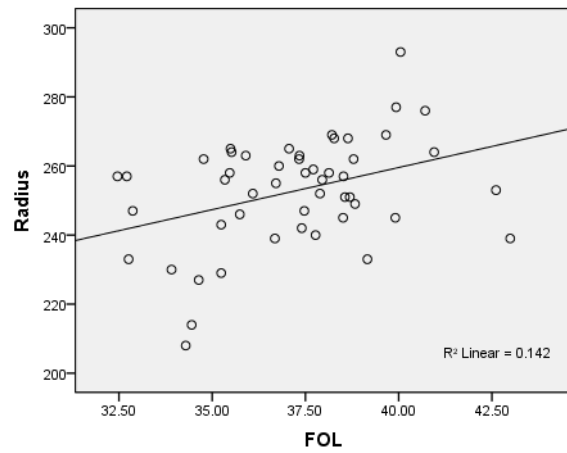
NLH-CLAXLN correlation of SAB males



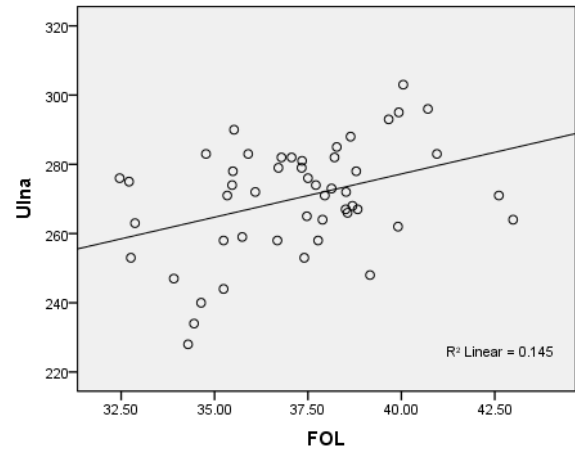
AUB-CLAXLN correlation of SAB males



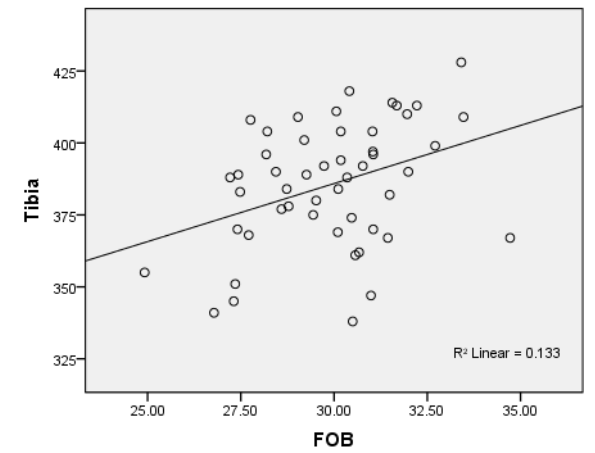
FOL-RADXLN correlation of SAB males



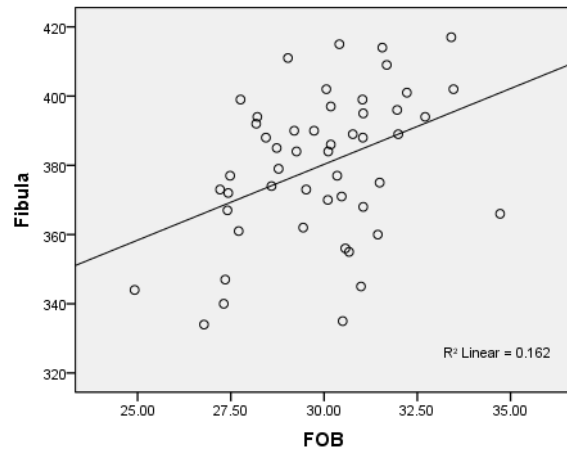
FOL-ULNXLN correlation of SAB males



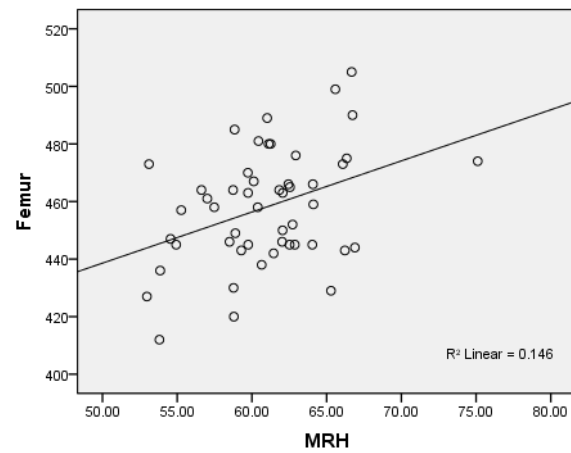
FOB-TIBXLN correlation of SAB males



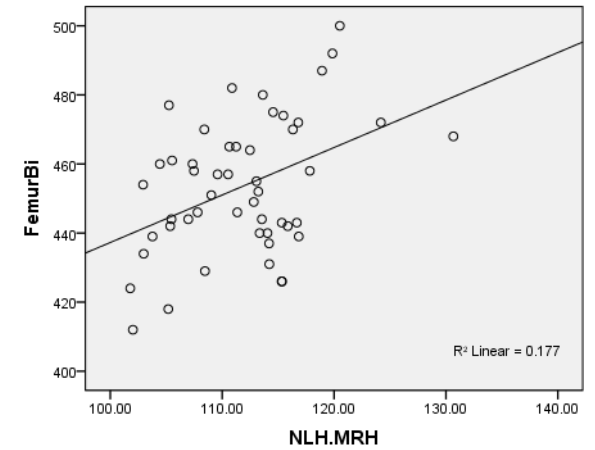
FOB-FIBXLN correlation of SAB males



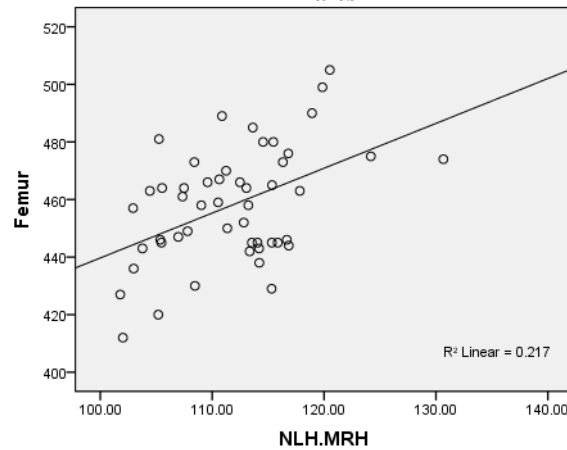
MRH-FEMXLN correlation of SAB males



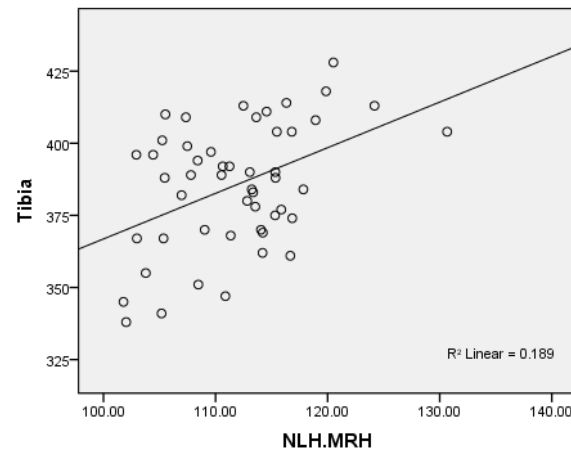
NLH.MRH-FEMBLN correlation of SAB males



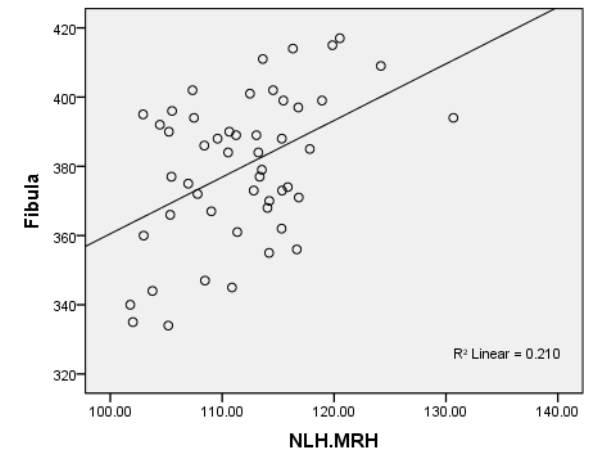
NLH.MRH-FEMXLN correlation of SAB males



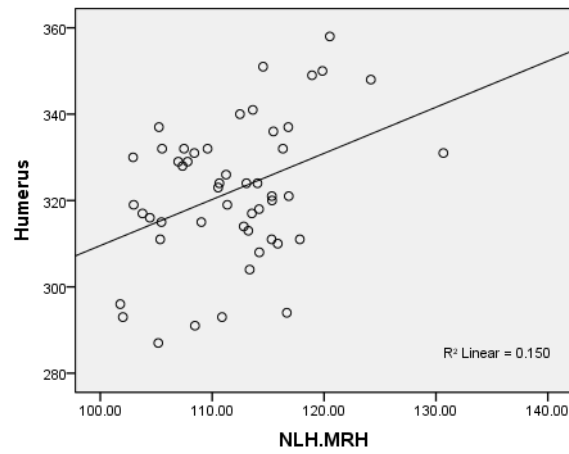
NLH.MRH-TIBXLN correlation of SAB males



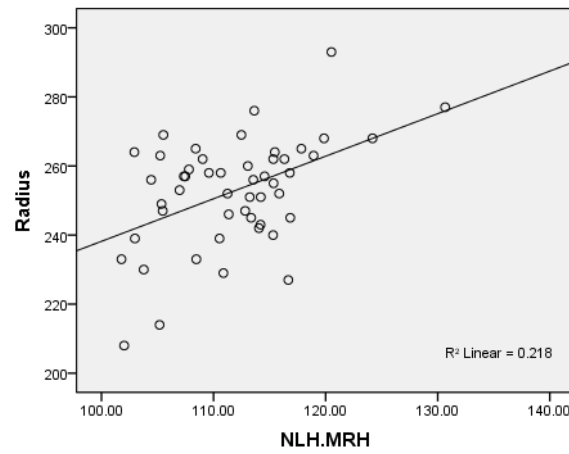
NLH.MRH-FIBXLN correlation of SAB males



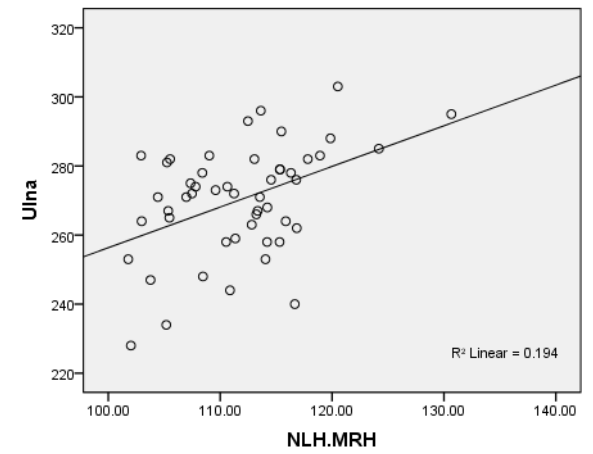
NLH.MRH-HUMXLN correlation of SAB males



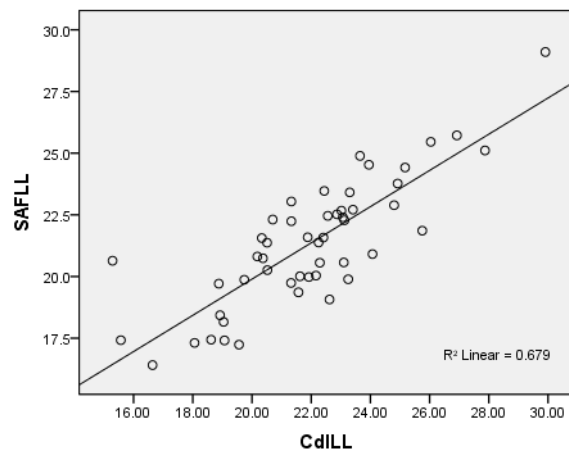
NLH.MRH-RADXLN correlation of SAB males



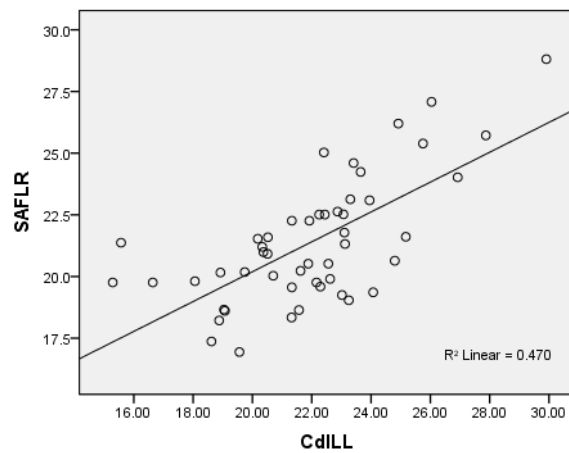
NLH.MRH-ULNXLN correlation of SAB males



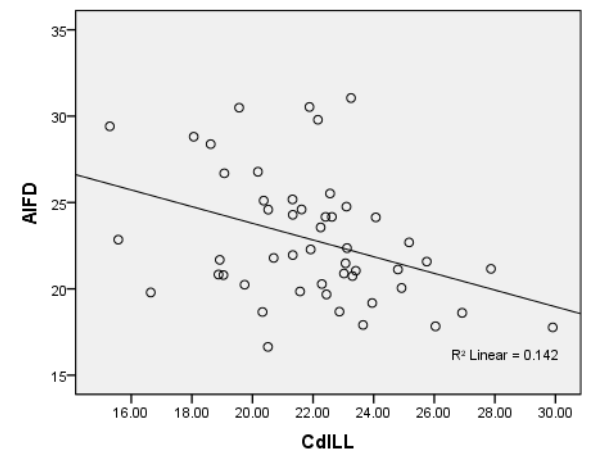
CdILL-SAFLL correlation of SAB males



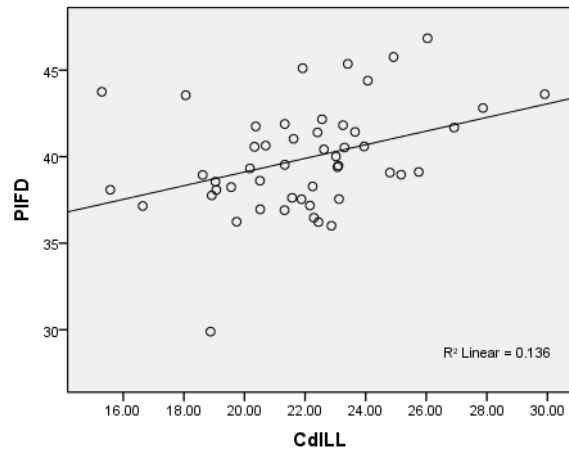
CdILL- SAFLR correlation of SAB males



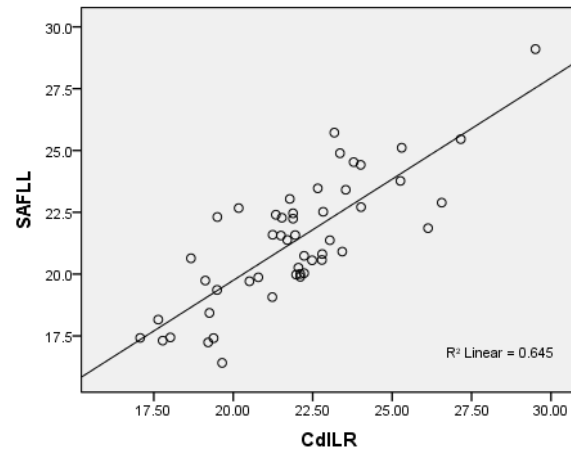
CdILL-AIFD correlation of SAB males



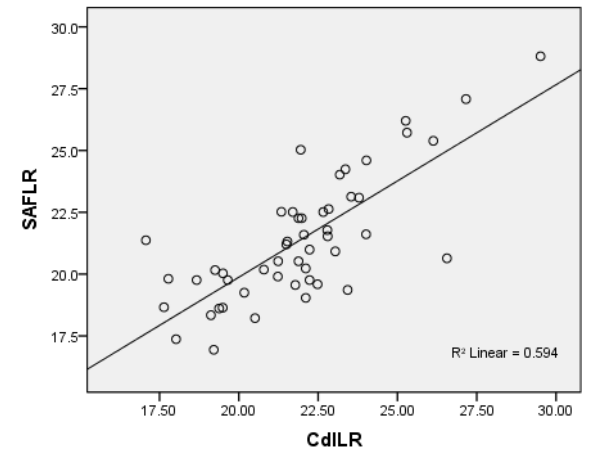
CdILL-PIFD correlation of SAB males



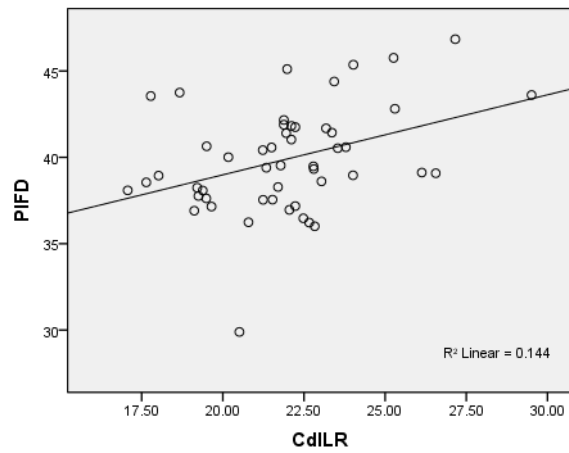
CdILR-SAFLL correlation of SAB males



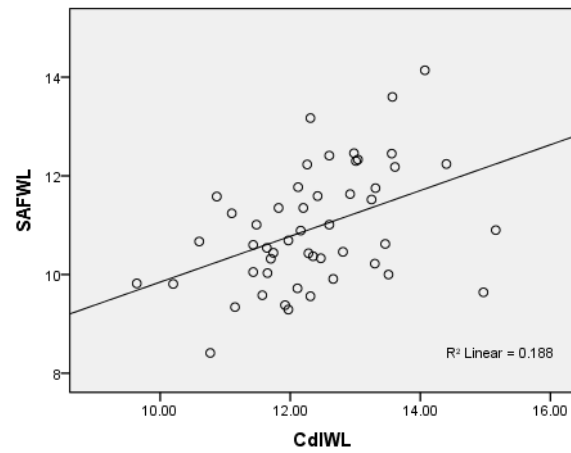
CdILR-SAFLR correlation of SAB males



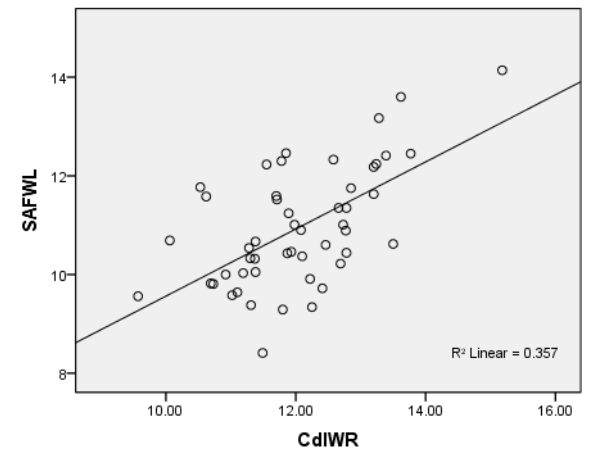
CdILR-PIFD correlation of SAB males



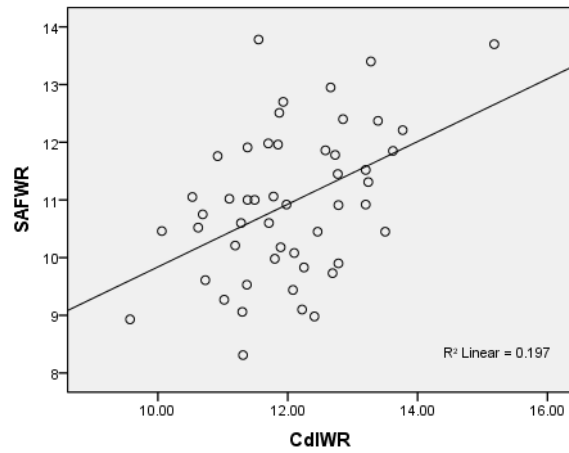
CdIWL-SAFWL correlation of SAB males



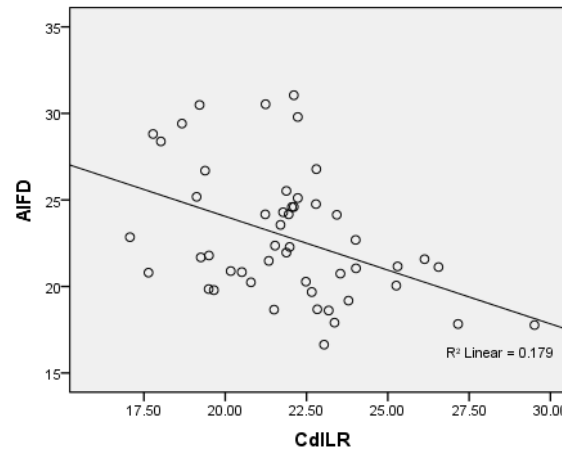
CdIWR-SAFWL correlation of SAB males



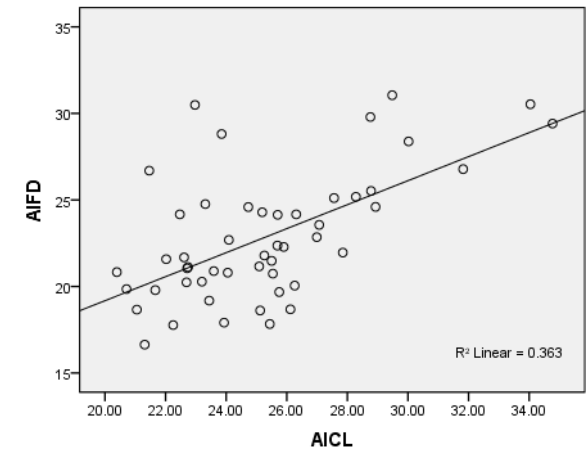
CdIWR-SAFWR correlation of SAB males



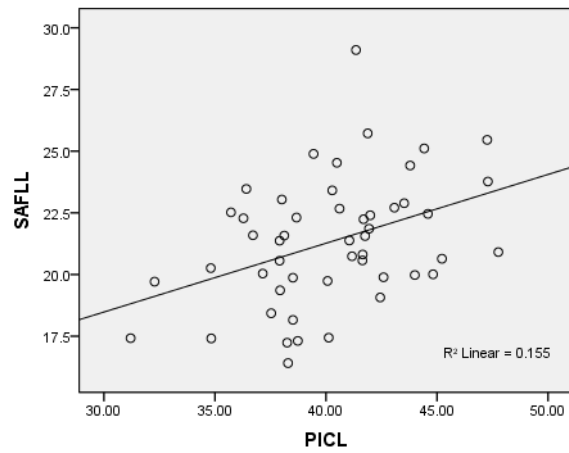
CdILR-AIFD correlation of SAB males



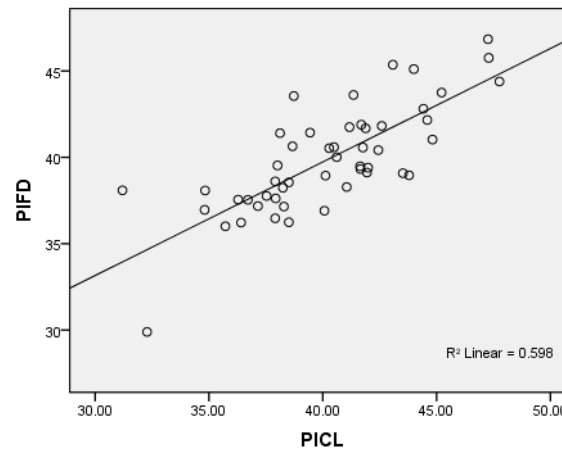
AICL-AIFD correlation of SAB males



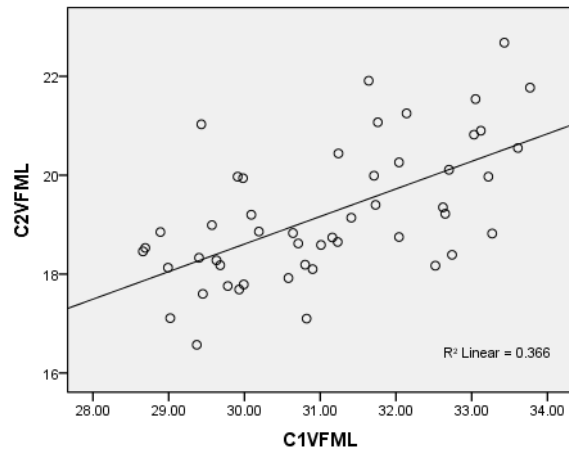
PICL-SAFLL correlation of SAB males



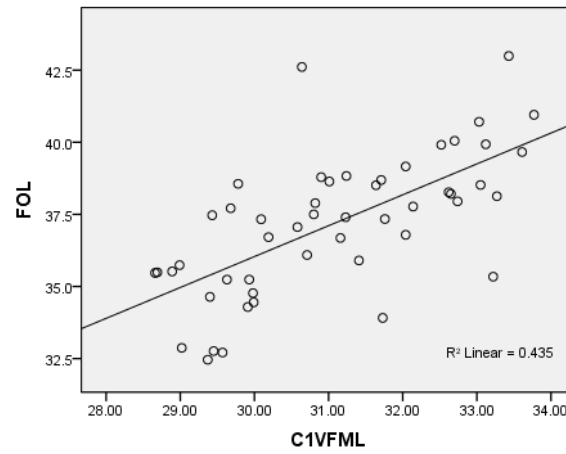
PICL-PIFD correlation of SAB males



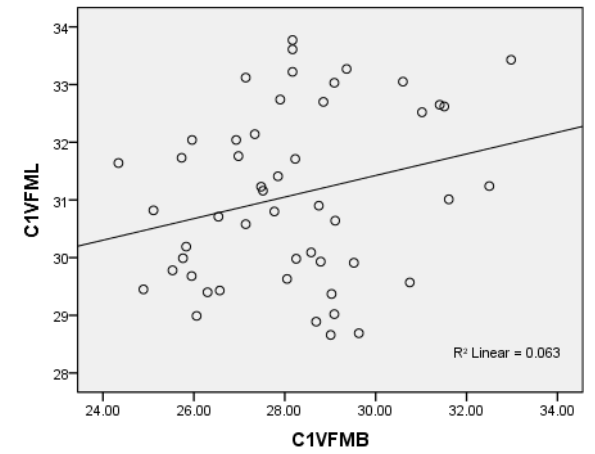
C1VFML-C2VFML correlation of SAB males



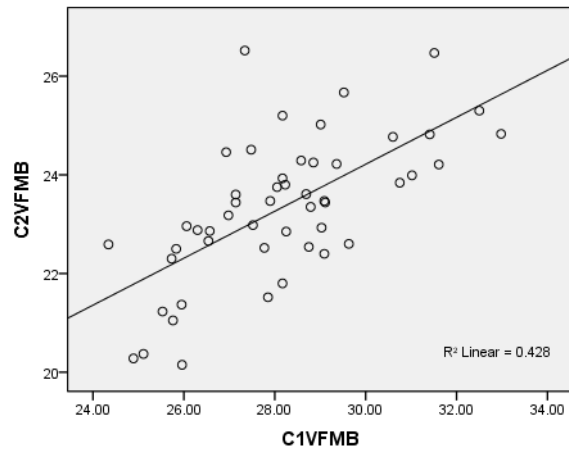
C1VFML-FOL correlation of SAB males



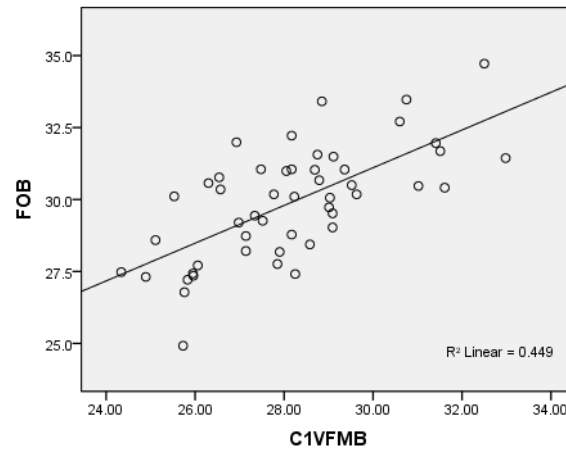
C1VFMB-C1VFML correlation of SAB males



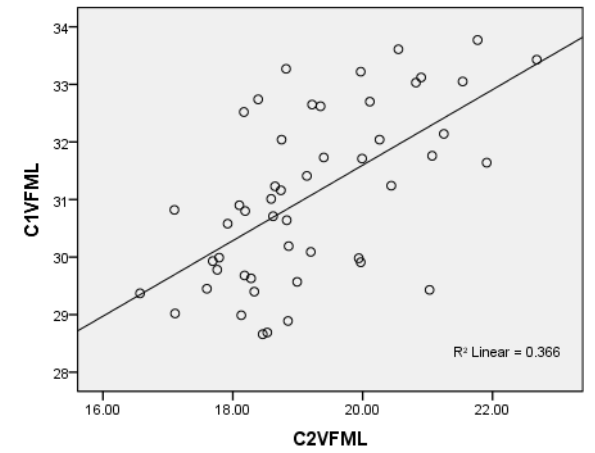
C1VFMB-C2VFMB correlation of SAB males



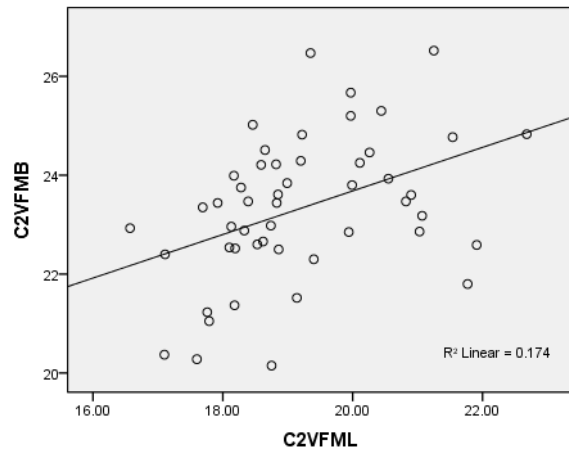
C1VFMB-FOB correlation of SAB males



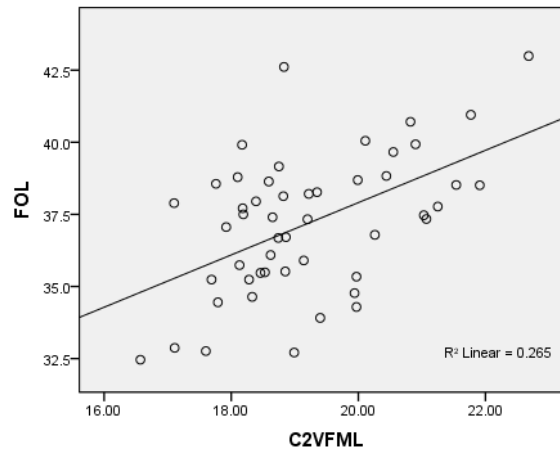
C2VFML-C1VFML correlation of SAB males



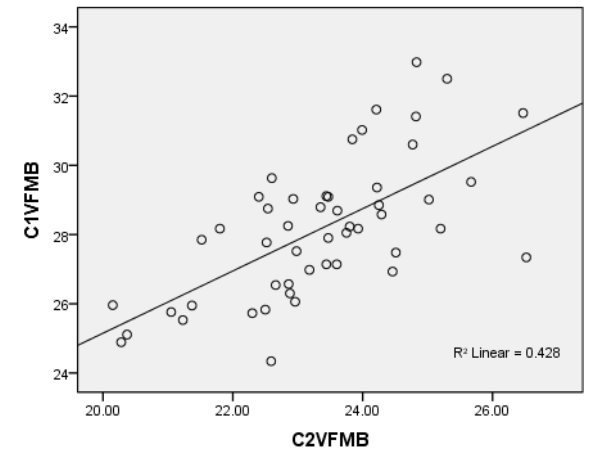
C2VFML-C2VFMB correlation of SAB males



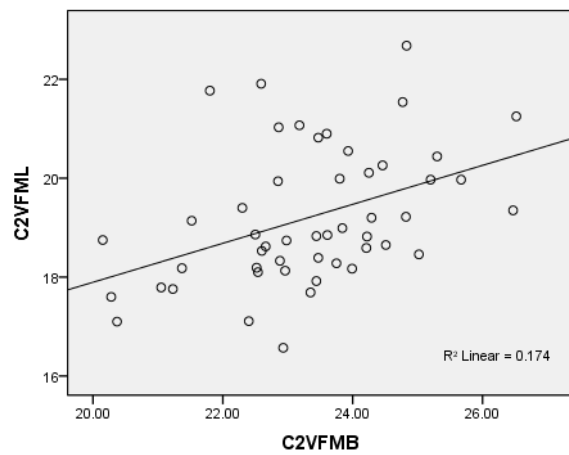
C2VFML-FOL correlation of SAB males



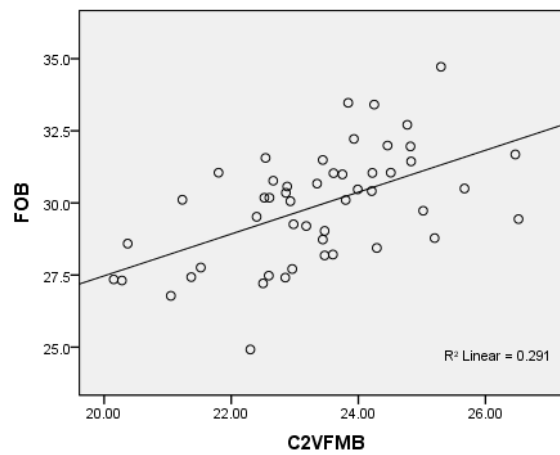
C2VFMB-C1VFMB correlation of SAB males



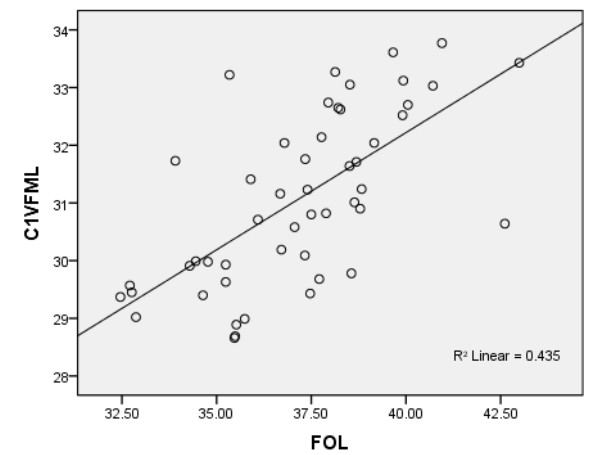
C2VFMB-C2VFML correlation of SAB males



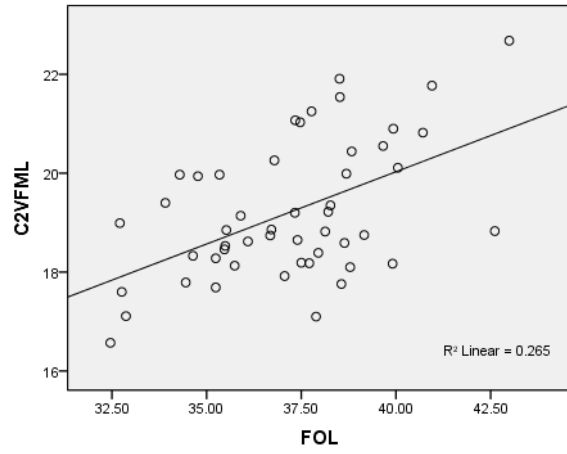
C2VFMB-FOB correlation of SAB males



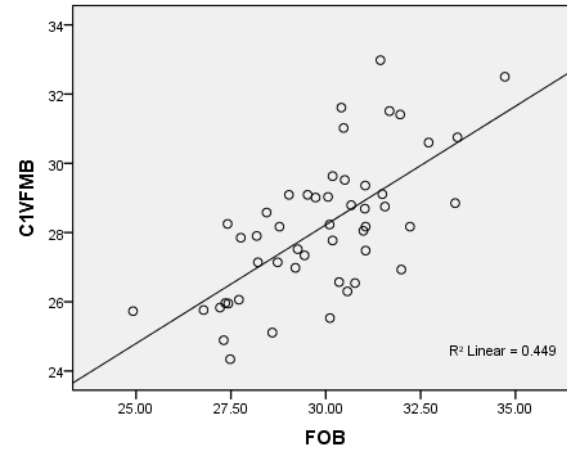
FOL-C1VFML correlation of SAB males



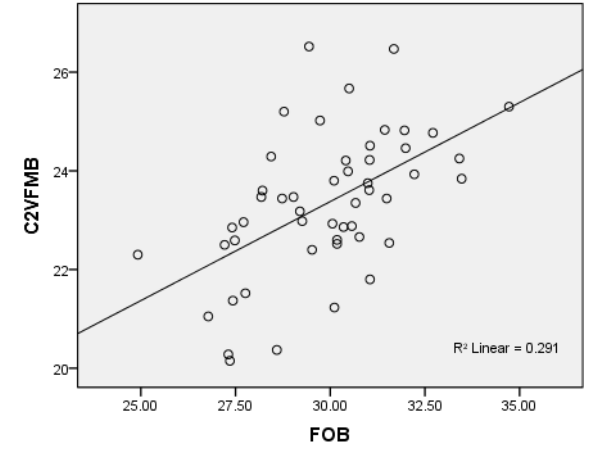
FOL-C2VFML correlation of SAB males



FOL-C1VFMB correlation of SAB males

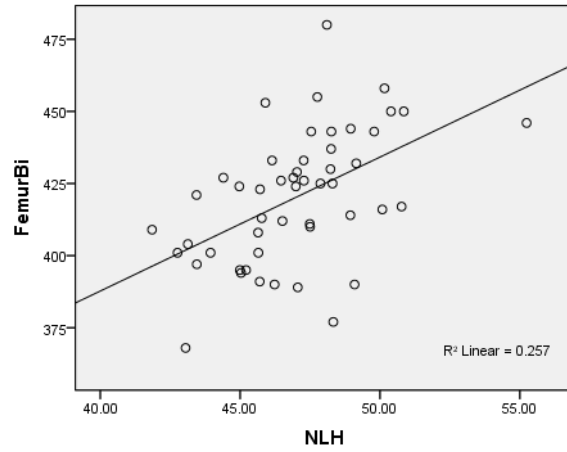


FOL-C2VFMB correlation of SAB males

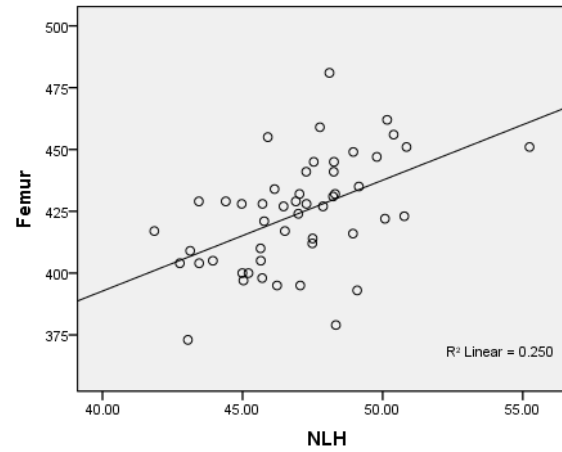


7.2 SOUTH AFRICAN BLACK FEMALES

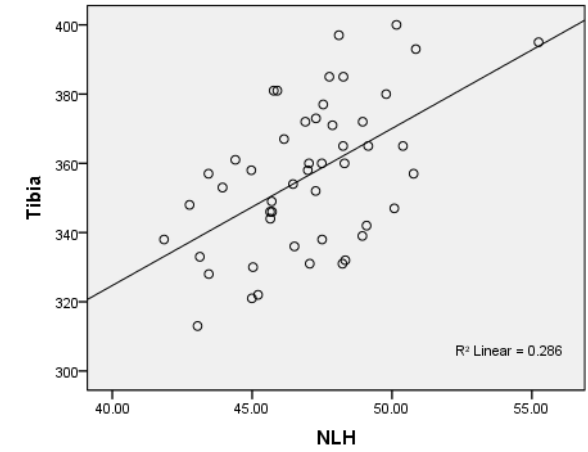
NLH-FEMBLN correlation of SAB females



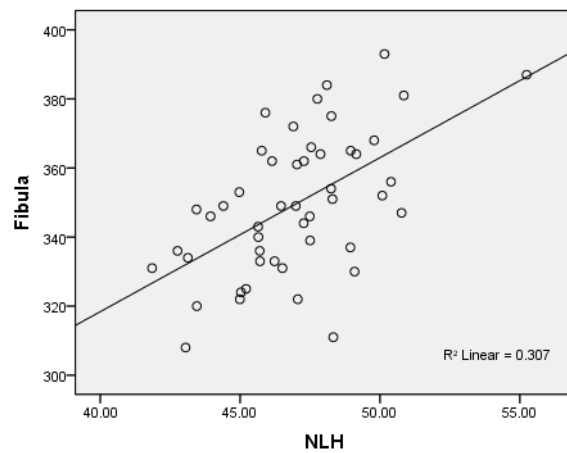
NLH-FEMXLN correlation of SAB females



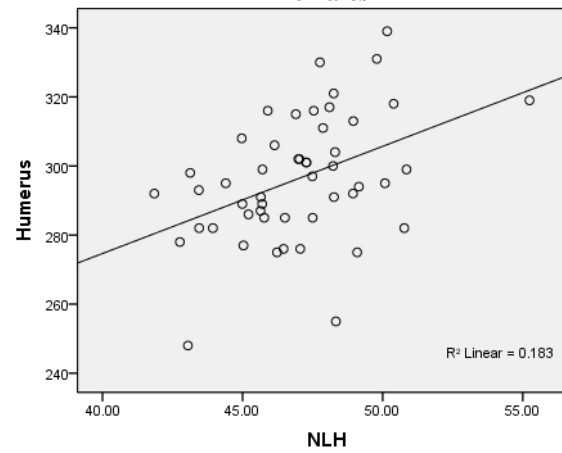
NLH-TIBXLN correlation of SAB females



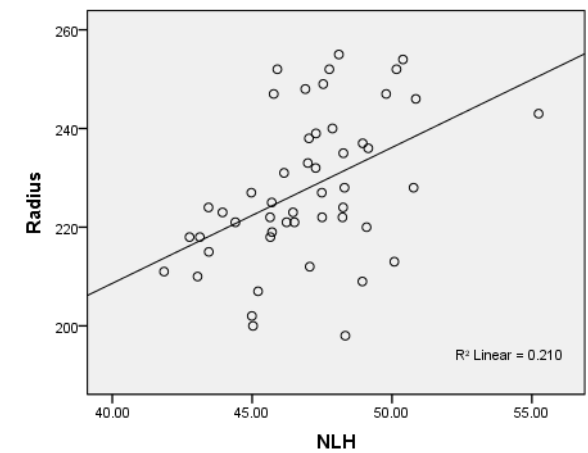
NLH-FIBXLN correlation of SAB females



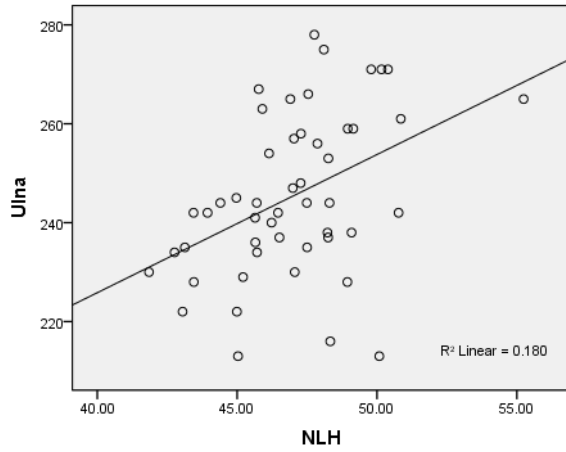
NLH-HUMXLN correlation of SAB females



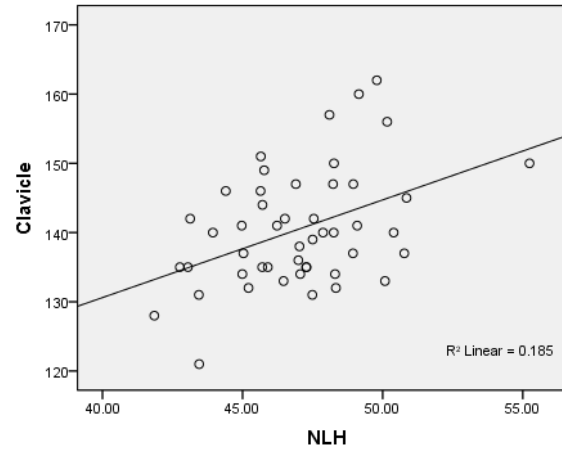
NLH-RADXLN correlation of SAB females



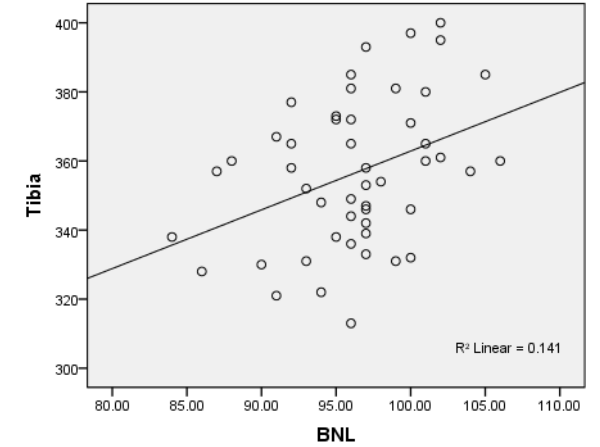
NLH-ULNXLN correlation of SAB females



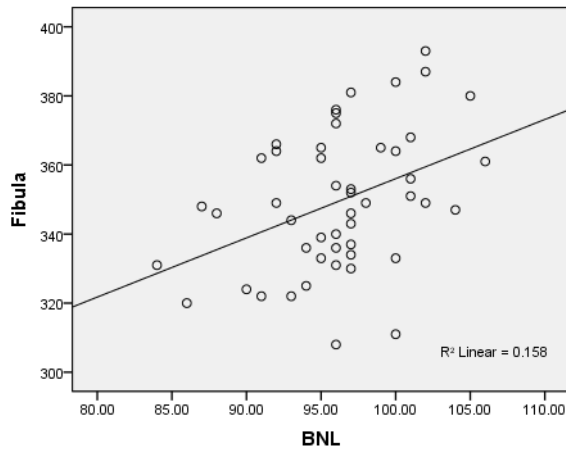
NLH-CLAXLN correlation of SAB females



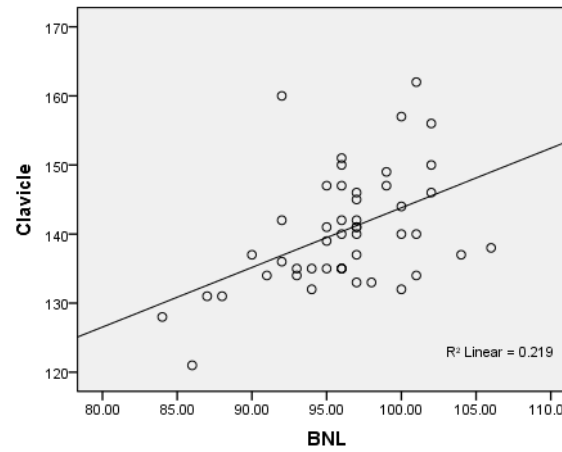
BNL-TIBXLN correlation of SAB females



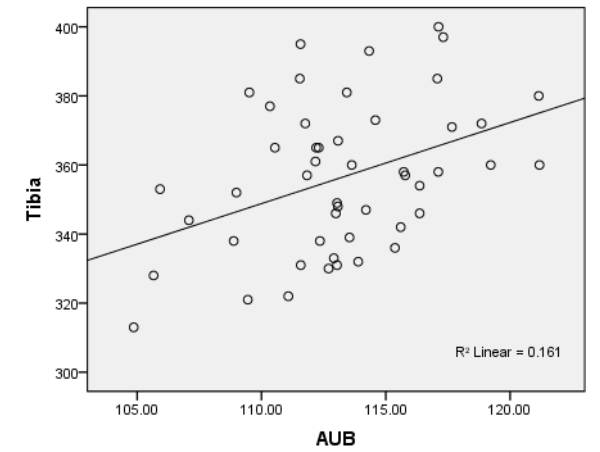
BNL-FIBXLN correlation of SAB females



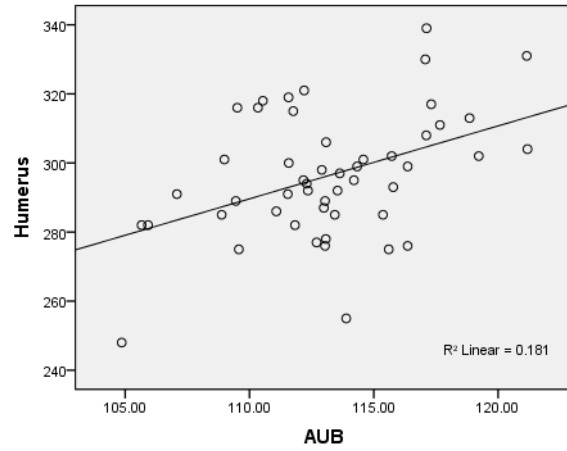
BNL-CLAXLN correlation of SAB females



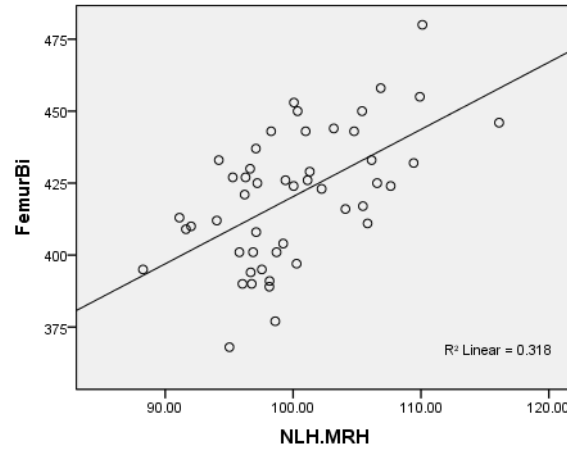
AUB-TIBXLN correlation of SAB females



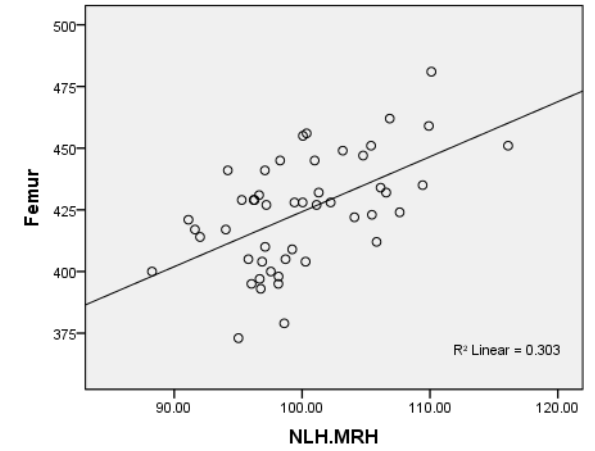
AUB-HUMXLN correlation of SAB females



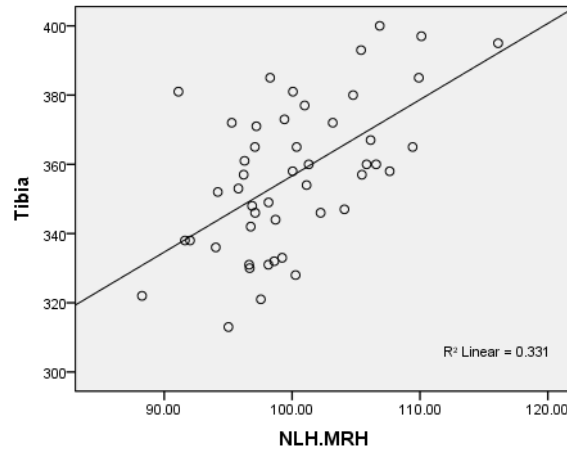
NLH.MRH-FEMBLN correlation of SAB females



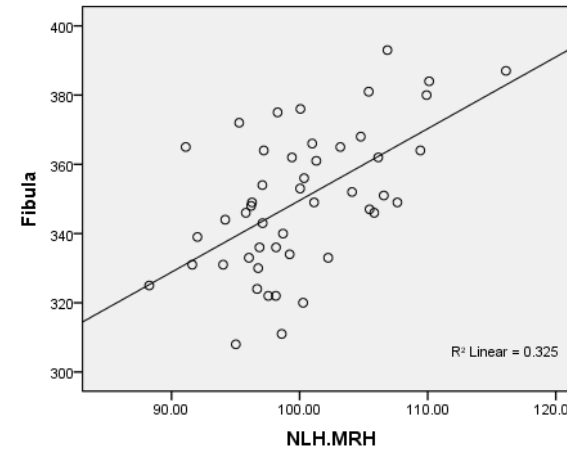
NLH.MRH-FEMXLN correlation of SAB females



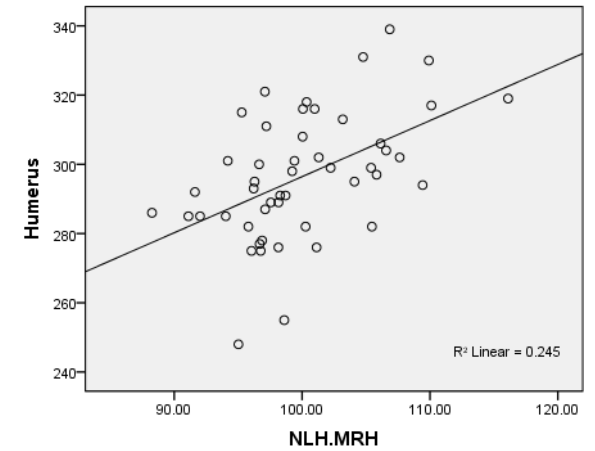
NLH.MRH-TIBXLN correlation of SAB females



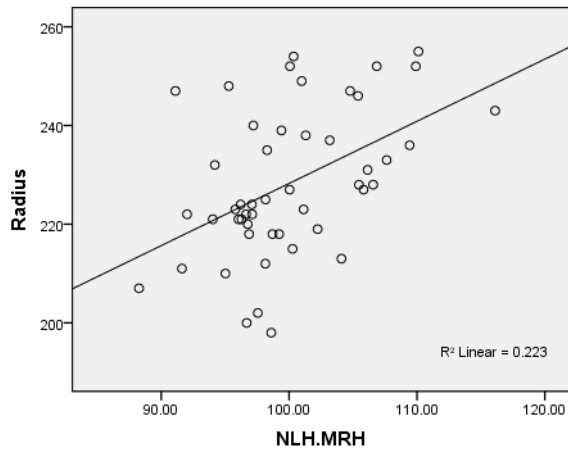
NLH.MRH-FIBXLN correlation of SAB females



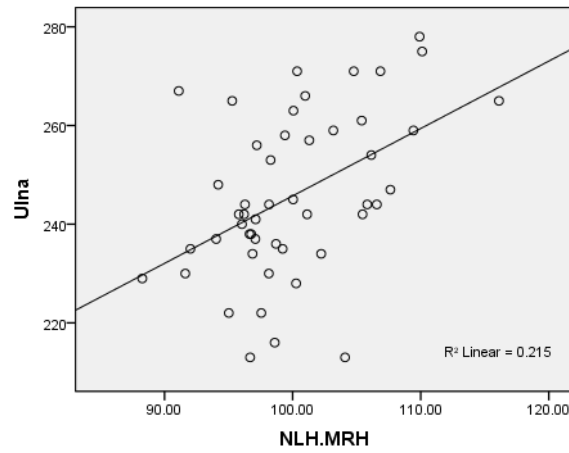
NLH.MRH-HUMXLN correlation of SAB females



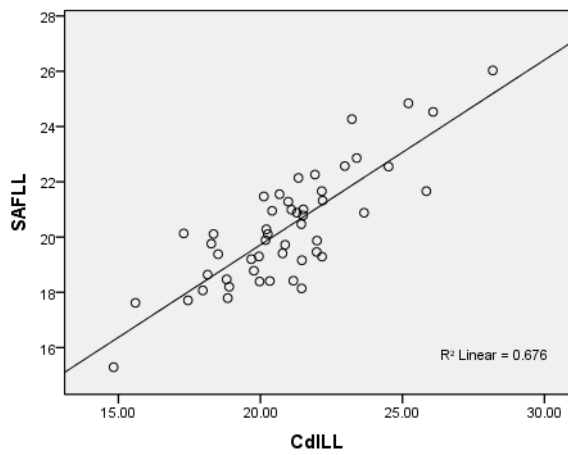
NLH.MRH-RADXLN correlation of SAB females



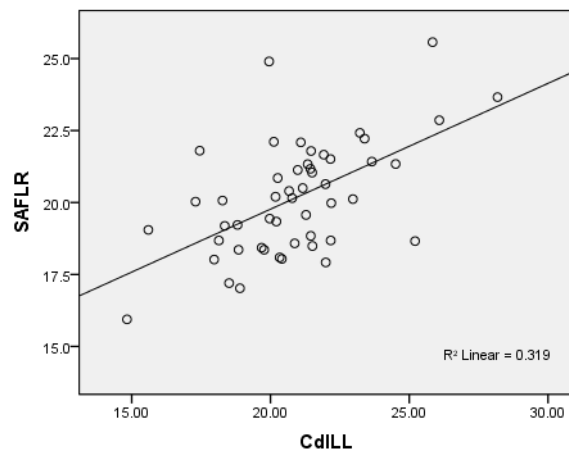
NLH.MRH-ULNXLN correlation of SAB females



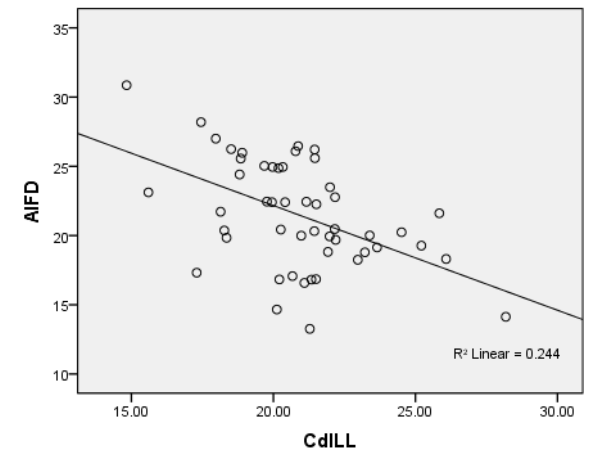
CdILL-SAFLL correlation of SAB females

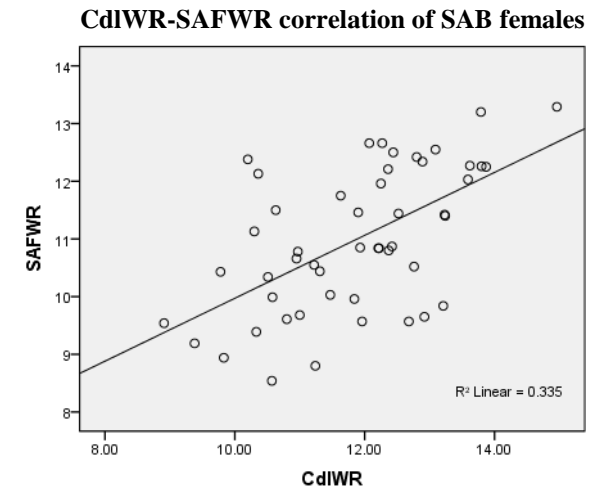
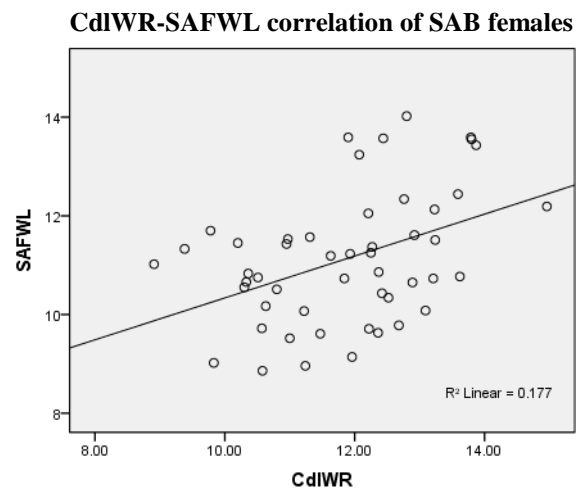
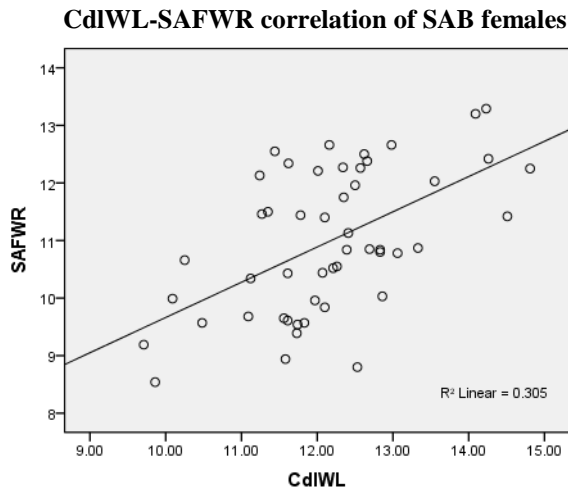
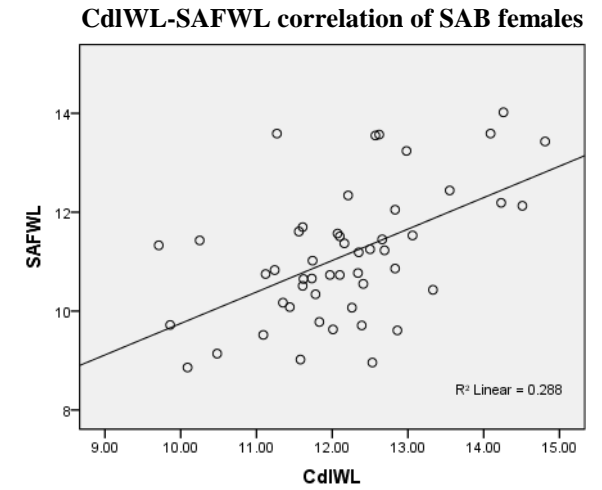
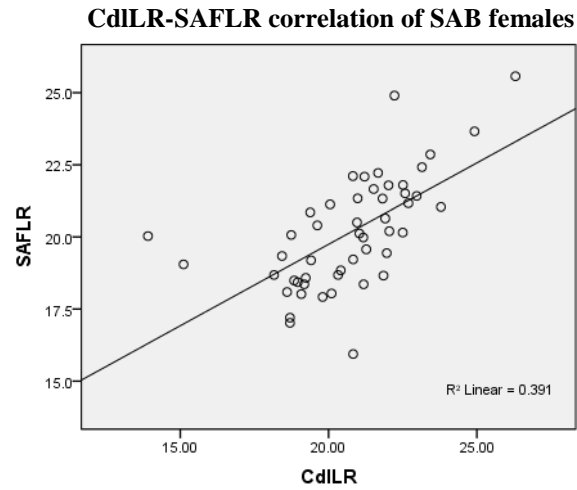
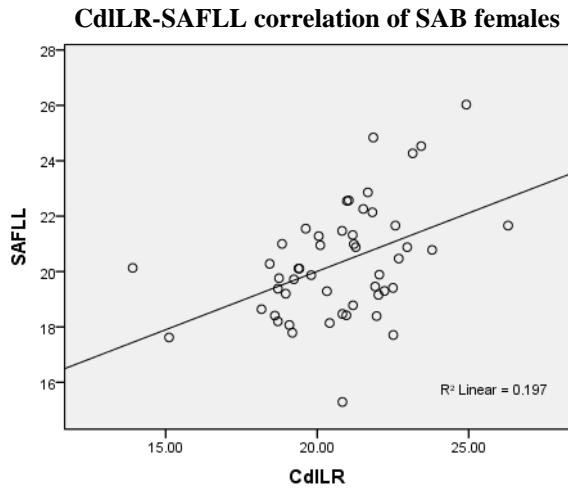


CdILL-SAFLL correlation of SAB females

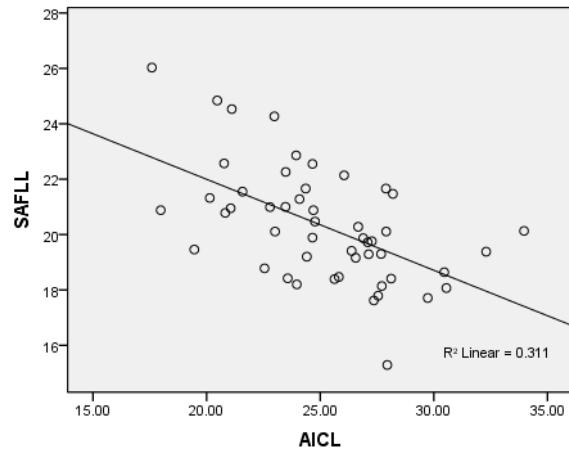


CdILL-AIFD correlation of SAB females

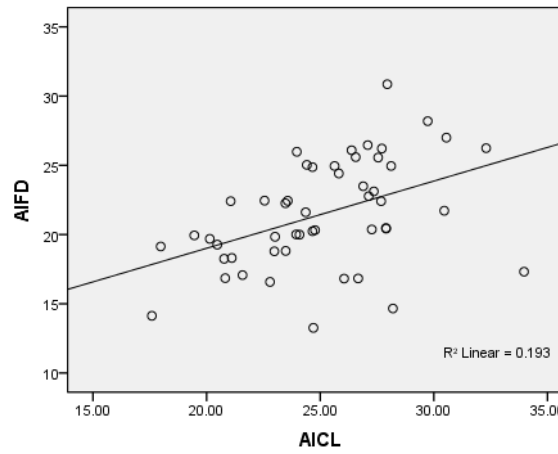




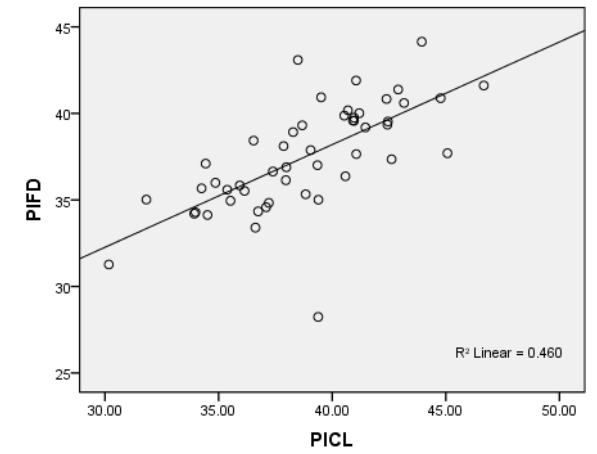
AICL-SAFLL correlation of SAB females



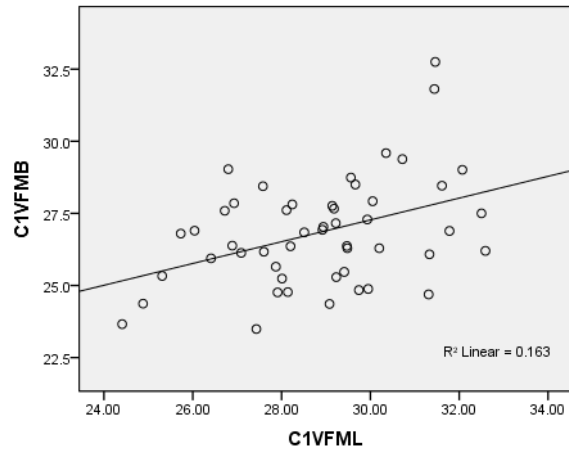
AICL-AIFD correlation of SAB females



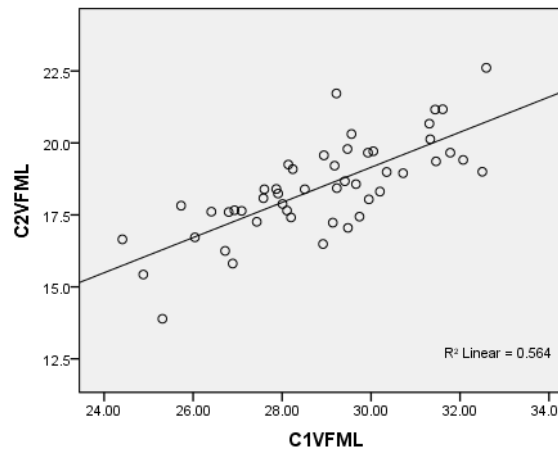
PICL-PIFD correlation of SAB females



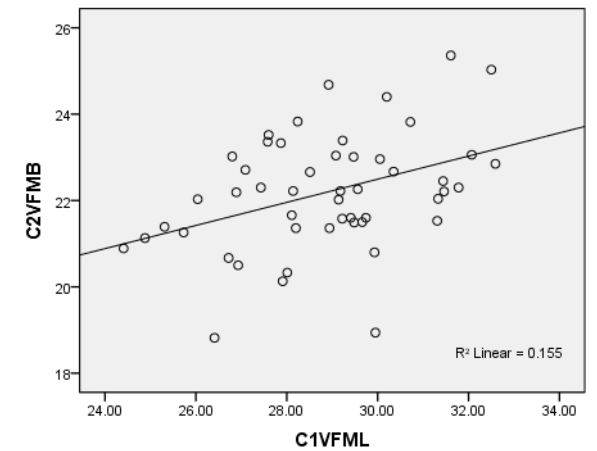
C1VFML-C1VFMB correlation of SAB females

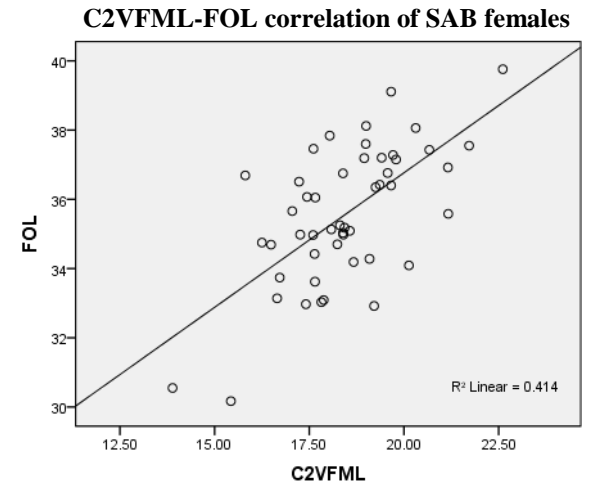
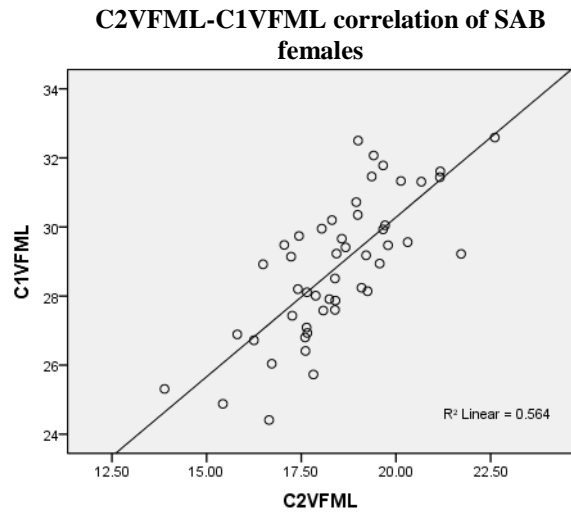
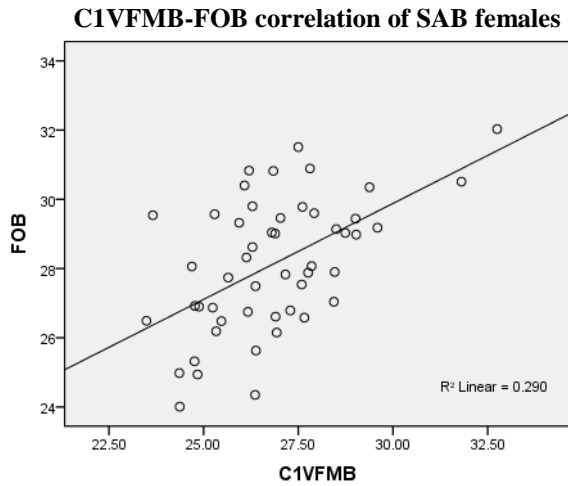
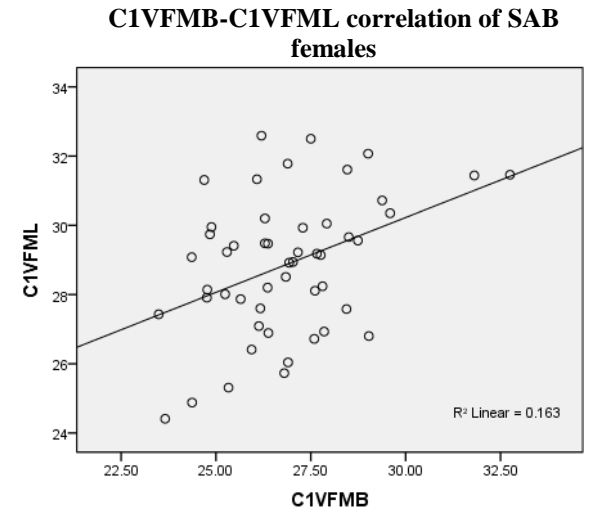
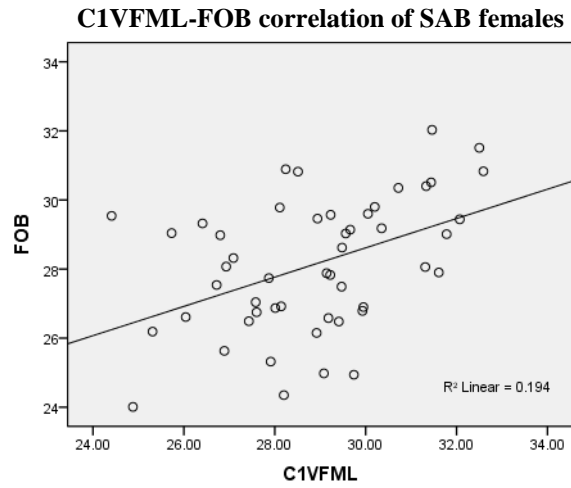
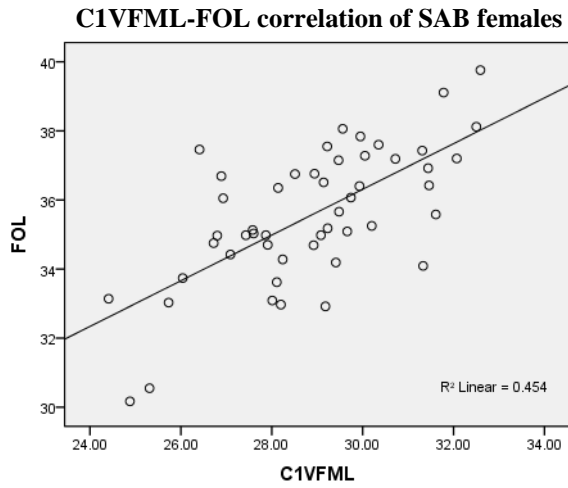


C1VFML-C2VFML correlation of SAB females

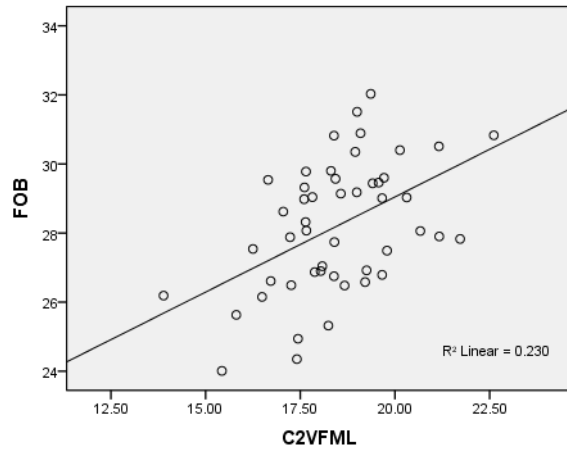


C1VFML-C2VFMB correlation of SAB females

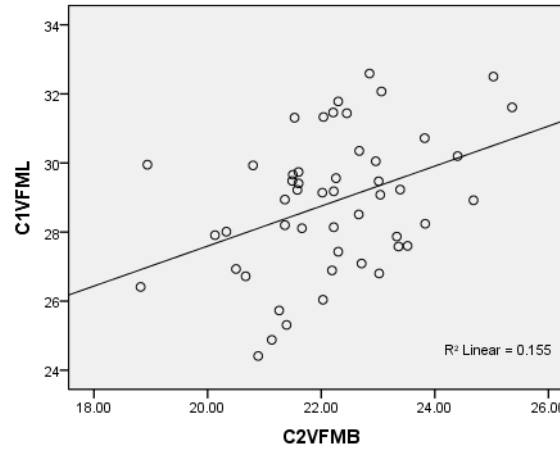




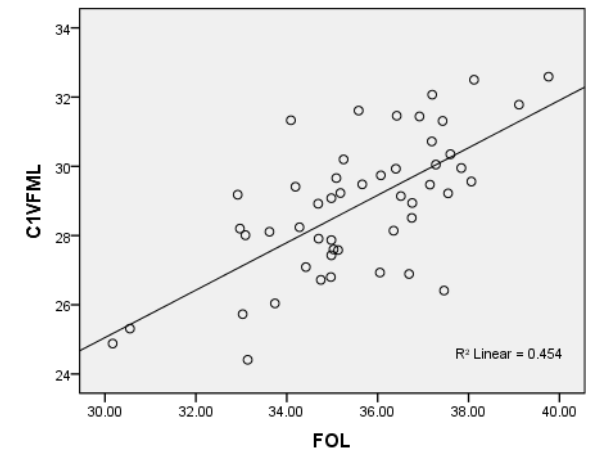
C2VFML-FOB correlation of SAB females



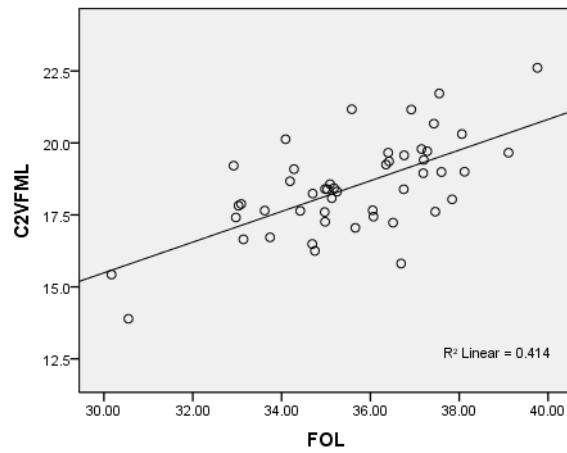
C2VFMB-C1VFML correlation of SAB females



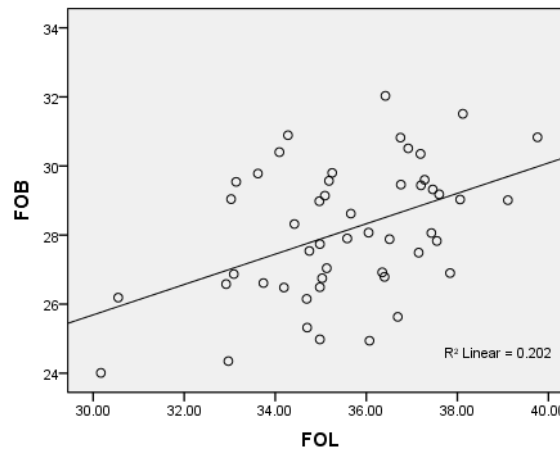
FOL-C1VFML correlation of SAB females



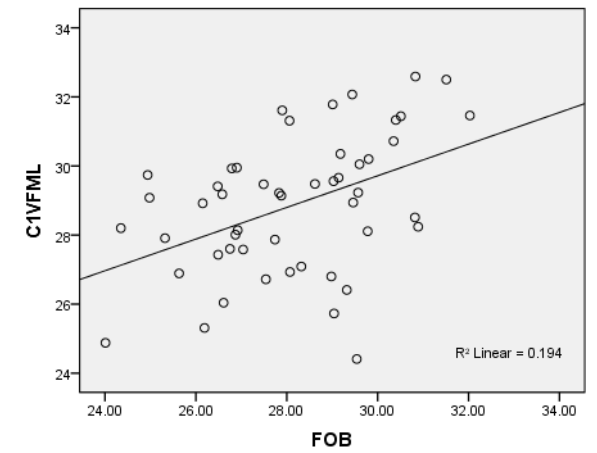
FOL-C2VFML correlation of SAB females



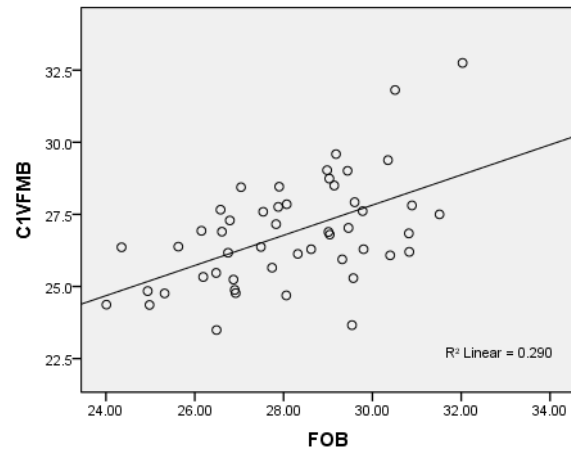
FOL-FOB correlation of SAB females



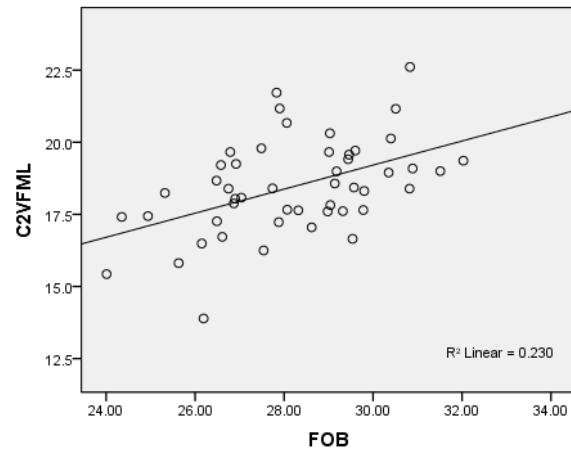
FOB-C1VFML correlation of SAB females



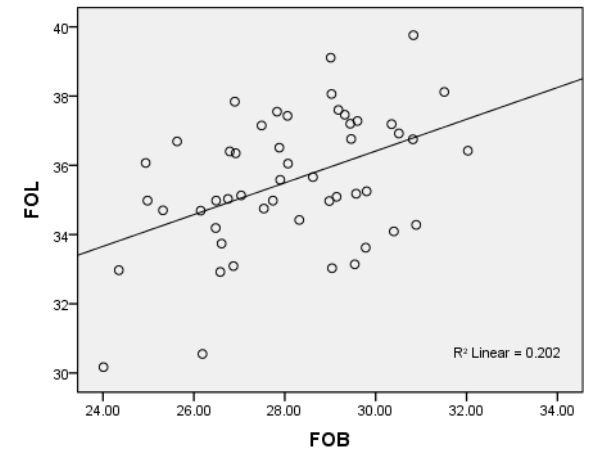
FOB-C1VFMB correlation of SAB females



FOB-C2VFML correlation of SAB females

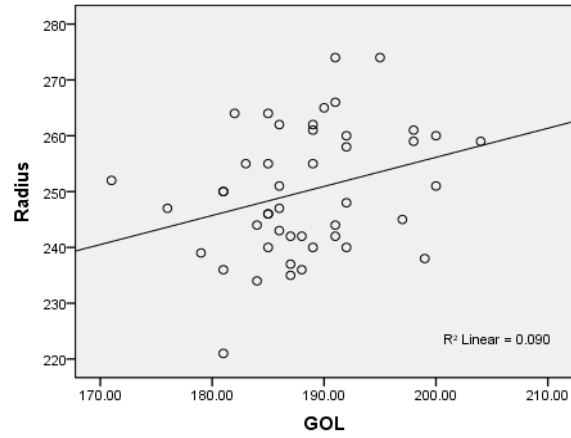


FOB-FOL correlation of SAB females

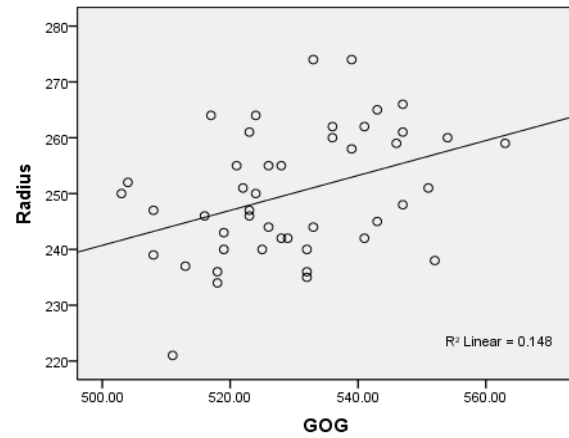


7.3 SOUTH AFRICAN WHITE MALES

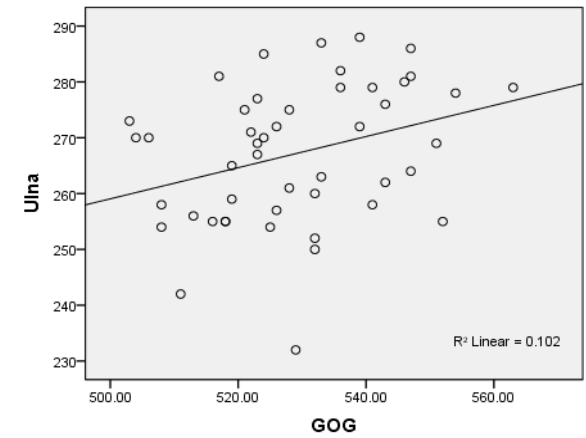
GOL-RADXLN correlation of SAW males



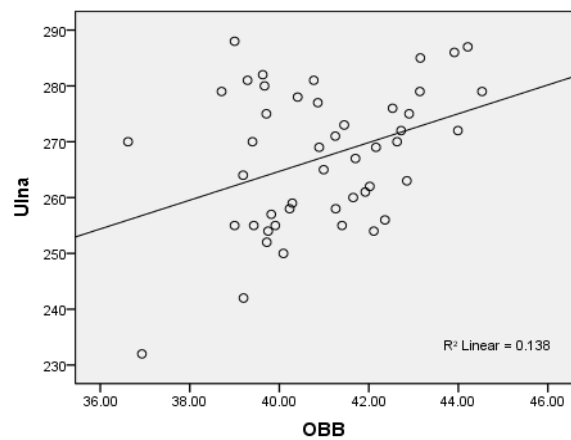
GOG-RADXLN correlation of SAW males



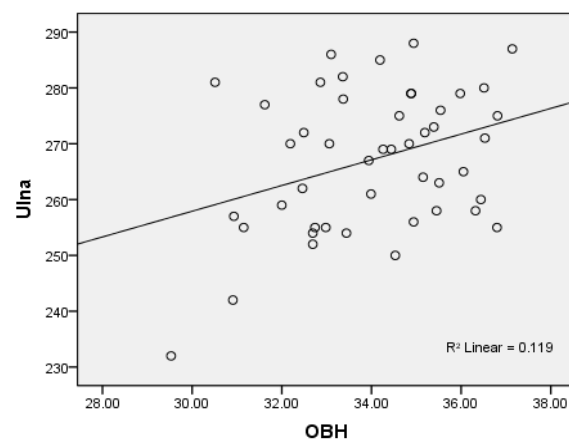
GOG-ULNXLN correlation of SAW males



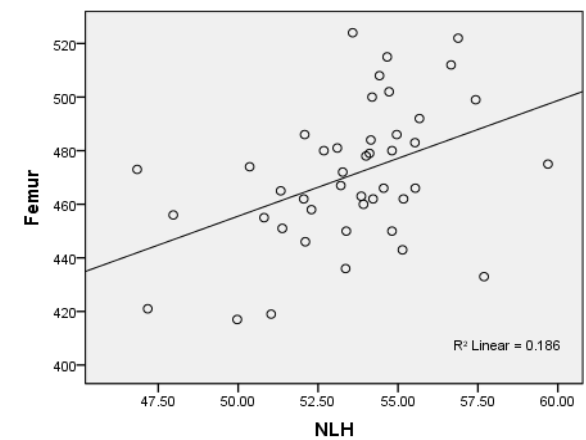
OBB-ULNXLN correlation of SAW males



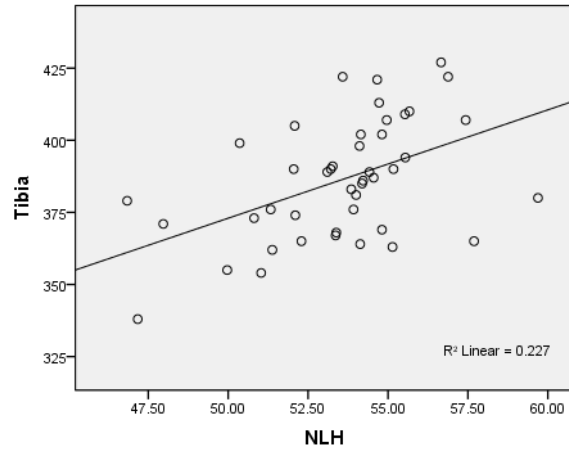
OBH-ULNXLN correlation of SAW males



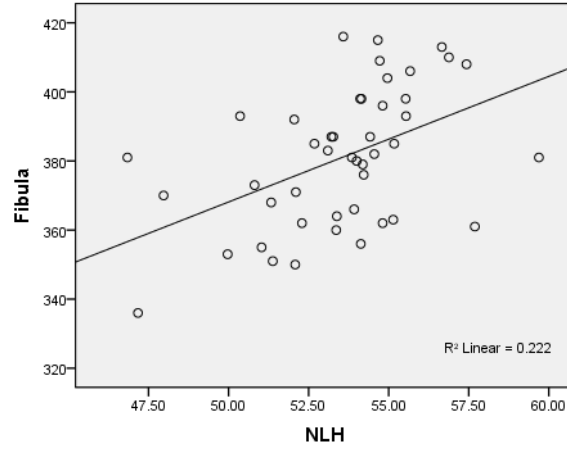
NLH-FEMXLN correlation of SAW males



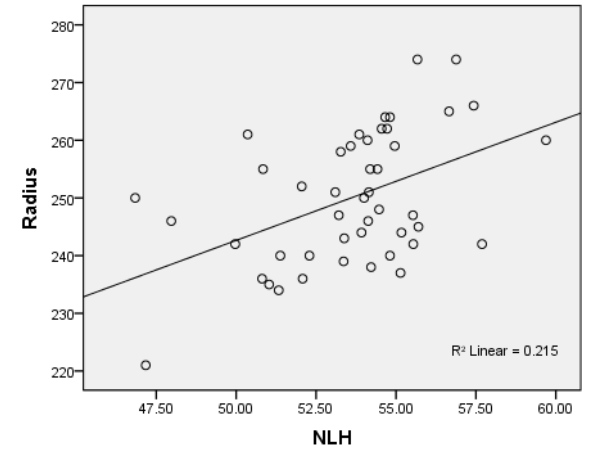
NLH-TIBXLN correlation of SAW males



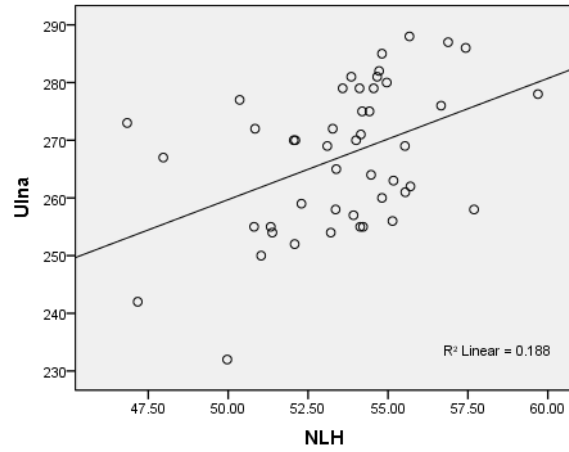
NLH-FIBXLN correlation of SAW males



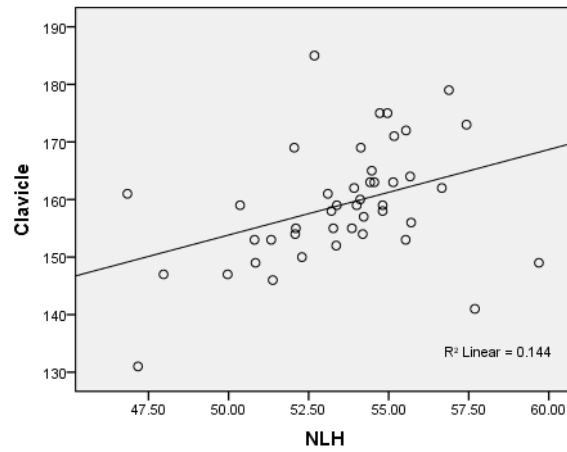
NLH-RADXLN correlation of SAW males



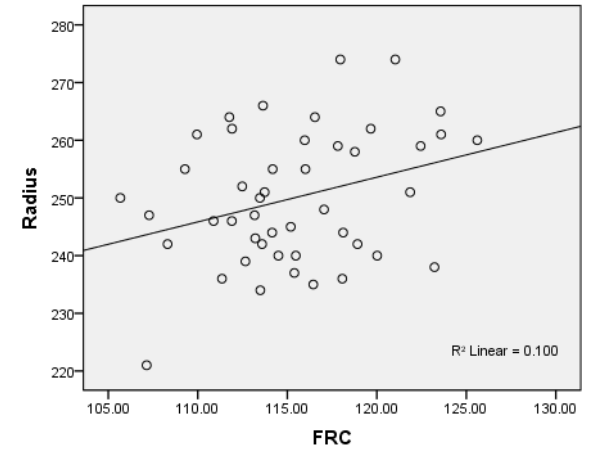
NLH-ULNXLN correlation of SAW males



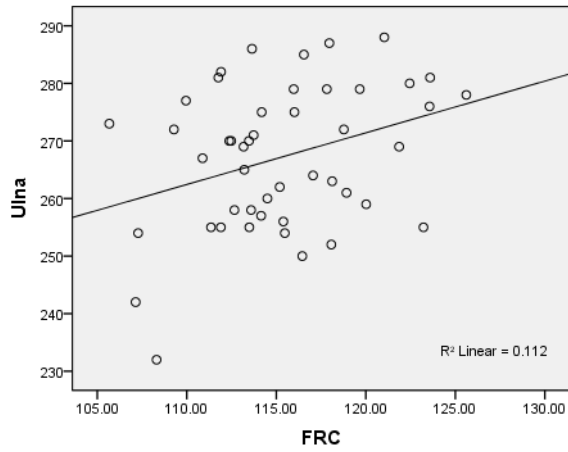
NLH-CLAXLN correlation of SAW males



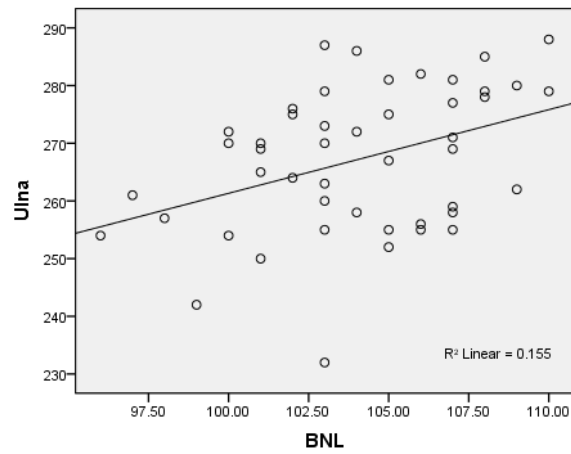
FRC-RADXLN correlation of SAW males



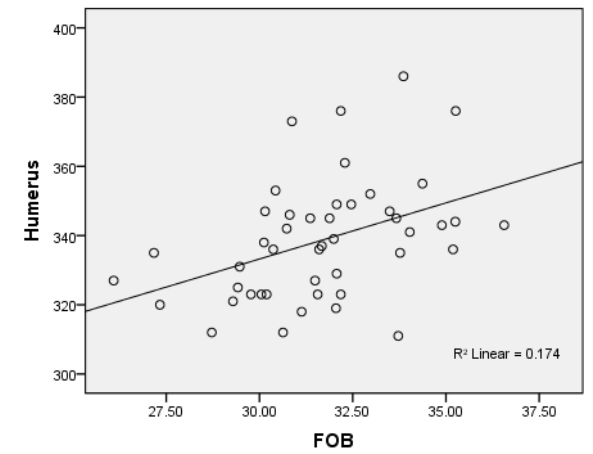
FRC-ULNXLN correlation of SAW males



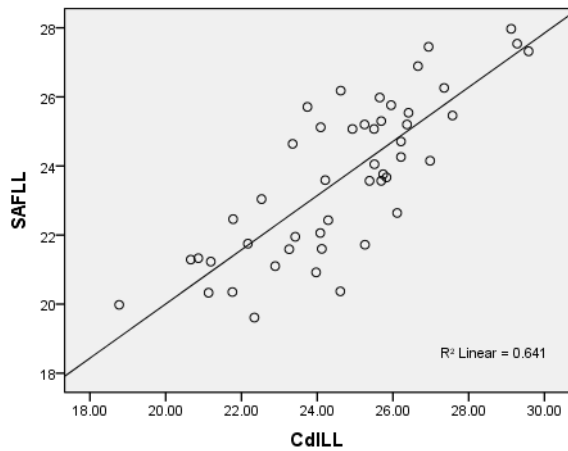
BNL-ULNXLN correlation of SAW males



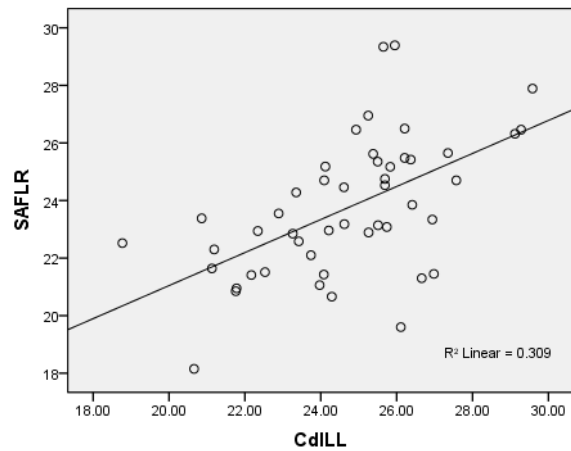
FOB-HUMXLN correlation of SAW males



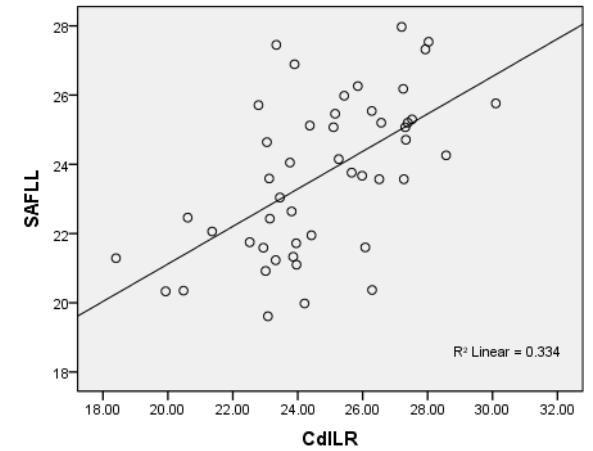
CdILL-SAFLL correlation of SAW males



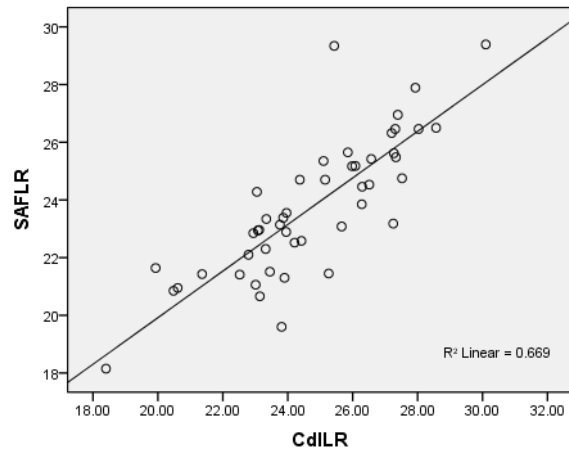
CdILL-SAFRLR correlation of SAW males



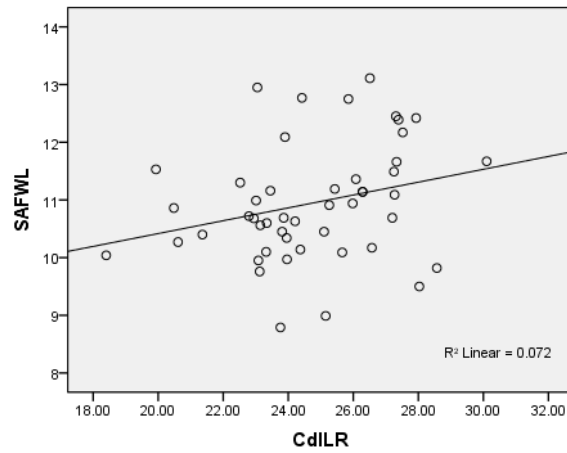
CdILR-SAFLL correlation of SAW males



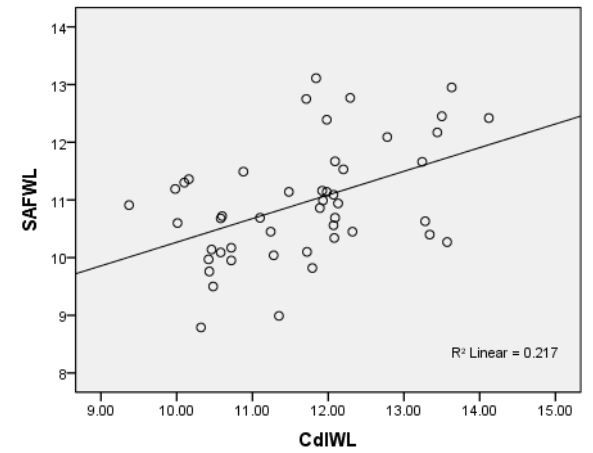
CdILR-SAFLR correlation of SAW males



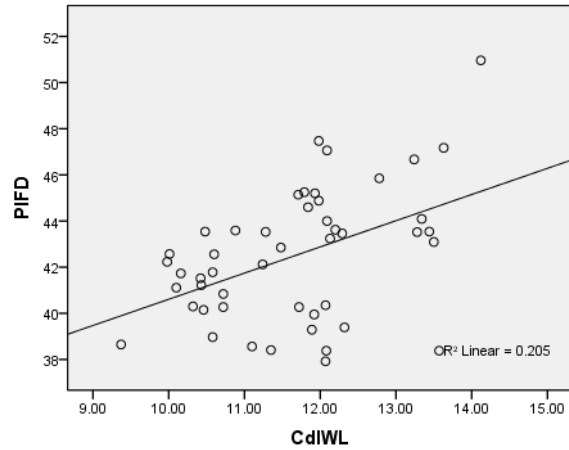
CdILR-SAFWL correlation of SAW males



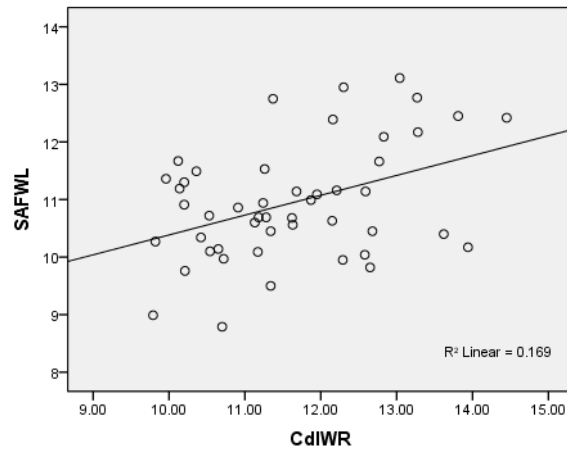
CdIWL-SAFWL correlation of SAW males



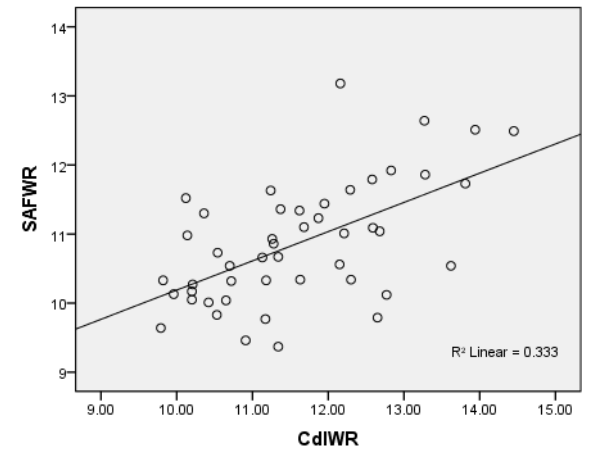
CdIWL-PIFD correlation of SAW males



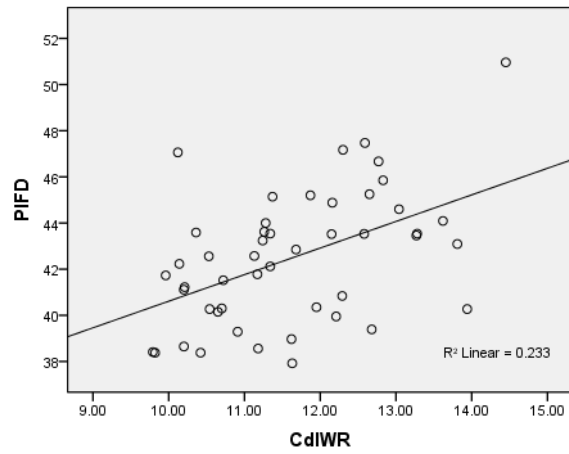
CdIWR-SAFWL correlation of SAW males



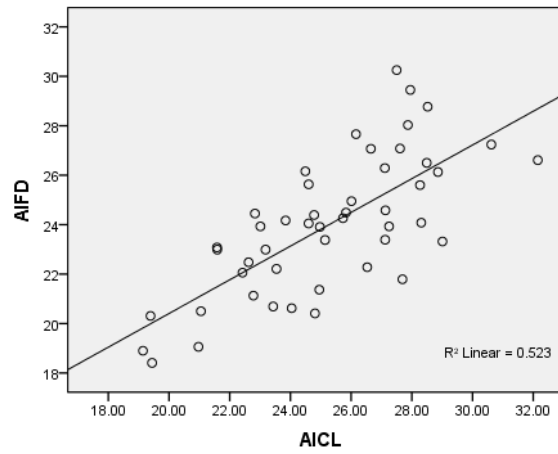
CdIWR-SAFWR correlation of SAW males



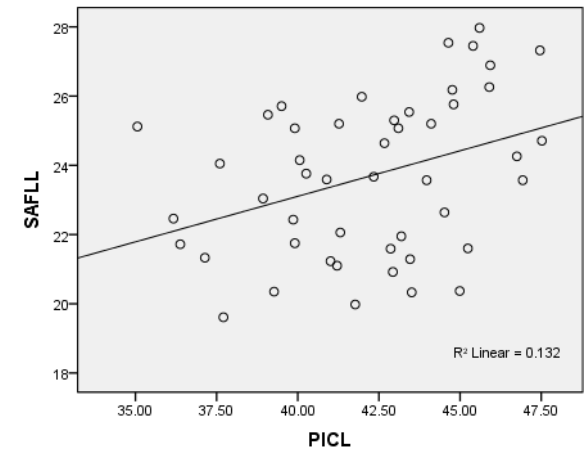
CdIWR-PIFD correlation of SAW males



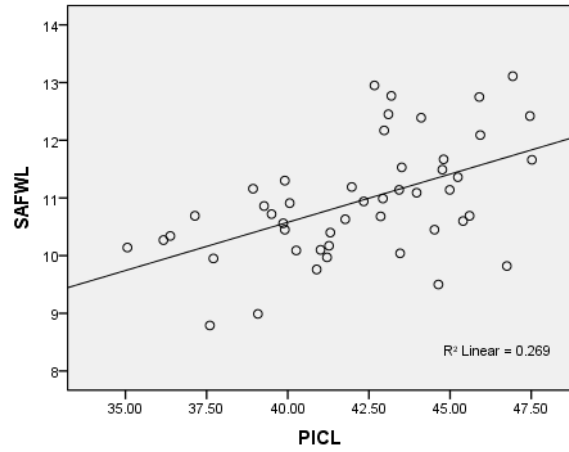
AICL-AIFD correlation of SAW males



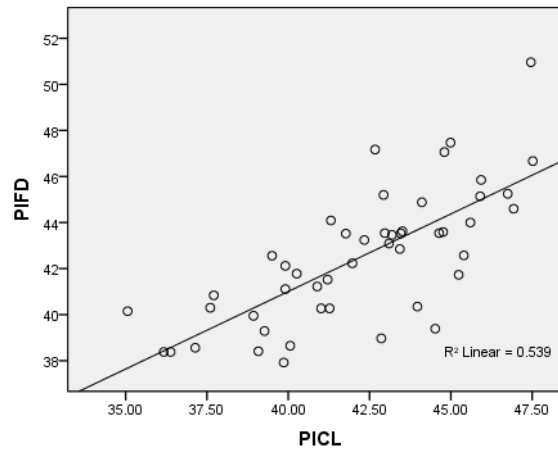
PICL-SAFLL correlation of SAW males



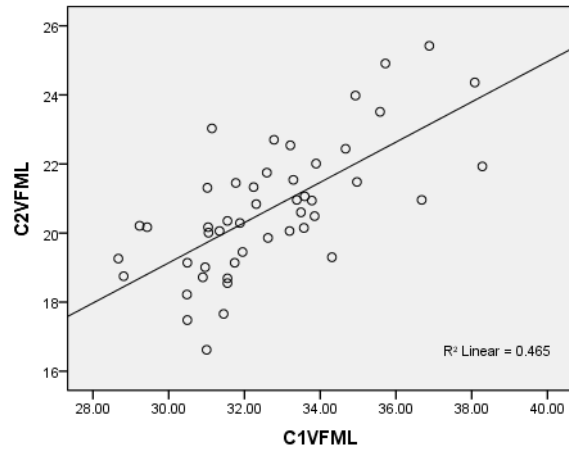
PICL-SAFWL correlation of SAW males



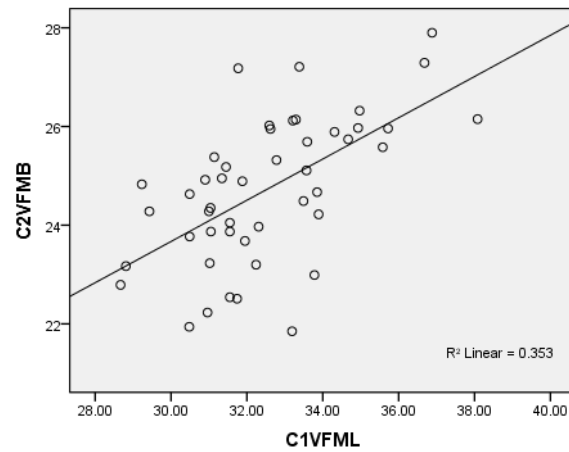
PICL-PIFD correlation of SAW males



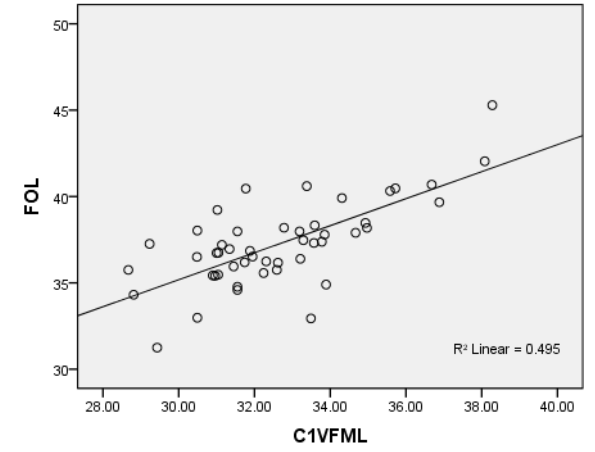
C1VFML-C2VFML correlation of SAW males



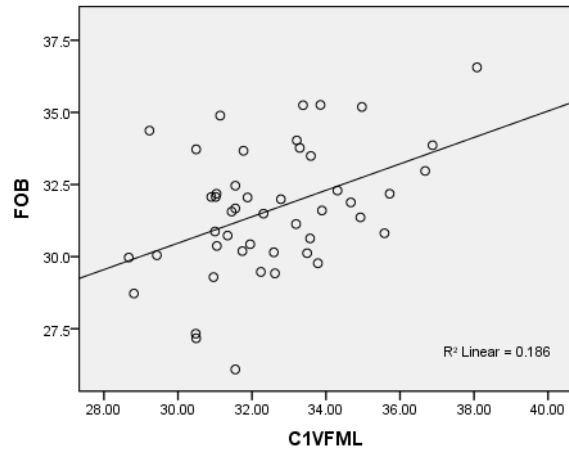
C1VFML-C2VFML correlation of SAW males



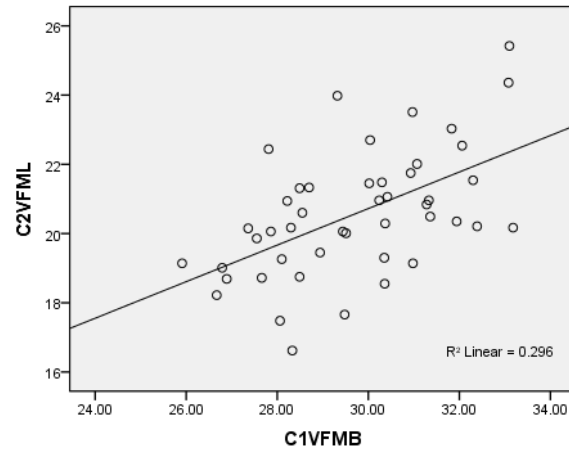
C1VFML-C2VFML correlation of SAW males



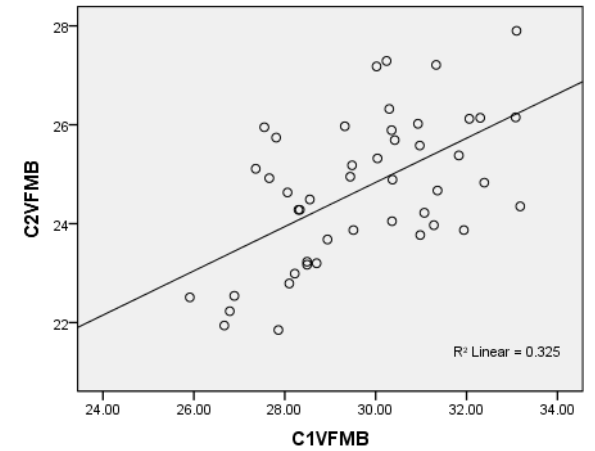
C1VFML-FOB correlation of SAW males

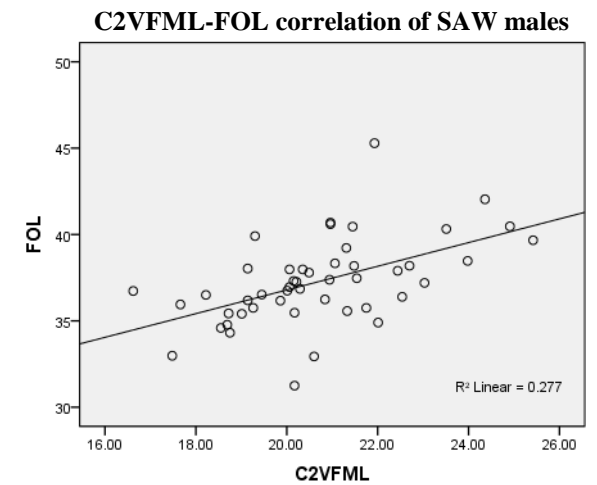
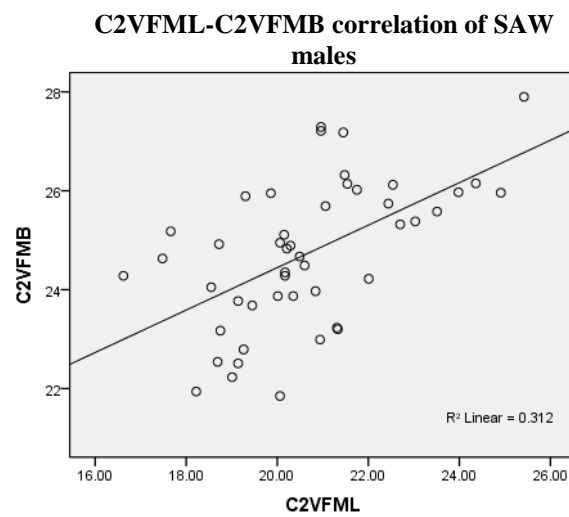
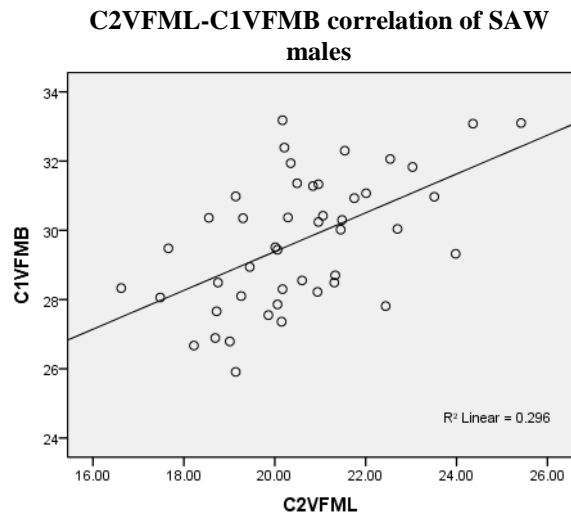
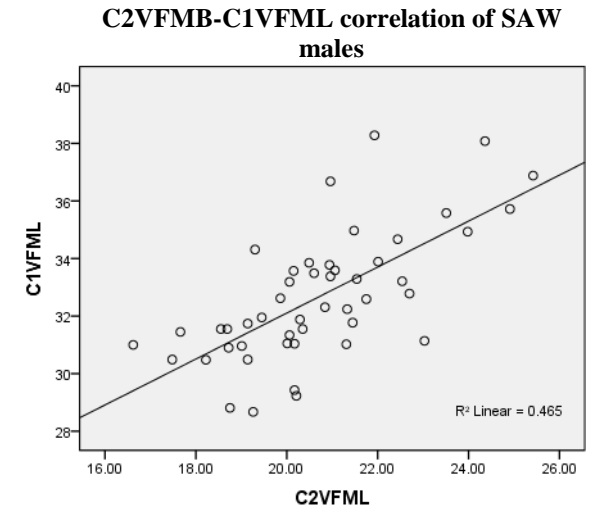
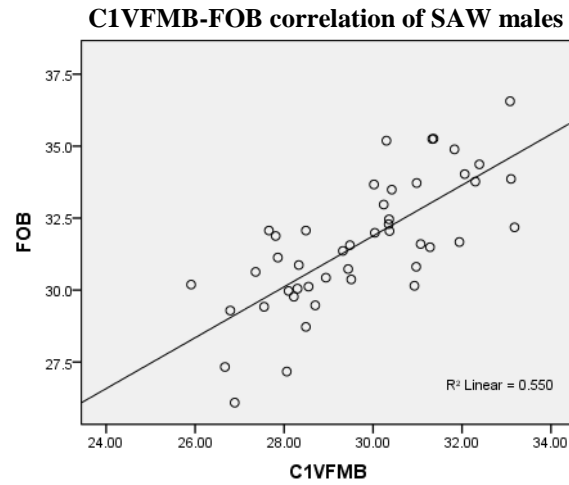
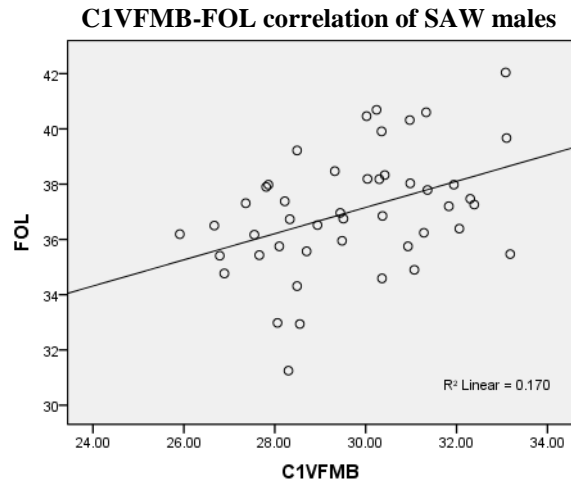


C1VFMB-C2VFML correlation of SAW males

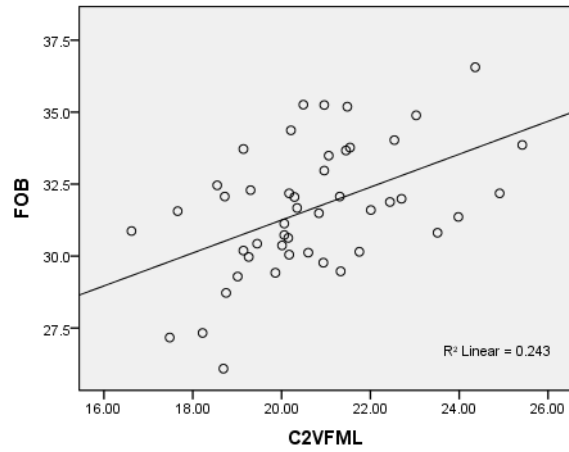


C1VFMB-C2VFMB correlation of SAW males

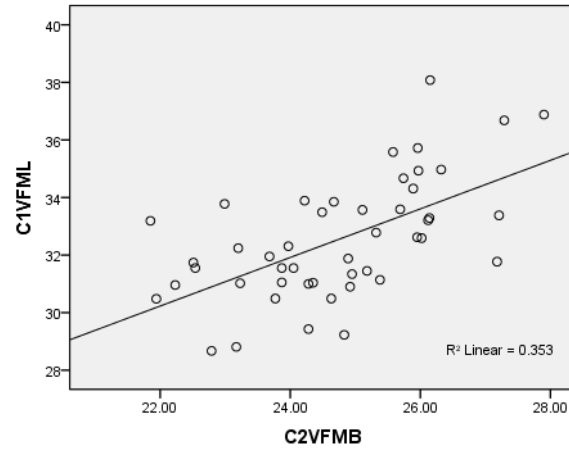




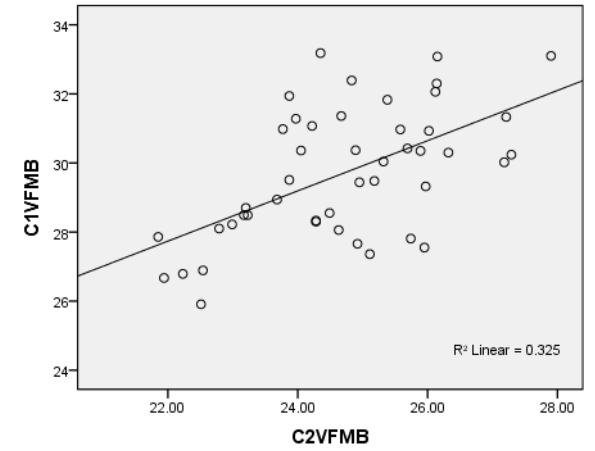
C2VFML-FOB correlation of SAW males



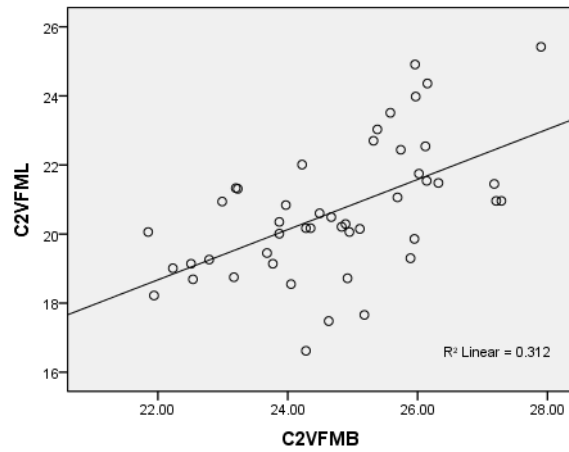
C2VFMB-C1VFML correlation of SAW males



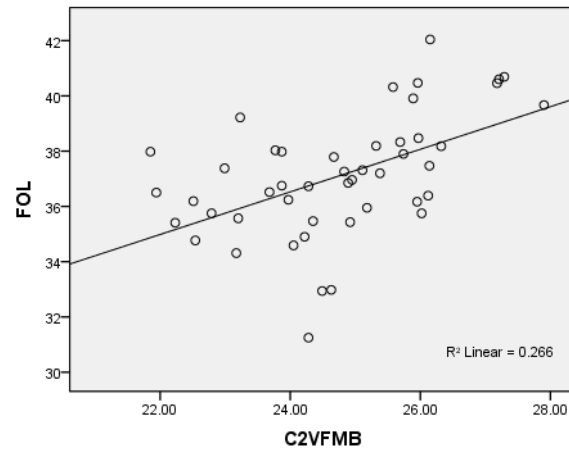
C2VFMB-C1VFMB correlation of SAW males



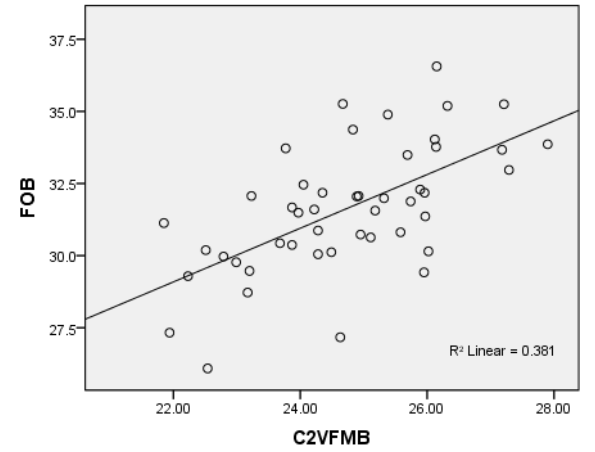
C2VFMB-C2VFML correlation of SAW males



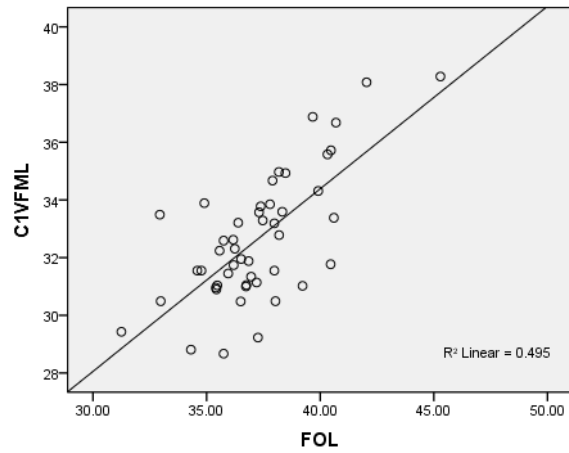
C2VFMB-FOL correlation of SAW males



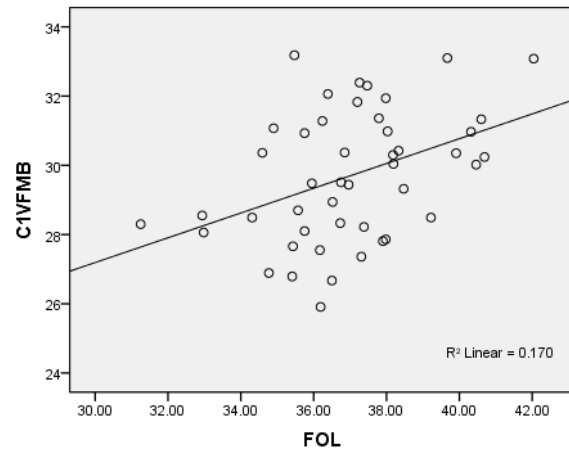
C2VFMB-FOB correlation of SAW males



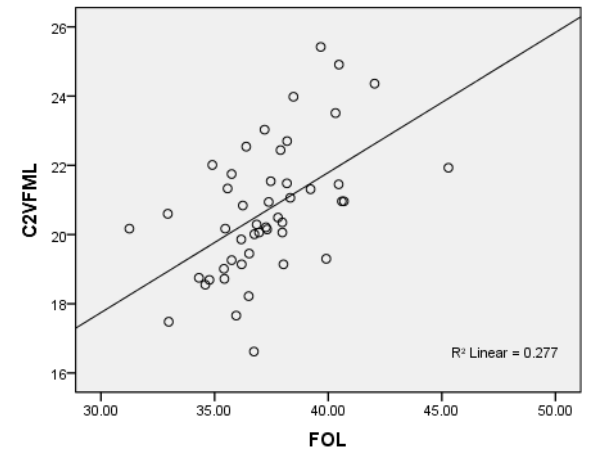
FOL-C1VMFL correlation of SAW males



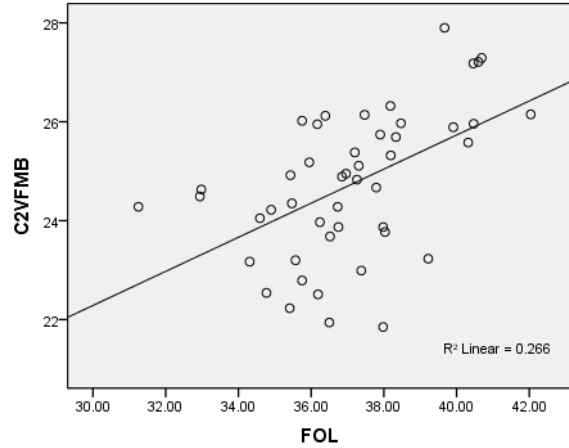
FOL-C1VMFB correlation of SAW males



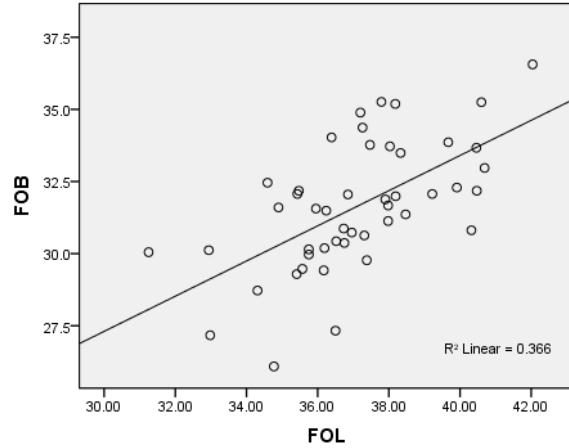
FOL-C2VFML correlation of SAW males



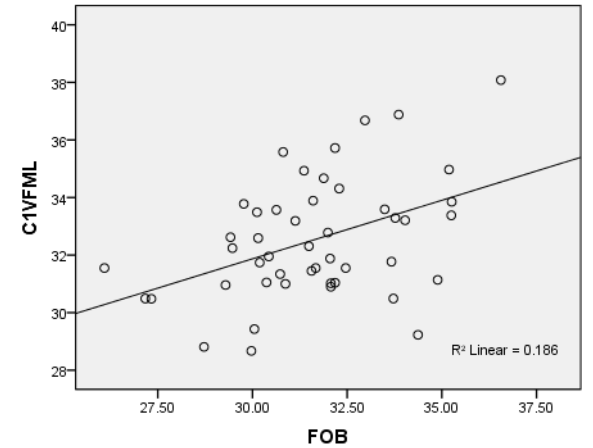
FOL-C2VFMB correlation of SAW males



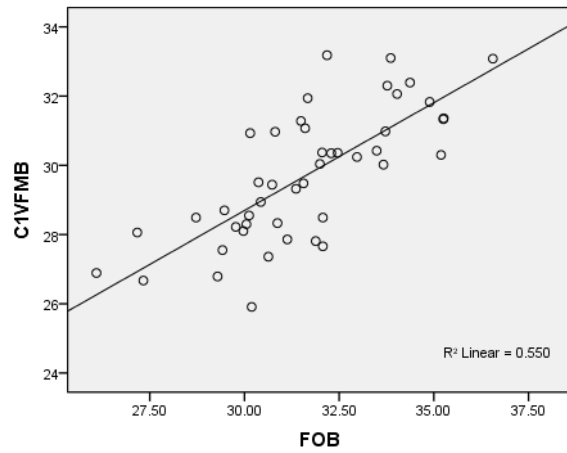
FOL-FOB correlation of SAW males



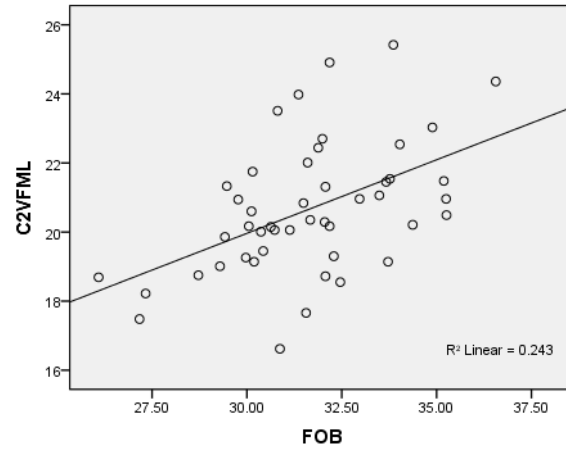
FOB-C1VMFL correlation of SAW males



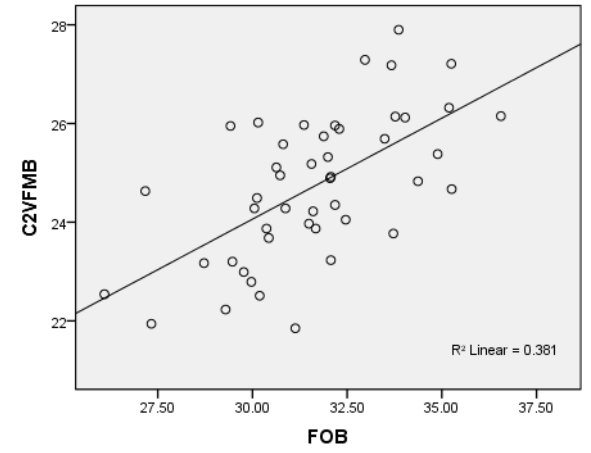
FOB-C1VFMB correlation of SAW males



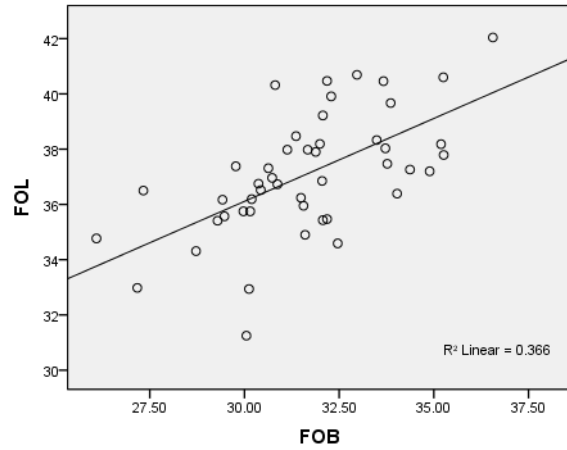
FOB-C2VFML correlation of SAW males



FOB-C2VFMB correlation of SAW males

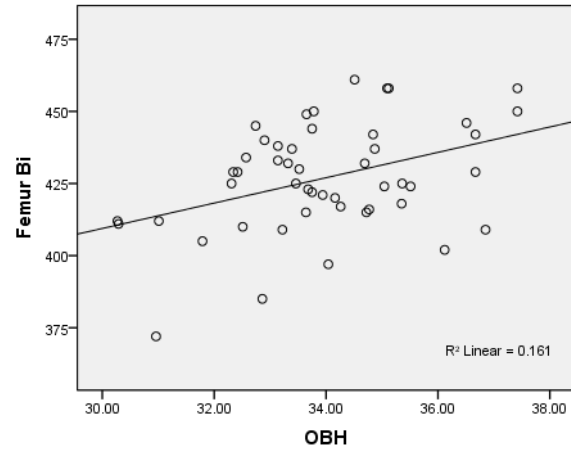


FOB-FOL correlation of SAW males

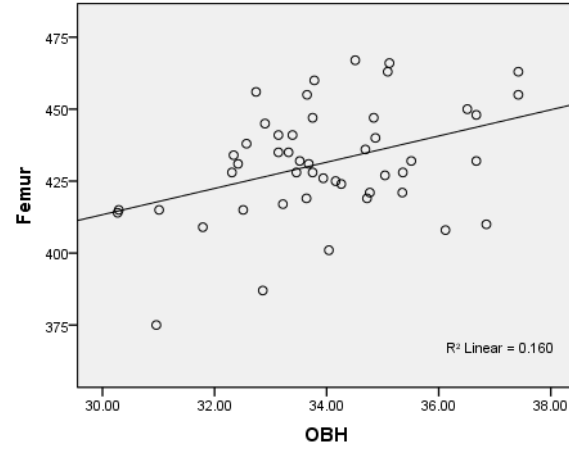


7.4 SOUTH AFRICAN WHITE FEMALES

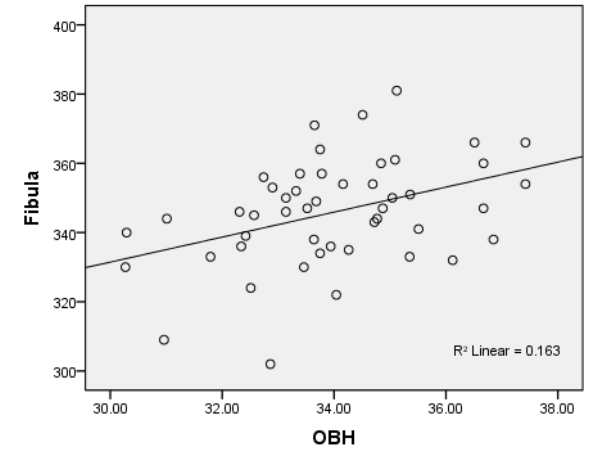
OBH-C1VFMB correlation of SAW females



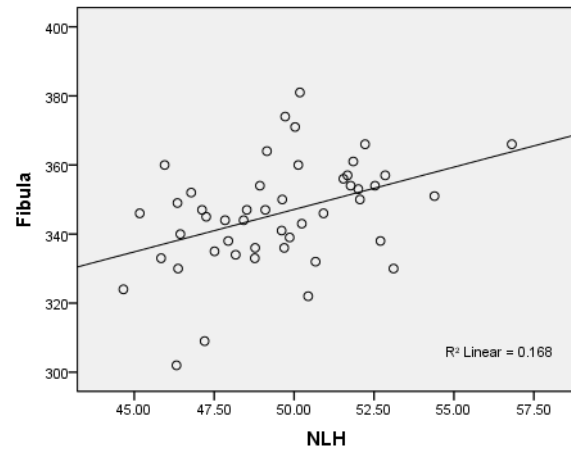
OBH-C1VFMB correlation of SAW females



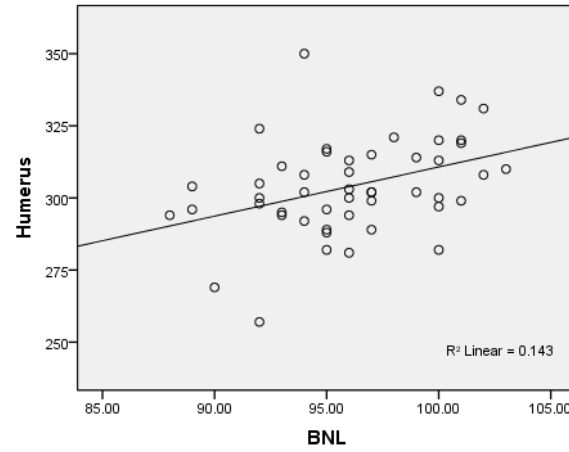
OBH-C1VFMB correlation of SAW females



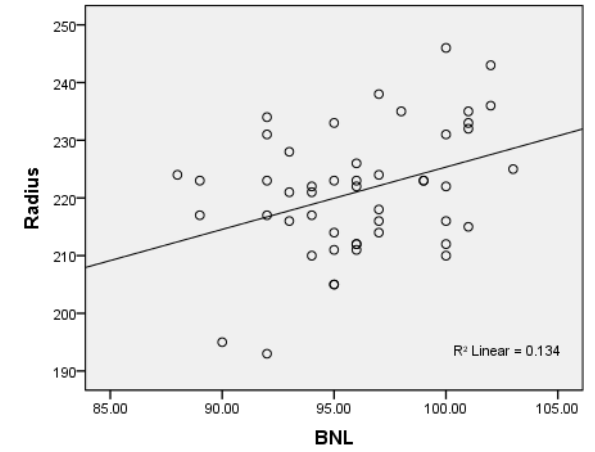
NLH-C1VFMB correlation of SAW females

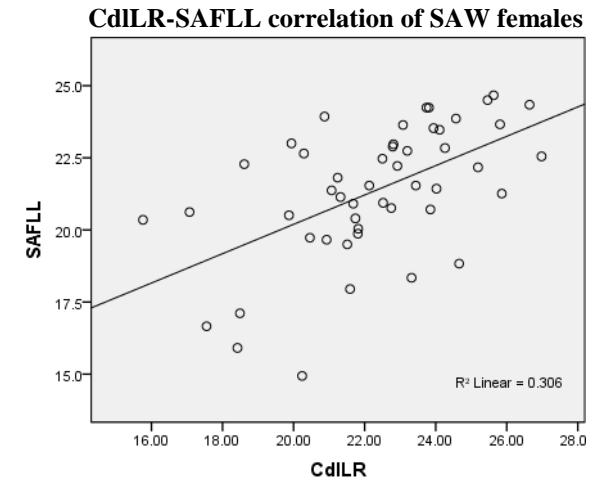
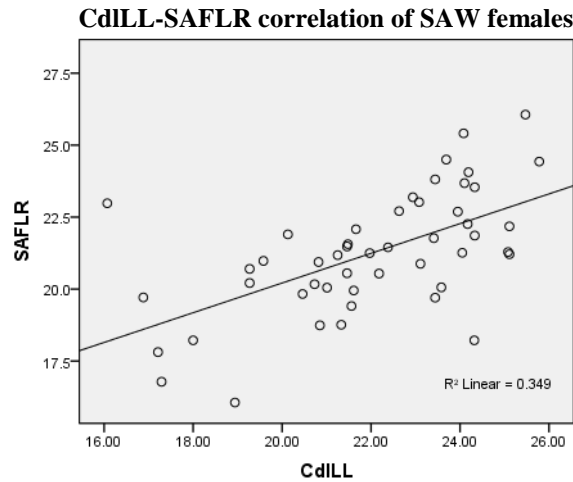
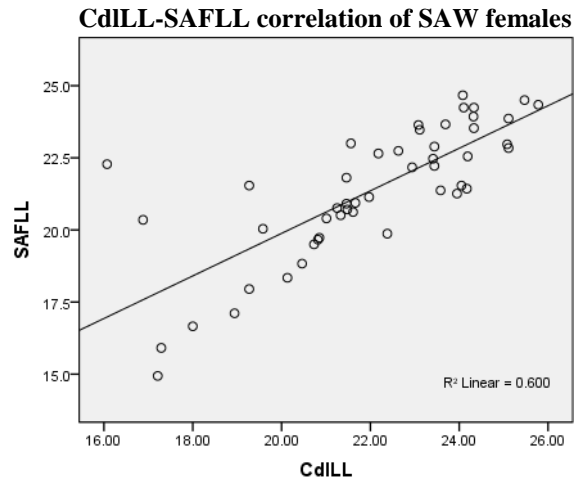
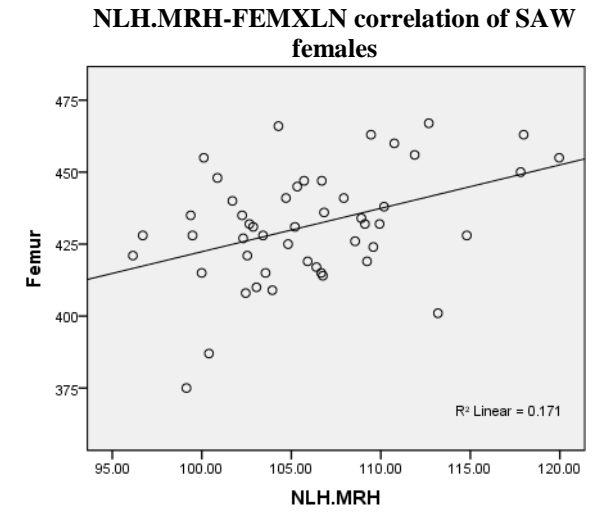
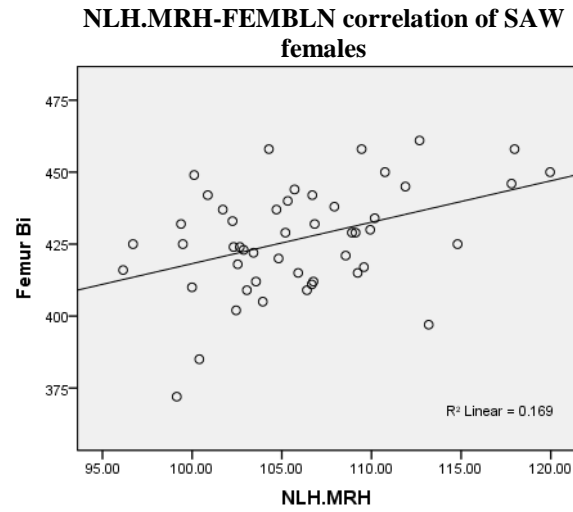
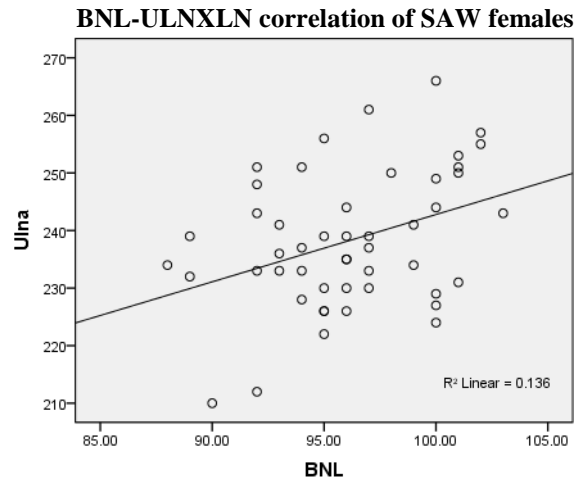


BNL-C1VFMB correlation of SAW females

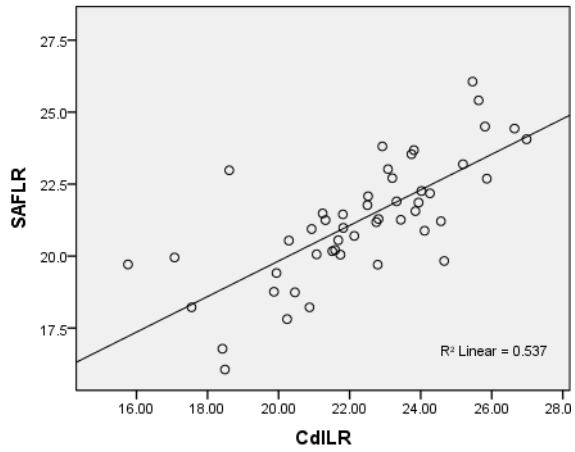


BNL-C1VFMB correlation of SAW females

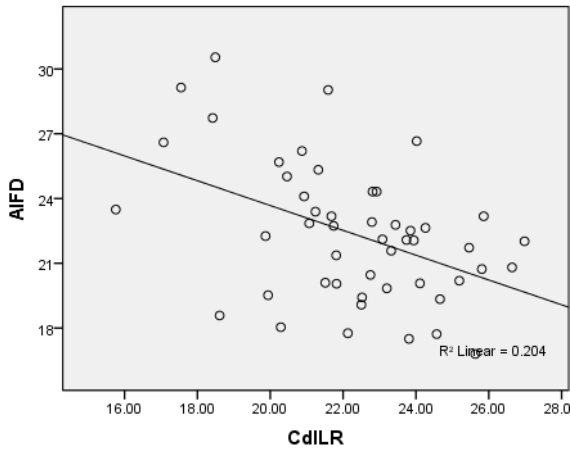




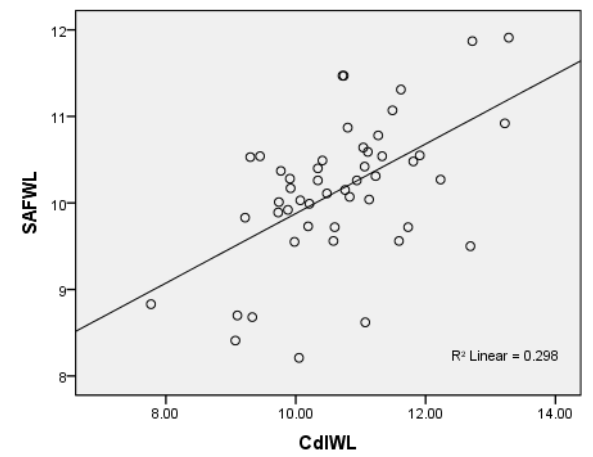
CdILR-SAFLR correlation of SAW females



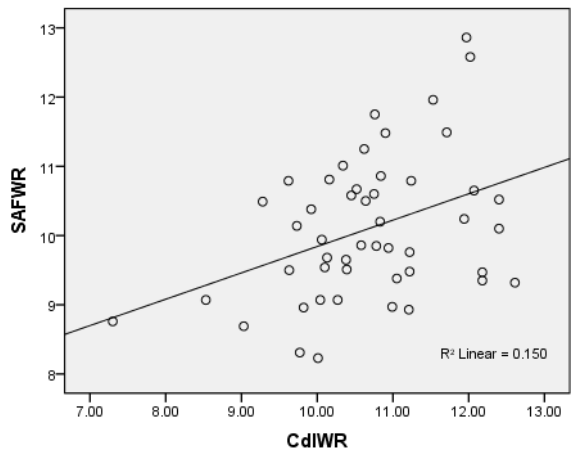
CdILR-AIFD correlation of SAW females



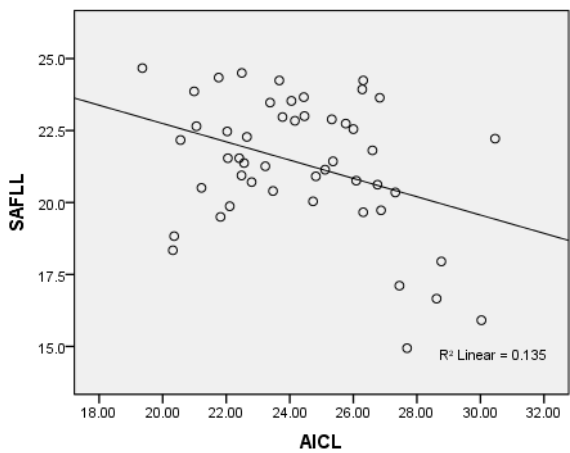
CdIWL-SAFWL correlation of SAW females



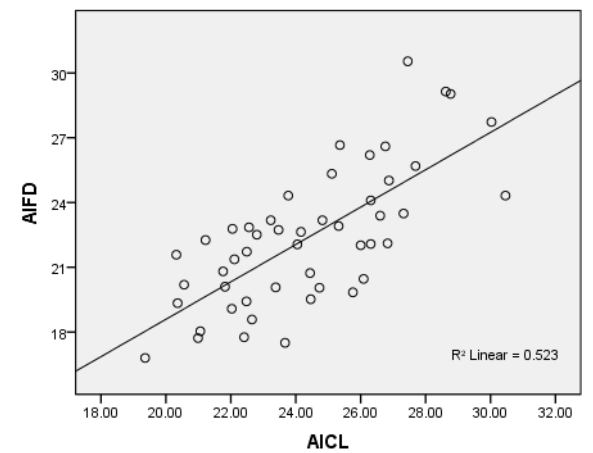
CdIWR-SAFWR correlation of SAW females



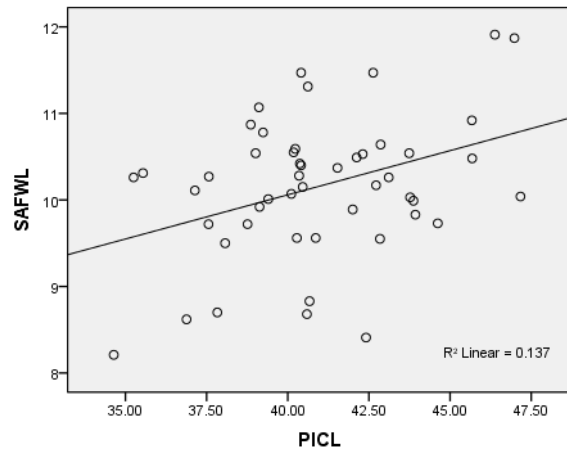
AICL-SAFLL correlation of SAW females



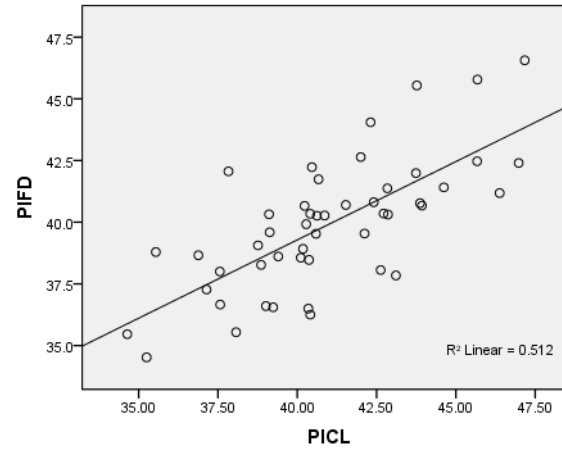
AICL-AIFD correlation of SAW females



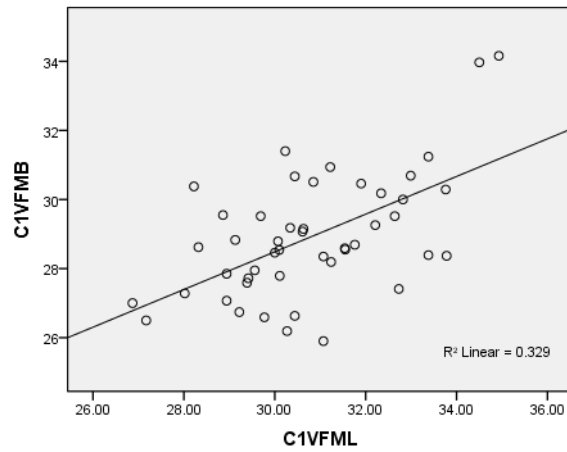
PICL-SAFWL correlation of SAW females



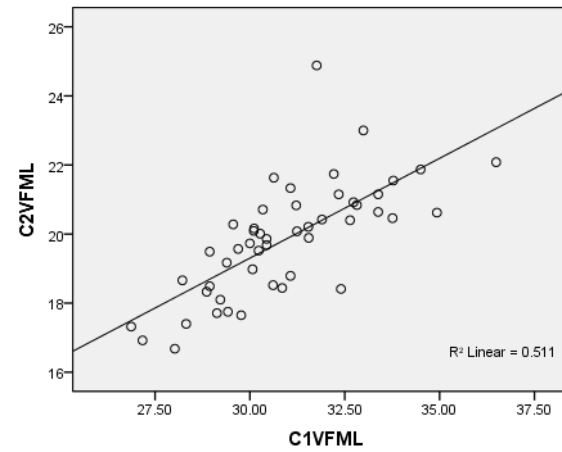
PICL-PIFD correlation of SAW females



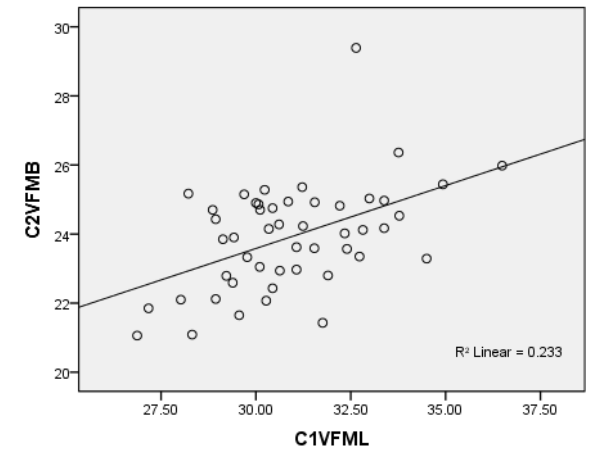
C1VFML-C1VFMB correlation of SAW females

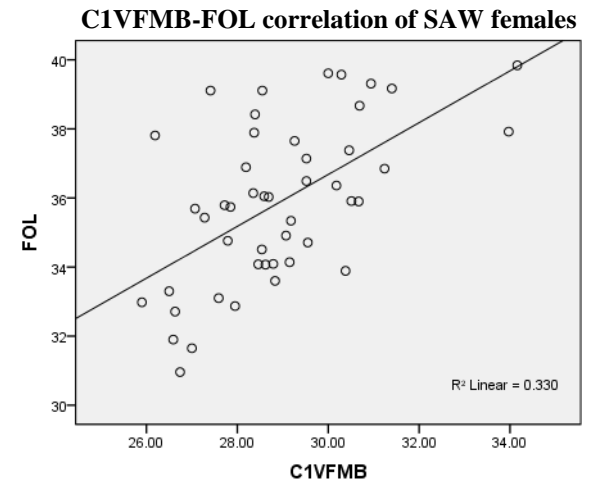
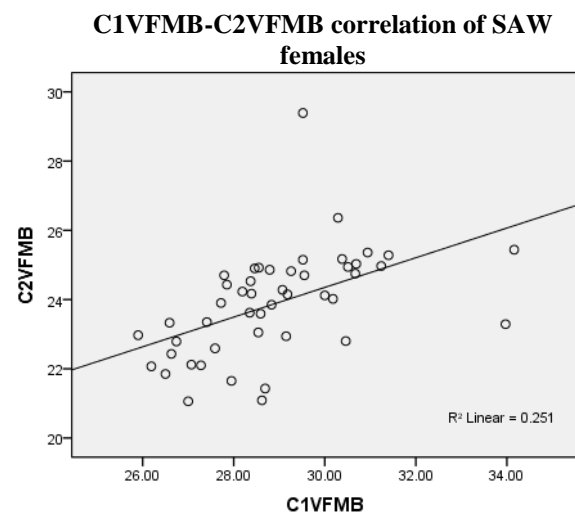
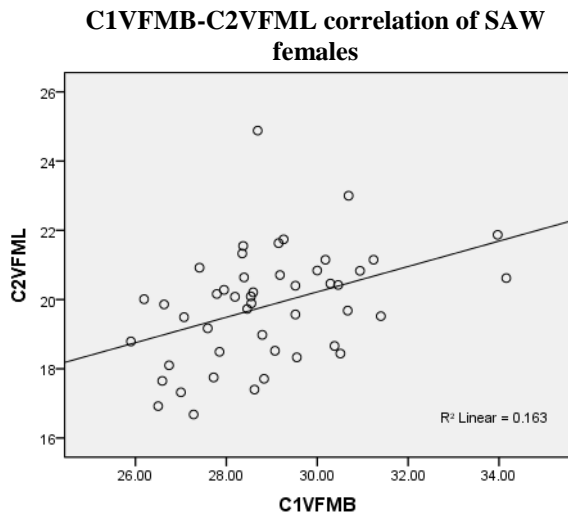
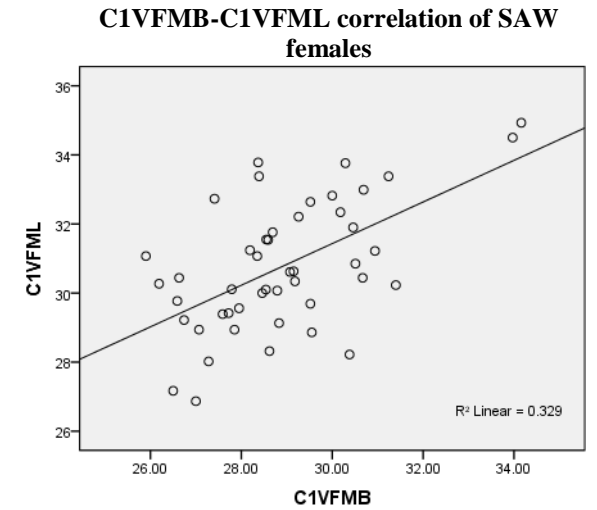
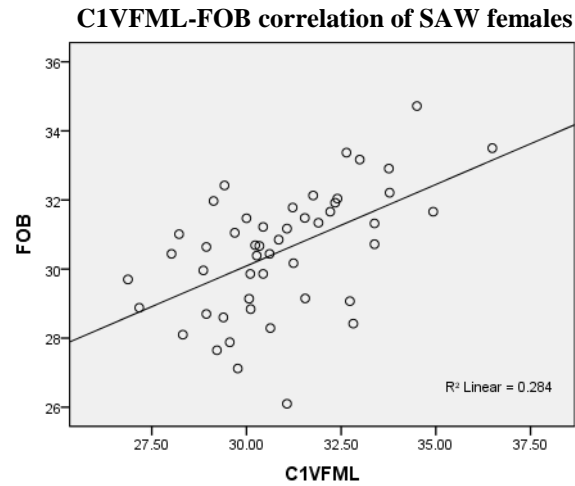
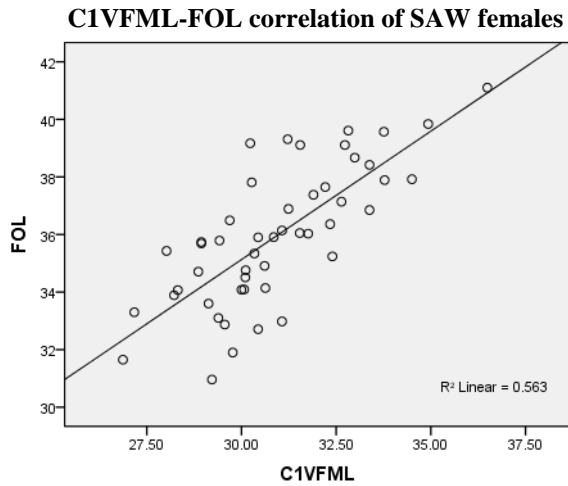


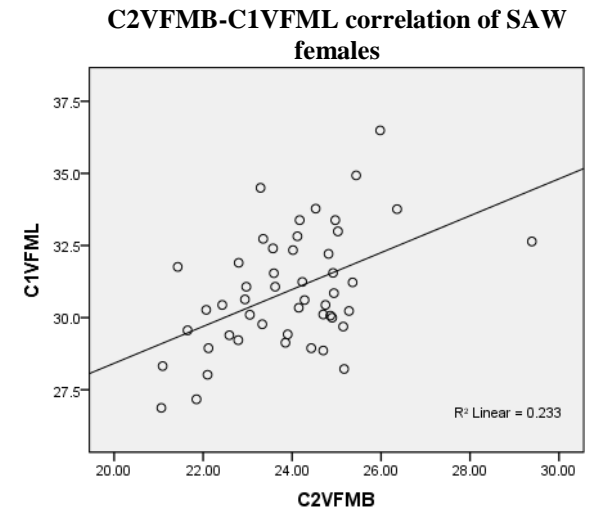
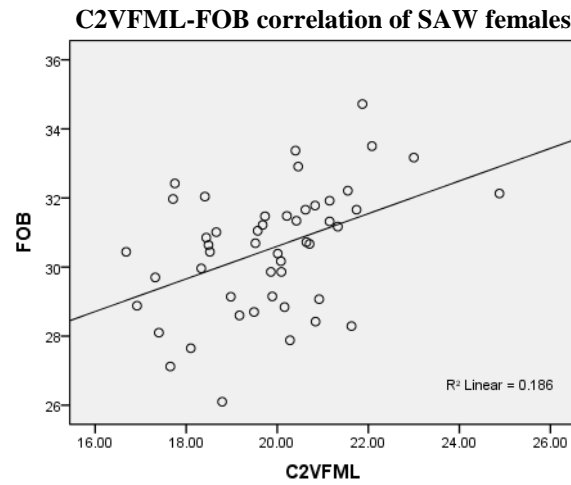
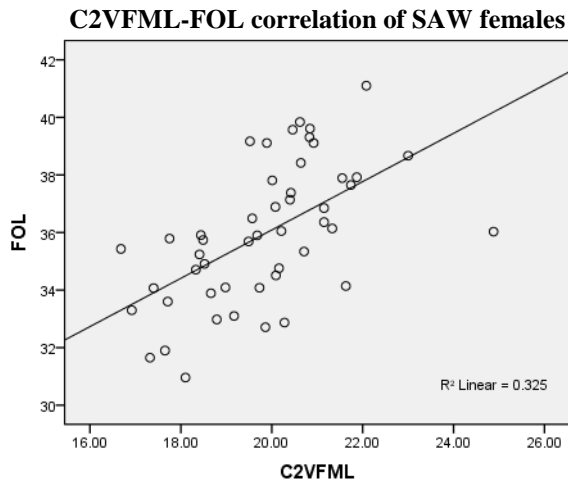
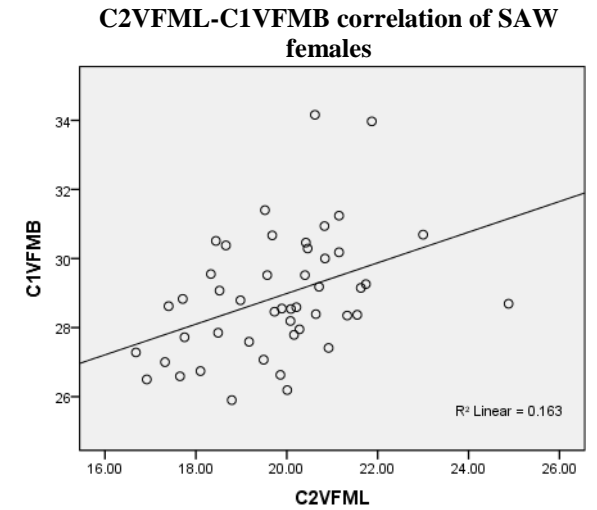
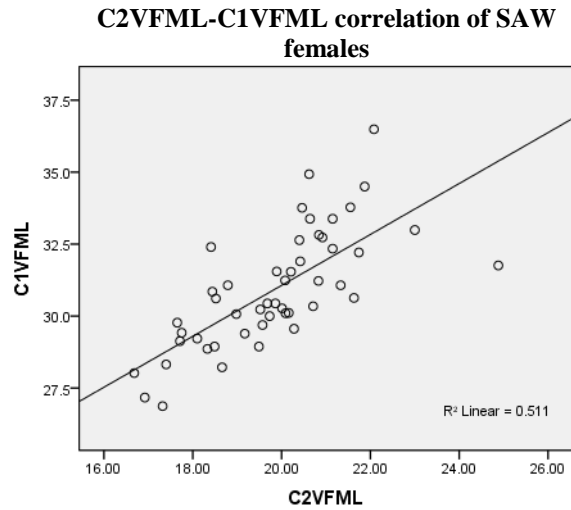
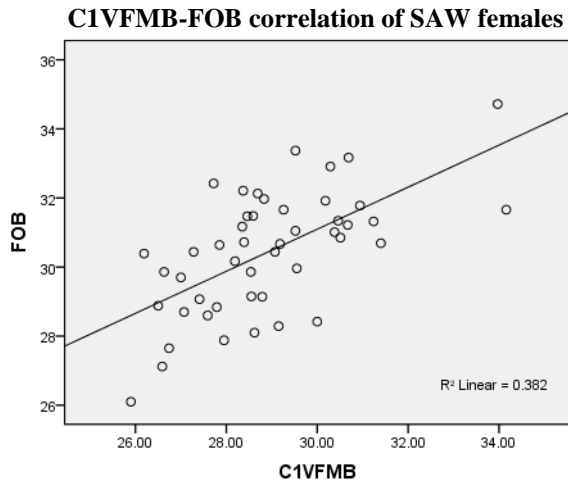
C1VFML-C2VFML correlation of SAW females



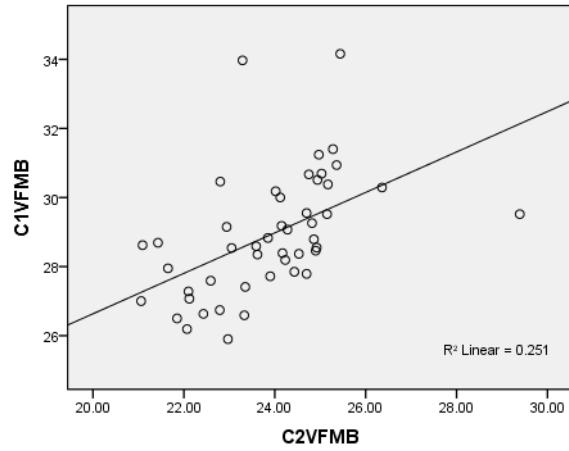
C1VFML-C2VFMB correlation of SAW females



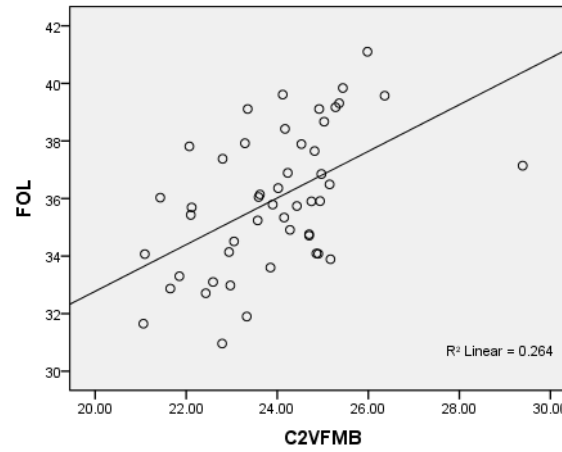




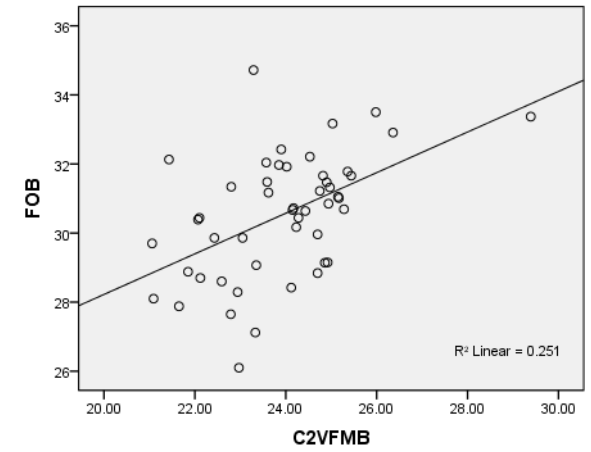
C2VFMB-C1VFMB correlation of SAW females



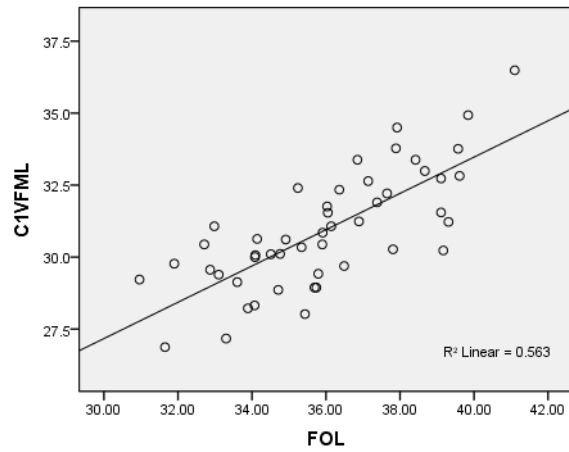
C2VFMB-FOL correlation of SAW females



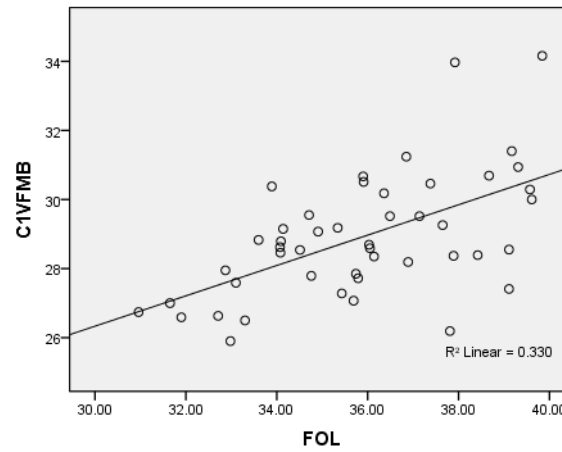
C2VFMB-FOB correlation of SAW females



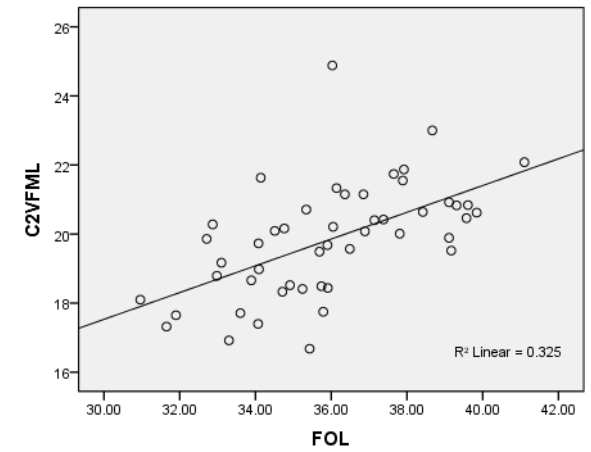
FOL-C1VFML correlation of SAW females



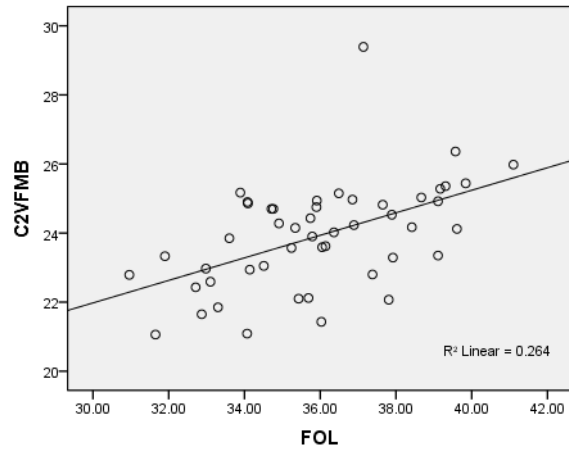
FOL-C1VFMB correlation of SAW females



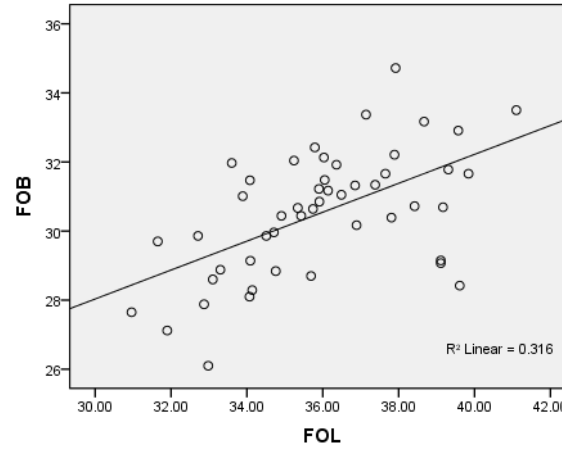
FOL-C2VFML correlation of SAW females



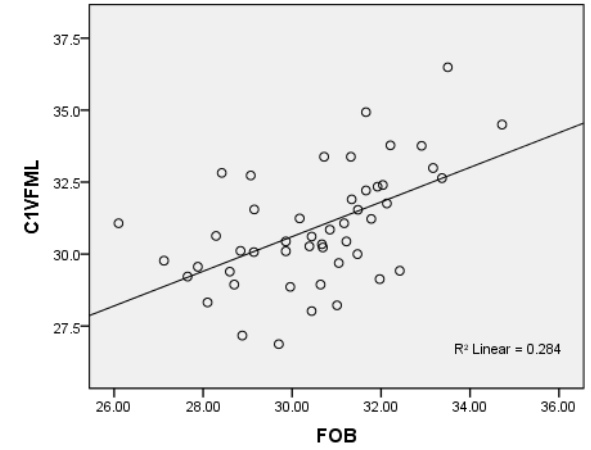
FOL-C2VFMB correlation of SAW females



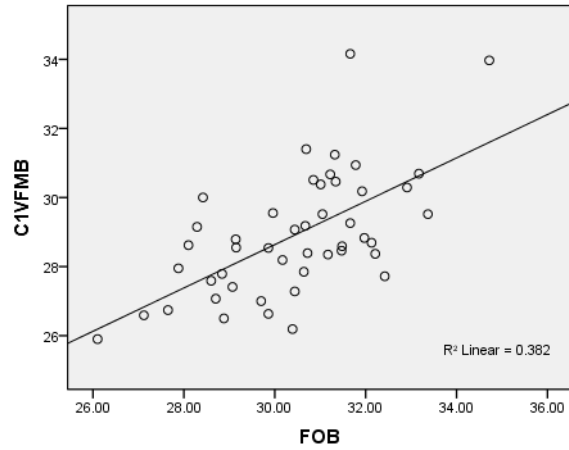
FOL-FOB correlation of SAW females



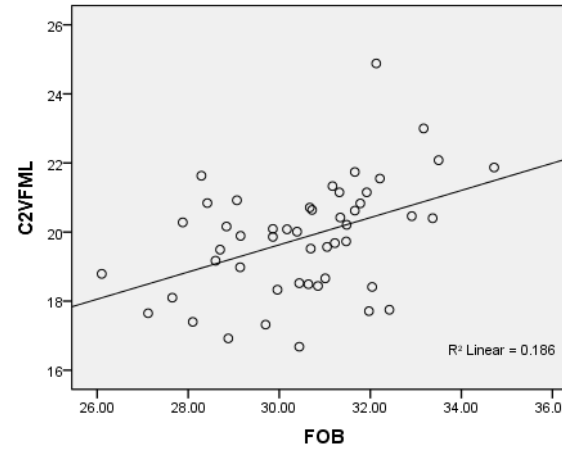
FOB-C1VFML correlation of SAW females



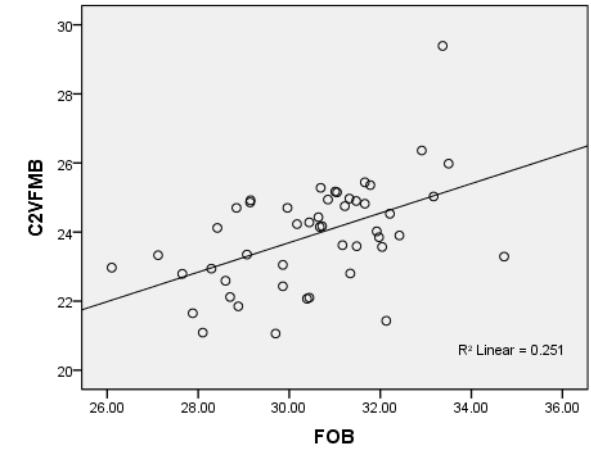
FOB-C1VFMB correlation of SAW females

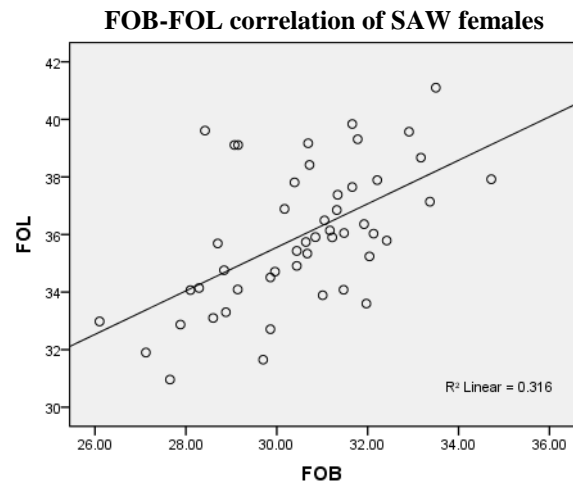


FOB-C2VFML correlation of SAW females



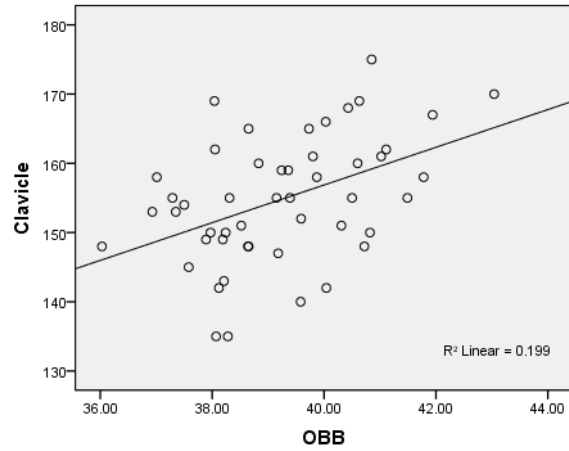
FOB-C2VFMB correlation of SAW females



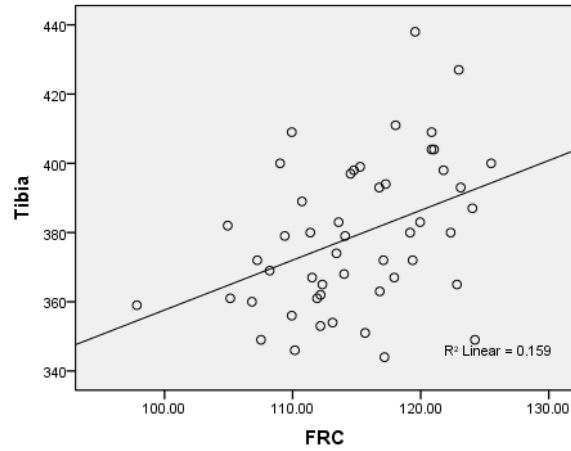


7.5 SOUTH AFRICAN COLOURED MALES

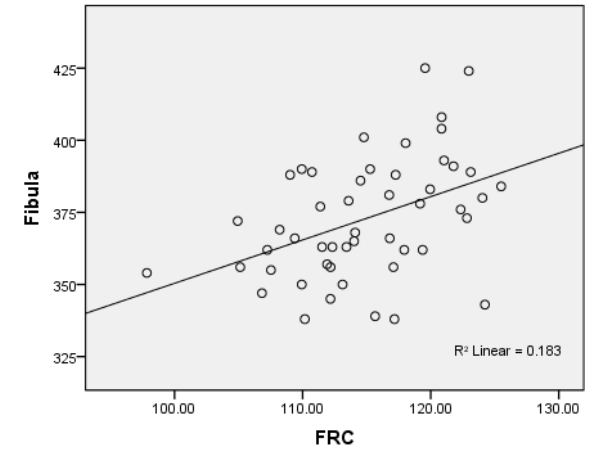
OBB-CLAXLN correlation of SAC males



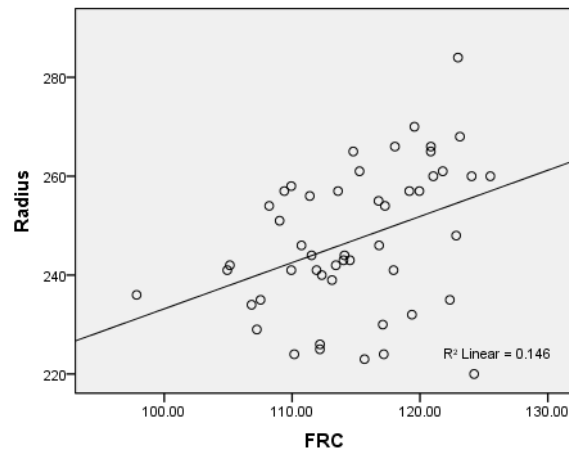
FRC-TIBXLN correlation of SAC males



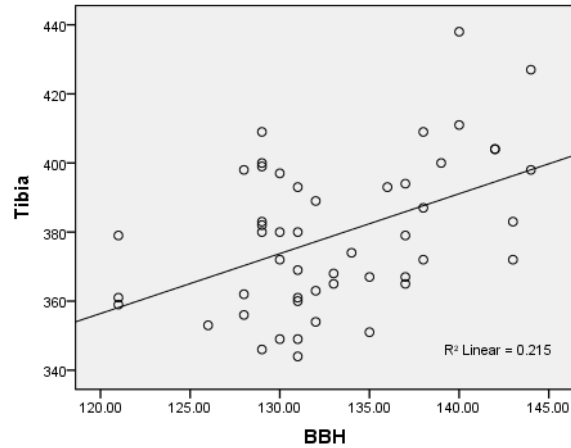
FRC-FIBXLN correlation of SAC males



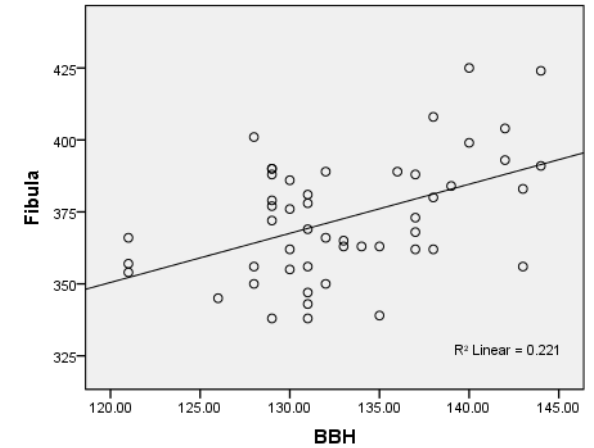
FRC-RADXLN correlation of SAC males



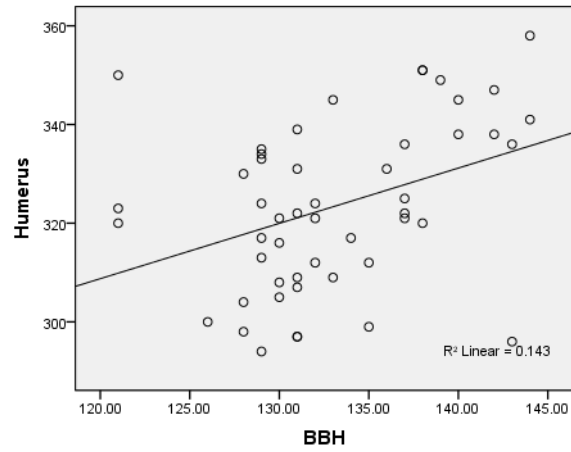
BBH-TIBXLN correlation of SAC males



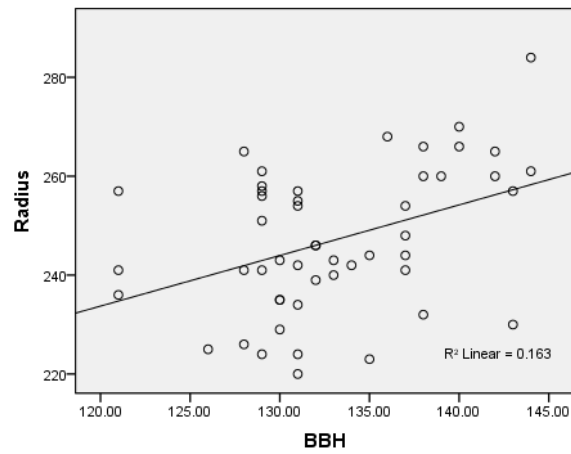
BBH-FIBXLN correlation of SAC males



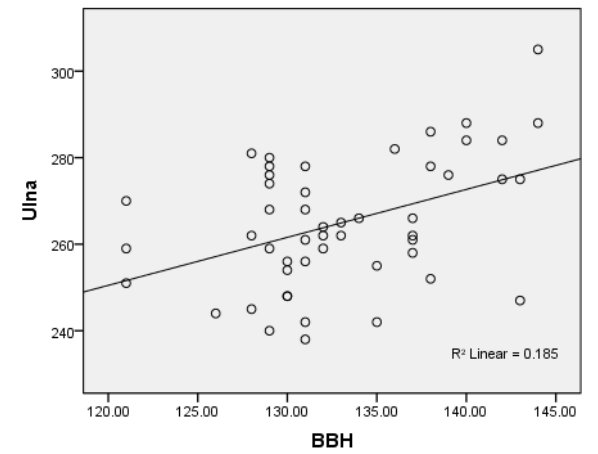
BBH-HUMXLN correlation of SAC males



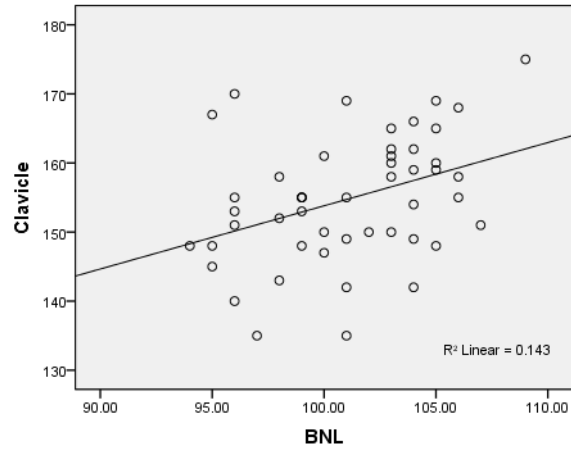
BBH-RADXLN correlation of SAC males



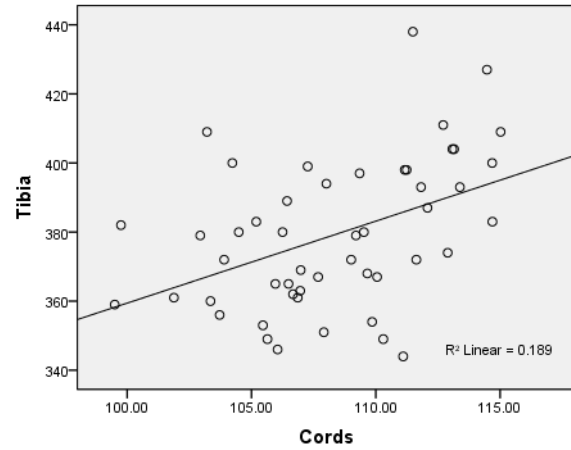
BBH-ULNXLN correlation of SAC males



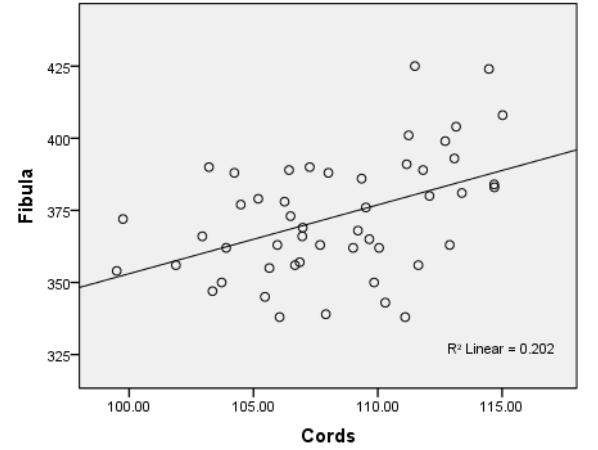
BNL-CLAXLN correlation of SAC males



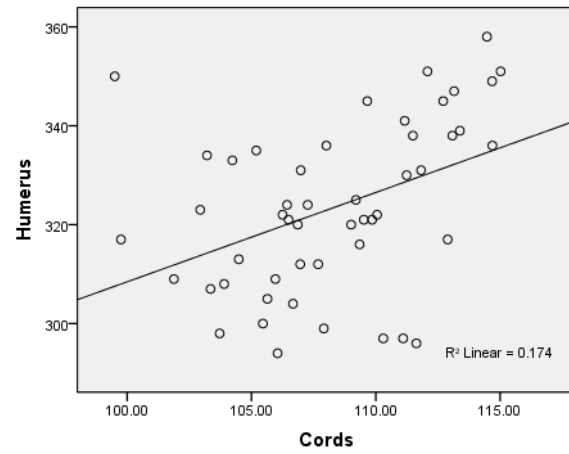
Cords-TIBXLN correlation of SAC males



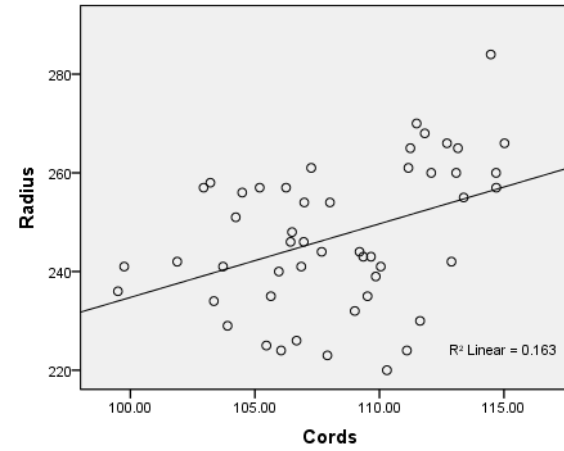
Cords-FIBXLN correlation of SAC males



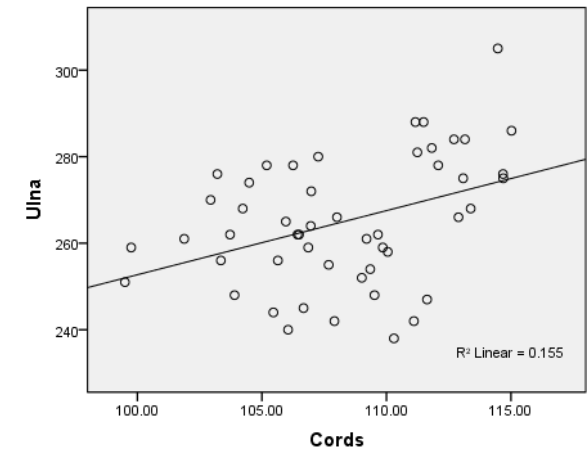
Cords-HUMXLN correlation of SAC males



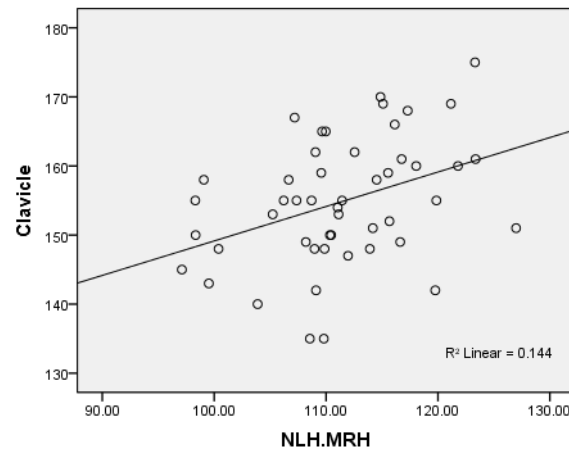
Cords-RADXLN correlation of SAC males



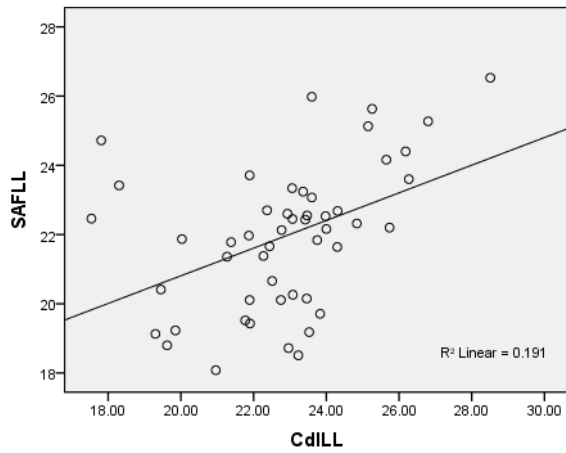
Cords-ULNXLN correlation of SAC males



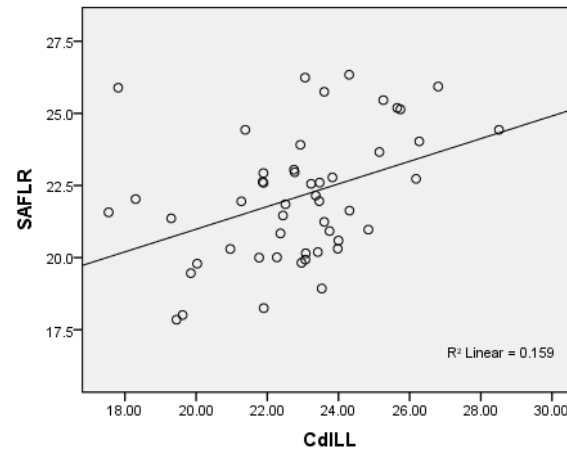
NHL.MRH-CLAXLN correlation of SAC males



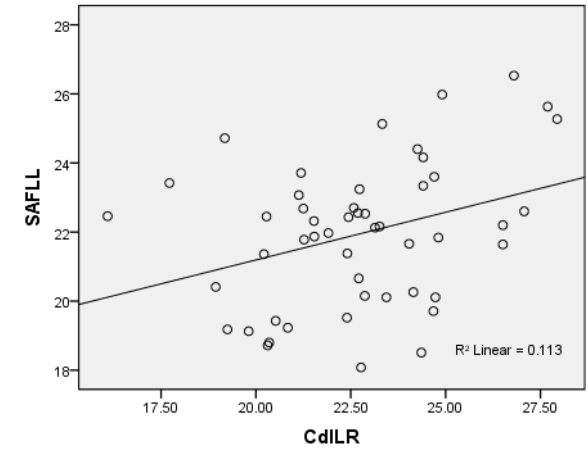
CdILL-SAFLL correlation of SAC males



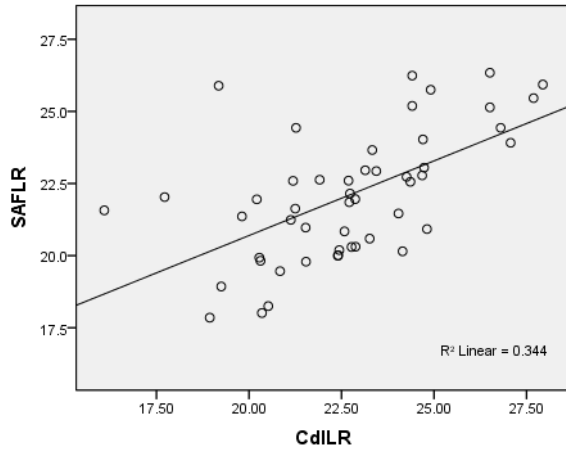
CdILL-SAFRL correlation of SAC males



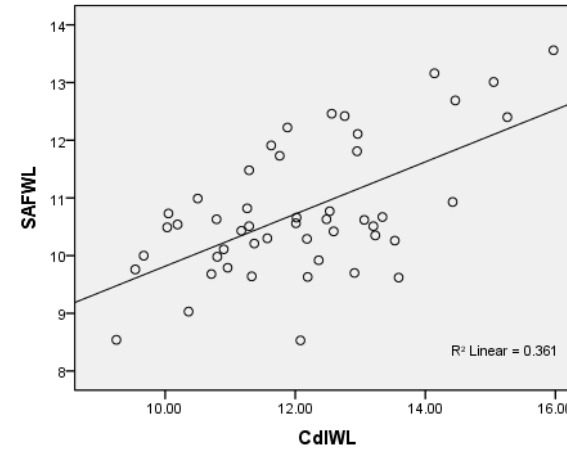
CdILR-SAFLL correlation of SAC males



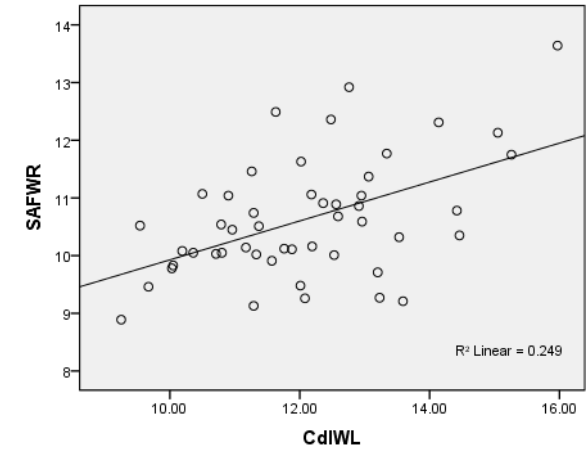
CdILR-SAFRL correlation of SAC males



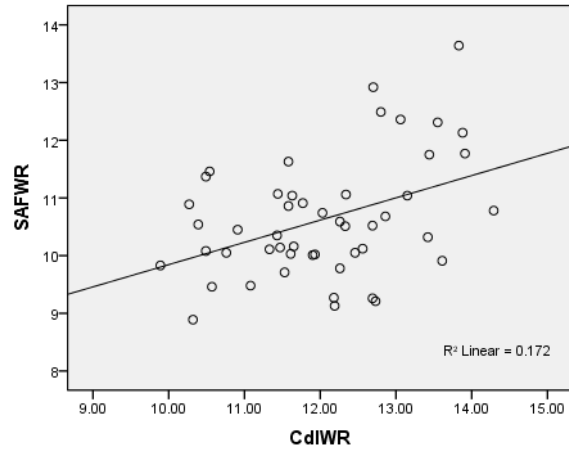
CdIWL-SAFWL correlation of SAC males



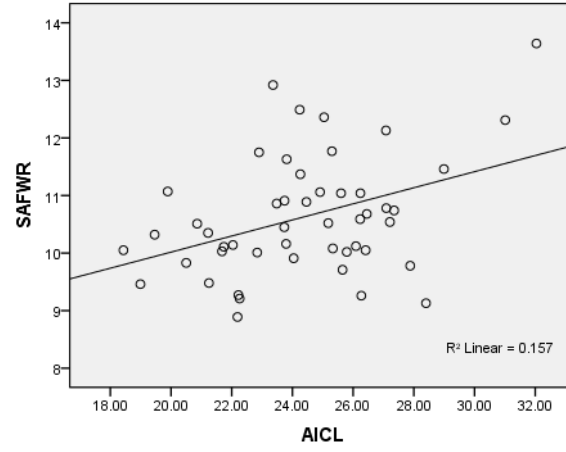
CdIWL-SAFWR correlation of SAC males



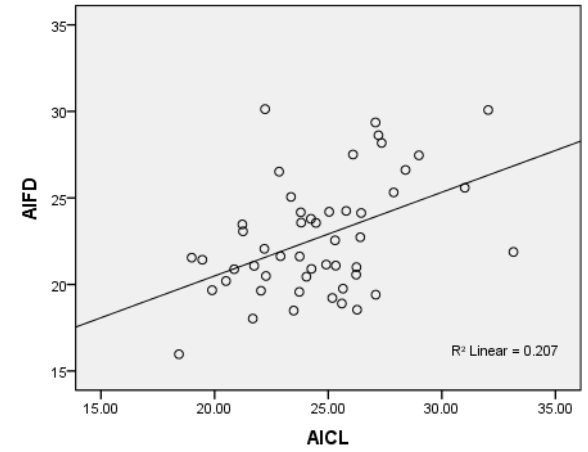
CdILR-SAFLR correlation of SAC males



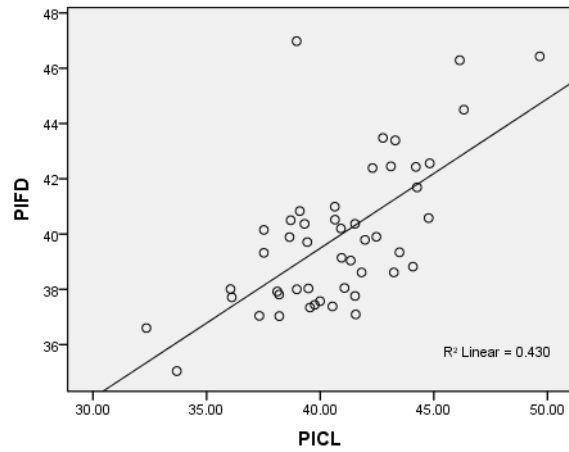
CdILR-SAFLR correlation of SAC males



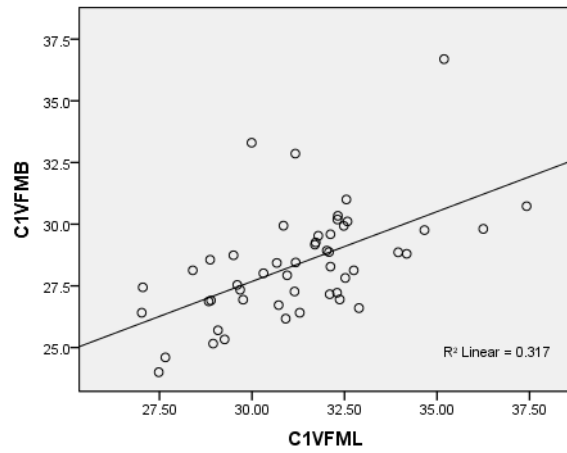
CdILR-SAFLR correlation of SAC males



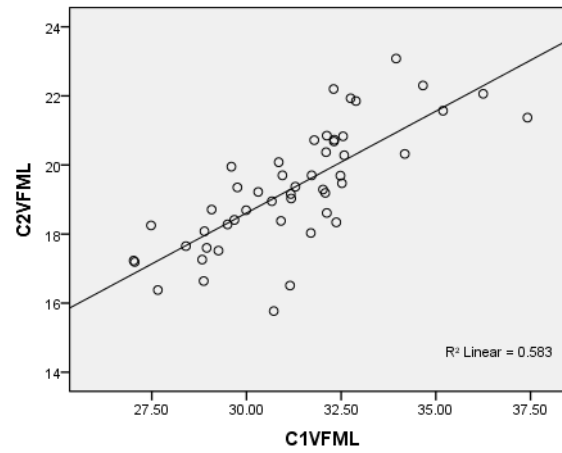
CdILR-SAFLR correlation of SAC males



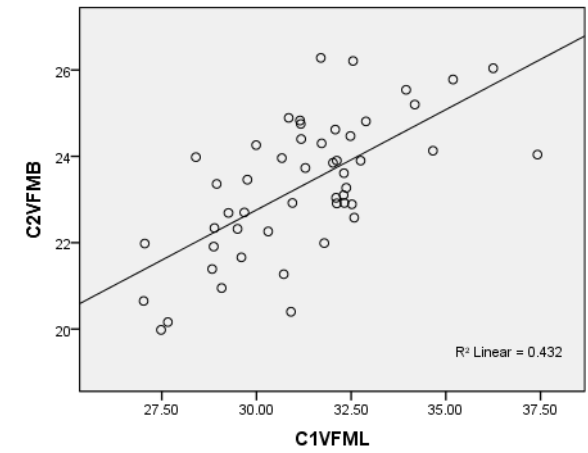
C1VFML-C1VFMB correlation of SAC males



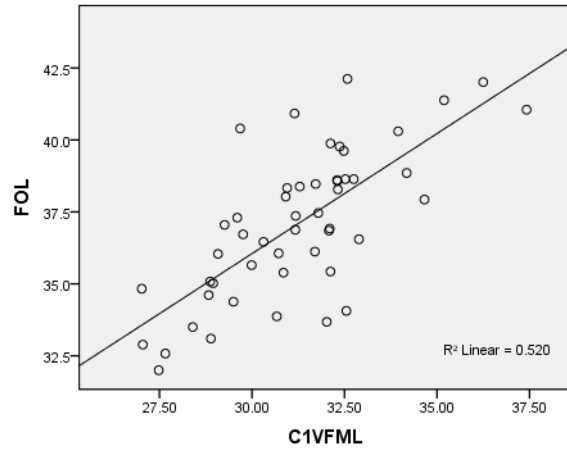
C1VFML-C2VFML correlation of SAC males



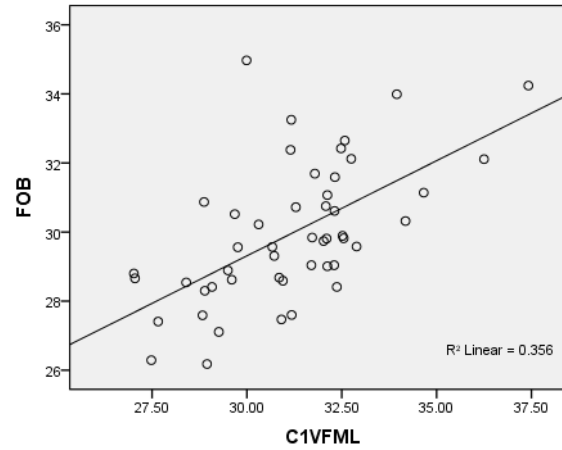
C1VFML-C2VFMB correlation of SAC males



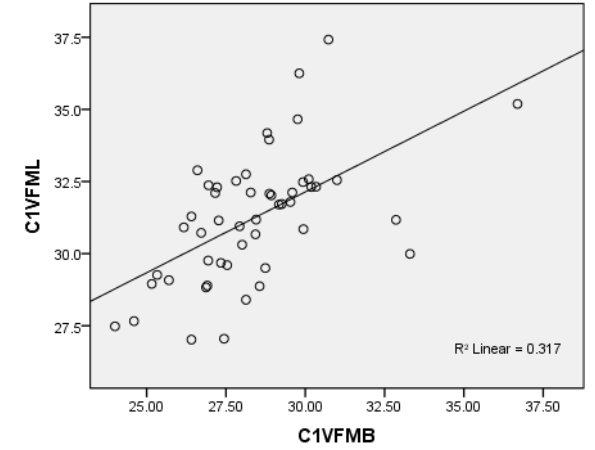
C1VFML-FOL correlation of SAC males



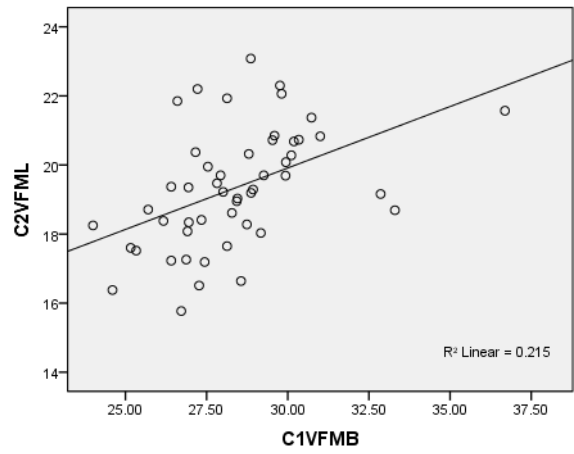
C1VFML-FOB correlation of SAC males



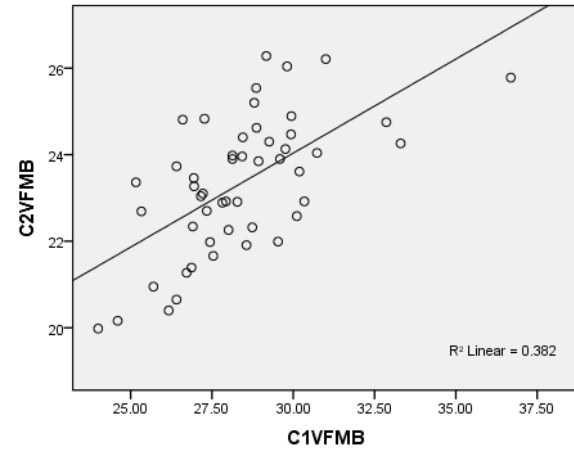
C1VFMB-C1VFML correlation of SAC males



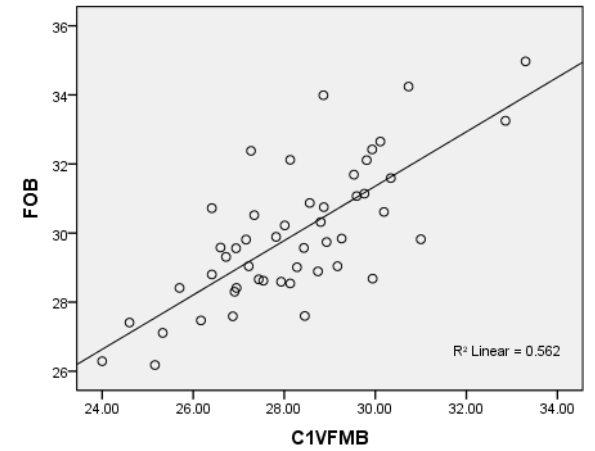
C1VFMB-C2VFML correlation of SAC males



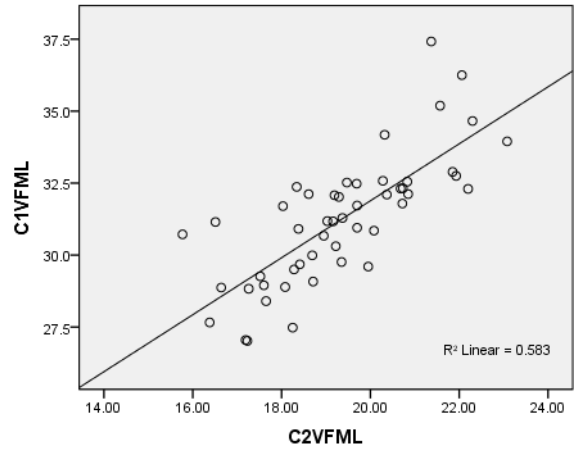
C1VFMB-C2VFMB correlation of SAC males



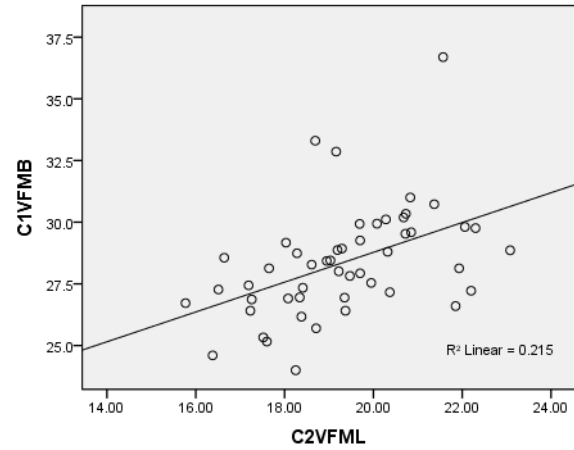
C1VFMB-FOB correlation of SAC males



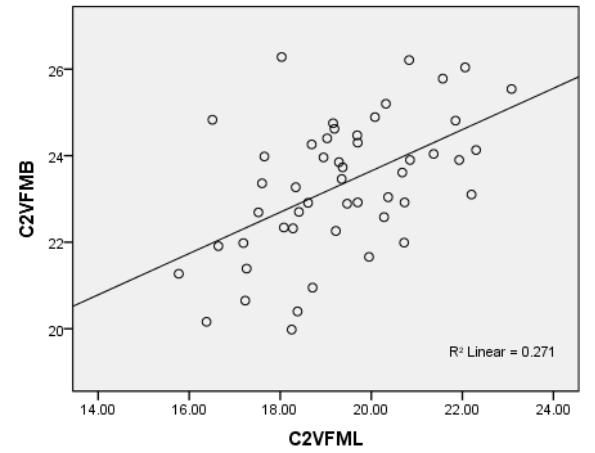
C2VFML-C1VFML correlation of SAC males



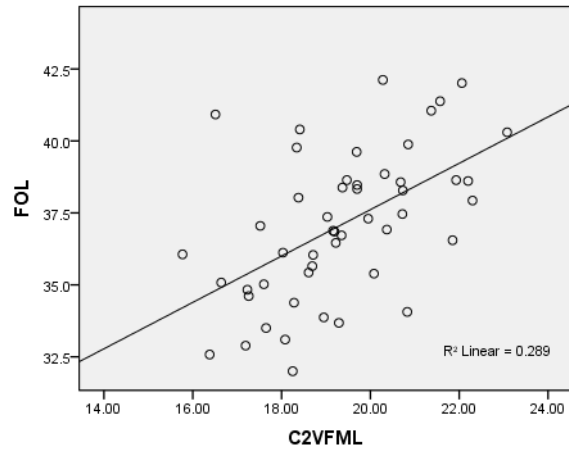
C2VFML-C1VFMB correlation of SAC males



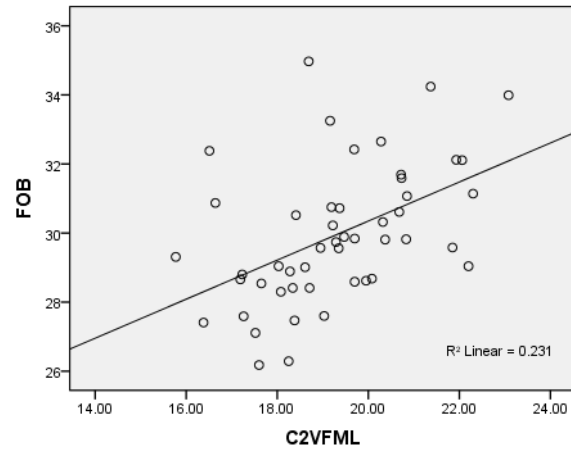
C2VFML-C2VFMB correlation of SAC males



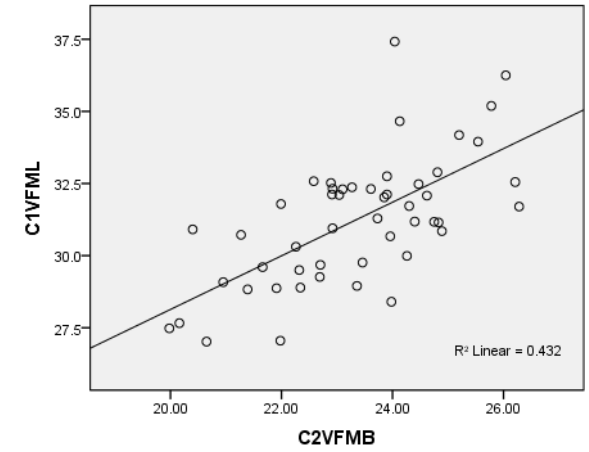
C2VFML-FOL correlation of SAC males



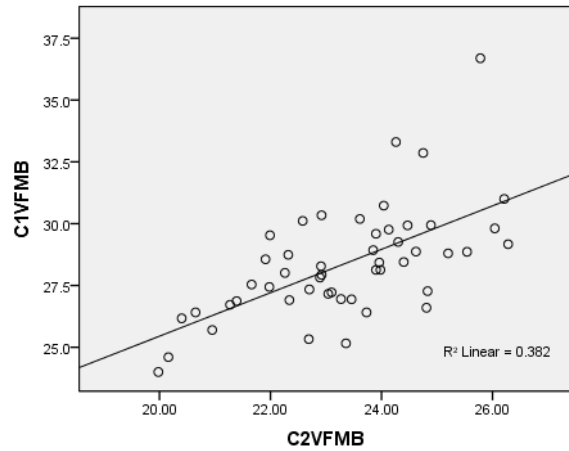
C2VFML-FOB correlation of SAC males



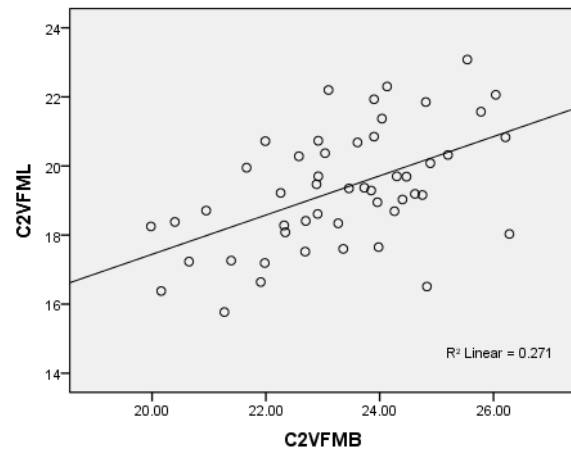
C2VFMB-C1VFML correlation of SAC males



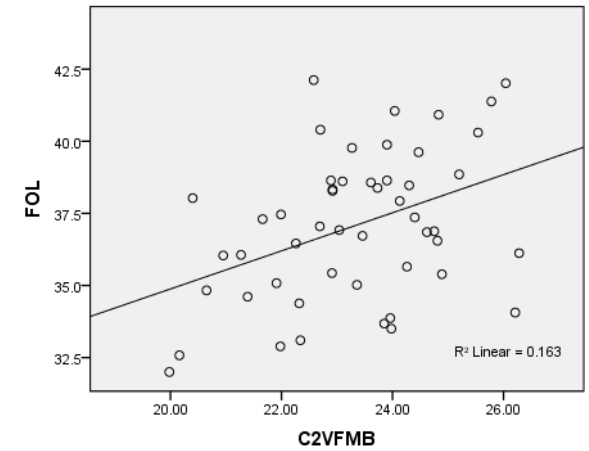
C2VFMB-C1VFMB correlation of SAC males



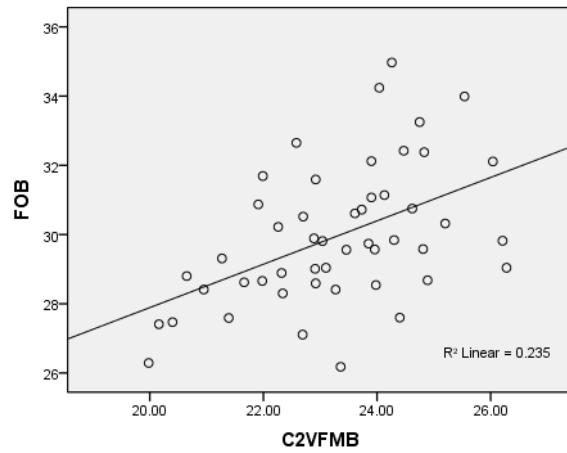
C2VFMB-C2VFML correlation of SAC males



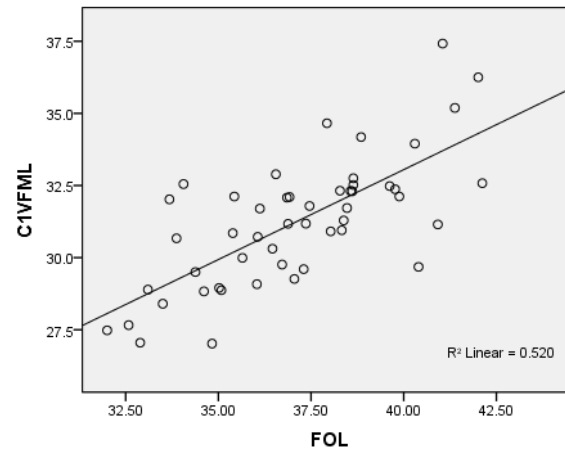
C2VFMB-FOL correlation of SAC males



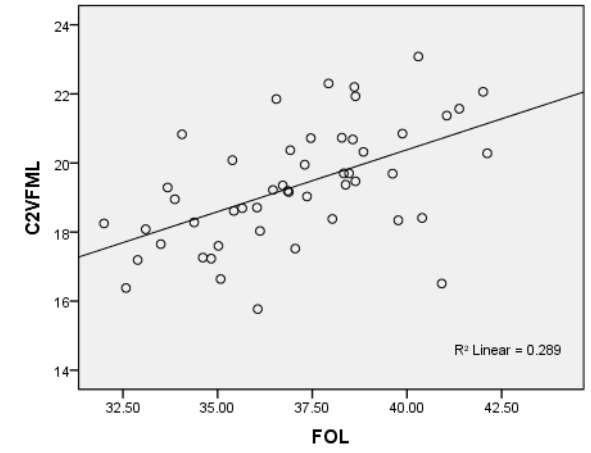
C2VFMB-FOB correlation of SAC males



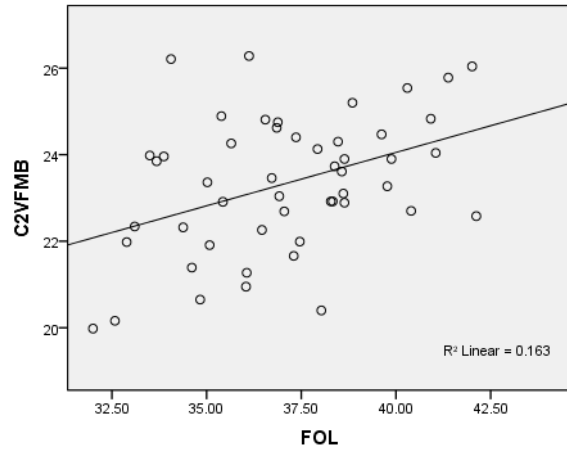
FOL-C1VFML correlation of SAC males



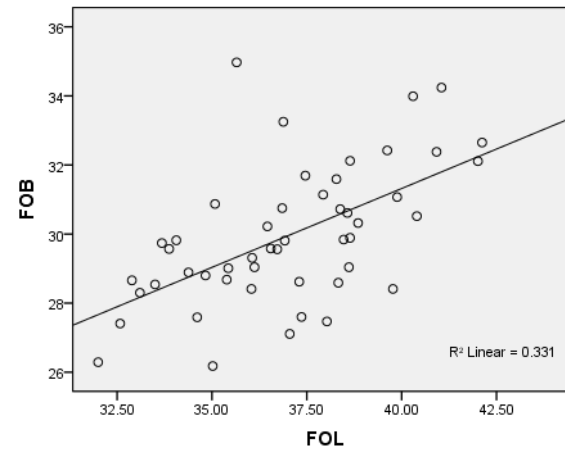
FOL-C2VFML correlation of SAC males



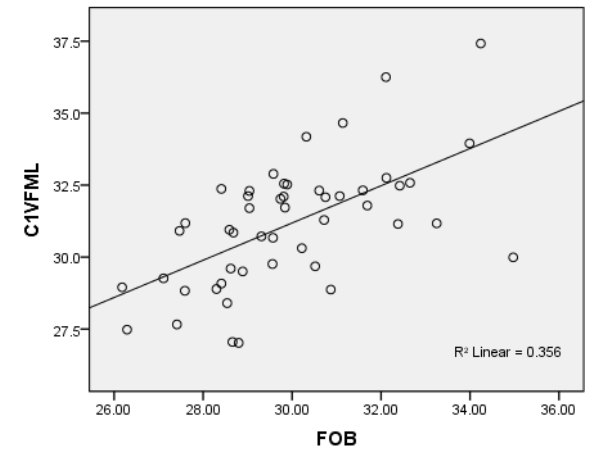
FOL-C2VFMB correlation of SAC males



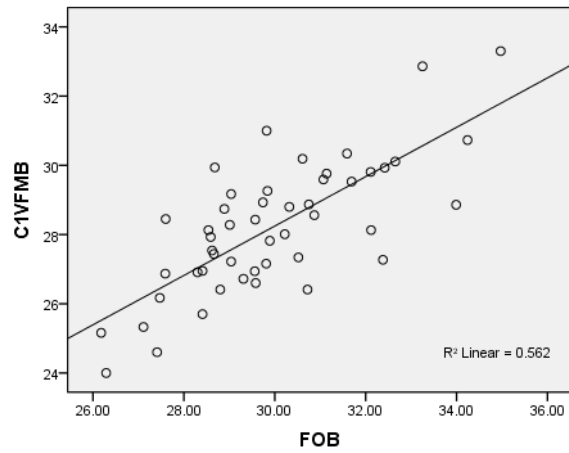
FOL-FOB correlation of SAC males



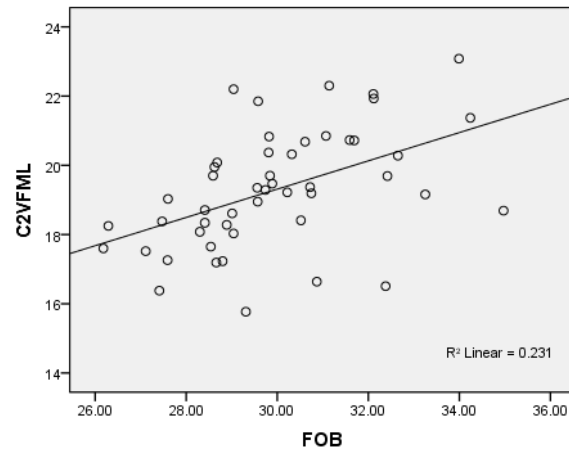
FOB-C1VFML correlation of SAC males



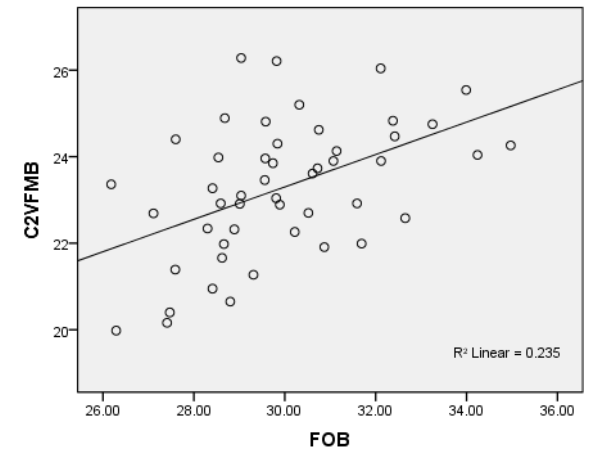
FOB-C1VFMB correlation of SAC males



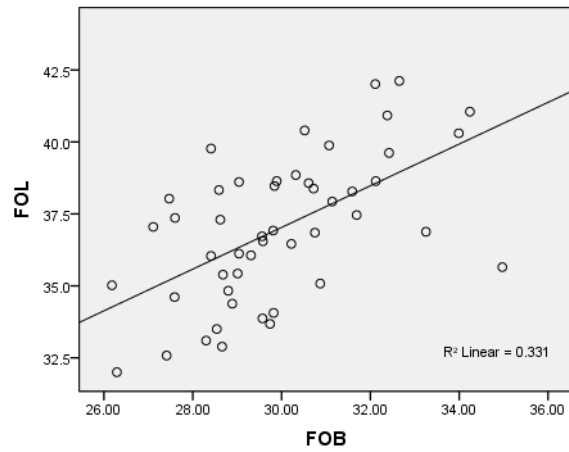
FOB-C2VFML correlation of SAC males



FOB-C2VFMB correlation of SAC males

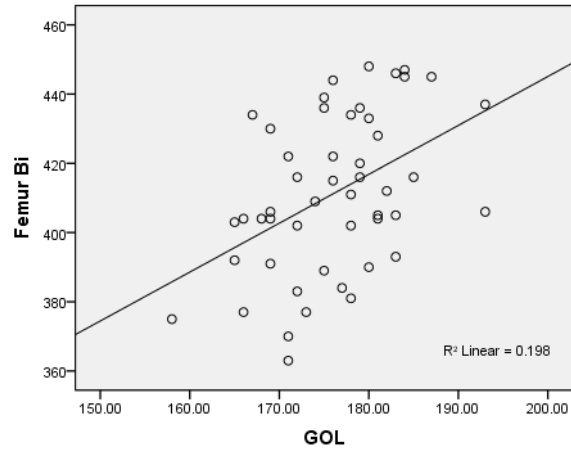


FOB-FOL correlation of SAC males

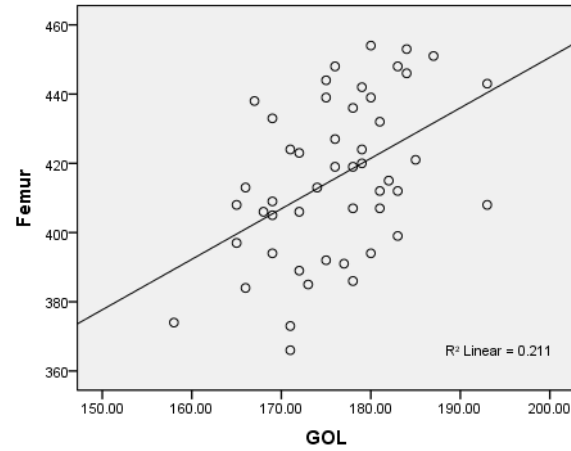


7.6 SOUTH AFRICAN COLOURED FEMALES

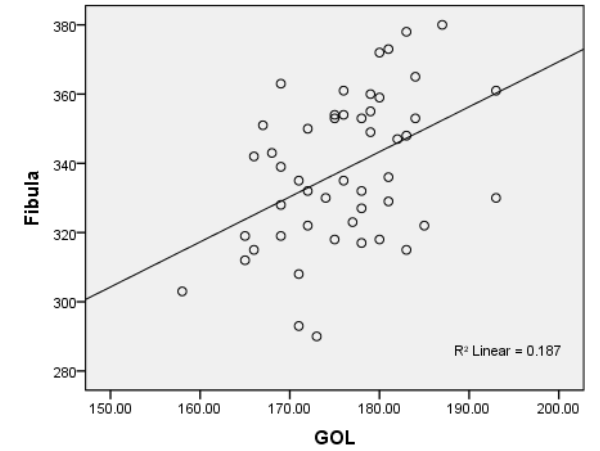
GOL-FEMBLN correlation of SAC females



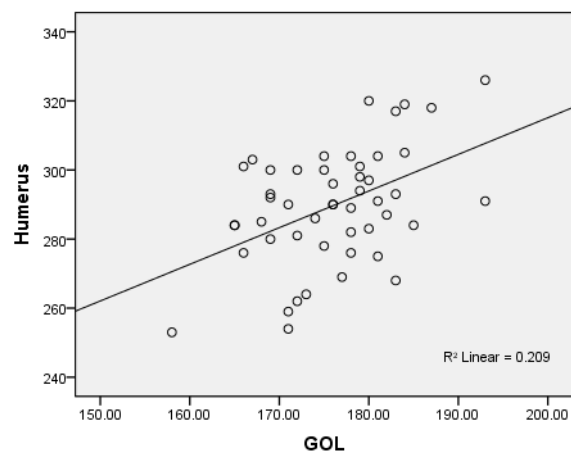
GOL-FEMXLN correlation of SAC females



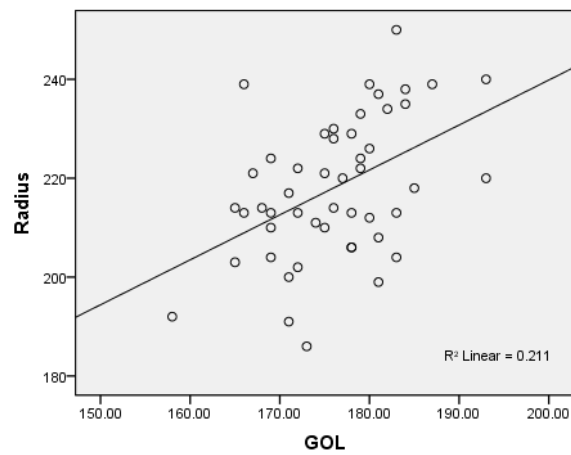
GOL-FIBXLN correlation of SAC females



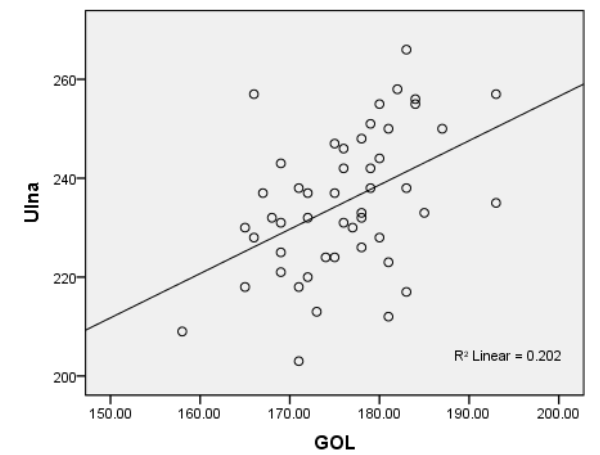
GOL-HUMXLN correlation of SAC females



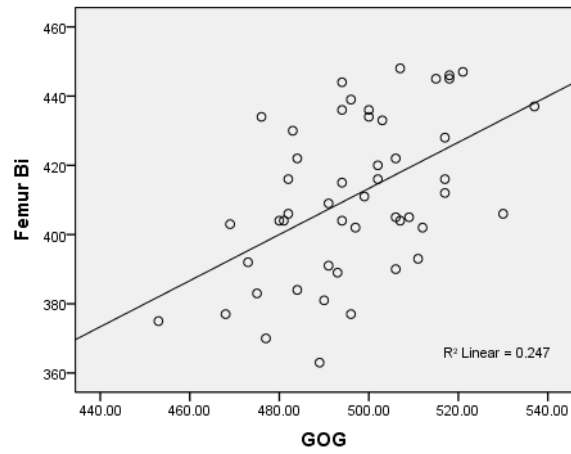
GOL-RADXLN correlation of SAC females



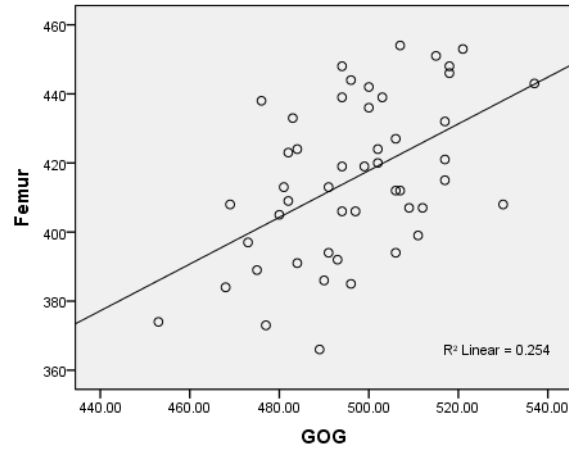
GOL-ULNXLN correlation of SAC females



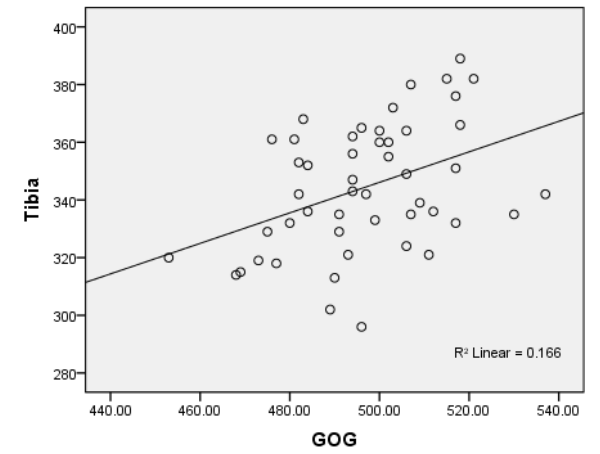
GOG-FEMBLN correlation of SAC females



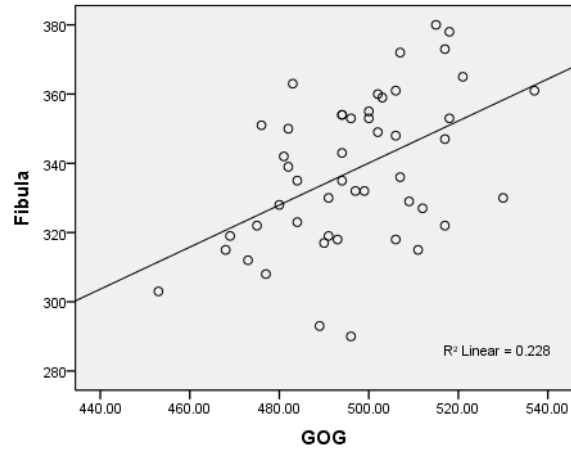
GOG-FEMXLN correlation of SAC females



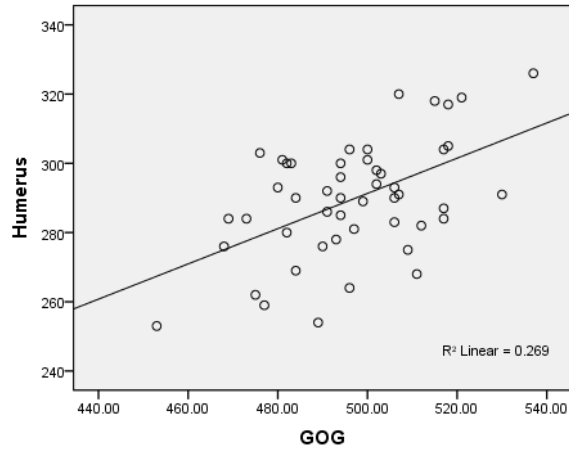
GOG-TIBXLN correlation of SAC females



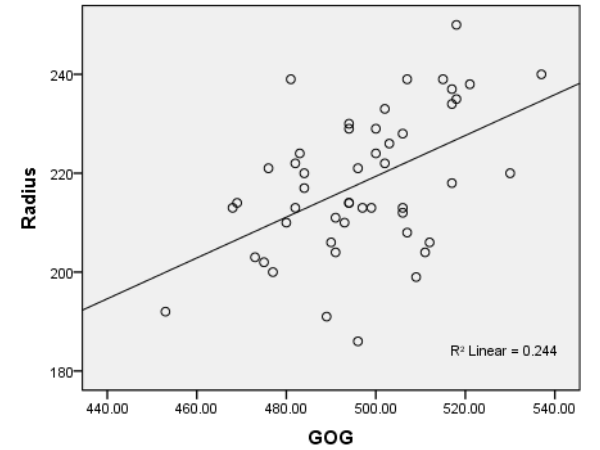
GOG-FIBXLN correlation of SAC females



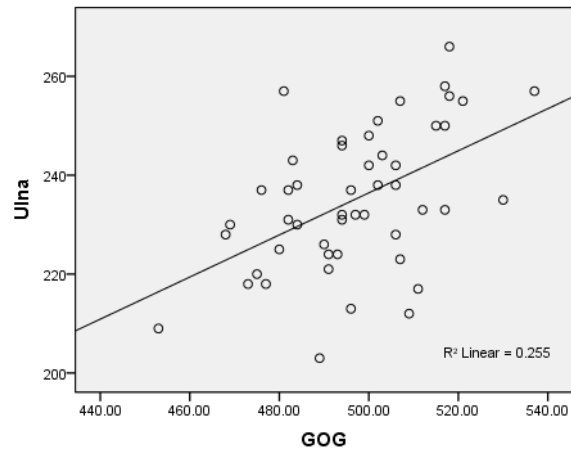
GOG-HUMXLN correlation of SAC females



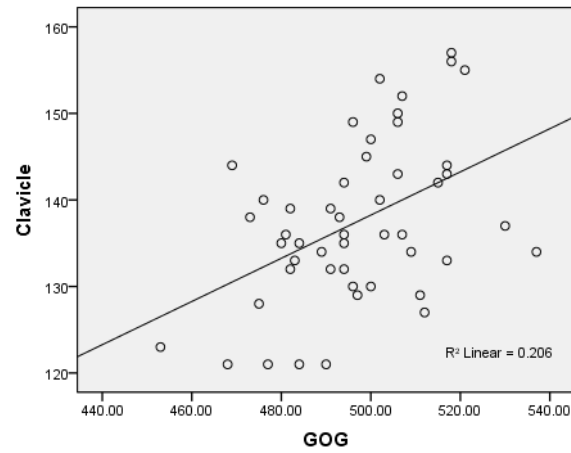
GOG-RADXLN correlation of SAC females



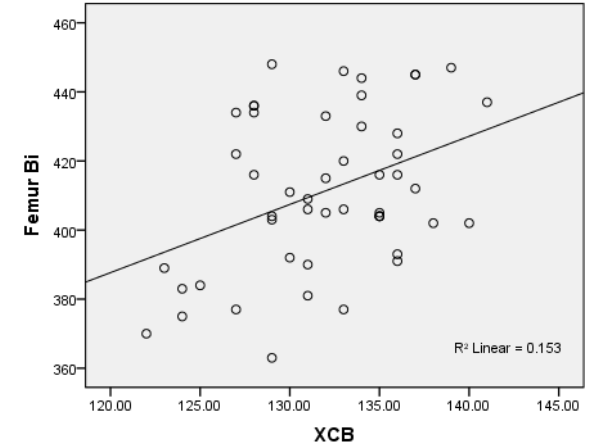
GOG-ULNXLN correlation of SAC females



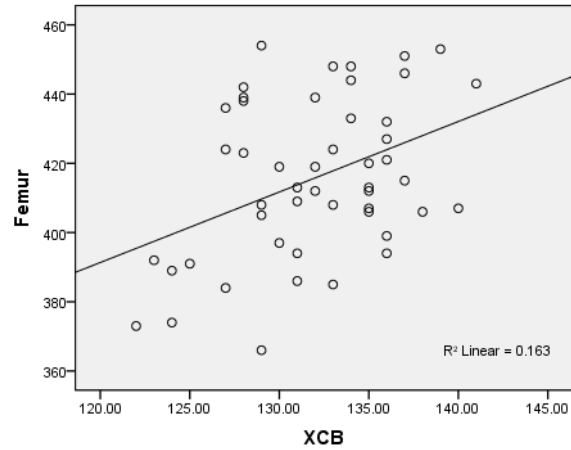
GOG-CLAXLN correlation of SAC females



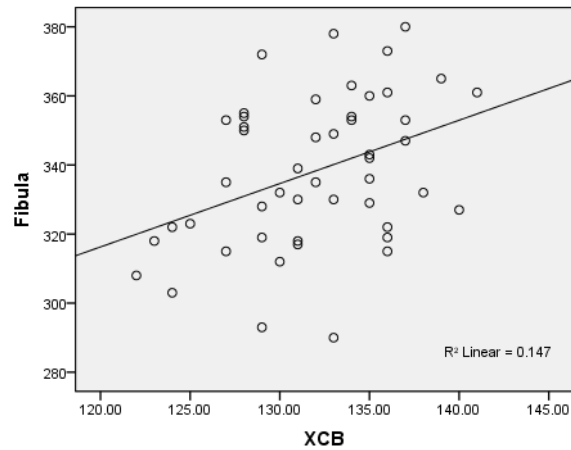
XCB-FEMBLN correlation of SAC females



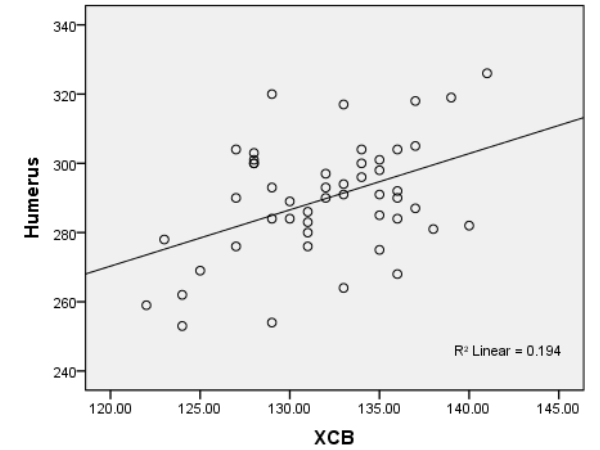
XCB-FEMXLN correlation of SAC females



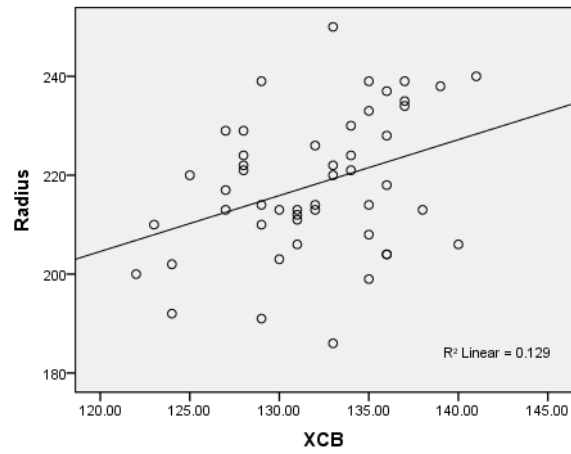
XCB-FIBXLN correlation of SAC females



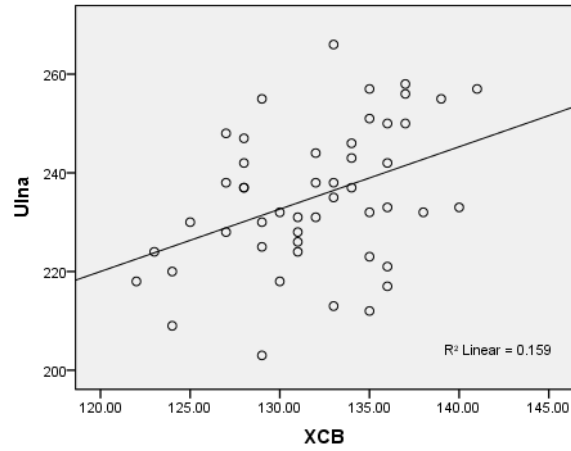
XCB-HUMXLN correlation of SAC females



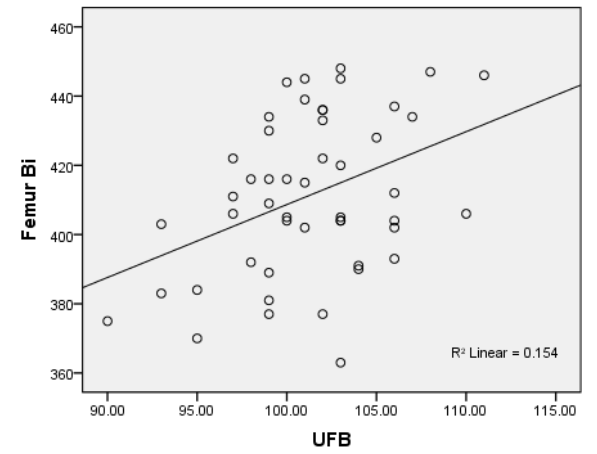
XCB-RADXLN correlation of SAC females



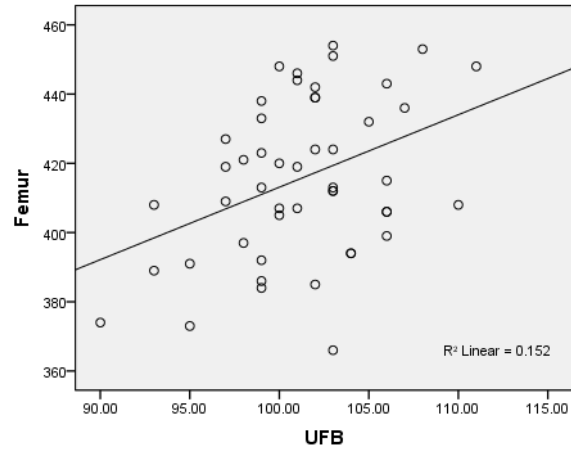
XCB-ULNXLN correlation of SAC females



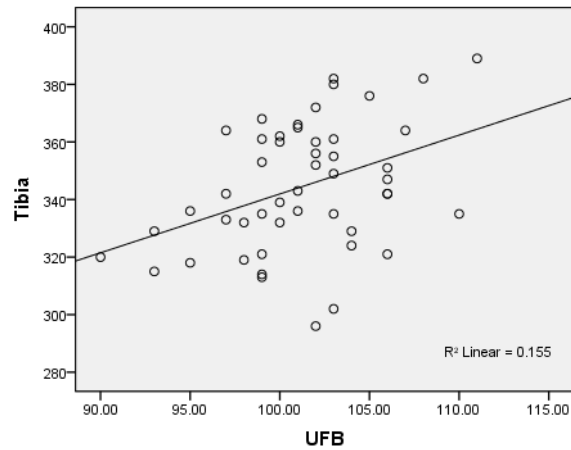
UFB-FEMBNL correlation of SAC females



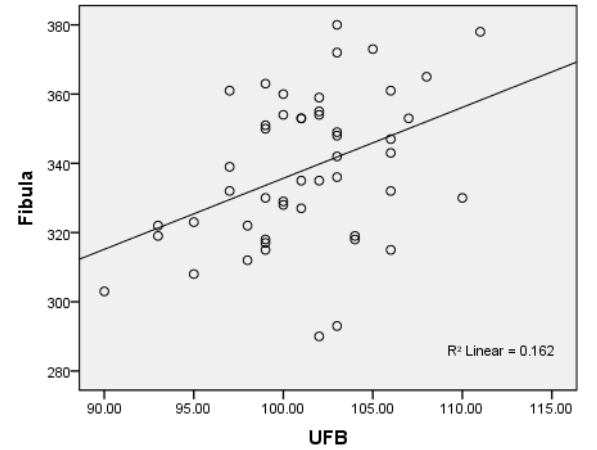
UFB-FEMXLN correlation of SAC females



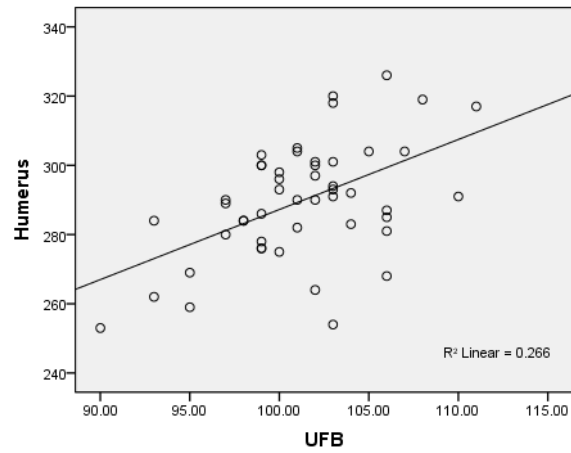
UFB-TIBXLN correlation of SAC females



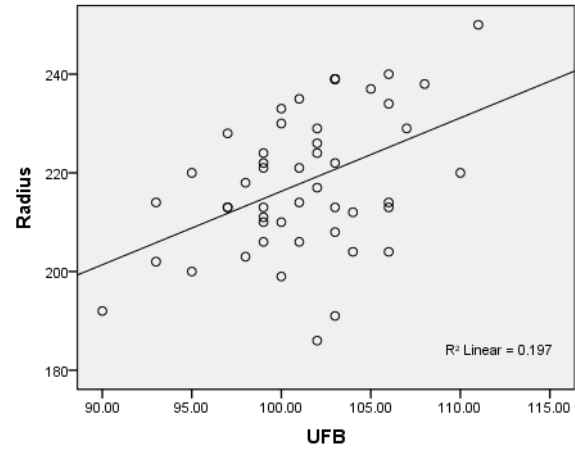
UFB-FIBXLN correlation of SAC females



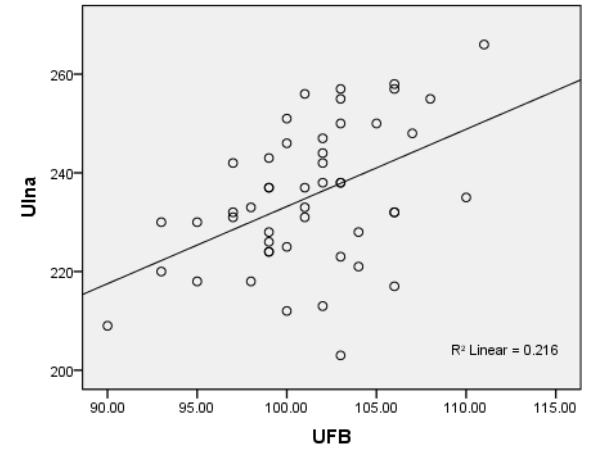
UFB-HUMXLN correlation of SAC females



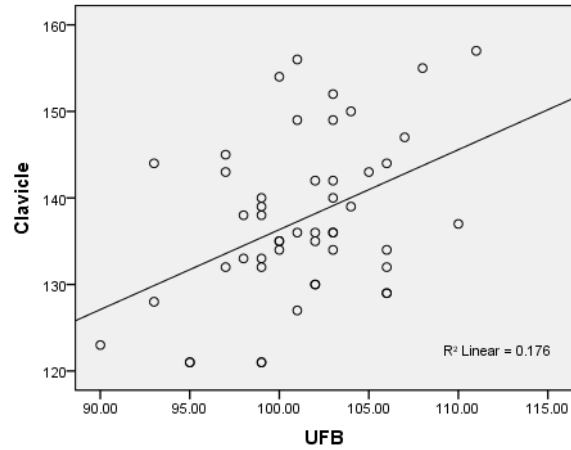
UFB-RADXLN correlation of SAC females



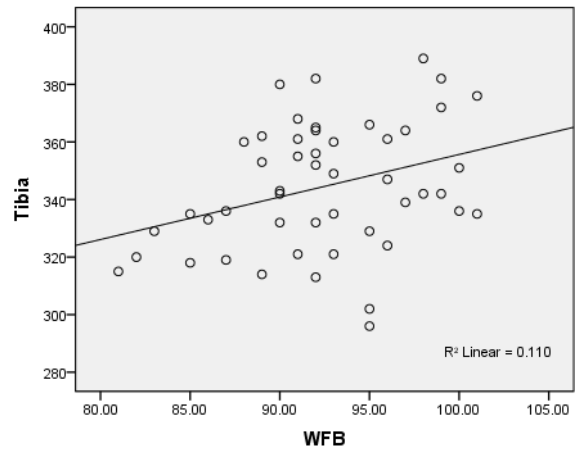
UFB-ULNXLN correlation of SAC females



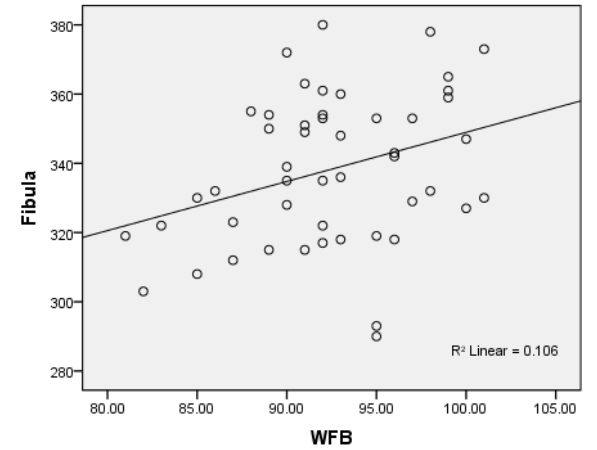
UFB-CLAXLN correlation of SAC females



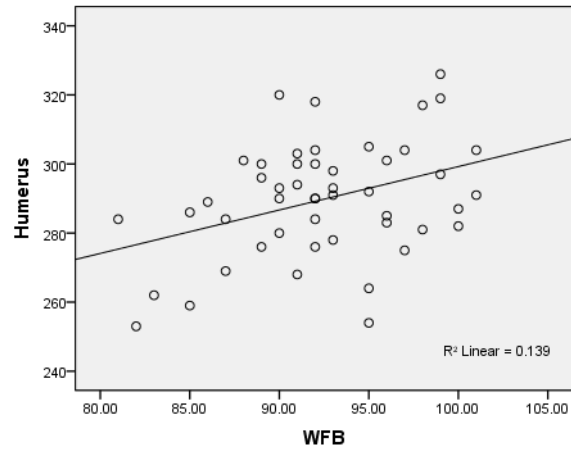
WFB-TIBXLN correlation of SAC females



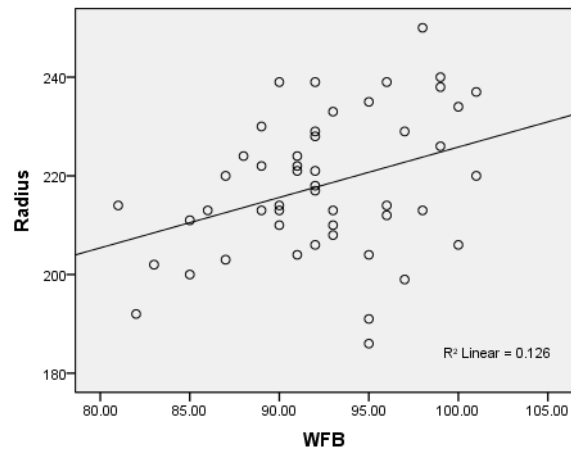
WFB-FIBXLN correlation of SAC females



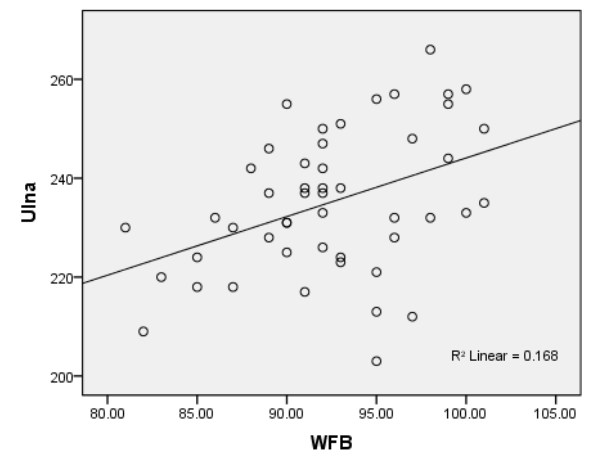
WFB-HUMXLN correlation of SAC females



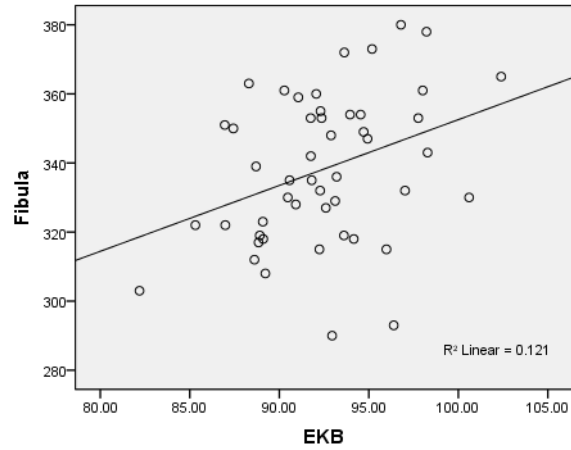
WFB-RADXLN correlation of SAC females



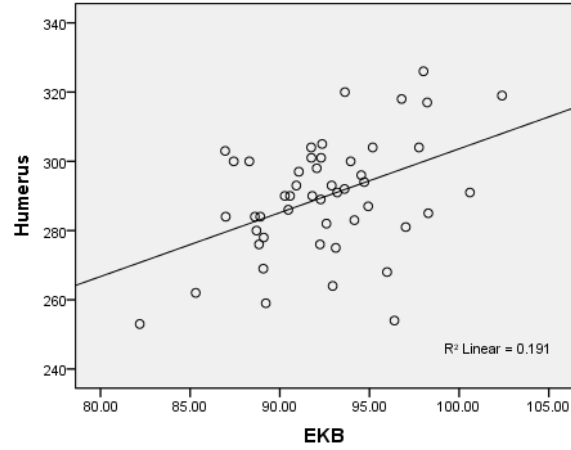
WFB-ULNXLN correlation of SAC females



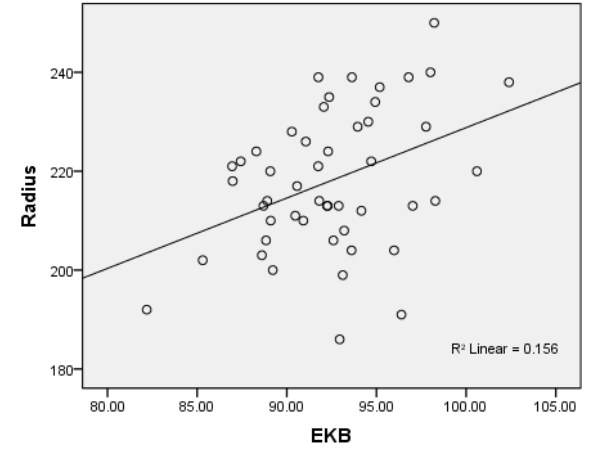
EKB-FIBXLN correlation of SAC females



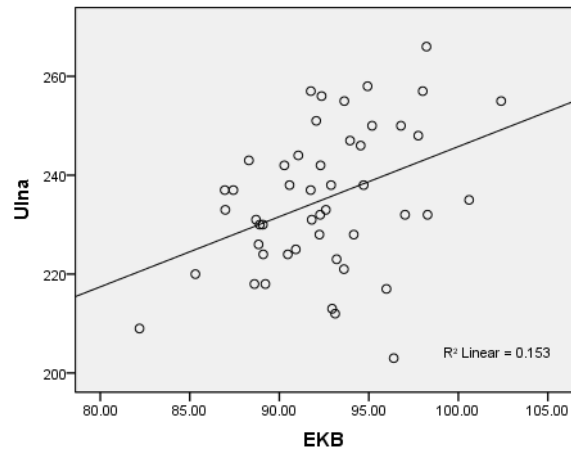
EKB-HUMXLN correlation of SAC females



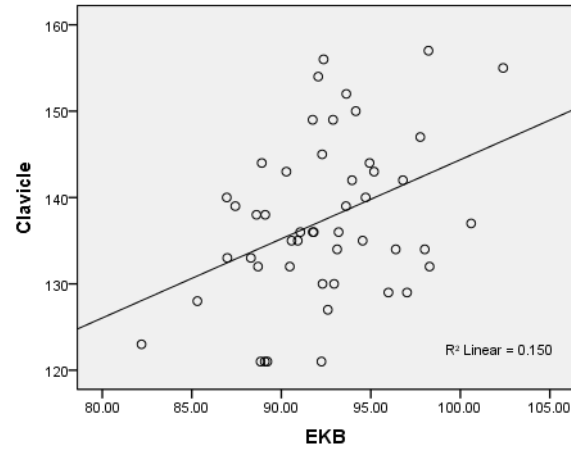
EKB-RADXLN correlation of SAC females



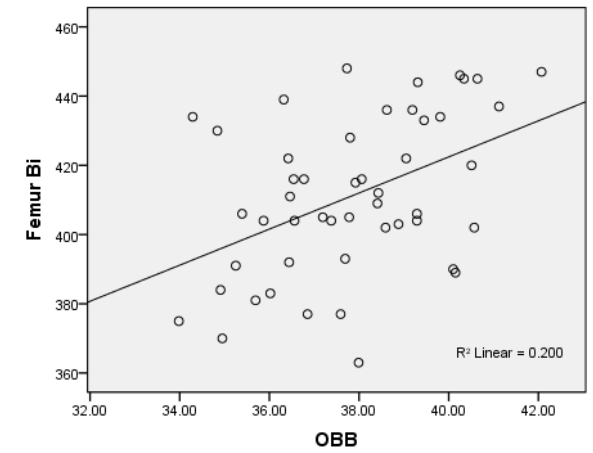
EKB-ULNXLN correlation of SAC females



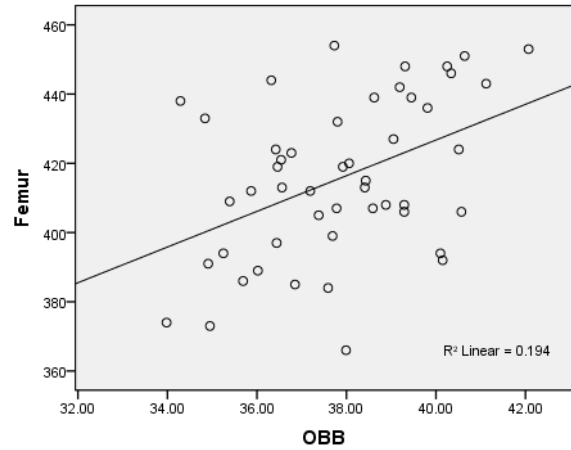
EKB-CLAXLN correlation of SAC females



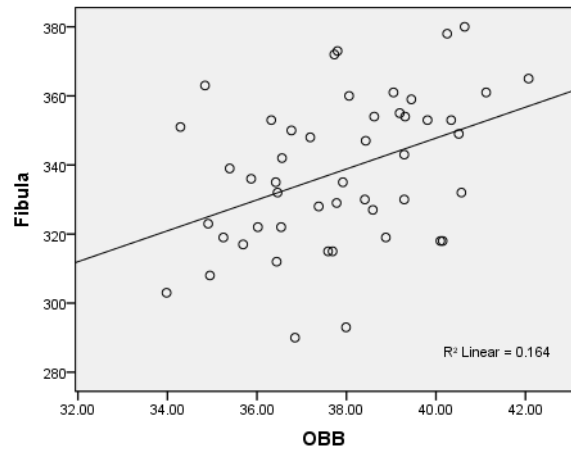
OBB-FEMBNL correlation of SAC females



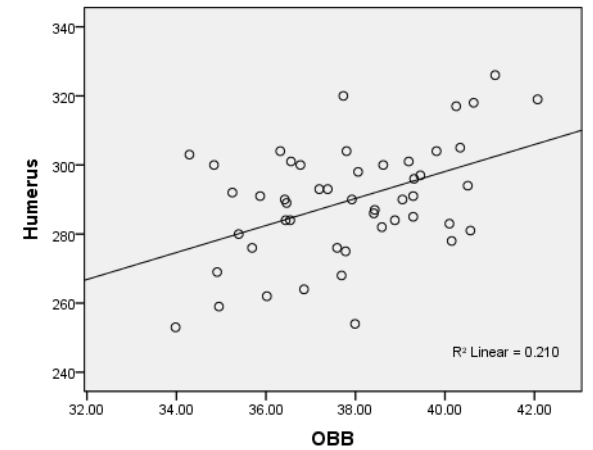
OBB-FEMXLN correlation of SAC females



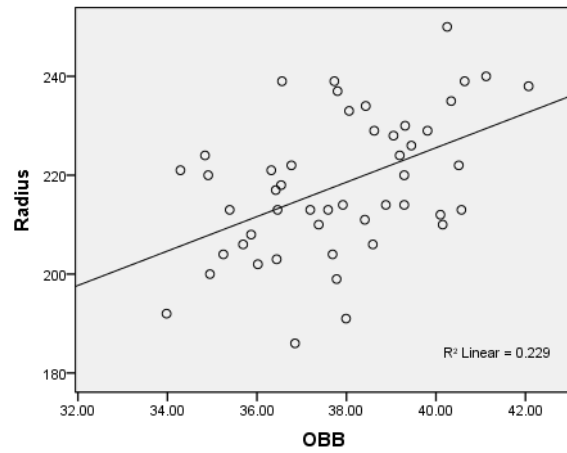
OBB-FIBXLN correlation of SAC females



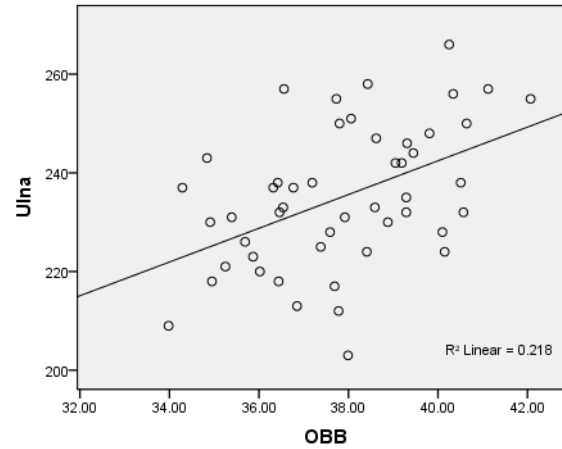
OBB-HUMXLN correlation of SAC females



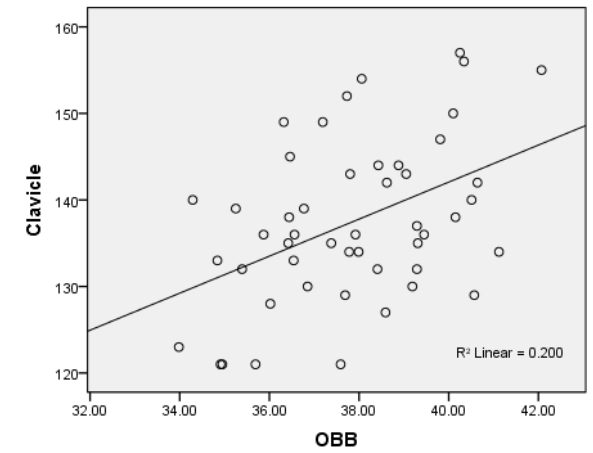
OBB-RADXLN correlation of SAC females



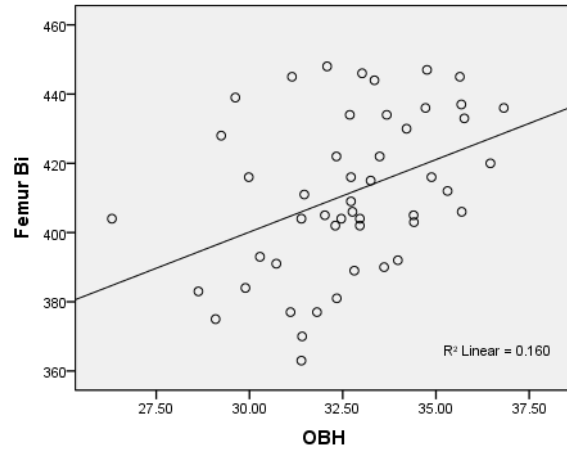
OBB-ULNXLN correlation of SAC females



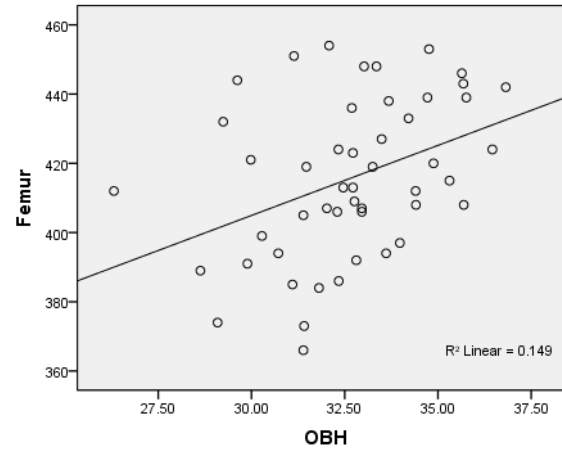
OBB-CLAXLN correlation of SAC females



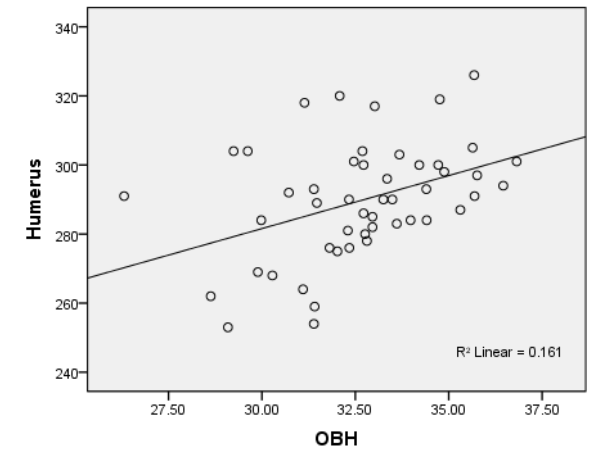
OBH-FEMBLN correlation of SAC females



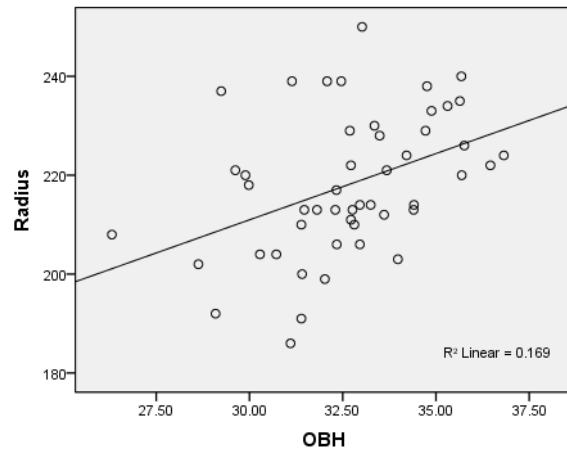
OBH-FEMXLN correlation of SAC females



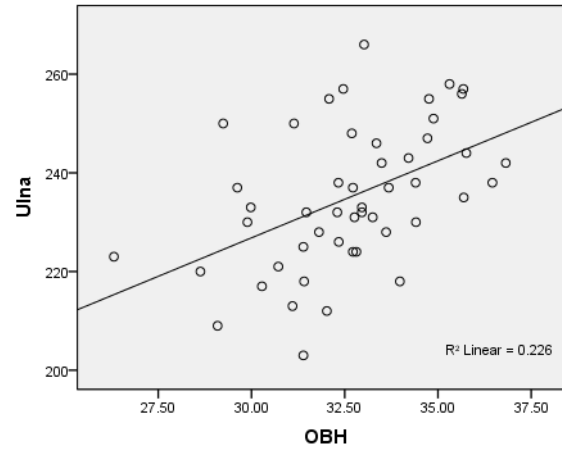
OBH-HUMXLN correlation of SAC females



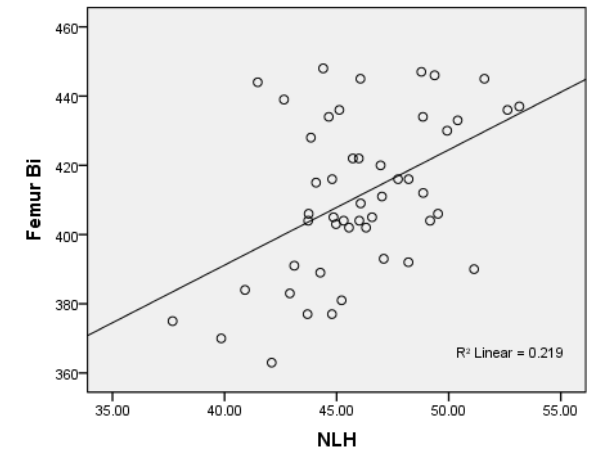
OBH-RADXLN correlation of SAC females



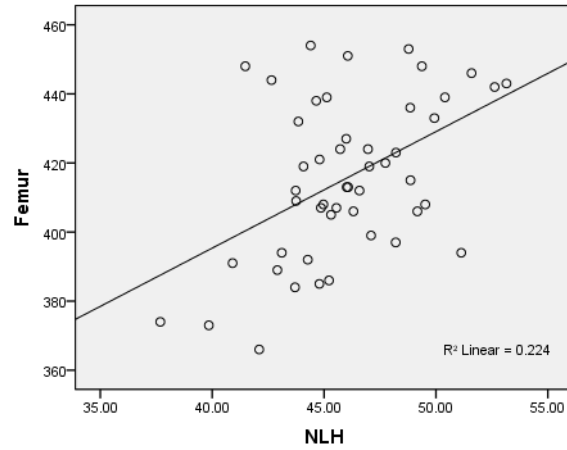
OBH-ULNXLN correlation of SAC females



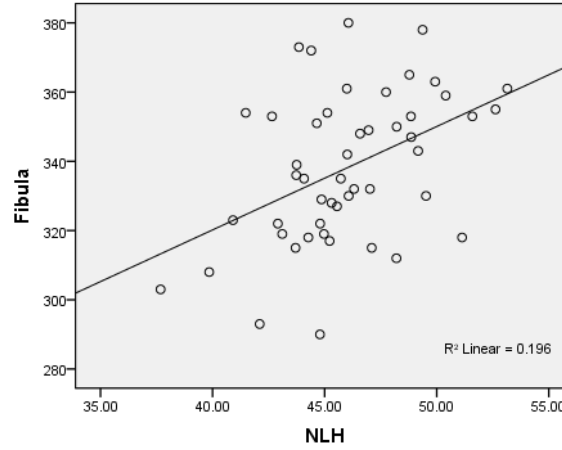
NLH-FEMBLN correlation of SAC females



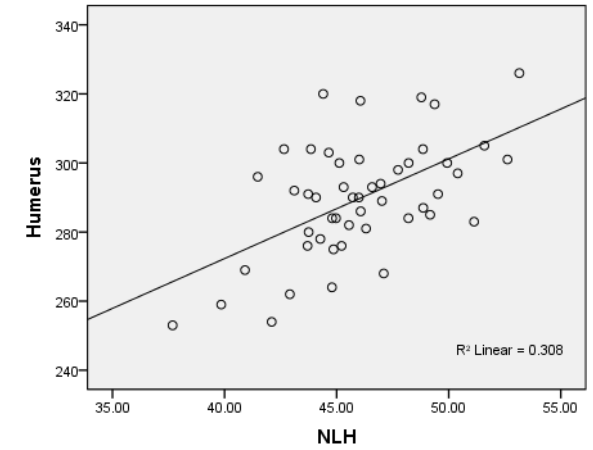
NLH-FEMXLN correlation of SAC females



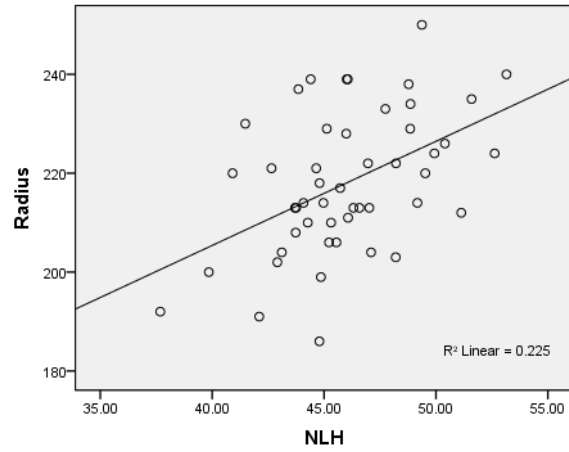
NLH-FIBXLN correlation of SAC females



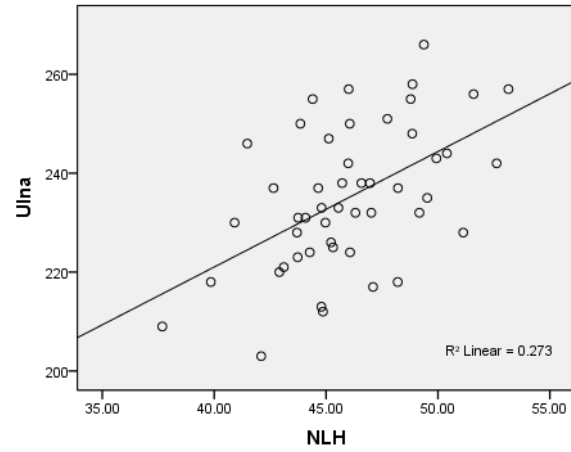
NLH-HUMXLN correlation of SAC females



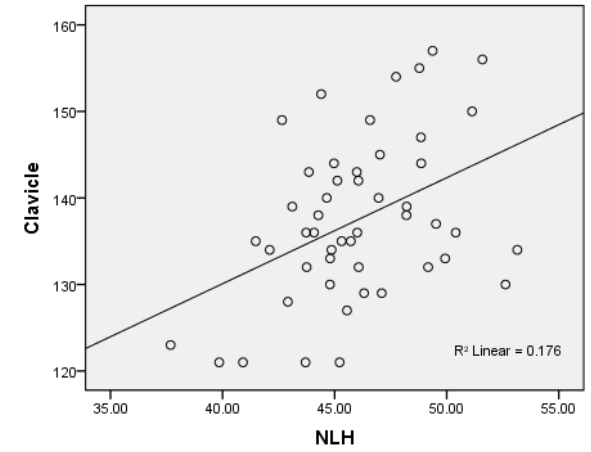
NLH-RADXLN correlation of SAC females



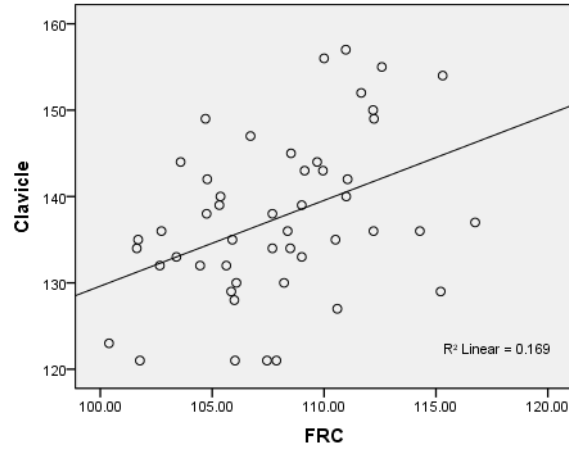
NLH-ULNXLN correlation of SAC females



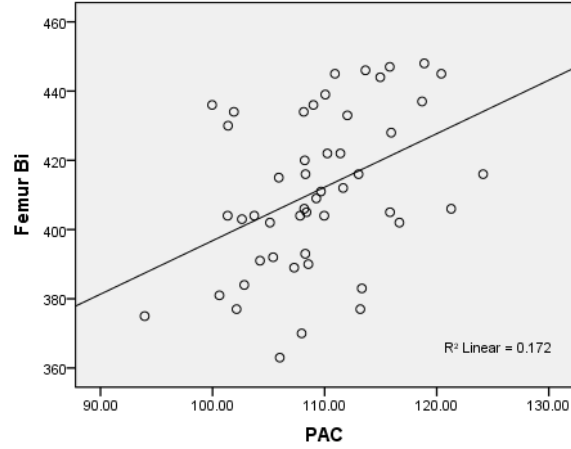
NLH-CLAXLN correlation of SAC females



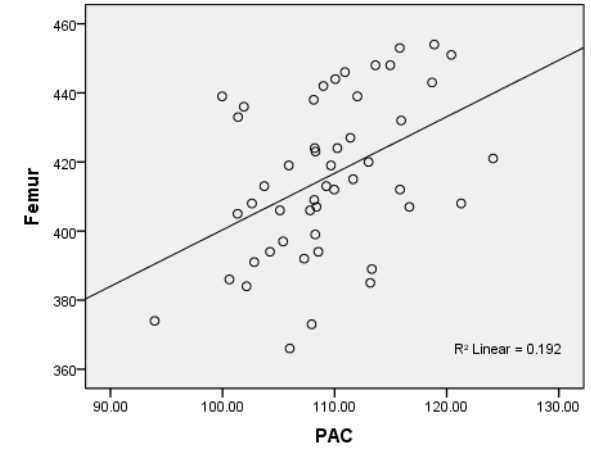
FRC-CLAXLN correlation of SAC females



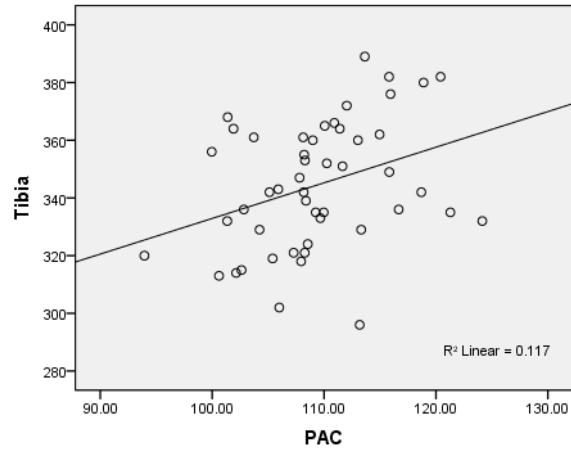
PAC-FEMBLN correlation of SAC females



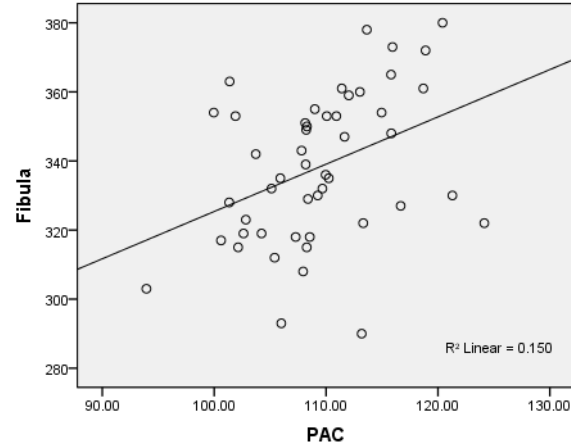
PAC-FEMXLN correlation of SAC females



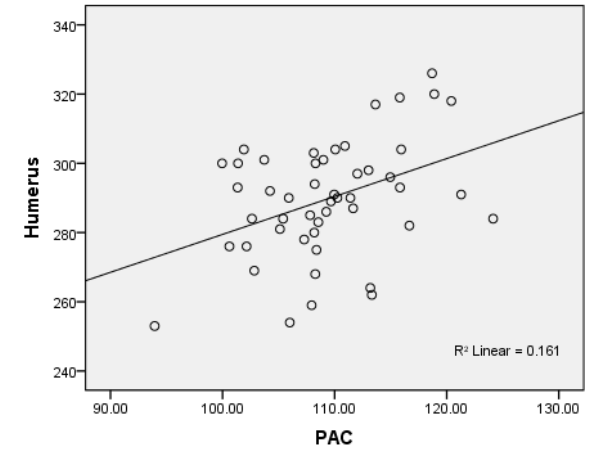
PAC-TIBXLN correlation of SAC females



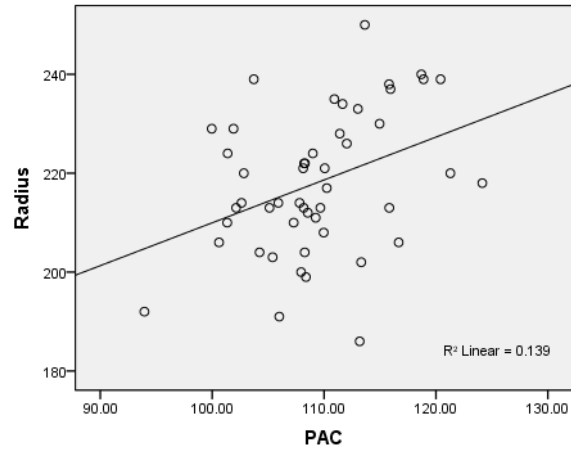
PAC-FIBXLN correlation of SAC females



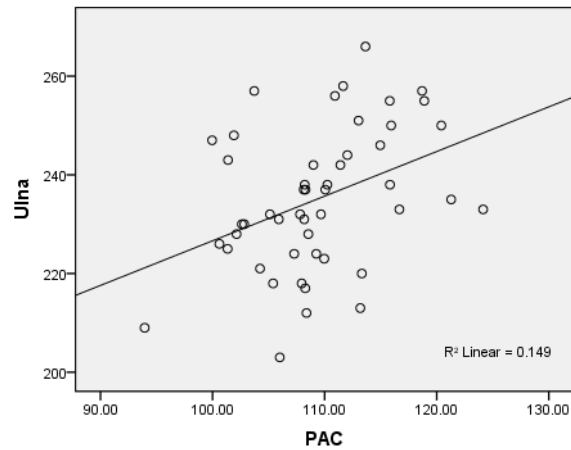
PAC-HUMXLN correlation of SAC females



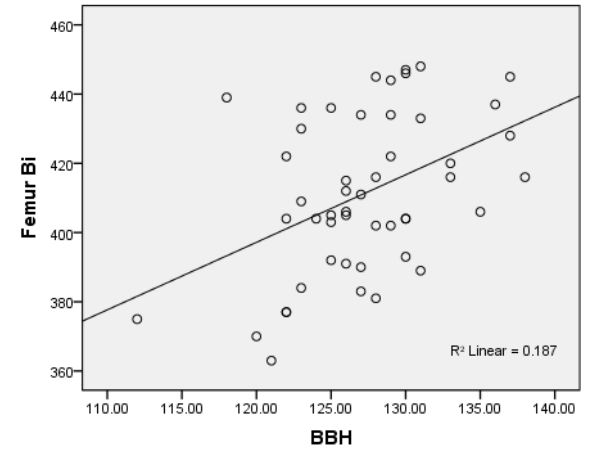
PAC-RADXLN correlation of SAC females



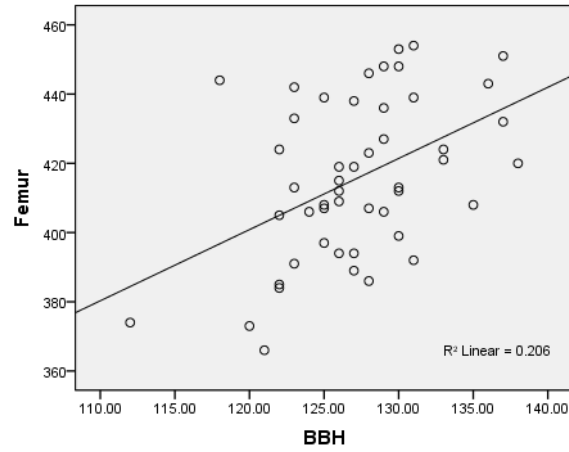
PAC-ULNXLN correlation of SAC females



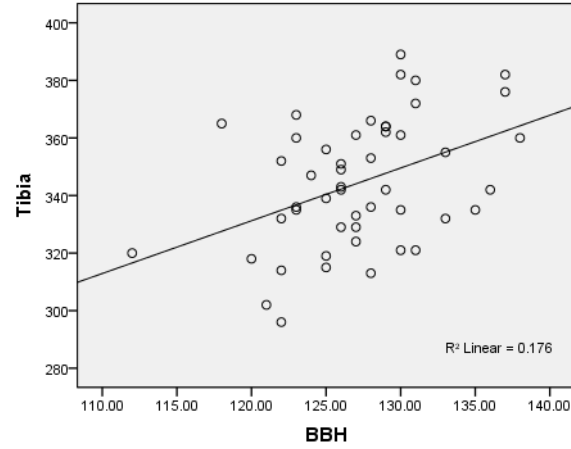
BBH-FEMBLN correlation of SAC females



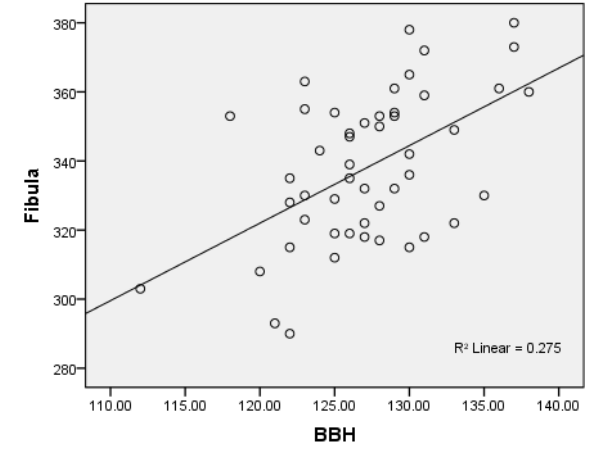
BBH-FEMXLN correlation of SAC females



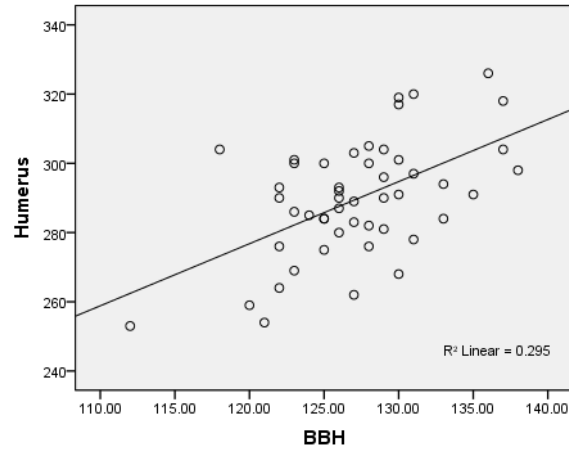
BBH-TIBXLN correlation of SAC females



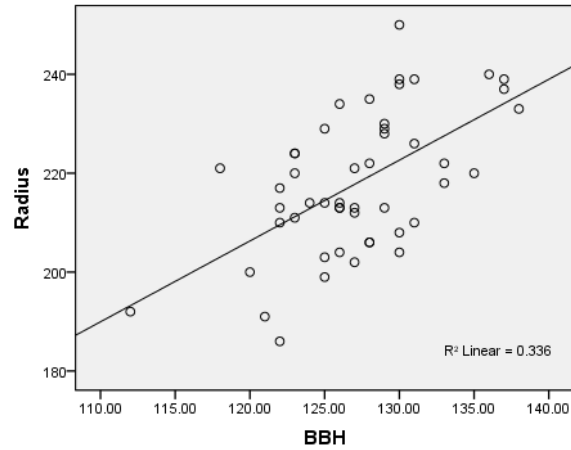
BBH-FIBXLN correlation of SAC females



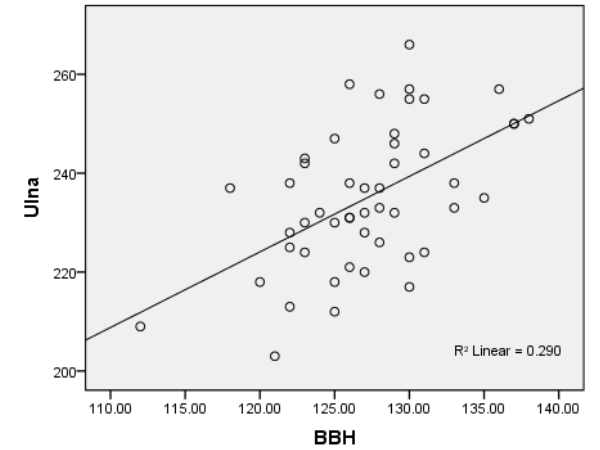
BBH-HUMXLN correlation of SAC females



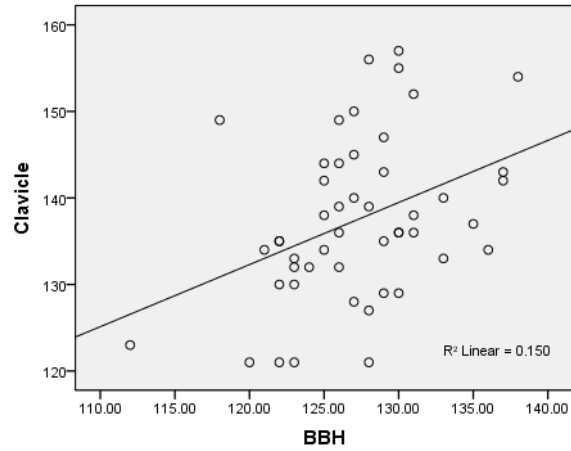
BBH-RADXLN correlation of SAC females



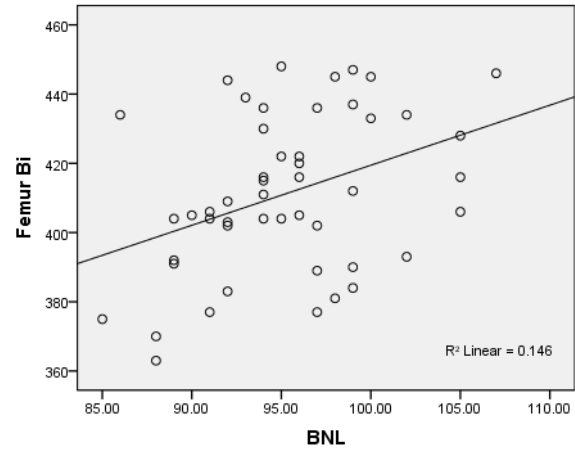
BBH-ULNXLN correlation of SAC females



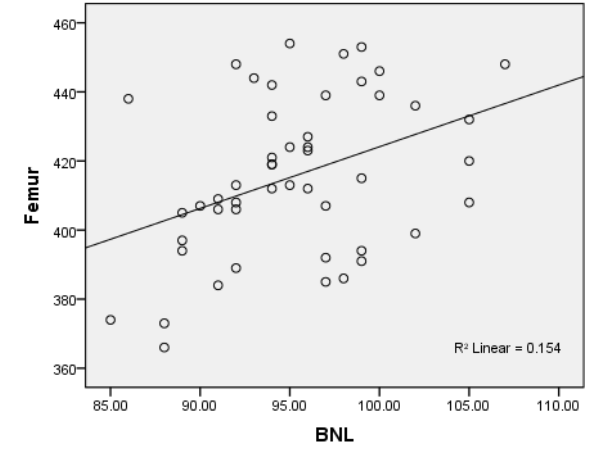
BBH-CLAXLN correlation of SAC females



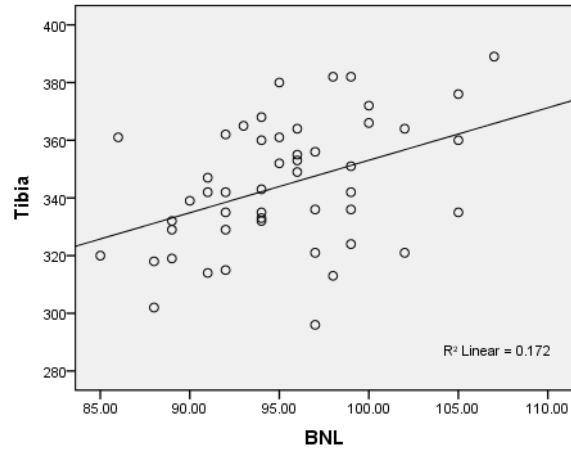
BNL-FEMBLN correlation of SAC females



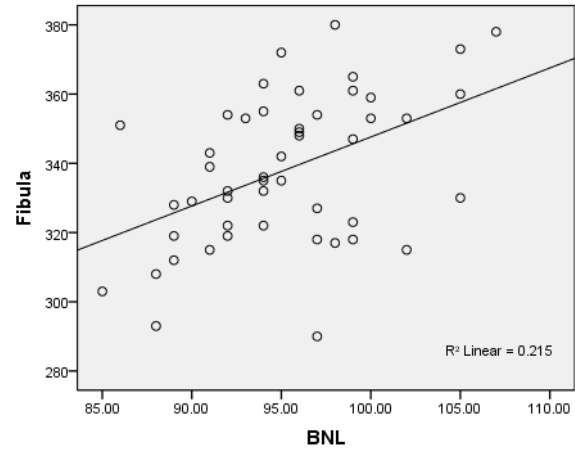
BNL-FEMXLN correlation of SAC females



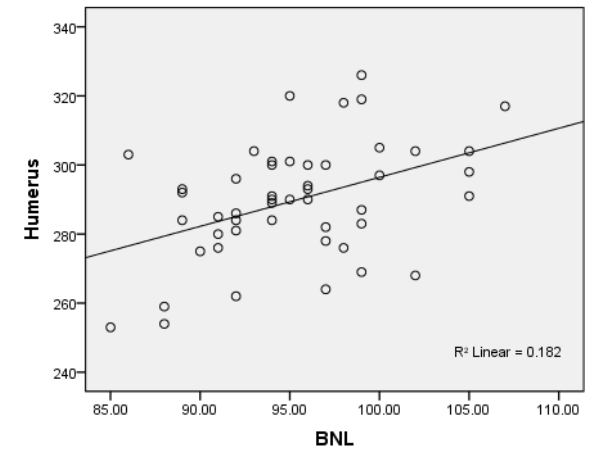
BNL-TIBXLN correlation of SAC females



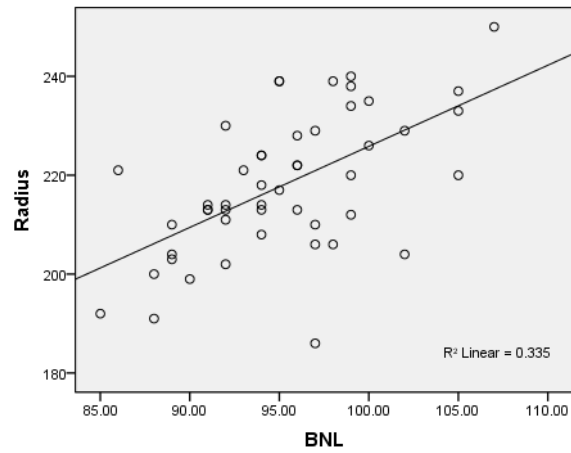
BNL-FIBXLN correlation of SAC females



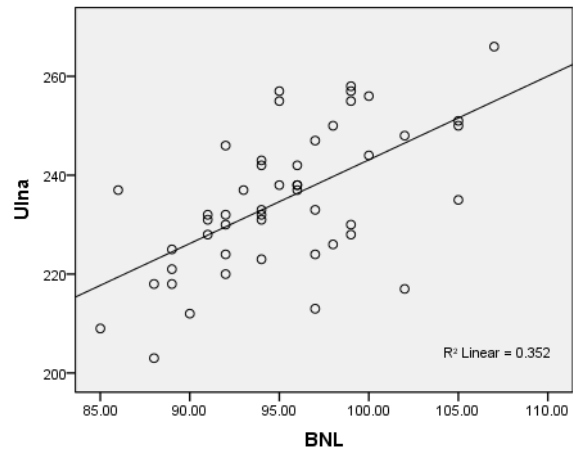
BNL-HUMXLN correlation of SAC females



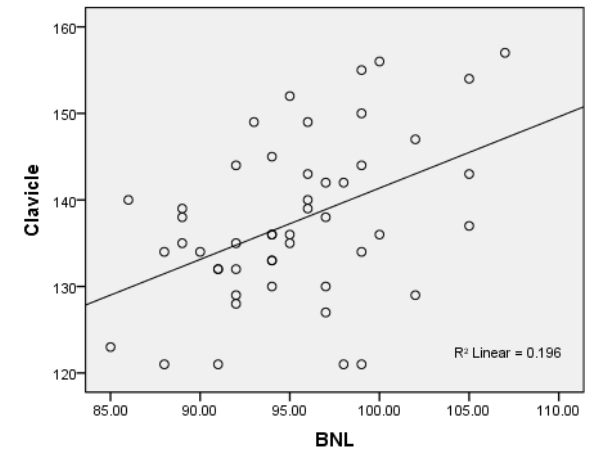
BNL-RADXLN correlation of SAC females



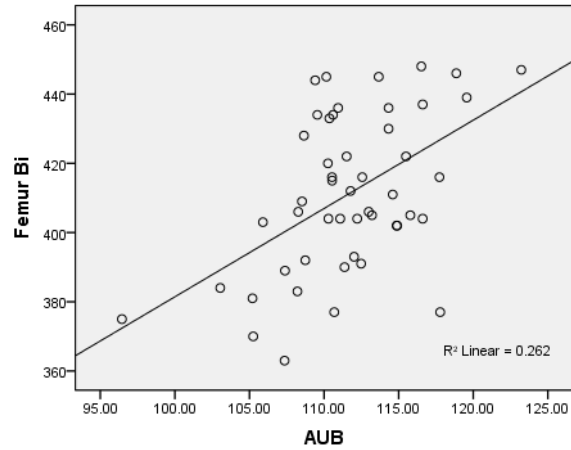
BNL-ULNXLN correlation of SAC females



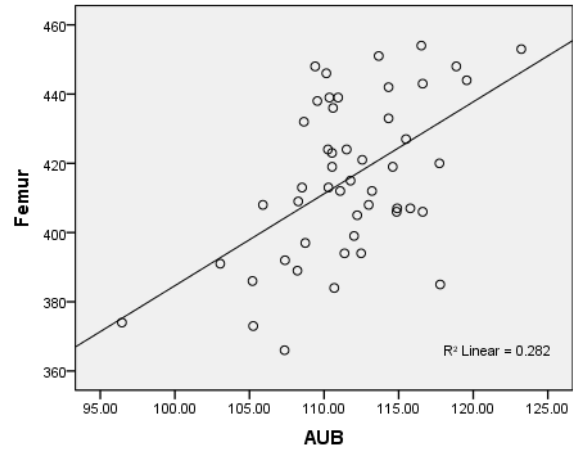
BNL-CLAXLN correlation of SAC females



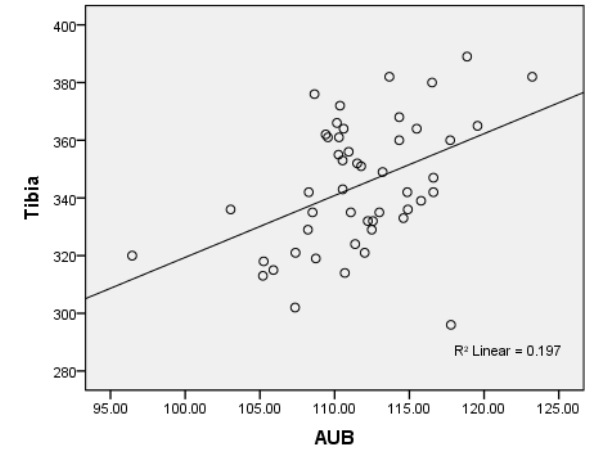
AUB-FEMBLN correlation of SAC females



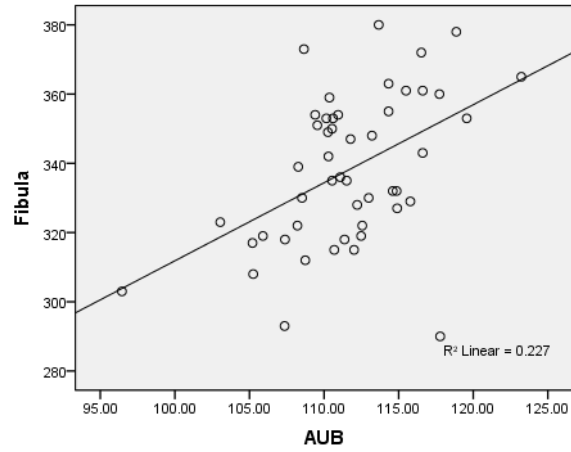
AUB-FEMXLN correlation of SAC females



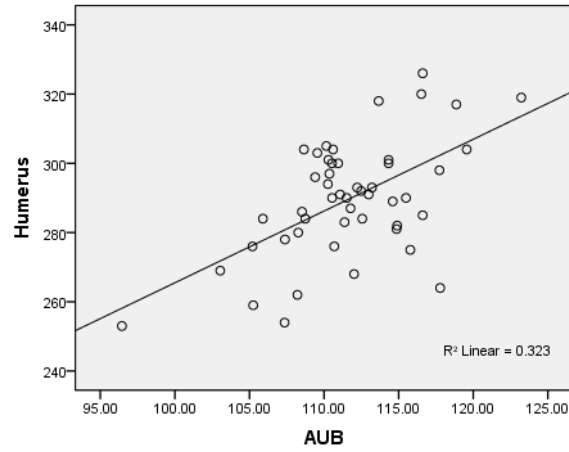
AUB-TIBXLN correlation of SAC females



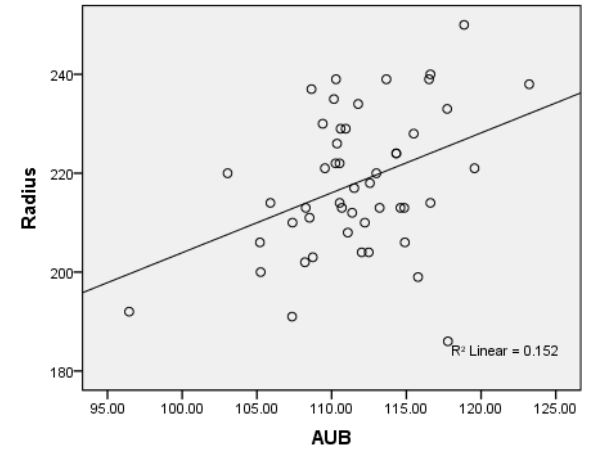
AUB-FIBXLN correlation of SAC females



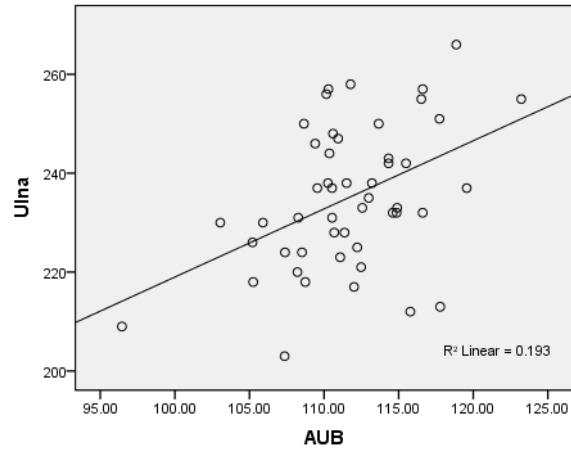
AUB-HUMXLN correlation of SAC females



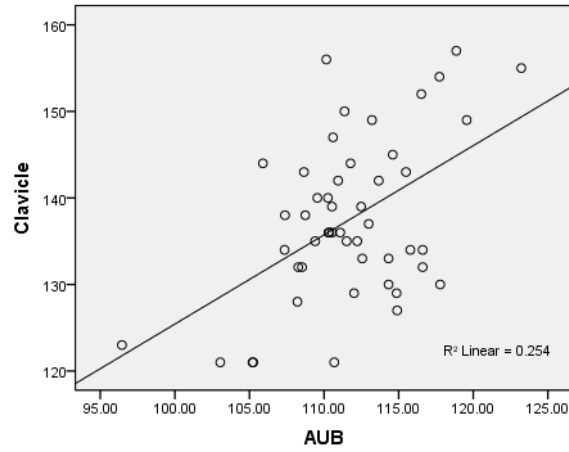
AUB-RADXLN correlation of SAC females



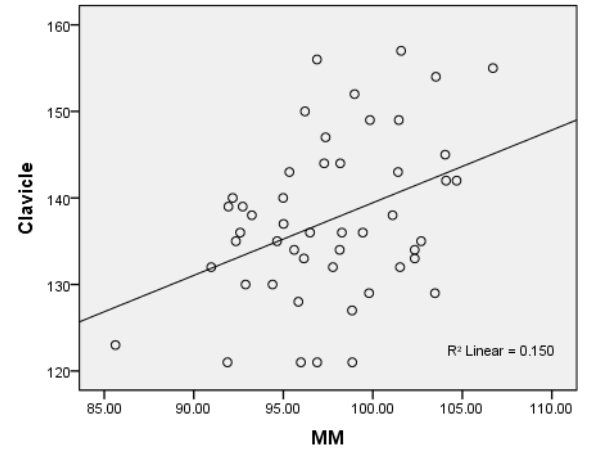
AUB-ULNXLN correlation of SAC females



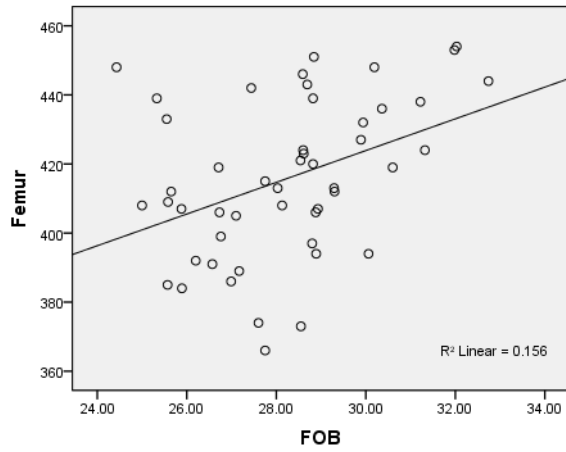
AUB-CLAXLN correlation of SAC females



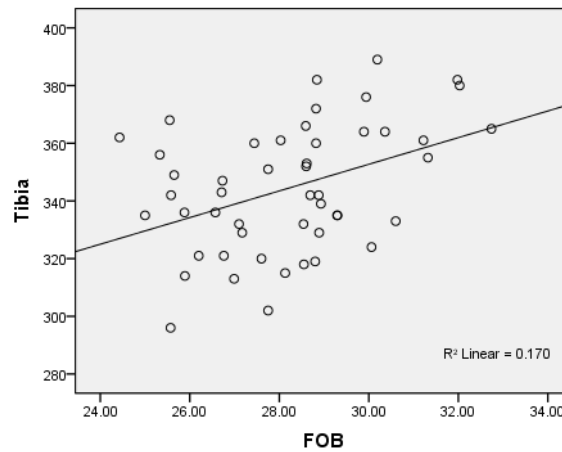
MM-CLAXLN correlation of SAC females



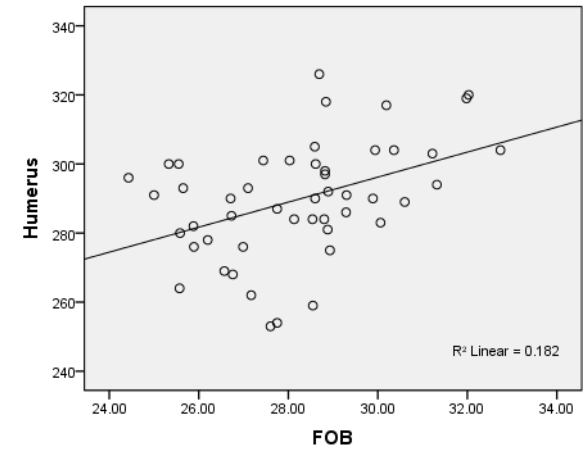
FOB-FEMXLN correlation of SAC females



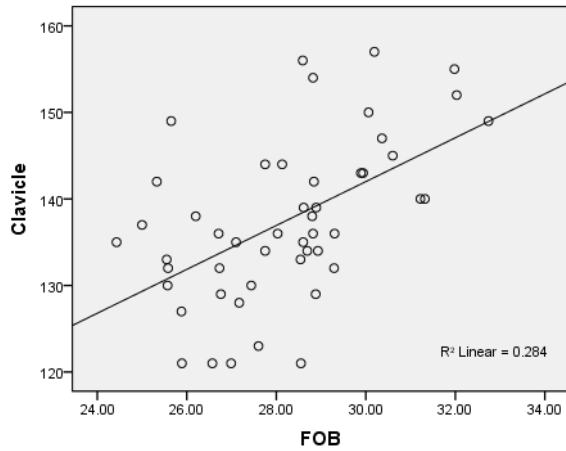
FOB-TIBXLN correlation of SAC females



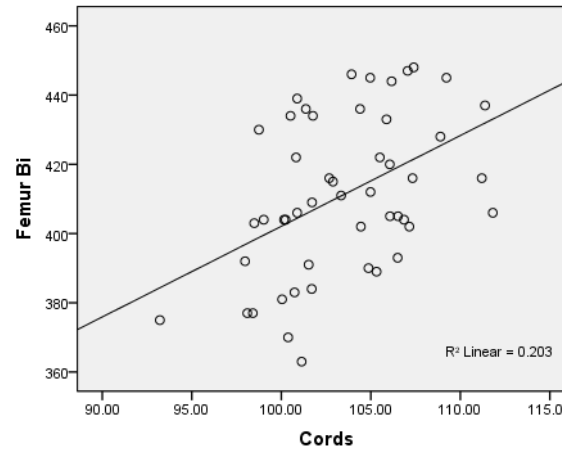
FOB-HUMXLN correlation of SAC females



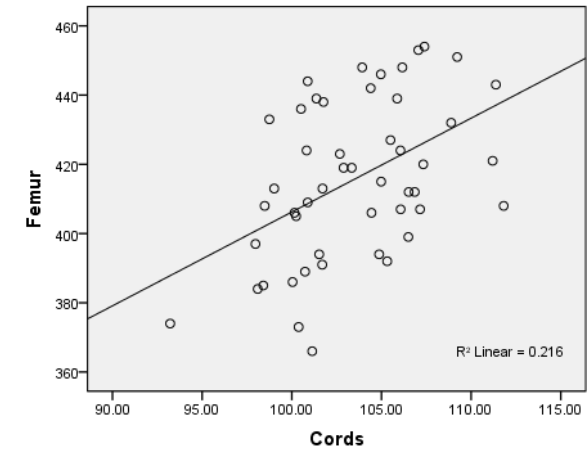
FOB-CLAXLN correlation of SAC females



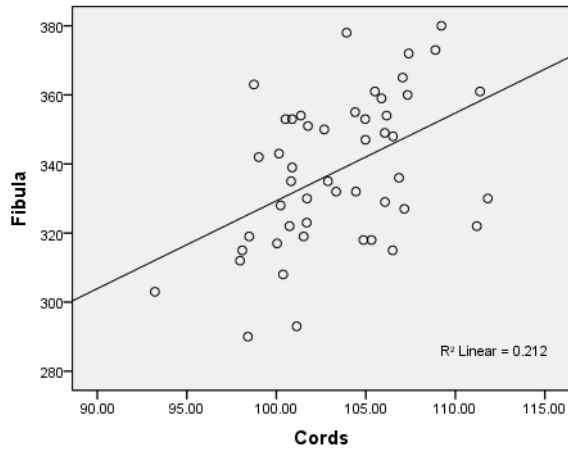
Cords-FEMBLN correlation of SAC females



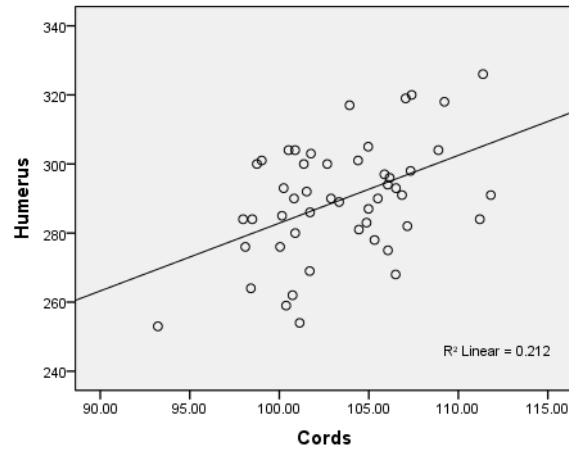
Cords-FEMXLN correlation of SAC females



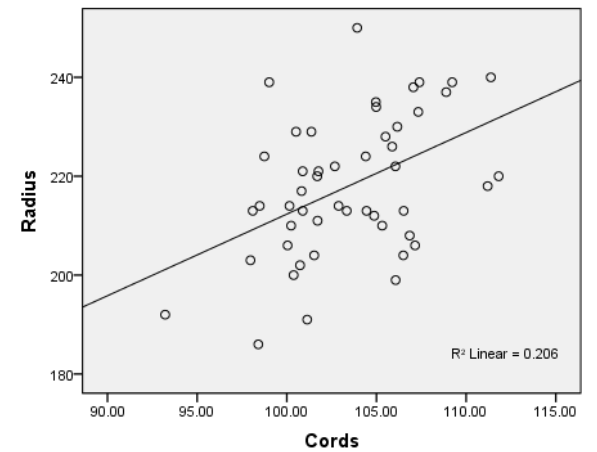
Cords-FIBXLN correlation of SAC females



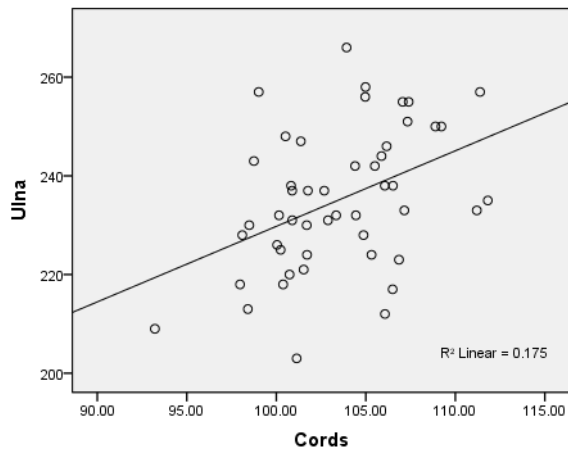
Cords-HUMXLN correlation of SAC females



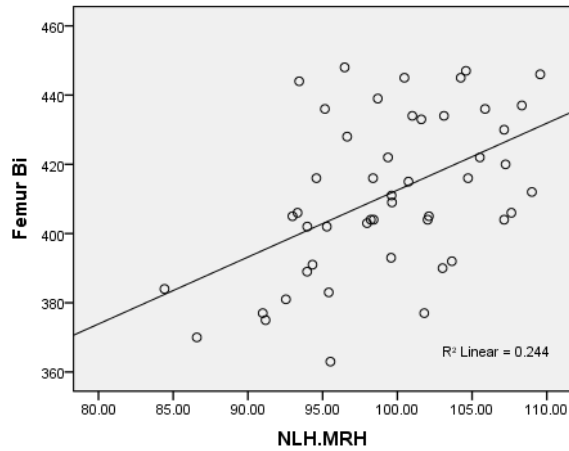
Cords-RADXLN correlation of SAC females



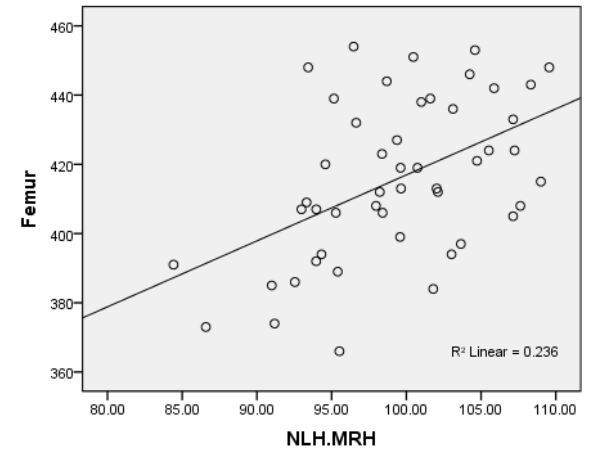
Cords-ULNXLN correlation of SAC females



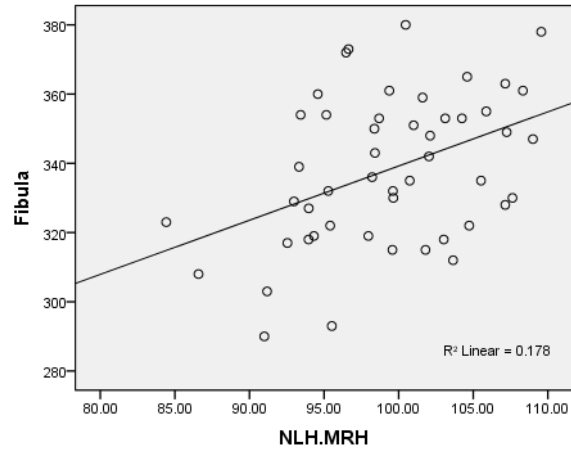
NLH.MRH-FEMBLN correlation of SAC females



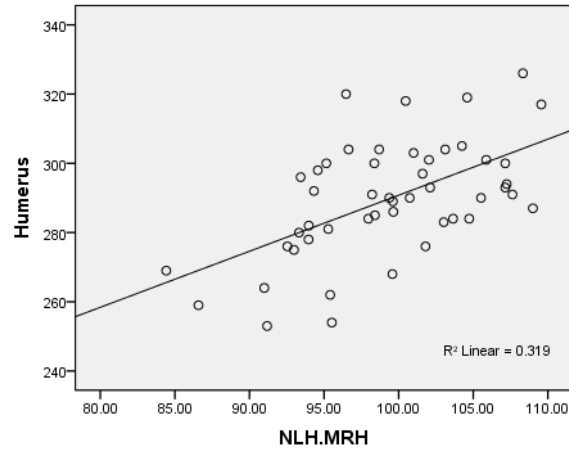
NLH.MRH-FEMXLN correlation of SAC females



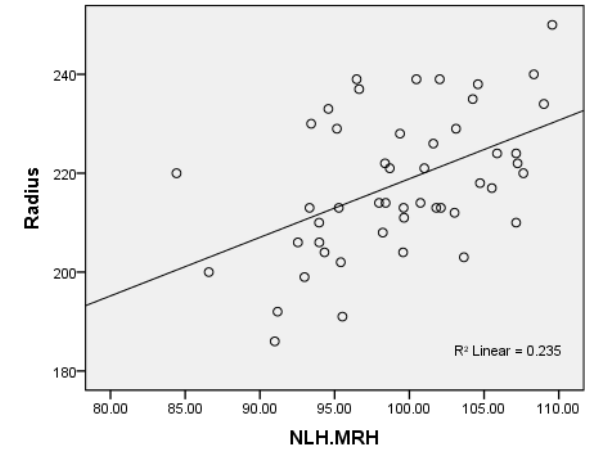
NLH.MRH-FIBXLN correlation of SAC females



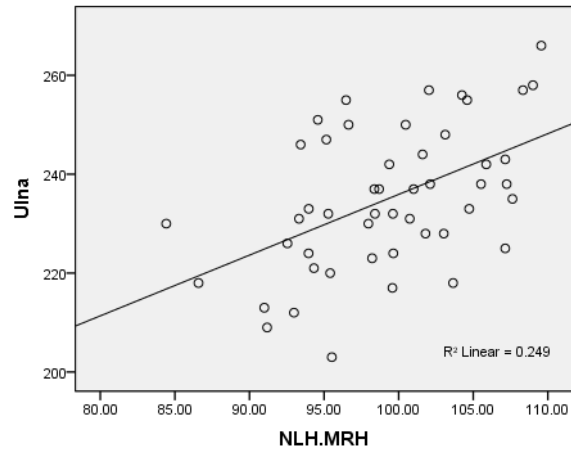
NLH.MRH-HUMXLN correlation of SAC females



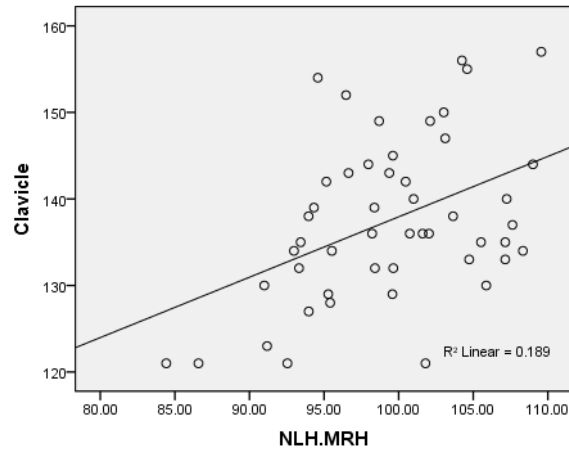
NLH.MRH-RADXLN correlation of SAC females

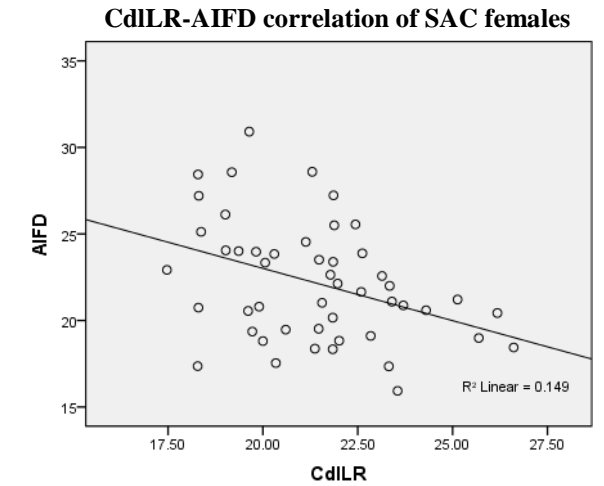
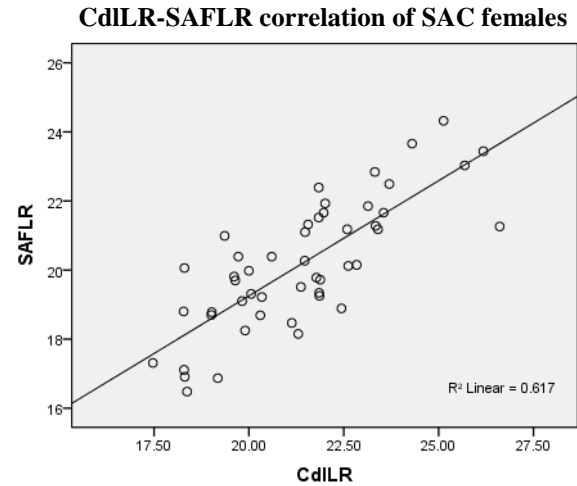
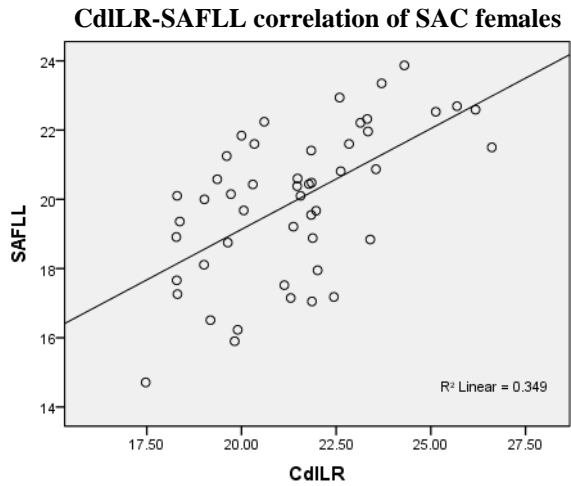
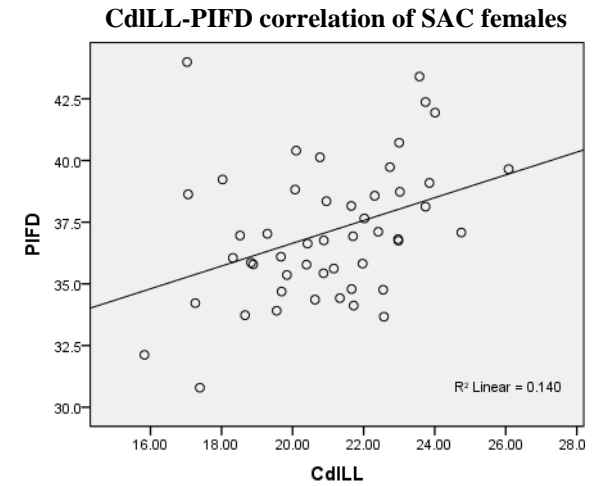
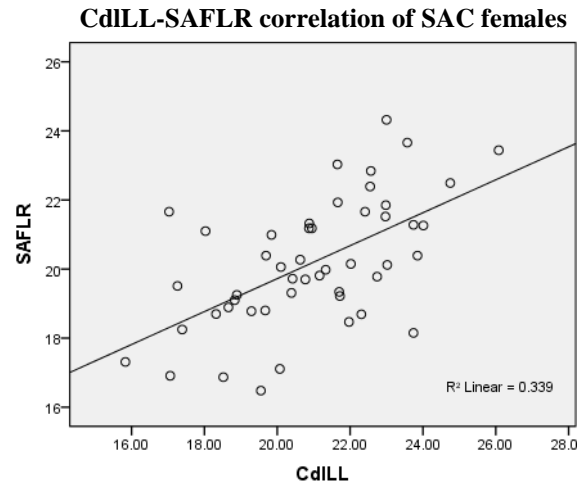
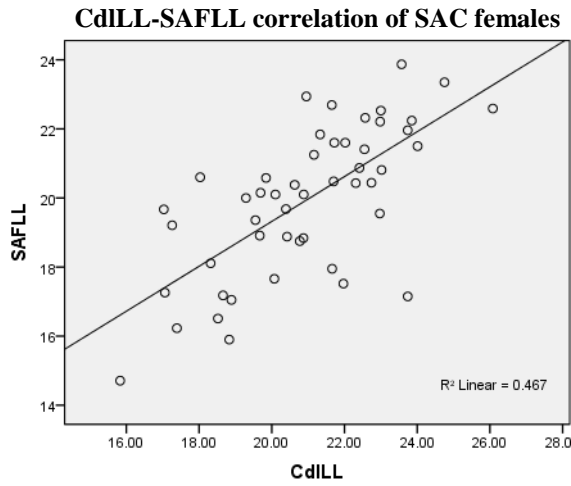


NLH.MRH-ULNXLN correlation of SAC females

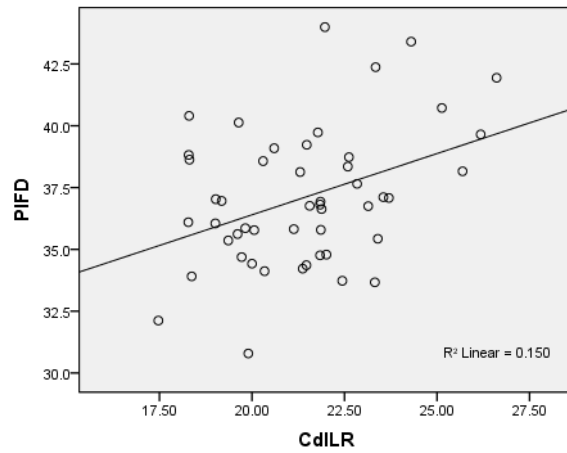


NLH.MRH-CLAXLN correlation of SAC females

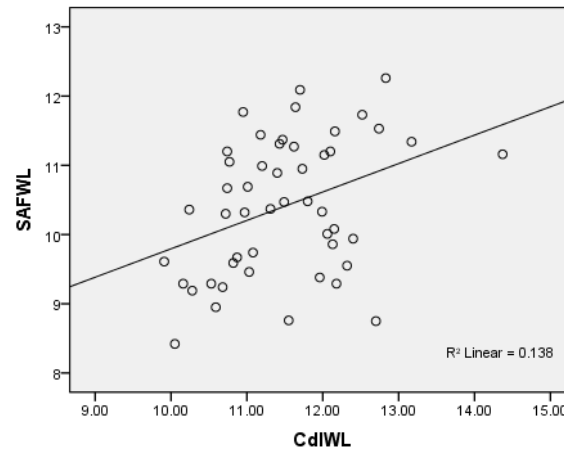




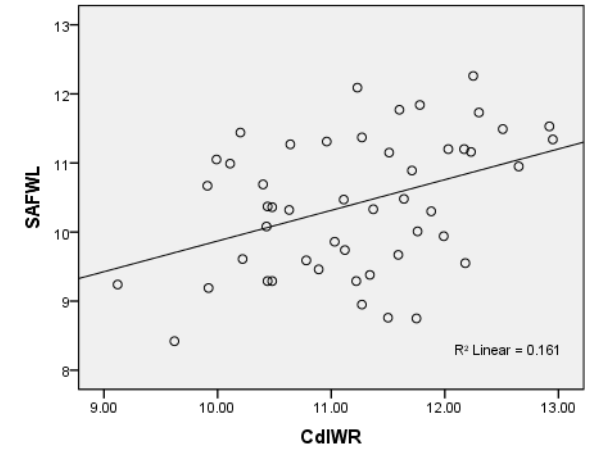
CdILR-PIFD correlation of SAC females



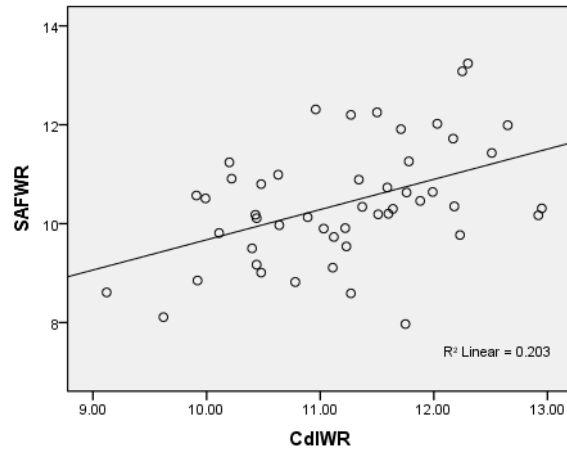
CdIWL-SAFWL correlation of SAC females



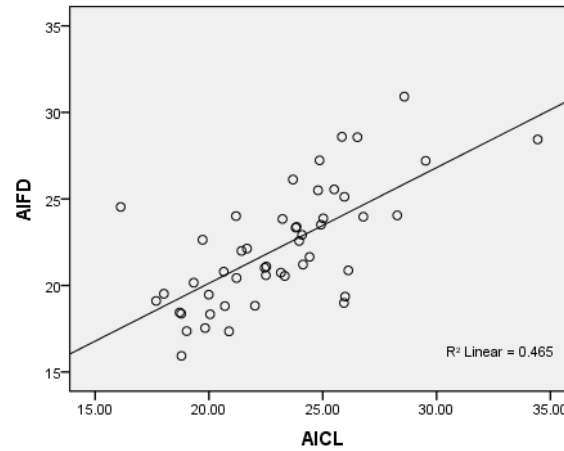
CdIWR-SAFWL correlation of SAC females



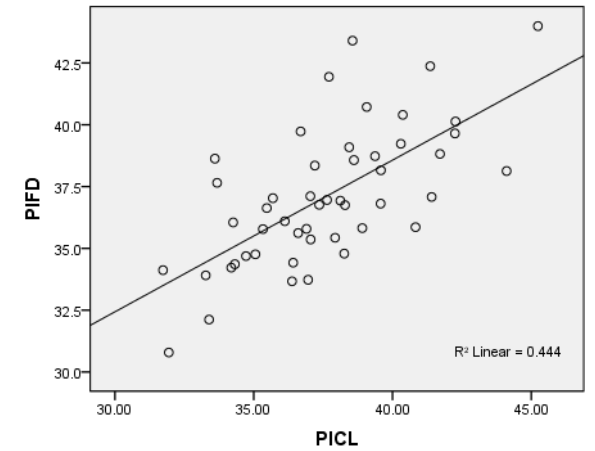
CdIWR-SAFWR correlation of SAC females



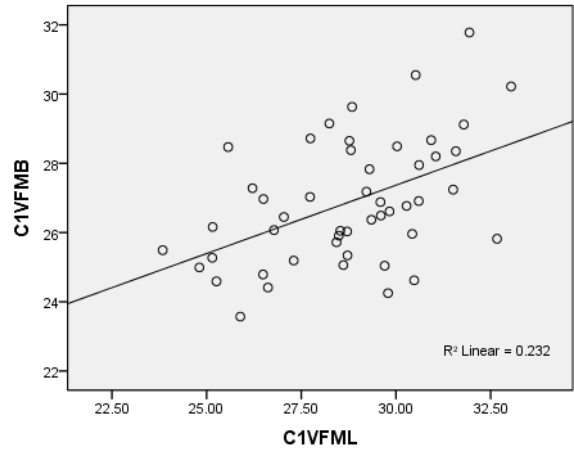
AICL-AIFD correlation of SAC females



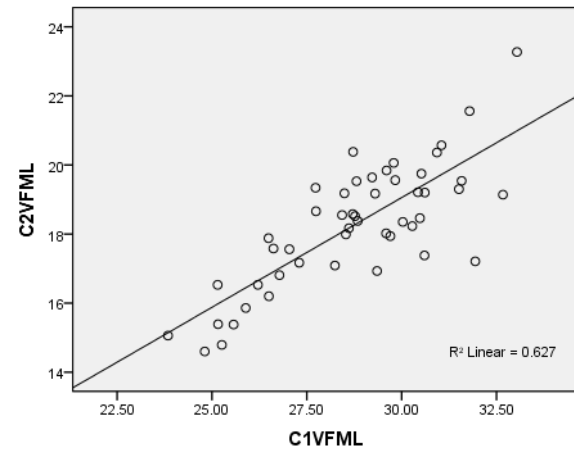
PICL-PIFD correlation of SAC females



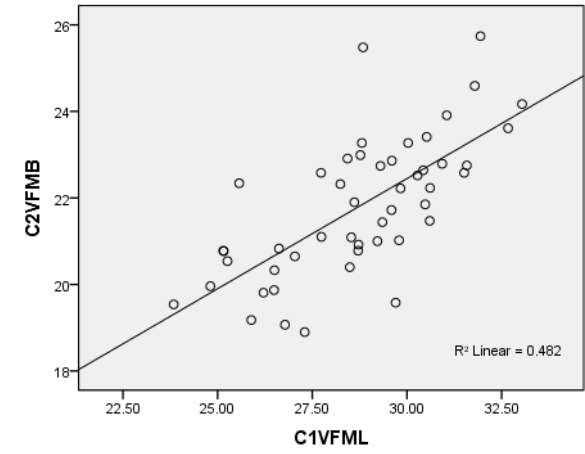
C1VFML-C1VFMB correlation of SAC females



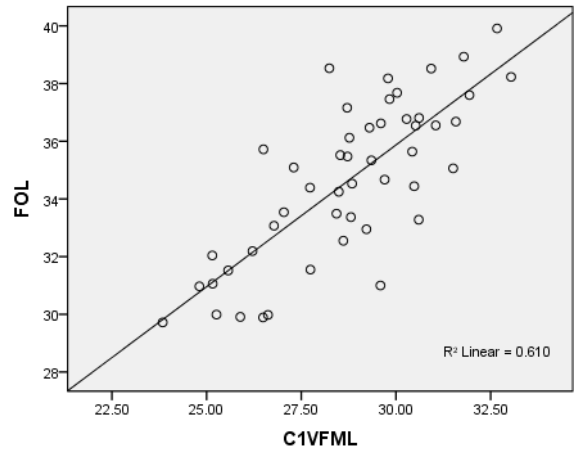
C1VFML-C2VFML correlation of SAC females



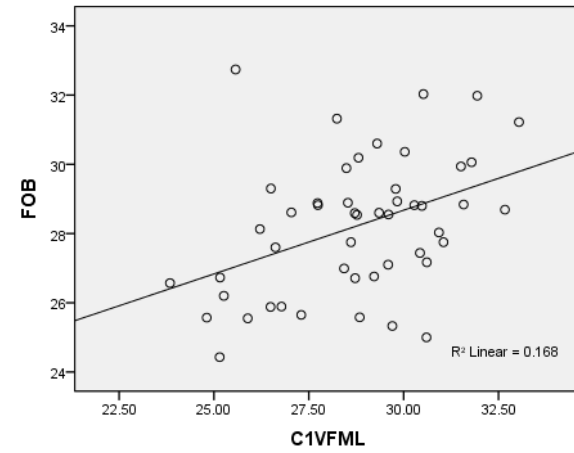
C1VFML-C2VFMB correlation of SAC females



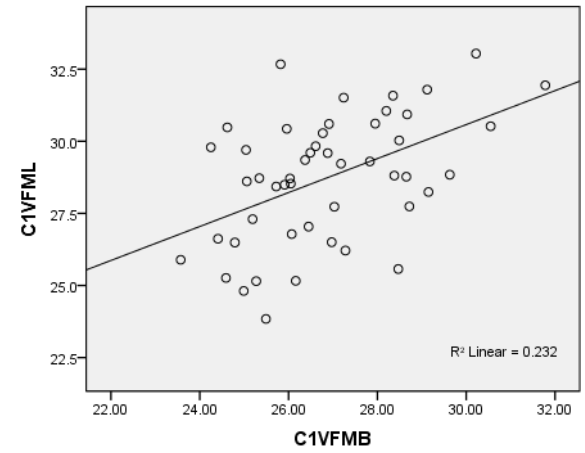
C1VFML-FOL correlation of SAC females



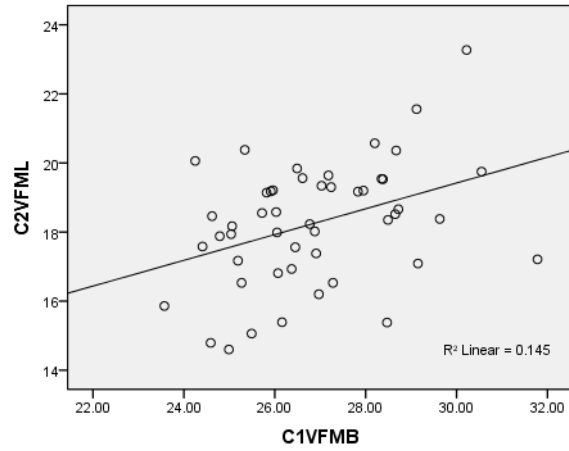
C1VFML-FOB correlation of SAC females



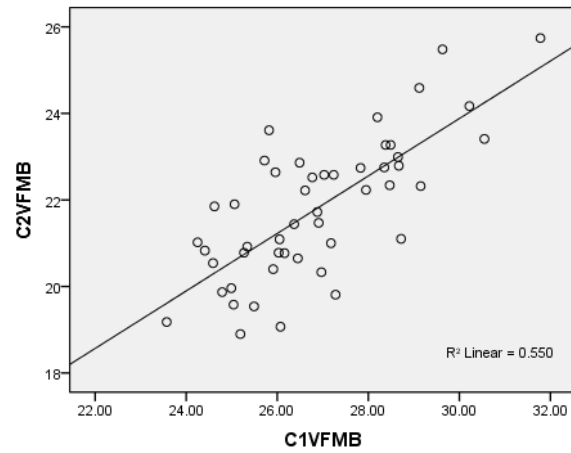
C1VFMB-C1VFML correlation of SAC females



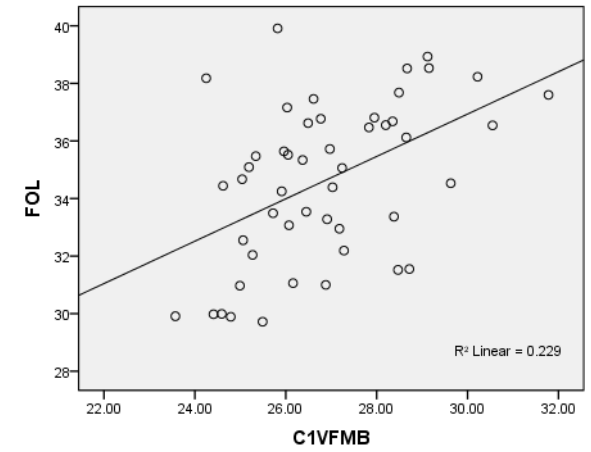
C1VFMB-C2VFML correlation of SAC females



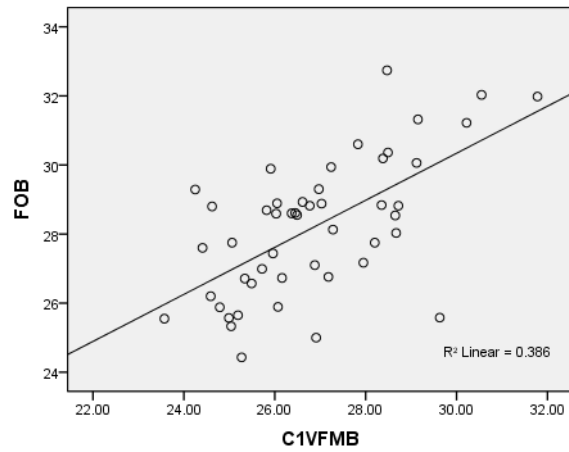
C1VFMB-C2VFMB correlation of SAC females



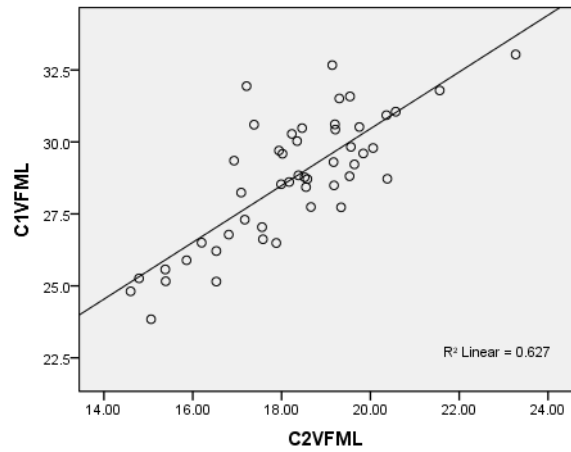
C1VFMB-FOL correlation of SAC females



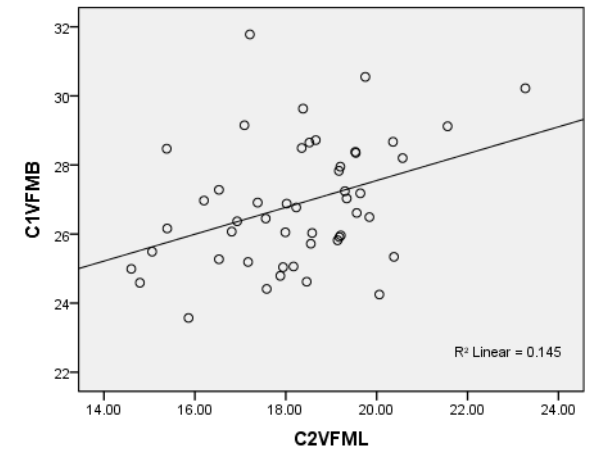
C1VFMB-FOB correlation of SAC females



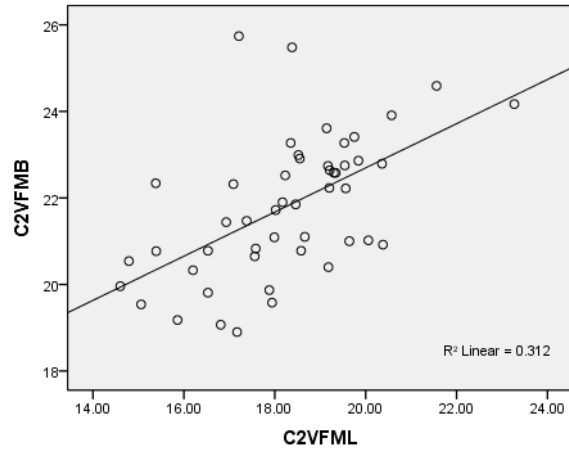
C2VFML-C1VFML correlation of SAC females



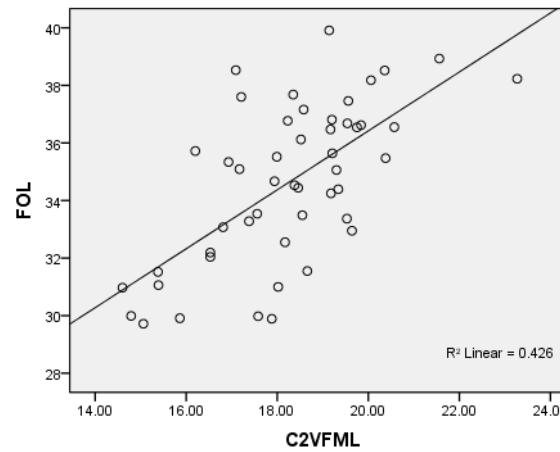
C2VFML-C1VFMB correlation of SAC females



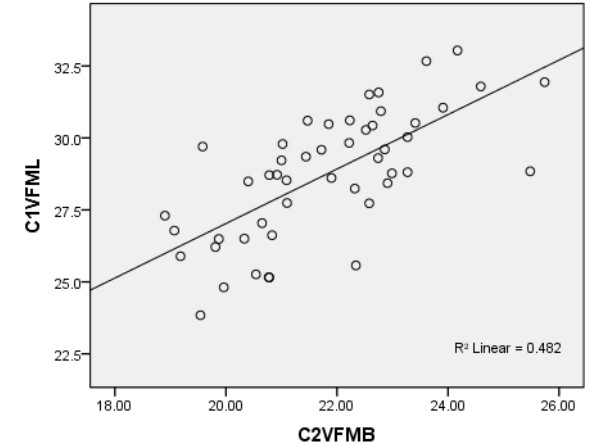
C2VFML-C2VFMB correlation of SAC females



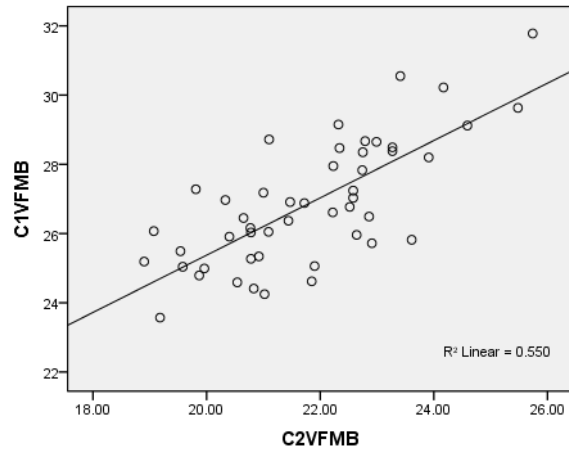
C2VFML-FOL correlation of SAC females



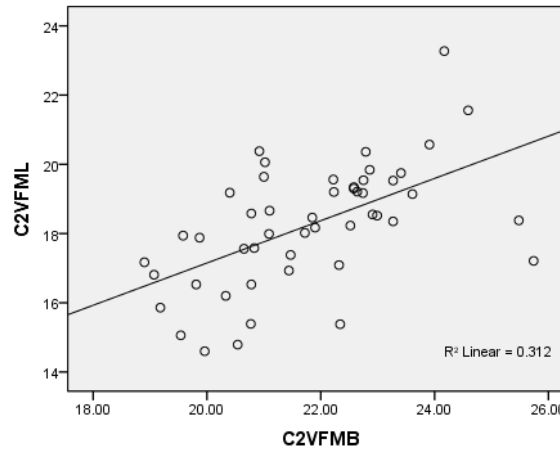
C2VFMB-C1VFML correlation of SAC females



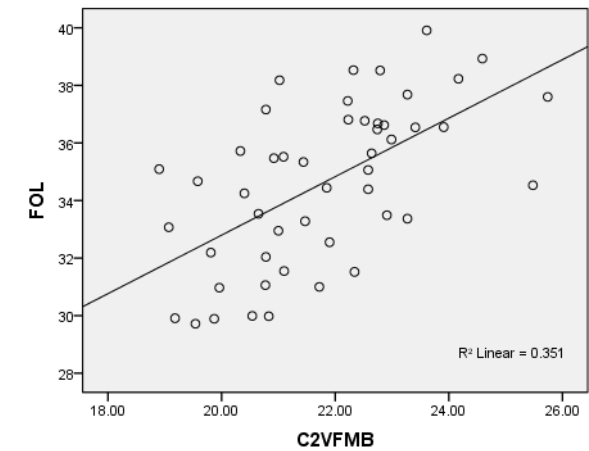
C2VFMB-C1VFMB correlation of SAC females



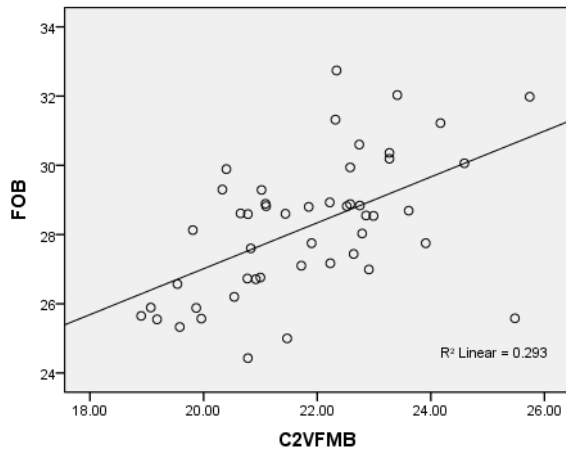
C2VFMB-C2VFML correlation of SAC females



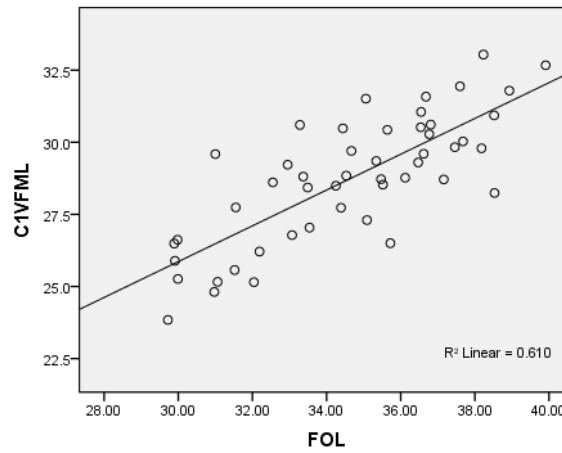
C2VFMB-FOL correlation of SAC females



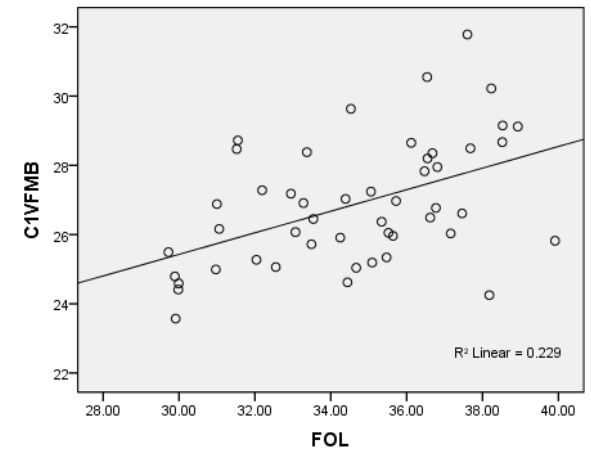
C2VFMB-FOB correlation of SAC females



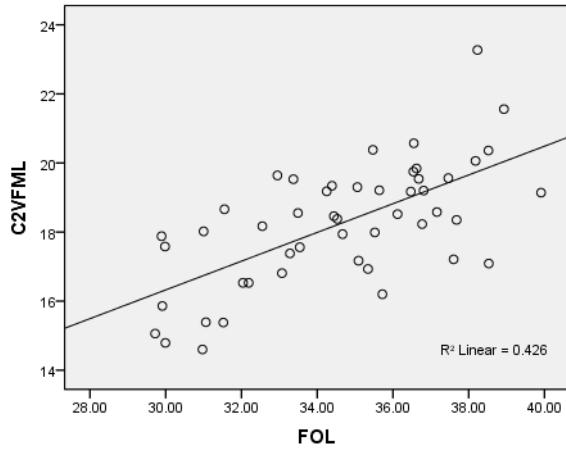
FOL-C1VFML correlation of SAC females



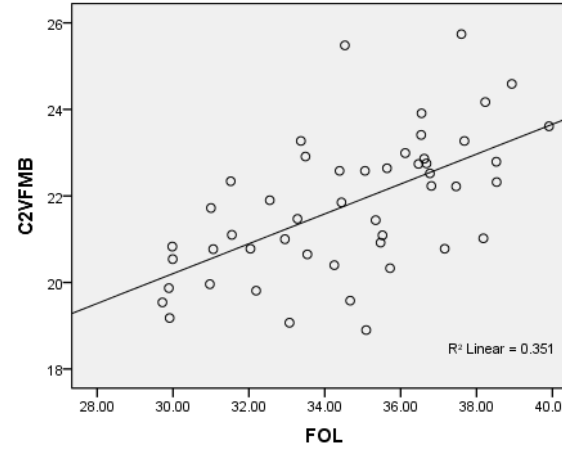
FOL-C1VFMB correlation of SAC females



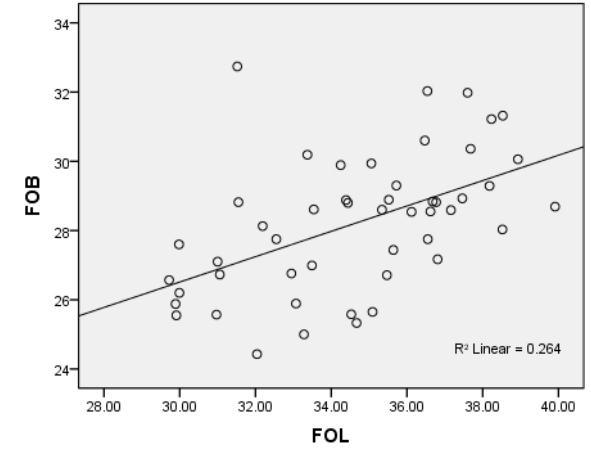
FOL-C2VFML correlation of SAC females



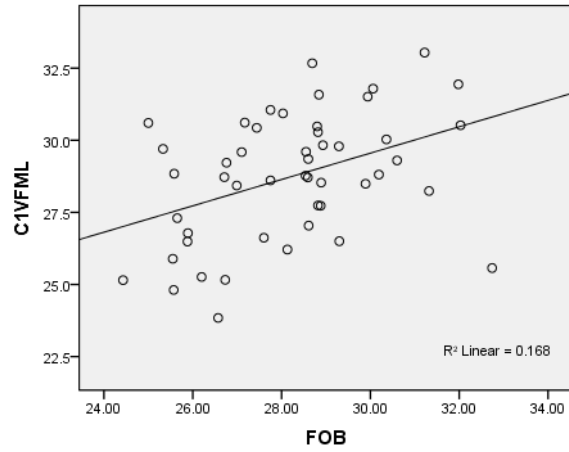
FOL-C2VFMB correlation of SAC females



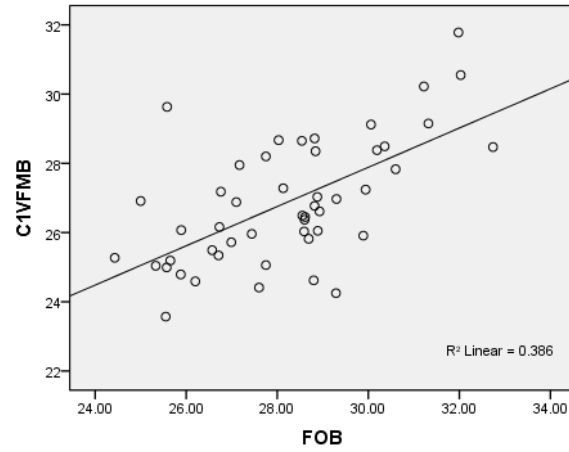
FOL-FOB correlation of SAC females



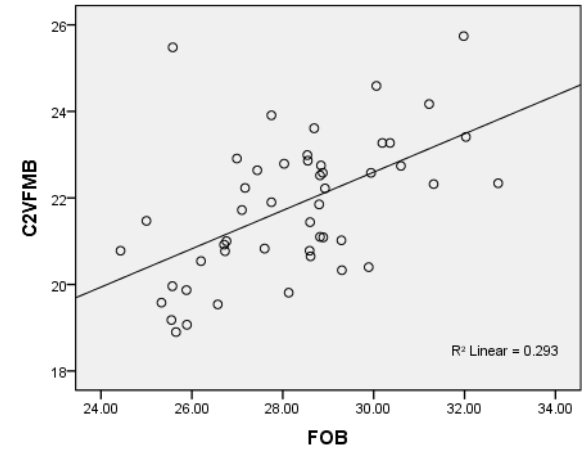
FOB-C1VFML correlation of SAC females



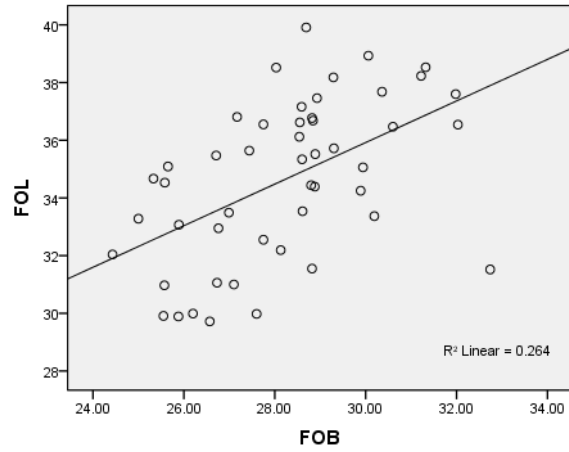
FOB-C1VFMB correlation of SAC females



FOB-C2VFMB correlation of SAC females



FOB-FOL correlation of SAC females



feedback studio Johan Christian Marais | MSc Thesis Marais

Match Overview

2%

- 1 Handbook of Anthro... (Publication) <1% >
- 2 Submitted to University... (Student Paper) <1% >
- 3 'ECR 2018 - BOOK OF ... (Publication) <1% >
- 4 Submitted to National ... (Student Paper) <1% >
- 5 Submitted to University... (Student Paper) <1% >
- 6 'A selection of abstract... (Publication) <1% >
- 7 journals.viamedica.pl <1% >

ABSTRACT

Upon discovery of comingled disarticulated skeletons, actual matching of different skeletal elements to a particular individual can be extremely difficult. Available literature regarding the matching of skeletal elements, show few studies correlating skull measurements with post-cranial elements, with the majority of cases determining correlations with stature. The aim of this study is to assess the degree of correlation between cranial and post-cranial skeletal elements, of the three dominant South African population groups, by means of direct correlations of measurements.

Skeletons of individuals (N=296) of both males (n=148) and females (n=148) of South African black (n=100), South African white (n=97) and South African coloured (n=99) population groups, were assessed in three distinct manners. Firstly, three correlation sets were recorded: 21 cephalometric elements were correlated with eight long-bone measurements, and six

Word Count: 17700

The maximum size of a document uploaded (Word, Excel, PDF) is 20 MB or 500 pages

Refresh Submissions

Submission Turnitin Overall

turnitin

Digital Receipt

This receipt acknowledges that Turnitin received your paper. Below you will find the receipt information regarding your submission.

Submission Author	Johan Christian Marais
Turnitin Paper ID (Ref. ID)	1047743172
Submission Title	MSc Thesis Marais
Assignment Title	PG Skills Turnitin Sandbox
Submission Date	30/11/18, 11:19

Print